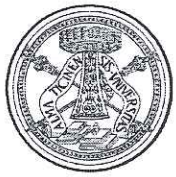

UNIVERSITÀ DEGLI STUDI DI PAVIA

DOTTORATO IN SCIENZE CHIMICHE E FARMACEUTICHE

XXIX CICLO

Coordinatore: Chiar.mo Prof. Mauro Freccero

DRUG DELIVERY IN 3D POLYMERIC SCAFFOLD FOR TISSUE REGENERATION

Tutore

Chiar.ma Prof. Bice Conti

Tesi di Dottorato di

Antonella DE TRIZIO

a.a. 2015- 2016

Ai miei genitori

Table of content:

Chapter 2-*Thermosetting hydrogel and moldable composite scaffold as drug delivery systems for osteomyelitis treatment*

Chapter 3- *An experimental design approach to the preparation of pegylated polylactide-co-glicolide gentamicin loaded microparticles for local antibiotic delivery*

Chapter 4- *Formulation and in vitro characterization of a composite biodegradable scaffold as antibiotic delivery system and regenerative device for bone*

SECTION I

General Introduction

SECTION I

GENERAL INTRODUCTION

Tissue engineering (TE) aims to restore loss of tissue and organ's functionality resulting from injury, aging or disease [1]. Biomaterials, cells and bioactive factors, are commonly considered the key elements needed for preparation of 3D tissue engineered construct aimed to manage the damaged tissue regeneration. After an acute injury to cells or tissue, regeneration process can occur and consequently restoration of tissue structure or repair by scar formation. Regeneration corresponds to complete restitution of lost or damaged tissue; instead repair involves restoring of some original structure with scar formation. Regeneration is typical for tissue with high proliferation capacity such as hematopoietic system, skin epithelia, gastrointestinal tract and bone tissue because of their capacity to renew continuously after an injury. Repair is often consisted by a combination of regeneration and scar formation by collagen deposition. The contribution of regeneration and scarring in tissue repair depends on tissue ability to regenerate but also on injury extent [2]. This repairing/regeneration of damaged site is regulated by several cell types, matrix proteins, growth factors and cytokines. Tissue engineering has focused on design of constructs promoting regeneration of several types of tissue, e.g.: skin, cartilage, bone, tendon and cardiac tissue. The classical approach to induce tissue regeneration at the defective site is to artificially build an environment for cells that can induce tissue regeneration by providing a scaffolds as artificial ECM (extracellular matrix), which can assist cell attachment and subsequent proliferation and differentiation. The approach considers that cells around the scaffold infiltrate into the scaffold and proliferate if artificial ECM is biocompatible. Scaffold should be used in combination with cells and/or growth factors, cytokines and genes, in order to promote tissue regeneration expecially when tissue has not inherent self-regenerating potentiality. Growth factors (GFs) are important therapeutic agents to regenerate many tissues such as, muscoloskeletal, neuronal, hepatic and vascular [3, 4]. Their direct injection into the specific site to be regenerated is generally not effective because of their rapid diffusion from injected site and enzymatic digestion and deactivation. This comes in a new technology of tissue regeneration combined with Drug Delivery System (DDs) (**Figure 1**). In the field of tissue regeneration drugs includes proteins and genes in order to promote cells proliferation and differentiation. For example, control delivery of GFs is achieved by incorporation of these GFs into polymeric carrier [5].

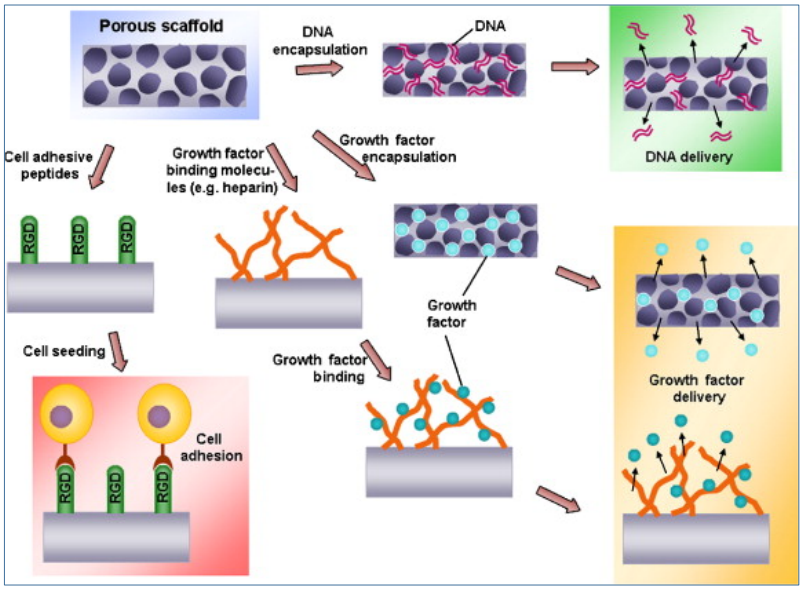

Figure 1: Surface engineered and growth factor releasing scaffolds for tissue engineering: Scaffolds can be either immobilized with cell specific ligands for cell adhesion, or encapsulated with growth factors or DNA to promote cell proliferation and morphogenesis. Reprinted from Chung et al. (2007).

Therefore an ideal scaffold should possess a 3D and well-defined micro-architecture with an interconnected pore network, mechanical properties similar to those of natural tissue, it should be biocompatible and bio-resorbable at a controllable degradation and resorption rate, as well as it should provide control delivery of specific bioactive factors in order to enhance or guide the regeneration process [6]. Polymer matrix or scaffold are 3D platforms that can get dual purpose of cell support and cells/GFs/drugs delivery, where macropores (> 50nm, <300nm) are most useful for cell and tissue penetration, and smaller pores such as micropores (< 2nm) and mesopores (>2nm, <50nm) contribute to drugs diffusion allowing nutrient transport and waste of metabolic products, to achieve cells growth. Furthermore, based on scaffold material composition, degradation rate can be tuned to match the rate of tissue growth, in such a way that the regenerated tissue can progressively replace scaffold matrix. Functionality enhancement of these already complex matrices, by using them as drug releasing scaffold or by incorporation of drug delivery devices, permits local delivery of an adequate dose of bioactive molecules for a desired time frame, minimizing active agent release to not-targeted sites and supporting tissue regeneration which normally occurs in long time span. In this perspective, TE can be viewed as a special case of controlled drug delivery combined to scaffolding materials and leading to new multifunctional platforms able to achieve drug delivery with high loading and efficiency to specific sites, controlling tissue regeneration process [7]. Different form of polymeric scaffolds for cell/drug

delivery are available: 1) typical 3D porous matrices 2) nanofibrous matrices 3) thermosensitive sol-gel transition hydrogels and 4) porous microspheres (**Figure 2**).

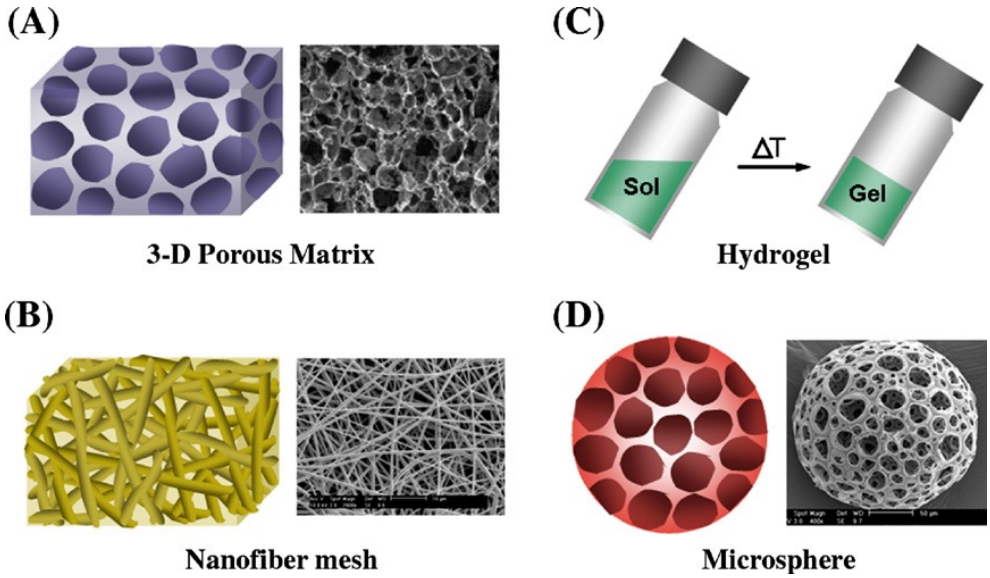

Figure 2: Different forms of 3D polymeric scaffold for tissue regeneration: (A) a typical 3D-porous matrix, (B) a nanofibrous matrix, (C) a thermosensitive sol-gel transition hydrogel, (D) porous microspheres. Reprinted from Chung et al. (2007).

Scaffolds are used successfully in various fields of tissue engineering such as bone formation, periodontal regeneration, repair of nasal and auricular malformations, cartilage development, artificial corneas, heart valves, tendon repair, ligament replacement and tumors. They are also used in joint pain inflammations, diabetes, osteochondrogenesis and wound healing. Alternatively, they are applied for delivering drugs and genetic materials, such as plasmid DNA at controlled rate over a long period time. In addition, incorporation of drugs (inflammatory inhibitors and /or antibiotics) into scaffolds may be used to prevent infection after surgery and other latent chronic diseases. Scaffolds can be used to provide adequate signals (using adhesion peptides and growth factors) to induce and maintain cells in their desired differentiation stages and to maintain their survival and growth.

Drugs (growth factors and genes) and cells, can be integrated within scaffolds by simply interspersion them into polymer matrix. Examples in the literature have been found where a biodegradable hydrogel could act simultaneously as scaffold and controlled delivery system. In addition the hydrogel system can even release more than one type of growth factor at the same time or in time-order way [6, 8]. Depending on incorporation method used, GFs release rate may be controlled by processes included diffusion, polymer erosion or degradation, swelling of polymer followed by diffusion, whereas covalently immobilization of proteins is followed by chemical/enzymatic reaction controlled mechanism release. GFs release profile can be altered by modifying polymer properties or adjusting

vehicle physical and chemical properties such as porosity, pore size, tortuosity, degree of crosslinking and its degradation rate. Additionally, cells, GFs and genes can be encapsulated into biodegradable particulate systems having the potential to be retained in a specific tissues providing sustained release (**Figure 3**).

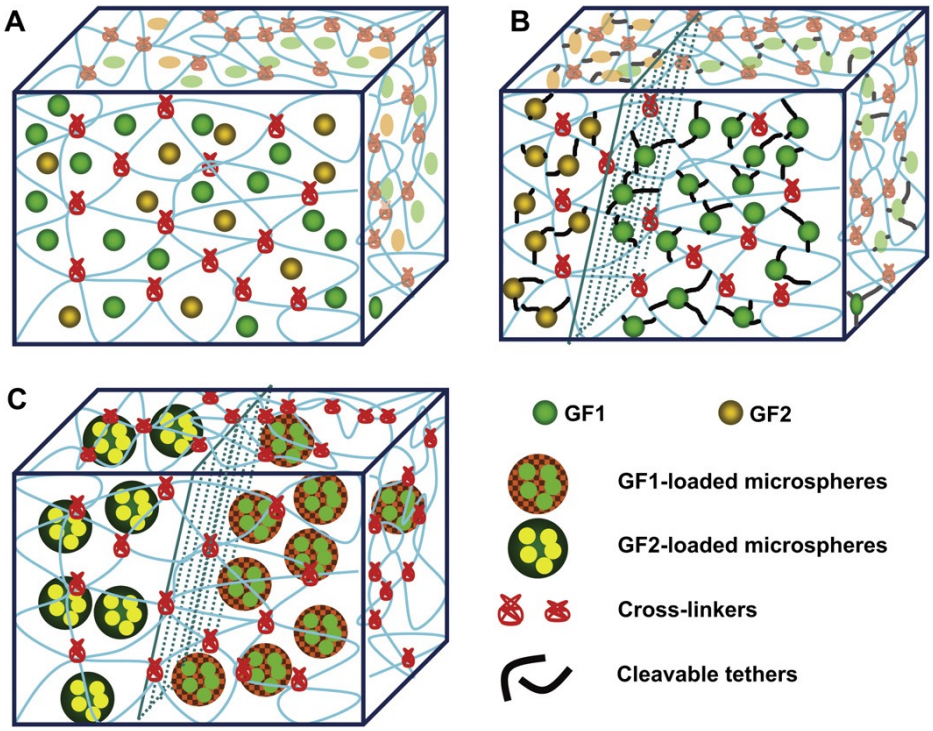

Figure 3: (a) non covalent immobilization of GF1 and GF2 directly entrapped into hydrogel; (b) covalent immobilization: GFs are modified and covalently crosslinked to the hydrogel via crosslinkable and cleavable bonds that can degrade hydrolytically and enzymatically, leading to spatially and sequential delivery of two types of GFs; (c) particulate-based delivery: GFs are pre-loaded into microspheres that are subsequently entrapped into the hydrogel. Reprinted from F.-M. Chen et al. (2010).

Biomaterials for drug delivery can be designed in various morphologies (e.g. micelles, vesicles, particles tubes, scaffolds or gels) and architecture (reservoirs or matrices). The GFs can be safely encapsulated in non-cytotoxic and biodegradable synthetic polymers such as polylactic acid (PLA), polyglycolic acid (PGA) their copolymer polylactic-co-glycolic acid (PLGA), poly-ε-caprolactone (PCL), polyethylene, polymethylmetacrylate (PMMA) or natural hydrogels such as alginate, gelatin, fibrin, collagen and chitosan in which chemical or physical cross-linking offers the possibility to control diffusion of solubilized hydrophilic molecules. Moreover, a particulate system loaded with drugs such as GFs, can be further incorporated into hydrogel or porous scaffolds in order to simultaneously or sequentially deliver one or more GFs. In this way, delivery systems can be designed to produce different drugs

release profiles with distinct spatial and temporal gradients also in response to specific cues from cellular microenvironment, in order to better simulate natural healing process. In addition, inorganic materials such as calcium orthophosphates (including calcium phosphate cements and sintered ceramics, calcium sulphate cements and Bioglasses) have also been used as drug carriers. A combination of several materials may offer the best beneficial clinical outcome combining the individual benefits from each material to efficiently deliver drugs. Moreover, nanotechnology development in recent years focused on nanoparticles delivery systems, with diameter between 50 to 700 nm, as carriers for therapeutic agents, such as GF and genes, able to penetrate through capillaries into cells and enabling new tissue regeneration [9].

The thesis is focused on regeneration of infected bone defects, in particular infection by bacteria as a consequence of orthopedic implant surgery. Pathology refers to osteomyelitis infection, an overview of the major occurring events and features in osteomyelitis was highlighted with emphasis on bacterial adhesion process on implants and conventional therapeutic strategies, since they are the basis to design new bioactive scaffolds. The research project was focused on local drug delivery systems for bone regeneration and it involves a deep study on drug delivery technologies approaches that can be included into scaffolds.

Osteomyelitis is caused by pyogenic bacteria including certain strains of mycobacteria and fungi. It involves inflammation, subsequent bone loss and spreading of bacterial infection to soft tissue. It has three sub categories: i) acute (develops within 10 days) ii) sub-acute (develops within two weeks to one month) and iii) chronic (after several months). Acute osteomyelitis can occur from bacterial presence in the blood with edema, local anoxia and pus formation. Chronic osteomyelitis exhibits osteonecrosis, formation of a large area of devascularized sequestrum and generally is due to untreated or incorrect treatment of acute phase. On the basis of pathogenic mechanism and infections source osteomyelitis can be divided into three categories: a) microbial infection due to trauma, surgical operation or incorporation of prosthetic joint; b) infection with hematogenous spread, most frequent in vertebral and children; c) infection associated to vascular insufficiency as happens in diabetes mellitus and/or peripheric vascular disease. Despite infection of bone in average conditions is found to be quite rare, foreign materials implantation and bone damage like trauma or open fracture, can often lead to osteomyelits. The highest possibility of osteomyelitis includes patients suffering from diabetes, hepato-renal failure, immune suppression. It has been reported that infection rate is lowest after primary joint replacement (1%) to open fractures (23%). However, in acute infection, bacteria after entry and been phagocytosed, release toxic oxygen radicals and proteolytic enzymes which cause surrounding tissue lysis. Further, inflammation of surrounding blood vessels leads to increase

intraosseous pressure, making blood flow less effective in the infected area. Finally, the unvascolarized sequestrum is generated from necrotic bone tissue formation that can create a fistula which breaks through skin. Typical micro-organisms which are prevalent causative agents of the disease are *Staphilococcus aureous* followed by *Pseudomonas and Enterobacteriaceae, Salmonella, Clostridium and Pasteurella multocida*, while osteomyelitis involving diabetic foot is caused bypolymicrobial infections, finally osteomyelitis following implantation of prosthesis is prevalently caused by *Staphilococcus aureous* [10]. *Staphilococcus aureous* gets attached to the bone with help of expressed receptors (adhesins) for bone matrix components like fibronectin, lamin, collagen and bone sialoglycoprotein.

Conventional therapy of osteomyelitis includes surgical debridement, removal of implant and necrotic tissue, blood supply and soft tissue restoration, oral/systemic antibiotic administration. Surgical removal of sequestra and infected bone tissue involves additional surgery that can lead to more chances of infections with elevated medical costs and subsequent bone loss with general difficulty in healing. An alternative antibiotic therapy is the traditional therapy for the chronic osteomyelitis treatment. Systemic antibiotic therapy needs high doses to successfully eradicate bacteria, with subsequent rising of systemic toxicity and expensive hospitalization costs. Intravenous administration of glycopeptides drugs like vancomycin and drugs such as daptinomycin and teicoplanin demonstrated scarcity of bone penetration.

Despite several numbers of antibiotic exist, a good solution has not been yet found to treat this condition because of the poor vascularization that hinders antibiotics penetration facilitating rising-bacterial resistance. Moreover, traditional antibiotic therapy is sometimes unable to control infection because of the different antibiotics and host defences mechanisms such as slow metabolic rate, living in dormant state inside osteoblast and/or developing a biofilm. Bacteria pass from a planktonic phase into a sessile form with a high metabolic rate and rapid multiplication reducing their sensitivity to antibiotics by a factor 10^3 [11].

Oral therapy of osteomyelitis is done with fluoroquinone drugs. Ciprofloxacin, moxifloxacin, levofloxacin, clindamycin, metronidazole, fosfomycin and trimethoprim-sulphamethoxazole are the most common antibiotic used on this purpose, but therapy must be continued for 12-16 weeks at very high doses [12].

Local delivery of antibiotics has emerged as new therapeutic strategy to overcome the limitations and effectively manage osteomyelitis cases [13-15]. Local application justifies elevated antibiotics concentration in an avascular zone able to destroy the persistent infection originated from microrganisms residuals in biofilms [16]. In osteomyelitis therapy, local antibiotic delivery has many

advantages over parenteral and oral administration: antibiotic concentration is much higher and is maintained for a long time, keeping its concentration at minimum level, thus it can favor healing process, several studies demonstrate a decrease of adverse hypersensitivity reactions and shorter hospital stay with lower costs. One of the most severe drawback is a slow residual release of antibiotics for prolonged time enhancing risk of resistance. Local antibiotic delivery system could be non-biodegradable or biodegradable. The gold standard for treatment of infection associated with bone and soft tissue are antibiotic loaded carriers based on inert carrier such as cements or beads of polymethylmethacrylate (PMMA) impregnated with antibiotics able to release sustained high levels of antibiotic at local site [17]. Polymethylmethacrylate (PMMA) could be in form of beads chains impregnated with antibiotic frequently used for arthoplasties and muscoskeletal infections. Two types of PMMA beads are available in the market with different antibiotic dosages. They are uniform in size with about 7 mm diameter. However, poor antibiotic elution and drug stability at high temperature when PMMA beads are polymerized represents some limitations. Because of their stability at high temperature, aminoglycoside including streptomycin, gentamicin, amikacin, and tobramycin are the most used to impregnate PMMA beads. Moreover, PMMA can trigger some immune response and thus some cytotoxic effects, and a second surgical intervention is needed to remove them.

Other studies were carried out investigating elution kinetics, mechanical properties and antimicrobial effects of diverse antibiotics (impregnated to acrylic cements). Vancomycin, gentamicin, rifampicin and moxifloxamicin showed excellent results with sustained and high elution rates for the entire experimental time and keeping *in situ* antimicrobial effect. On the other hand, elution rate of etrapemen, meropenem and daptinomycin decreased after 4 days. The type and bioavailability of the antibiotics can influence drug elution, also depending on structural characteristics of bone grafts. As an alternative, biodegradable materials are mostly used by researchers. Biodegradation time must be correlated to infection status and amount of required reconstructed or repaired tissue. Antibiotic delivery results to be more effective using biodegradable systems, also because antibiotic delivery by PMMA beads is incomplete with persistent release of low amounts of antibiotics from the beads.

On the opposite, use of biodegradable carriers ensures a complete and effective delivery of antibiotics. Biodegradable devices can be divided in three categories:

1) Proteins such as collagen, gelatin, thrombin. Collagen materials are usually prepared from skin or tendon of animals and can provide sufficient stimulation for bone regeneration with osteoblast proliferation and increased mineralization. Collagen is found in all organs as an elemental part of connective tissue and it does not induce toxicity. Moreover, drug content and elution properties depend on system porosity. Recent studies of antibiotic loaded collagen sponges locally

administration associated with parenteral therapy show promising results for open fracture treatment [18].

2) Synthetic polymers like copolymer of polylactide and polyglicolide and polycaprolactone. They are highly compatible with several antibiotics, ampicillin, gentamicin and polymixin-B. These materials degrade very slowly at physiological pH and thus can provide sustained release of antibiotics. Moreover, drug elution kinetics from these synthetic polymers can be modulated by changing physical, biochemical and molecular structural properties of the polymer [19].
3) Bone graft materials and substitutes. Antibiotic can be added by directly mixing antibiotic powder to bone graft or soaking bone graft in an antibiotic solution. Calcium sulphate for its low immune-reaction, structural properties and easy reabsorption, was also used to manage chronic osteomyelitis. Application of tobramycin and vancomycin impregnated calcium sulphate was effective to reduce infection due to implantation of prosthesis, preventing also colonization of bacteria and subsequent biofilm formation.

Correct use of antibiotics is very important to reduce morbidity and mortality from osteomyelitis. My research has been focused on developing new local biodegradable drug delivery systems in order to increase drug concentration at infected tissue. Limited data are available on these new systems in animals and human osteomyelitis patients so more work and study is needed to improve solutions for treating osteomyelitis.

This work is a deep investigation on a biodegradable thermosetting hydrogel containing antibiotic such as gentamicin sulphate for improving the chronic osteomyelitis treatment.

Chitosan (CHS) plays an important role in bone regeneration and its adhesive nature and bacteriotatic property are very important when associated to osteomyelitis treatment [20]. B-glycerol phosphate (β-GP) is a catalyst to induce sol-gel transition of chitosan solution at physiological environment at 37°C and it also promotes bone regeneration. Moreover, recent researches addressed to formulation of composite biocompatible and biodegradable materials. For this reason, we propose an CHS-β-GP hydrogel combined with bovine bone granules (BBS) from Geislich Orthoss®, a natural bone substitute material made from the mineral part of bovine bone, in form of granules (1-2 mm). Orthoss® is available in micro-sized granules dimension.

REFERENCES:

[1] R.Lanza, R. Langer, J. Vacanti, Principles of tissue engineering. Academic press, 3 rd Ed., 2011, 54-58.

[2] V. Kumas, A.K. Abbas, N. Fousto, J. Aster, Tissue renewal, Regeneration, and Repair. Robbins and Cotran Pathologic basis of Disease, chapter 3, Eighth Ed, 2010

[3] Richardsson T.P., Peters M.C., Polymeric system for dual growth factor delivery. Nature Biotechnol, 19 (2001), 1029-1034

[4] N.J. Turner, S.F. Badylak, Biological scaffolds for muscolotendinous tissue repair, Eur Cell Mater. 25 (2013), 130-43.

[5] F.B. Basmanav, G.T. Kose, Hasirci V, Sequential growth factor delivery from complexed microspheres for bone tissue engineering. Biomaterials 29 (2008), 4195-4204

[6] M. Biondi, F. Ungaro, F.Quaglia, P.A.Netti, Controlled drug delivery in tissue regeneration. Adv Drug Deliv Rev. 60 (2008), 229-242.

[7] M.A Hupcey , S. Ekins, Improving the drug selection and development process for combination devices. Drug Discov Today. 12 (2007), 844-852

[8] Y. Tabata, Significance of release technology in tissue engineering. Drug Discov Today.,10 (2005), 1639-1646

[9] F.M Chen , M. Zhang , Z.F. Wu , Towards delivery of multiple growth factors in tissu engineering. Biomaterials, 31 (2010), 6279-6308

[10] W. Reizner, J.G. Hunter, N.T. O'Malley, R.D. Southgate, E.M. Schwarz, S.L. Kates, A systemic review of animal models for staphylococcus aureous osteomyelitis. Eur. Cell. Mater 27 (2014), 192-212

[11] H. Winkler, P. Haiden, Treatment of chronic bone infection. Oper. Tec. Orthop, 26 (2016), 2-11

[12] S.K Nandi, S. Bandyopadhyay, P. Das, I. Samanta, P. Mukherjee, S. Roy, B. Kundu, Understanding osteomyelitis and its treatment through local drug delivery system. Biotechnol Adv., 28 (2016), 30113-30116

[13] Ribeiro M., F.J. Monteiro , M.P. Ferraz , Infection of orthopedic implants with emphasis on bacterial adhesion process and techniques used in studying bacterial-material interactions. Biomatter, 2 (2012), 176-194

[14] H. Lu , Y. Liu , J. Guo , H. Wu , J. Wang , G. Wu , Biomaterials with abtibacterial and osteoinductive properties to repair infected bone defects. Int J Mol Sci, 17 (2016), 334

[15] A.E. Eltorai, J. Haglin, S. Perera, B.A. Brea , R. Ruttiman, D.R. Garcia, C.T. Born , A.H. Daniels, Antimicrobial technology in orthopedic and spinal implants. World J Orthop., 7 (2016), 361-369

[16] Meital, Z., Antibiotic-eluting medical devices for various applications. Journal of controlled release, 2008. 130.

[17] H. van de Belt , D. Neut , W. Schenk , J.R. van Horn , H.C. van der Mei , H.J. Busscher, Infection of orthopedic implants and the use of antibiotic -loaded bone cements. Acta Orthop Scand, 72 (2001), 557-571

[18] H. Knaepler, Local application of gentamicin-containing collagen implant in the prophylaxis and treatment of surgical site infection in orthopaedic surgery. Int J Surg. 10 (2012)

[19] M. Aviv, I. Berdicevsky, M. Zilberman, Gentamicin-loaded bioresorbable films for prevention of bacterial infections associated with orthopedic implants. J Biomed Mater Res A, 83 (2007), 10-19

[20] M.Kong, X.G. Cheng, K. King and H.J. Park,, Antimicrobial properties of chitosan and mode of action: a state of the art. Int. J. Food Microbiol., 144 (2010), 51-63

Outlines

SECTION II

OUTLINES

The research work carried out during my PhD aimed to develop a combination device at the interface of pharmaceutical and medical devices research and consisting in two components, i.e. a polymer device to support tissue regeneration, and a drug or a drug delivery system incorporated in the polymeric matrix to handle infections. In orthopedics, due to numerous surgical procedures involving invasive implant materials, infections have a huge impact in morbidity, mortality and medical costs. For this reason, it is important to devolp therapeutic strategies starting from a clear view of anatomic bone structure, pathogenesis and epidemiology of bone infection, with a special attention to alarming phenomenon of antibiotic resistance.

To reach this goal was preliminary designed a bone grafting based on inorganic bone components (bovine bone granules) combined with the chitosan polymeric solution (chapter I) that could be injectable or moldable system for minimally invasive or invasive chirurgical procedure, respectively as the surgen prefers according to the site of applications.

Morover, the bone grafting could be a drug delivery system followed by the addition of an antibiotic such as gentamicin-free (chapter II) and/or micro-nano encapsulated (Chapter III, IV, V and VI). The complete system could present several advantages respect the conventional therapy (oral or intravenous administration): could be biodegradable, biomimetic and should be able to directly release the antibiotics into bone defects for local drugs delivery system. In addition, the possibility to control the incorporation of several antibiotics and their amounts permits to obtain the desired profile: high local release rate in order to reduce the risk of infection of bacteria introduced during the implantation procedure, followed by prolonged release of antibiotics at effective level (over than *minimum inhibitory concentration,* MIC) for inhibiting the persistent infections.

The experimental section (section III) of my thesis is divided in 6 chapters, organized according with defined aims, the nature of the experiments performed and the results obtained. Level of complexity of the problem being studied and assays used to characterize the developed systems were the main parameters taken into account in the organization and sequence of those chapters. Chapters division corresponds related papers published in international journals which are identified in the front page of each chapter, or to be submitted for publication. Therefore, each thesis chapter is presented in an adapted version of the published or ready to be submitted manuscript style, keeping its contents, but intended to have a consistent structure between the various thesis chapters.

The first chapter reports the development of an injectable *in situ* forming composite scaffolds (ISFcG) based on bovine bone substitute granules (BBS, Orthoss®) and biodegradable and biocompatible

thermogelling polymeric solution (chitosan), in order to combine in the same system the advantages of natural bone graft substitutes and polymer. For minimal invasive surgical procedures, the liquid suspension of BBS into the hydrogel show a feasibility as fiiling because of its ability to undergo *in situ* gelation at 37°C, upon injection. For invasive procedures, IsFcG could be lyophilized obtaining a moldable composite scaffold (mCS), a 3D highly porous spongy structure, unchanging hydrogel physical structure. The moldable scaffold resulted to be easy to manipulate from surgeons after rapid rehydratation.

The second chapter presents a moldable composite scaffold (mCS) containing gentamicin sulphate. The antibiotic is reported in literature to be the most common antibiotic used because of a broad antibacterial spectrum with a greatest duration of antibacterial activity against all more common bacteria involved in osteomyelitis (*Staphylococcus aureous, Pseudomonas aeruginosa and Escherichia coli*). Quickly antibiotic release from mCS permits to release all the drug directly to the infected site in order to immediately destroy bacteria growth and consequently bacteria biofilm formation. On the contrary, if drug release is delayed, the infection may set further and then is more complicated to deal with it.

Third chapter is focused on e development of polylactide-co-glycolide–PEG microparticles for gentamicin prolonged release in order to treat latent infections which typically occur in the first months post surgery, or biofilm. The gentamicin loaded microparticles show several advantages over conventional antibiotic administration and/or gentamicin powder mixing with hydrogel: ability to deliver the drug to a specific site, gentamicin activity preservation reducing its lysosomes accumulation and achieving gentamicin prolonged release, minimizing dosing regimens and reducing systemic toxicity and macrophages phagocytosis due to their stealth behavior.

In the fourth chapter gentamicin loaded microparticles (Mps) are embedded into the 3D moldable composite scaffold (3D-DDs) without any change in the micro-architecture and physical-mechanical properties with respect to placebo mCS without Mps. Prolonged release of gentamicin loaded into MPs embedded into the mCS is achieved. The polymeric component of MPs was susceptible to degradation during the *in vitr*o incubation in simulated physiological conditions (PBS pH 7.4, 37 C). MPs *in vitro* degradation rate was slower when they were embedded into the chitosan matrix, showing that chitosan has a protective effect on PLGA hydrolisis.

Fifth chapter is focused on gentamicin encapsulation in PLGA-PEG/PLGA-H nanoparticles. The aim is to improve gentamicin activity, also on the basis of what is reported in the literature. Few data in the literature suggest that nanoparticulate (Nps) approach could enhance gentamicin antimicrobial on biofilm. From the pharmaceutical stand point, the chapter represents a significant contribution to

overcome limitations in obtaining high encapsulation efficiency with small molecules, like gentamicin sulphate into PLGA-PEG and PLGA-H nanoparticles, with focus on solid/oil/water emulsion. On this purpose a Design of Experiment (DoE) deep evaluation has been performed.

Sixth chapter presents the project that I carried out abroad in the laboratories of 3B's Research Group, Biomaterials, Biodegradable and Biomimetic in Portugal. The main research is to study and develop a strategy to functionalize the surface of natural based eumelanin nanoparticles extract from the *Officinalis Sepia* by dopamine sel-assembly. Eumelanin nanoparticles coated with polydopamine can be further evaluated as gentamicin sulphate local drug delivery system.

In this thesis final section, section IV, overall conclusions obtained from collection of the research works are presented and discussed in global view together with future perspectives and future research activity.

SECTION II

Experimental Section

SECTION III

Chapter I

CHAPTER I

IN VITRO CHARACTERIZATION OF AN INJECTABLE *IN SITU* FORMING COMPOSITE SYSTEM FOR BONE RECONSTRUCTION

ABSTRACT

Injectable *in situ* forming composite scaffolds (ISFcG) have been prepared combining bovine bone substitute granules with a biodegradable and biocompatible thermogelling polymeric solution (chitosan). The presence of the organic component affects both physico-chemical features of ISFcG, as porosity, interconnectivity, mechanical properties and biofunctionality. The high water retention ability and the hydrophilic nature of the ISFcG polymer matrix promote the attachment and the infiltration of cells into the matrix and their growth. The polymeric component of ISFcG was susceptible to degradation during the *in vitro* incubation in simulated physiological conditions (DMEM pH 7.4, 37°C). The degradation products did not present remarkable toxicity level, as the MTT data resulted to be constant. The stability study showed an excellent *in vitro* physical stability even after mechanical stress. These features make the ISFcG based on chitosan and bovine bone substitute granules an excellent injectable composite scaffold for bone tissue regeneration.

Keywords: composite scaffold; tissue regeneration; cell adhesion; biodegradation; mechanical properties; gentamicin

This chapter is based on the following publication:

Polymer Degradation and Stability 119 (2015) 151 e 158 Elsevier.

R.Dorati, C. Colonna, I. Genta, A. De Trizio, T. Modena, H. Kloss, B. Conti

1. INTRODUCTION

Injectable bone substitutes (IBSs) are used in several clinical conditions, as osteoporotic and osteoarthritis fractures [1], congenital deformity corrections, tumor resection and reconstruction [2], generic infections [3], pathological degenerative bone destruction, and other degenerative diseases [4], [5].

In situ forming composite gel (ISFcG) present many advantages; first, the system consists in a suspension of solid material into a suitable liquid vehicle easily be injected and placed into complex defect sites or cavities. Moreover, the application of the ISFcG requires a cannula minimizing the procedure invasivity with respect to other surgical techniques [6 - 8].

In addition to these advantages, the ISFcG shows many other challenges. They present good physical properties maintaining the physical integrity when are subjected to extensive manipulation and they show excellent handling features and good operative flexibility [9].

The composite systems can be considered an ideal option because they combine the advantages of multiple materials as polymer and natural bone graft minimizing the drawbacks of these components. The polymers have lower hardness an insufficient compressive modulus with respect to the natural bone tissue, while the natural bone substitute material and ceramics fail mechanically presenting high elastic modulus and low ductility [10].

This research project implement an inter- and multi-disciplinary research area focused on the design and development of IBSs intended for bone tissue regeneration. The main goal of the research was to develop an ISFcG combining a thermogelling polymer solution based on a natural polymer (chitosan), with bovine bone substitute granules (Orthoss® granules). Orthoss® is a natural bone graft substitute, its inorganic bone matrix has the macro- and micro-structure similar to human spongeous bone, interconnecting pore structure and high inner surface area. Moreover, it presents excellent osteoconductive properties. The ISFcG was designed and developed as alternative to the solid-preformed block or granules shape which can be exclusively used in invasive procedures. The formulation obtained combining the polymer solution with the bovine bone substitute granules presents all the advantages of the IBS: ready-to-use, designed for minimally invasive surgical procedures, easy to be placed into an irregular surgical site reducing the spreading of granules in the tissues near the surgical area, good physical properties maintaining its physical integrity when subjected to extensive manipulation and excellent handling characteristic. Moreover, the designed ISFcG can be used for the controlled local release of therapeutic and active agents, as growth factor and antibiotics.

2. MATERIALS

Orthoss spongious granules were supplied by Geistlich Surgery (Geistlich Pharma AG, Wolhusen Switzerland), with size and size distribution of d_{10} (141.44 μm), d_{50} (721.03 μm) and d_{90} (1340.25 μm) and Span value 1.66. Chitosan chloride (CL213, Protosan CL213, deacetylation degree 82%, hydrochloric acid content 10-20%) was purchased from Pronova Biomedical, Norway. Glycerol 2-phosphate disodium salt hydrate was purchased from Sigma Aldrich, Milan (Italy). Human adult dermal fibroblasts as primary cells were purchased from International PBI, Milan (Italy). The water used in the preparation of thermogelling polymeric solutions was distilled and filtered through 0.22 μm membrane filters (Millipore Corporation, Massachusset, USA). Unless specified, all other solvents and reagents were of analytical grade. Whole human blood was provided by I.R.R.C.S. Policlinico S.Matteo Pavia, Italy.

3. METHODS

3.1 Preparation of thermogelling polymer solution

The thermogelling polymer solution based on chitosan and glycerol phosphate disodium salt (β-GP) was used as vehicle for the *in situ* injection of bovine bone spongious granules [8]. Briefly, chitosan was dissolved in sterile water at 2% w/v under magnetical stirring. Chitosan solutions were sterilized by high pressure saturated steam at 121°C for 15 min (Autoclave Vapor Matic 770, Milan, Italy) following the conditions reported in Eu. Pharm. β-GP was dissolved in sterile water (10% w/v) under magnetical stirring and sterile filtered before use (Filter 0.22 μm, Whatman®). The prepared chitosan and β-GP solutions were cooled down to 4°C in an ice bath. To form hydrogels, β-GP solutions (172.4 μL) were dropped into chitosan solutions (827.6 μl) and were mixed in an ice bath for about 1 h.

3.2 Characterization of sterilized thermogelling polymer solution

3.2.1 Effect of autoclave sterilization on chitosan Mw

Chitosan solution (2% w/v) and the selected thermogelling polymer solution were sterilized in autoclave for 15 minutes, at 121°C and 2 atm following the Eu Pharmacopoeia (Eu. Pharmacopoeia 7.0, 5.1.1. Methods of preparation of sterile products). The molecular weight was measured by GPC using monodisperse polysaccharide standards (Mw 180–708 KDa) and 2M $NaNO_3$ and 0.01M NaH_2PO_4 as the eluent, at a flow rate of 1 mL/min. The GPC apparatus consisted of a guard column (PL aquagel-OH Guard 8 μm, 50 x 7.5 mm, Agilent, Milan, Italy) and two PLaquagel-OH MIXED-H 8 μm columns connected in series (300×7.5 mm), a pump (Varian 9010, Milan, Italy), a Prostar 355 RI detector (Varian Milan, Italy), and software for computing Mw distribution (Galaxie Ws, ver. 1.8 Single-Instrument,

Varian Milan, Italy). Samples were dissolved in acetic acid 0.1 M at a concentration of 0.5-1 mg/mL, the solution were filtered through a 0.45 µm filter (Millipore, Massachusset, USA) before injection into the GPC system.

3.2.2 Rheological characterization of the selected thermogelling polymeric solution

The rheology of the selected thermogelling polymeric solutions was studied by means of a rotational rheometer (Rheostress 600, Haake, Spinea, I). A cone plate combination 35/1° Ti L was used as the measuring system. All measurements were carried out at 4°C storage temperature, 25°C reconstitution temperature and 37°C as body temperature, after a rest time of 3 min. The apparent viscosity was measured by increasing shear rate values in the range 10–300 s^{-1}.

The oscillatory measurements were performed by Haake^{TM} Mars III rotational Rheometer. The elastic modulus (G′) and the viscous modulus (G′′) were evaluated as function of the temperature at a frequency of 1 Hz. The temperature was modified at the rate of 2°C/min. A temperature sweep was used to study the thermal behavior of selected thermogelling polymer at physiological conditions, while a time sweep at a constant shear frequency (1 Hz) in the linear viscoelastic region (LVR) was performed to monitor the *in situ* gelation behavior of the thermogelling polymer solution, allowing the monitoring of the evaluation of elastic stored modulus, *G*′, and the viscous loss modulus, *G′′*, with time.

3.3 Preparation of *in situ* forming composite gel (ISFcG)

Different amounts of bovine bone spongious granules (150, 200 and 300 mg) were placed in 6-well culture plates and the thermogelling solution (1 ml) was added. The granules were homogeneously incorporated into the polymeric solutions till they were completely embedded into thermogelling polymeric solutions, the addition of the granules was performed at room temperature using a mild stirring to facilitate the distribution of the granules in the polymer solution avoiding precipitation phenomena [8]. All the procedures were performed in aseptic conditions.

To optimize the bovine spongious granules/thermogelling solution (w/v) ratio, a short-term culture study was performed on *in situ* forming composite samples. Briefly, samples were fixed in 6-well culture plates and conditioned by 8 ml of DMEM supplemented with 10% FBS for 4 h. After conditioning, $2 \cdot 10^5$ cells were seeded onto each ISFcG and incubated at 37°C and 5% CO_2 for 3 h and 3 days to assess their cell seeding capacity and short term cell growth, respectively. The thermogelling polymer solution was considered as blank. Fibroblasts were chosen as the model cells. After scheduled times, samples were collected and the cell mitochondrial activity was monitored by a slightly modified

MTT assay, based on a spectrophotometric technique [11]. The absorbance was measured at 570 nm with 655 nm as reference wavelength. The average of five samples was determined.

3.4 Characterization of *in situ* forming composite gel

3.4.1 Porosity and compressive strength

The porosity of the composite scaffolds was measured by a modified liquid displacement method [8, 12]. The porosity values were determined on five samples and expressed as mean±standard deviation. The compressive strength was measured with an electromagnetic testing machine (Enduratec Elf 3200, Bose Corporation, Eden Prairie, MN, USA) following the protocol previously optimized [12].

3.4.2 In vitro swelling and degradation studies

The *in vitro* swelling behavior of the scaffolds was investigated using three different solutions at specific pHs: buffer solution A (pH 6), buffer solution B (pH 8), and human blood (using human plasma as control, pH 7.35-7.45). The swelling behavior was quantified by measuring the change in the sample diameter as a function of incubation time in the medium. The experiment was performed in triplicate. Briefly, pure chitosan scaffolds and ISFcG were weighted (W_d) and incubated in 7 ml of DMEM supplemented with 10% v/v FBS, at 37°C for 24h, blotted with filter paper and re-weighted (W_w) to calculate the water uptake. Water retention capability was estimated after centrifugation at 500 rpm for 3 min, W'_w. The water absorption (Wa) and water retention (Wr) was calculated using Eqs, respectively:

$$Wa\ (\%) = \frac{Ww - Wd}{Wd} X\ 100 \qquad \text{Eq.1}$$

$$Wr\ (\%) = \frac{W'w - Wd}{Wd}\ X\ 100 \qquad \text{Eq.2}$$

The *in vitro* biodegradation properties of the scaffolds were studied as follows: briefly, the samples were incubated in physiological simulated conditions, in DMEM supplemented with 10% v/v FBS, at 37°C for 28 days. The incubation buffer was withdrawn from each test tube, collected and replaced with fresh buffer at regular intervals (twice a week). At scheduled times (3, 7, 10, 14, 21 and 28 days) samples were recovered, washed with distilled water and lyophilized (Lio 5P, Cinquepascal s.r.l., Milan, Italy) at about -50°C, for 24 h. The degradation performances were followed by monitoring the weight loss (WL) and the variations of polymer weight-average molecular weight (Mw) and number average molecular weight (Mn).

The weight loss (WL) of prototypes was determined gravimetrically (Mettler Toledo AG 245, Milan, Italy) using an optimized protocol [12], while the Mw and Mn were determined by GPC (section 3.2.1). The data are expressed as average of five parallel samples.

3.4.3 Syringeability test

The syringeability study was performed with a perfurmus^{TM} III (EFD Fluid Dispensing) which is a fluid dispensing equipment that can be used to dispense fluids. The system is equipped with fully electronic control of dispense time, air pressure and vacuum to ensure exceptionally high accuracy and repeatability.

Briefly, bovine bone granules (1 g) were mixed with thermogelling polymer solution (5 ml) and placed into a 10 ml syringe with a diameter of 19.1 mm and an opening of 5.5 mm. The filled syringe was connected to the air tube and 0.52 bar was applied to extrude the polymer thermogelling solution (gel) and ISFcG from the syringe at a crosshead speed of 15mm/min. Syringeability was determined from the ratio between the mass extruded from syringe and the original mass of the sample inside the syringe. Five specimens were tested for each formulation.

3.5 Biological studies

3.5.1 Cell cultures

Adult dermal fibroblasts, as primary cells were purchased from International PBI (Milan, Italy). The cells were cultured in DMEM containing 10% FBS and 1% antibiotic solution (100U/ml penicillin, 100 ug/ml streptomycin). After expansion, the cells were detached for the biological experiments. A cell seeding of 2 10^5 cells/scaffold was used for all 3D scaffolds.

3.5.2 Cell seeding capacity and long-term culture study

To assess the cell behavior during the long-term culture study, ISFcGs were fixed in 6-well culture plates and conditioned by 8 ml of DMEM supplemented with 10% FBS for 4 h. After conditioning, $2 \cdot 10^5$ cells were seeded onto each ISFcG and incubated at 37°C and 5% CO_2 for 3 h and 28 days to assess their cell seeding capacity and long term cell growth, respectively. At scheduled times (0.125, 3, 7, 14, 21 and 28 days), samples were collected and the cell mitochondrial activity was determined by a slightly modified MTT assay, based on a spectrophotometric technique [13, 8].

3.6 Statistical analysis

For all the experiments, including cell culture studies, a minimum of five samples were used. The results are expressed as the mean value of at least five replicates ± standard deviation (SD). Statistical analysis was carried out using a one-way analysis of variance with 95% confidence intervals. The error bars denote ± SD ($n \geq 5$).

4. RESULTS AND DISCUSSION

4.1 Preparation of thermogelling polymer solution

The thermogelling polymer solution was stable after sol-gel transition at 37°C presenting a rapid gelification kinetic, < 15 minutes. For our project purpose, a quite fast sol-gel transition phase is required in order to maintain the bovine bone granules entrapped into the polymer matrix and to create a simultaneous intimate contact with the surrounding tissues.

4.2 Characterization of thermogelling polymer solution

4.2.1 Effect of autoclave sterilization on chitosan Mw

The effect of the autoclave sterilization was evaluated measuring the Mw of chitosan polymer. The study was performed on the chitosan powder, chitosan solution (2% w/v) and on thermogelling polymer solution. The Mw of not-autoclaved chitosan (powder) was used as control.

The GPC results demonstrated that the autoclaving cycle affected chitosan polymer Mw with a percentage reduction of 20-30%. The chitosan powder showed a much higher variation (28.5%±1.42) with respect to polymer in the liquid state, namely chitosan solution and thermogelling polymer solution (21.99%±1.1 and 23.63%±1.2, respectively).

4.2.2 Rheological characterization of the selected thermogelling polymer solution

Figure 1 shows the viscosity curve of sterile thermogelling polymer solution at different temperatures, namely 4°C (as storage temperature), 22°C (as reconstitution temperature) and 37°C (as injection site temperature). The strong difference in the viscosity values obtained by the thermogelling polymer solution at the considered temperatures revealed that the liquid solution turned into a solid-like gel. An expanded y scale was used to evaluate the viscosity values at 4°C and 22°C which resulted to be negligible respect to the solution at 37°C (insert of **Figure 1**).

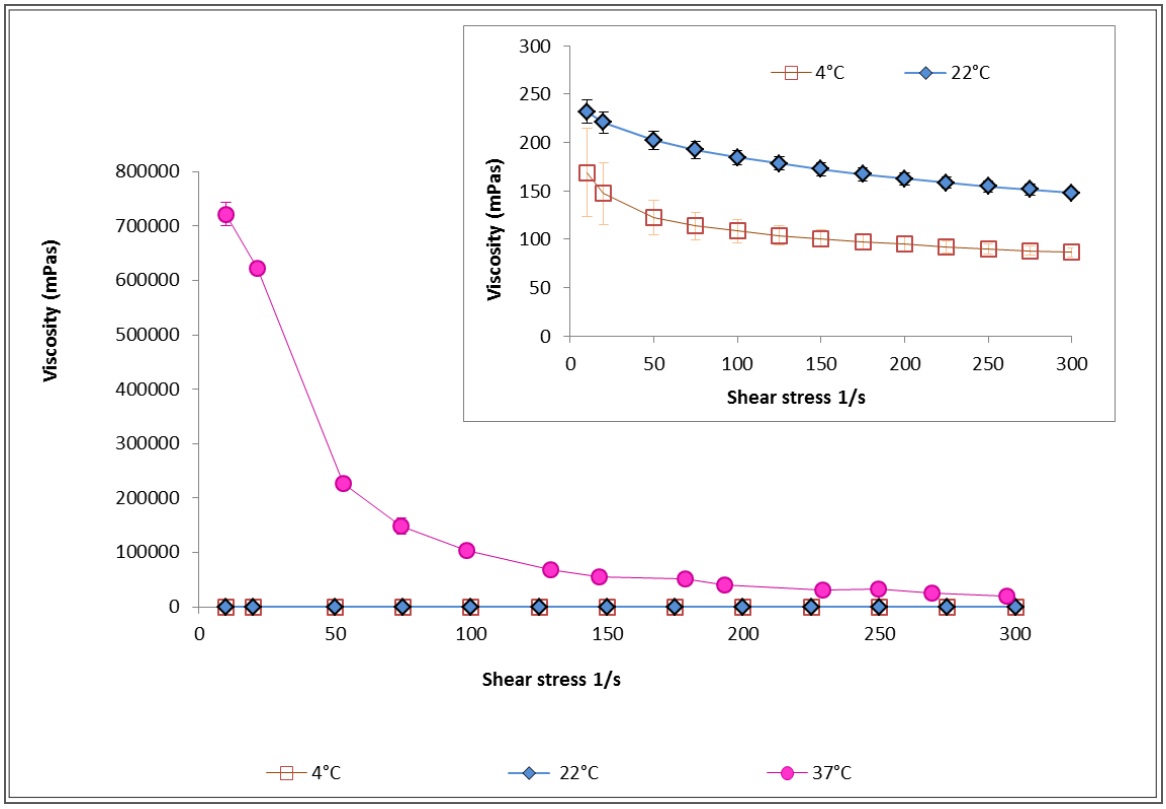

Figure 1: Viscosity curves of sterile thermogelling polymer solution (gel) at different temperatures: namely, 4°C (as storage temperature), 22°C (as reconstitution site temperature) and 37°C (as injection site temperature). **Insert:** Graph with an expended y scale (0-300 mPas).

The thermogelling solutions at the three temperatures presented similar viscosity profiles: they all showed a pseudoplastic behavior and it was more pronounced at 37°C than at lower temperatures. Considering the low viscosity values detected at 4° and 22°C and the revealed pseudoplastic behavior, which determines the change in viscosity in response to force application, the administration of the thermogelling polymer solution by injection through a needle/cannula into the bone defect could cause the transition of the formulation to a system that flows as a liquid. In these conditions, the liquid should easily spread into the bone defect.

The elastic modulus (G') and the viscous modulus (G''), as function of the temperature, were determined from oscillating measurements at a frequency of 1 Hz. **Figure 2** shows the sol-gel transition of thermogelling polymer solution at physiological pH (pH 7.4) during a heating-cooling cycle between 5 and 70°C, at 1°C/min rate.

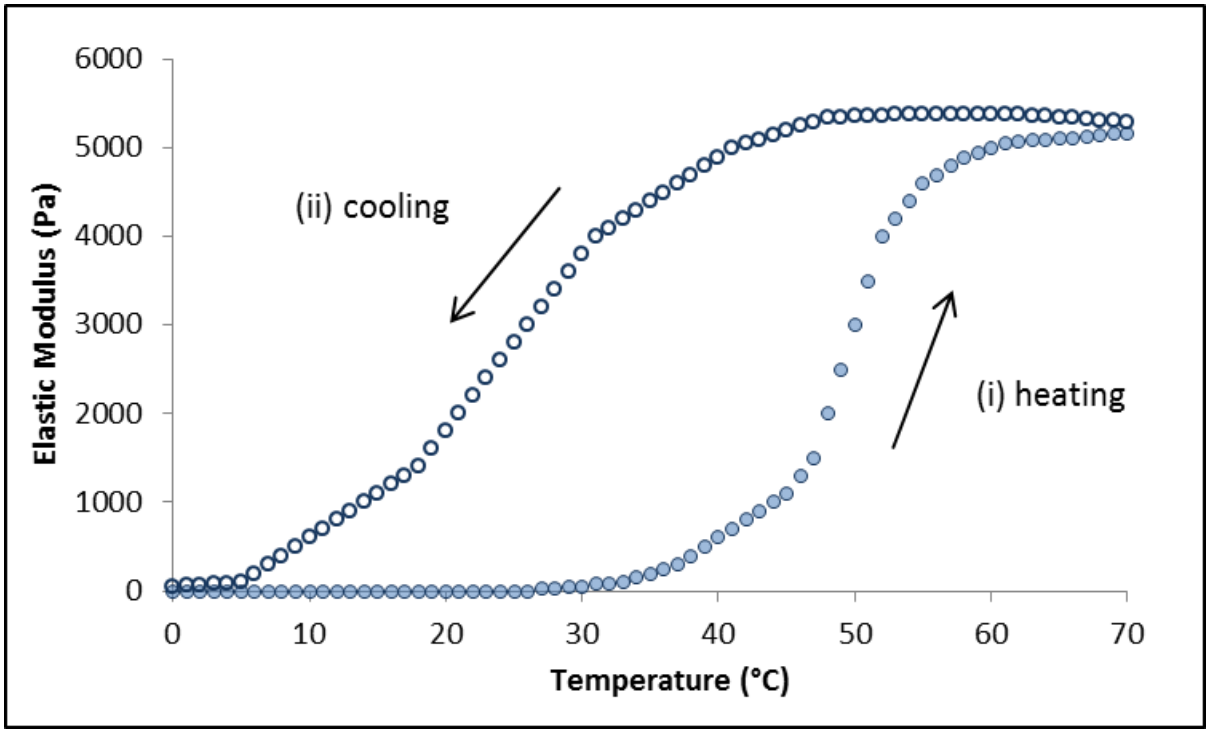

Figure 2: Sol-gel transition of thermogelling polymer solution (gel) at physiological pH (pH 7.4) during a heating-cooling cycle between 0 and 70°C, at 2°C/min.

The sharp rise of the elastic modulus upon heating (curve i), clearly indicates that the liquid solution turned into a solid-like gel at about 37°C, while the decrease of the elastic modulus upon cooling (curve ii) reveals the tendency of the gel to return to the liquid state. The temperature of incipient gelation was found to be between 35 and 40 °C.

4.3 Preparation of *in situ* forming composite gel

The *in situ* forming composite gels (ISFcG) were prepared combining the thermogelling polymer solution with bovine bone granules. Three different amounts of bovine bone granules were incorporated with thermogelling polymer solution (1 ml). To optimize the bovine bone granules/thermogelling polymer solution ratio a short-term culture study was performed using fibroblasts as model cells.

Results reported in **Figure 3** showed that ISFcG with 200 and 300 mg of bovine bone granules presented higher viability values with respect to pure chitosan scaffolds (gel), this evidence could be attributed to the higher stiffness and solidity of samples with bone granules which promote the proliferation of cells that normally grow in adhesion, such as fibroblasts, osteoblasts and chondrocytes. The best performances in cell seeding and growth were observed for ISFcG prepared combining the thermogelling polymer solution with 200 and 300 mg of bovine bone granules, indeed, the viability

was improved up to 50 and 75% ($p < 0.05$). The granules/thermogelling polymer solution ratio selected for the development of the ISFcG was 200 mg per 1 ml of thermogelling polymer solution because of the high physical stability of the ISFcG during the incubation time. Addition of 300 mg of bovine bone granules led to a more soft and fragile texture of the system with partial release granules into the culture medium.

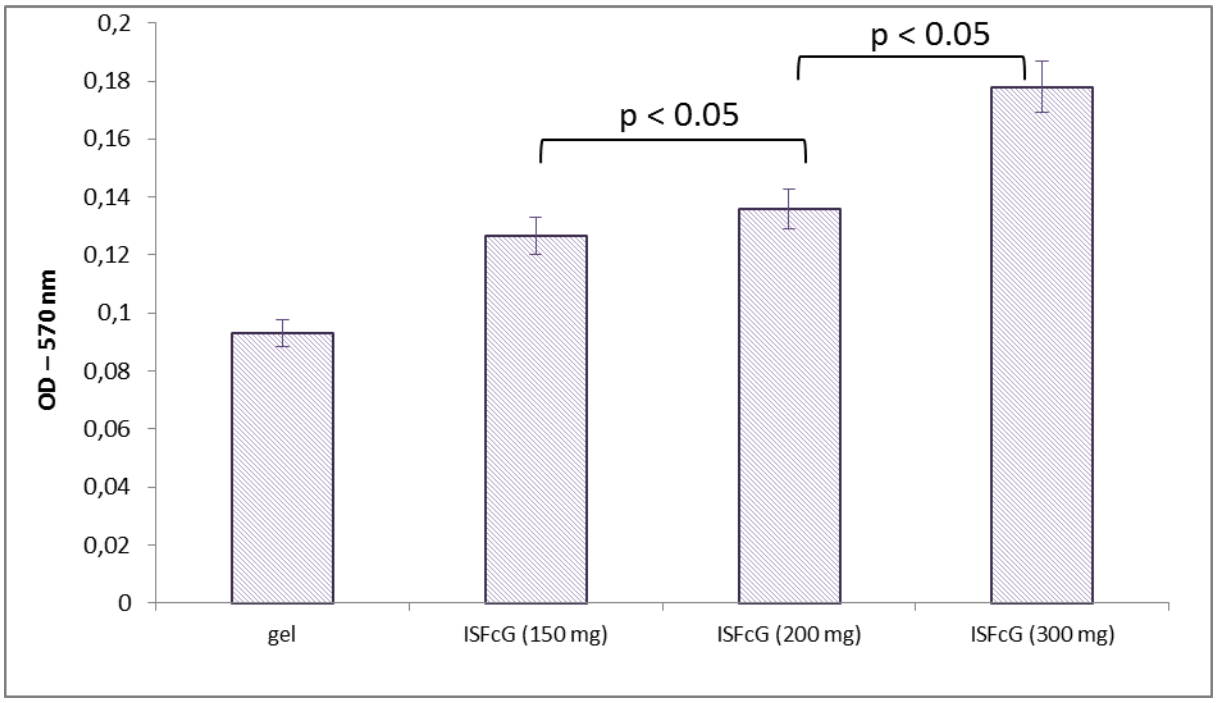

Figure 3: *In vitro* biological study (short-term) performed with fibroblasts seeded into pure chitosan scaffold (gel) and ISFcGs prepared combining thermogelling polymer solution with different amount of bovine bone granules: 150, 200 and 300 mg. The values are means ± SD (n=5). Time of culturing: 3 days.

4.4 Characterization of *in situ* forming composite gel

4.4.1 Porosity and mechanical properties

The porosity values of pure chitosan scaffold (gel) and ISFcG are summarized in **Table 1**, they result to be appropriate for bone tissue regeneration. The scaffolds have good porosity ranging between 89-91%, and the addition of the bovine bone granules did not negatively affect the porosity of ISFcG. The compressive strength of pure chitosan scaffold (gel) and ISFcG were measured using an electromagnetic testing machine, and results collected in **Table 1**. The compressive strength of ISFcG was found to be improved by 3 times in relation to pure chitosan scaffold (gel).

Table 1: Summary of physical and mechanical properties of pure chitosan scaffold (gel) and ISFcG

Scaffold/properties	Pure chitosan scaffold (gel)	ISFcG
Porosity (%)	91±3	89±6
Water uptake/water retention	306.43/176.61	253.96/163.14
Syringeability (%)	85±3	70±5
Cell seeding capacity (%)	35±2	50±5
Compressive strength (GPa)	0.036±0.08	0.096±0.6

4.4.2 In vitro swelling and degradation studies

The environmental pH could affect the gelification behavior as the chemical interactions among the thermogelling polymer solution components are strongly dependent on pH values. Shift of pH can promote the destabilization of ISFcG and eventually its failure. In **Figure 4** are plotted the shape retention data expressed as scaffold diameter as a function of incubation time in buffers at pH 6, 7.4, 8 and in complete blood at pH 7.4.

The ISFcG diameter was increased by ~ 19% within 2h, at a later stage the samples retained their size and shape in all tested solutions suggesting that the ISFcG were stable in the buffers at the different pHs and in complete blood. It was observed that the scaffold was able to uptake high amounts of water (water uptake, w_u) and more than 50% of the adsorbed water was maintained even after centrifugation (water retention, w_r), **Table 1**. The water uptake is favorable for the nutrients and oxygen exchanges, while the water retention should promote the cell adhesion. Moreover, the hydrophilic features of the ISFcG are expected to enhance both the cell attachment and the proliferation of cells during the regeneration of the new tissue [14].

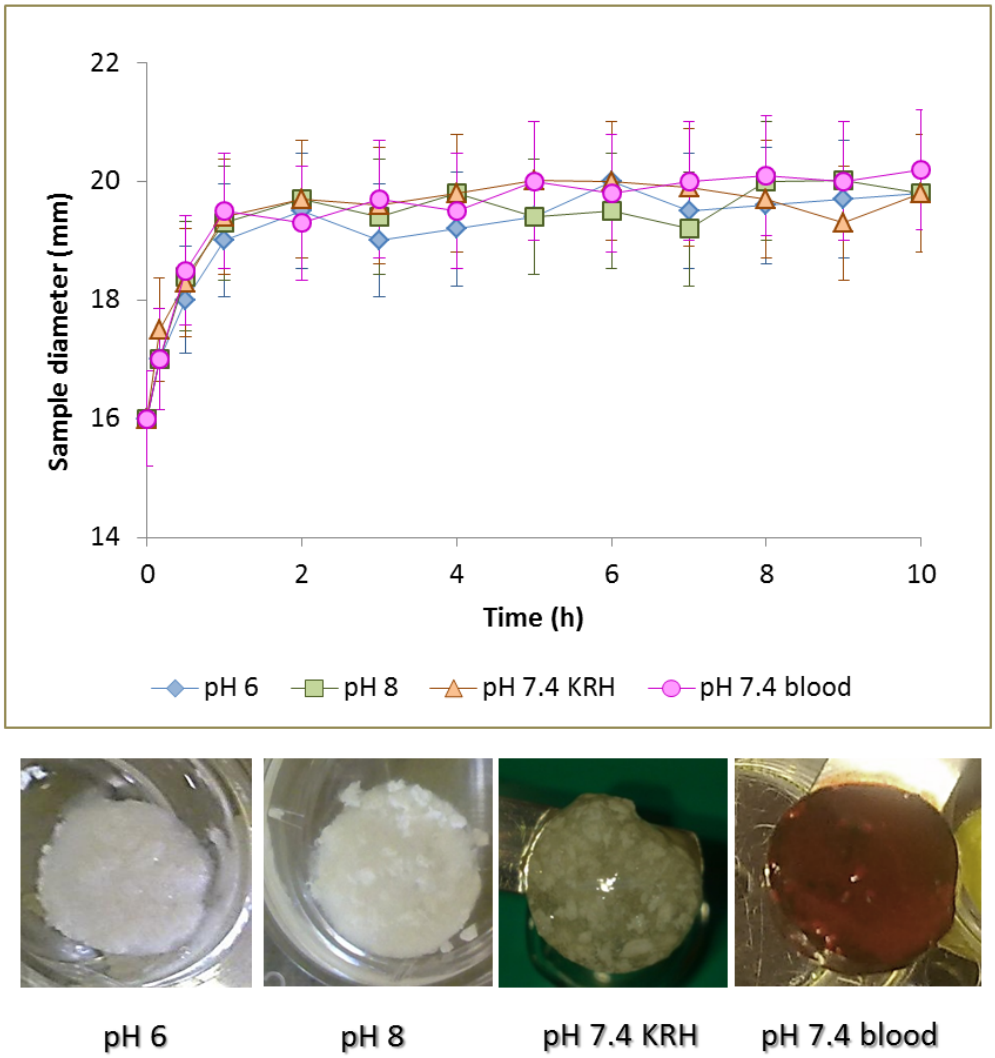

pH 6 pH 8 pH 7.4 KRH pH 7.4 blood

Figure 4: Diameter variation of pure chitosan scaffold (gel) and ISFcG as function of incubation time in media at different pHs. The values are means ± SD (n=5). Below, digital photographs of ISFcG after incubation in buffer pH 6, 8, 7.4 and in complete blood at pH 7.4.

Biodegradable scaffolds are expected to degrade through hydrolytic reactions; the degradation rate should be *in sync* with the regeneration rate of new tissue.

The chitosan degradation process is known to be a complex phenomenon. **Figure 5a** shows the mass changes of pure chitosan scaffolds (gel) and ISFcG, monitored during the *in vitro* degradation study.

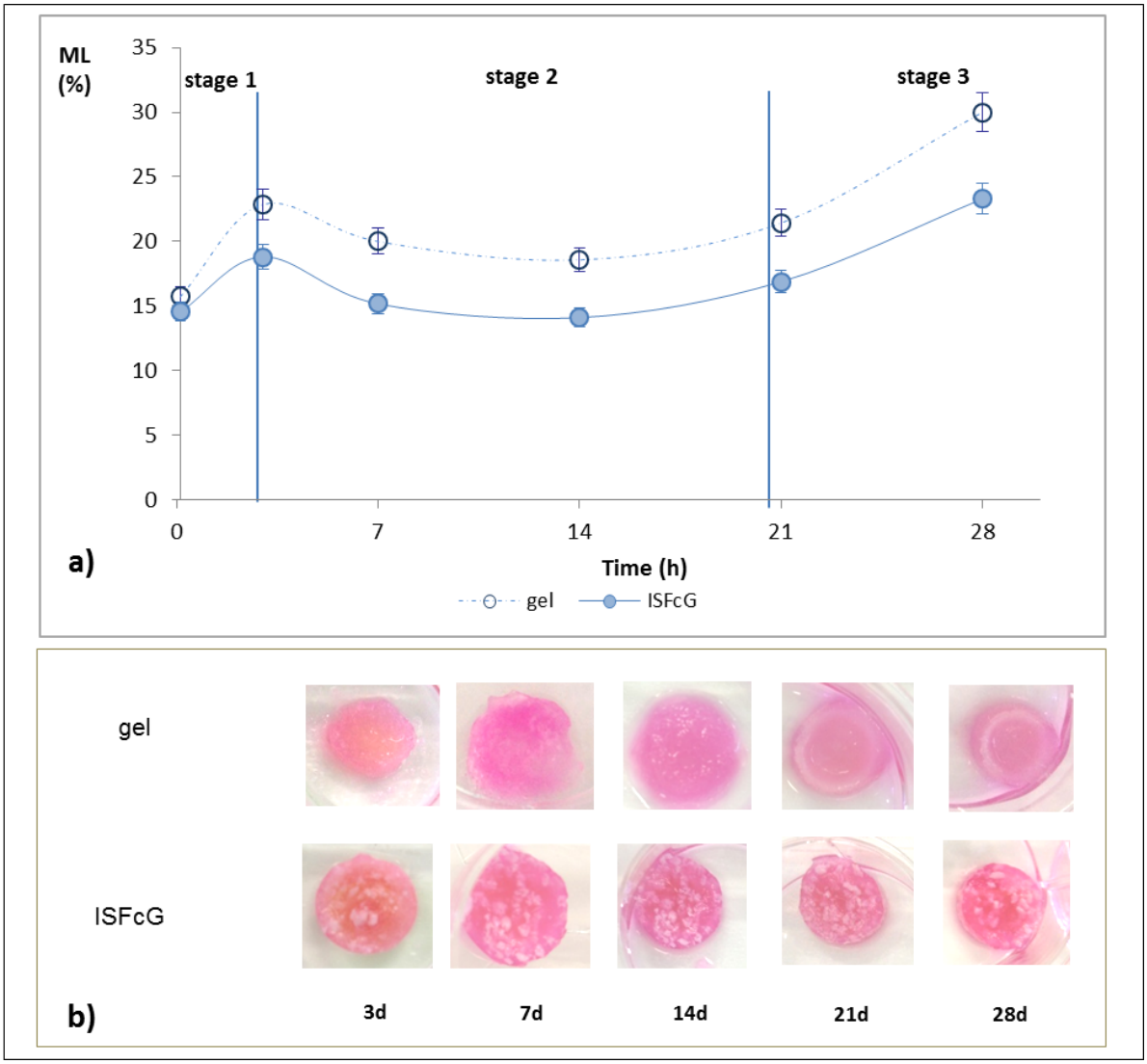

Figure 5: a) Mass loss (%) of pure chitosan scaffold (gel) and ISFcG as function of incubation time in DMEM supplemented with 10% v/v FBS, pH 7.4 at 37°C.The values are means ± SD (n=5). **b)** Digital photographs of gel and ISFcG after incubation.

The weight loss curves indicate that pure chitosan scaffold (gel) and ISFcG presents similar degradation trend throughout the degradation process, nevertheless rate of ML was higher for the pure chitosan scaffold (gel) than for ISFcG **(Figure 5a**). The results demonstrated a sensible mass loss percentage (~ 15%) after 3h, further mass loss was detected after 21 days. At day 28 the mass loss values of pure chitosan scaffold (gel) and ISFcG were maintained around 23-30%. The digital photographs of scaffolds (**Figure 5b**) after incubation in DMEM demonstrated the stability of both pure chitosan scaffold and ISFcG under physiological conditions, even after prolonged incubation (28 days).

The mass loss values were attributed to few concomitant phenomena: i) the removal of soluble polymeric fragments formed during the sterilization by steam autoclave and ii) the partial release of

the β-GP used as catalyst of the gelification process. The first hypothesis has been supported by GPC analysis, while the second one by the HPLC quantification of β-GP released during the incubation (data not reported).

The Mw reduction percentages determined during the degradation process are plotted in **Figure 6**.

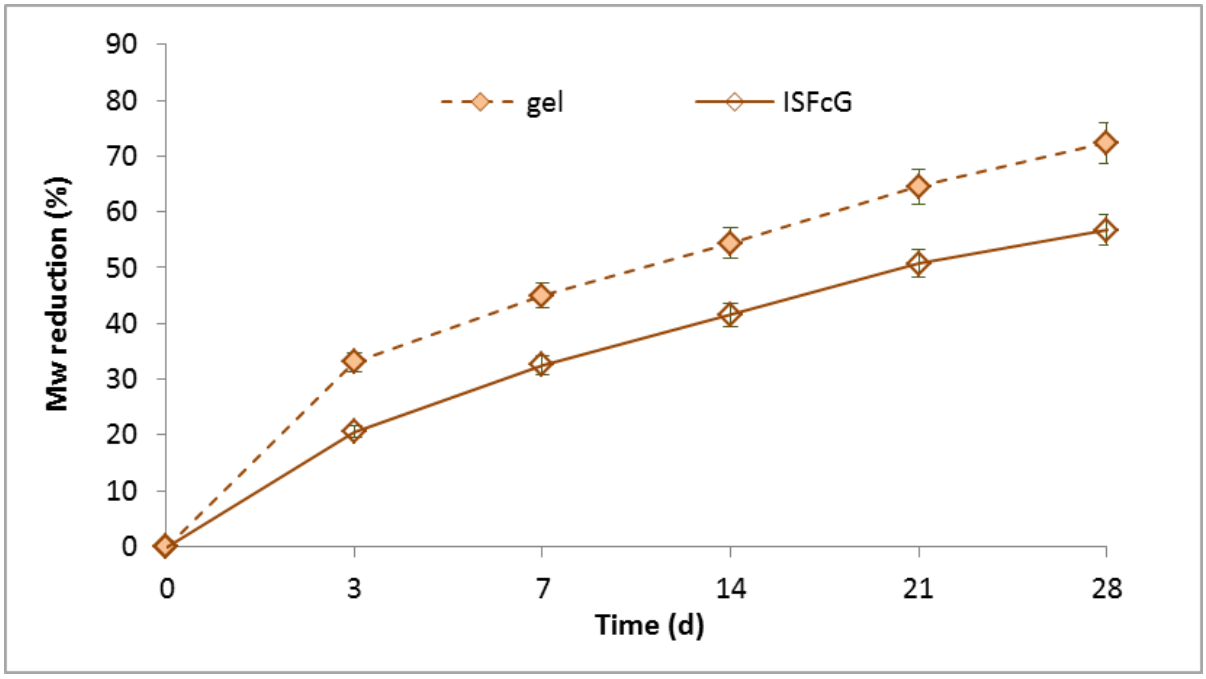

Figure 6: GPC results (Mw)of pure chitosan scaffold (gel) and ISFcGas function of incubation time in DMEM supplemented with 10% v/v FBS, at 37°C for 28 days. The values are means ± SD (n=5).

Initially, the measured average molecular weight (Mw) was 450 kDa and it significantly decreased by 3 days (23-35%), ($p<0.05$). The rapid Mw decrease detected at day 3 was attributed to degradation-induced by the sterilization process which is also responsible to the significant mass loss highlighted during the degradation process (**Figure 5a**). At day 28, the Mw reduction percentage was 56 and 72% for ISFcG and pure scaffold (gel), respectively ($p<0.05$).

Figure 7 shows the logarithmic plot of 1/Mw versus time for gel and ISFcG: the degradation rate constants (k_A) and half-life times ($t_{1/2}$) were obtained from equation 3 and 4:

$$-\frac{1}{2}\frac{dMw}{dt} = K(Mw)^2 = \frac{1}{Mw} = \frac{1}{Mw_0} + 2kt = \frac{1}{Mw_0} + k_A t \qquad \text{Eq.3}$$

$$t_{1/2} = \frac{1}{K_A(Mw_0)} \qquad \text{Eq. 4}$$

where, Mwt is the weight-averaged molecular weight at time t, Mw_0 is the initial weight-averaged molecular weight, k_A is the apparent degradation rate and $t_{1/2}$ is the half-life time of degradation.

From the results, it is revealed that the degradation of ISFcG was slow with a rate constant of 1.02 x 10^{-6}day^{-1} compare to the pure chitosan scaffold (1.7 x 10^{-6} day $^{-1}$), and half-life time degradation respectively 22.78 days and 13.38 days.

The degradation process can be divide in multiple stages: *Stage 1* - water permeate into the chitosan structure inducing swelling. The degradation can occur when the water molecules act on chitosan chains by cleavage of the β-(1→4) glycosidic bonds to form low Mw chitosan fragments, chito-oligomers and N-acetyl-D-glicosamine residues. The low Mw fragments remain in the bulk polymer matrix until they are small enough to dissolve into the surrounding media. *Stage 2* – the degradation process continues as the chitosan matrix undergoes hydrolytic reactions reducing its average Mw. At this point, the small fragments are released in the surrounding media which results in an increase of the average Mw of residual matrix. *Stage 3* - the chitosan matrix is further degraded with Mw reduction and mass loss. Composite scaffold loses the physical integrity with the complete dissolution of the polymer matrix in the incubation medium after 45 days.

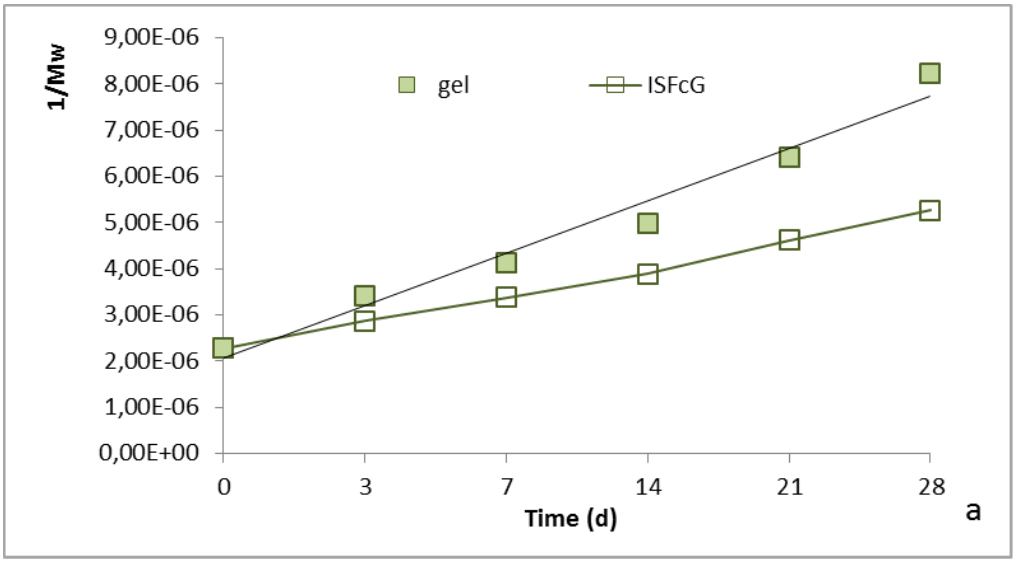

Sample	gel*	ISFcG**
Degradation rate (K_A, day-1)	1.7 x 10^{-6}	1.02 x 10^{-6}
Half life (t1/2, day)	13.38	22.78
Regression coefficient	0.972	0.995

* y= 1,7 $E^{-0,6}$x + 9 $E^{-0,7}$

**y= 1,02 $E^{-0,6}$x + 2 $E^{-0,6}$

b

Figure 7: 1/Mw versus time plot (a), degradation rate constant (k_A) and half-life ($t_{1/2}$) data (b).

4.4.3 Syringeability test

Syringeability results were reported in **Table 1**, the incorporation of bovine bone granules resulted in a reduction of the syringeability, nevertheless the ISFcG syringeability value (70±5 %) was considered appropriate for the clinical application. The syringeability value determined for pure chitosan scaffold (gel) was 85±3 %. Nevertheless, no evidence of solid-liquid separation and syringe or cannula clogging were detected during the syringeability test.

4.5 Cell culture studies

Cell seeding data determined by MTT assay (**Table 1**) revealed that ISFcG samples presented higher viability percentage values with respect to pure chitosan scaffold (gel). This evidence could be attributed to the higher stiffness and solidity of the composite scaffold (ISFcG), the bovine bone granules can promote the adhesion of cells that commonly grow in adhesion, such as fibroblasts. The substrate stiffness effects are not limited to soft tissue cells like epithelial cells and fibroblasts. Chondrocytes also exhibit morphological changes when cultured on substrates of different stiffness. It has been demonstrated that the cells assumed a rounded shape on softer substrates, while more stiff substrates changed the spherical morphology of chondrocytes into a flattened shape cells with increased spreading capability. By increasing the stiffness of the substrate, chondrocytes were found to attach more rapidly and to a greater degree. The ISFcG efficiency data seem to be in accordance with previous reports in which the authors found that fibroblasts attachment and proliferation are promoted by a stiffer environment [15].

Cell proliferation was studied by MTT assay incubating cells seeded onto scaffolds for 28 days, the results are summarized in **Figure 8.**

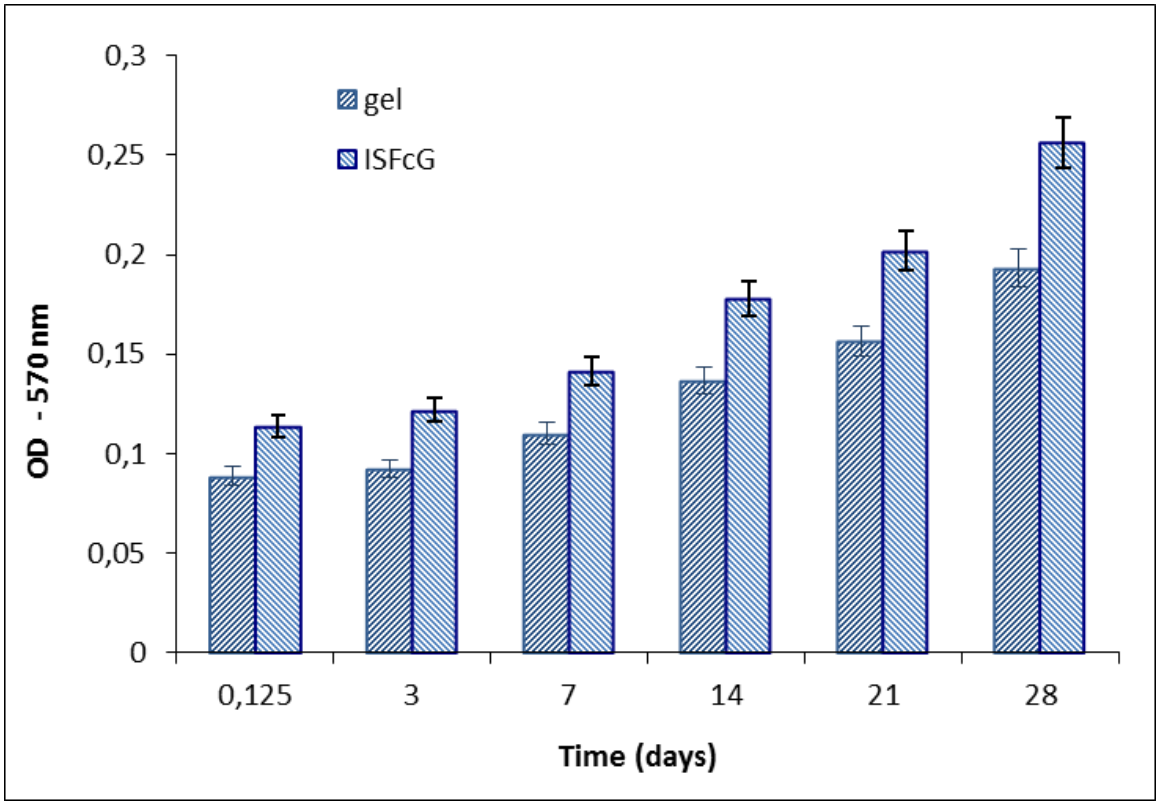

Figure 8: *In vitro* long-term cell growth study of pure chitosan scaffold (gel) and ISFcG prepared combining thermogelling polymer solution (1 ml) with bovine bone granules (200 mg). The values are means ± SD (n=5).

Good cell proliferation was shown after 28 days in culture, demonstrating that the excellent bioconductive properties of bovine bone granules were preserved when they were incorporated into chitosan polymer matrix. The cell density increased significantly on pure chitosan scaffold (gel) and ISFcG, which suggested that both the scaffolds could support the cell growth. Nevertheless, the cell proliferation on the composite scaffold (ISFcG) showed higher proliferation rate than that on pure chitosan scaffold (gel). These demonstrate that ISFcG could afford a more suitable 3D matrix for cell adhesion and proliferation.

5. CONCLUSIONS

ISFcG composite scaffold has been successfully prepared incorporating bovine bone substitute into a thermogelling polymer solution (chitosan and βGP), forming a porous 3D scaffold with a combination of excellent biofunctionality and good mechanical properties. The incorporation of bovine bone granules into thermogelling polymer solution positively modified the biological response, indeed the cell attachment and the proliferation and growth have been significantly enhanced. The biological response improvement could be correlated to the combination of several physical-chemical aspects,

such as high porosity and large surface area, good hydrophilic properties and high retention ability. The excellent physical stability and its injectable features make this system a promising candidate for bone regeneration, in particular for minimally invasive surgical procedures.

ACKNOWLEDGMENT

The authors acknowledge the support from Geistlich Pharma AG, Wolhusen, Schweiz, in particular Dr. Cesare Ferrari and Dr. Katja Martin. Moreover, the authors thank Dr. Alessandra Livraghi Dip. Medicina Diagnostica, I.R.R.C.S. Policlinico S.Matteo, Pavia, Italy, for human blood supplying.

6. REFERENCES

[1] Luyten FP, Vanlauwe J. Tissue engineering approaches for osteoarthritis. Bone 2012;51(2):289-296.

[2] Panetta NJ, Gupta DM, Slater BJ, Kwan MD, Liu KJ,. Longaker MT. Tissue engineering in cleft palate and other congenital malformations. Pediatr. Res. 2008;63(5):545-551.

[3] Nair MB, Kretlow JD, Mikos AG, Kasper FK. Infection and tissue engineering in segmental bone defects - a mini review. Curr. Opin. Biotech. 2011;22(5):721-725.

[4] Liu X, Wang X-M, Chen Z, Cui F-Z, Liu H-Y, Mao K, Wang Y. Injectable bone cement based on mineralized collagen. Biomed. Mater. Res. B 2010; 94B(1):72-79.

[5] Bose S, Roy M, Bandyopadhyay A. Recent advances in bone tissue engineering scaffolds. Trends Biotechnol. 2012;30(10):546-554.

[6] Larsson S, Hannink G. Injectable bone-graft substitutes: Current products, their characteristics and indications, and new developments. Injury 2011;42:S30-S34.

[7] Weiss P, Fatimi A. Injectable composites for bone repair. Biomed. Comp. 2009:255-275.

[8] Dorati R, Genta I, Conti B, Klöss H, Martin K. An injectable *in situ* forming composite gel to guide bone regeneration: Design and development of technology platform. Eur. Cells Mater. 2012;42:14.

[9] Heinemann S, Roessler S, Lemm M, Ruhnow M, Nies B. Properties of injectable ready-to-use calcium phosphate cement based on water-immiscible liquid. Acta Biomater. 2013;9(4):6199-6207.

[10] Jacquart S, Belime A, Pigasse C, Siadous R, Fatnassi M, Tadier S, Auzély-Velty R, Girod-Fullana S, Bareille R, Roques C, El Kissi N, Anagnostou F, Bignon A, Cordier D, Rey C, Brouillet F, Amédée J, Galliard H, Combes C. Development of an injectable composite for bone regeneration. Irbm 2013;34(2)176-179.

[11] Mosmann T. Rapid colorimetric assay for cellular growth and survival: application to proliferation and cytotoxicity assays. J. Immunological. Methods 1983;65:1-2.

[12] Dorati R, Colonna C, Genta I, Modena T, Conti B. Effect of porogen on the physico-chemical properties and degradation performance of PLGA scaffolds. Polym. Degrad. Stabil. 2010;95(4):694–701.

[13] Ismail AF, Abdalmonemdiilaanea, Awang M, Mohamed F. High initial burst release of gentamicin formulated as PLGA microspheres implant for treating orthopaedic infection. Int. J. Pharm. Pharm. Sci. 2012; 4(4):685-691.

[14] Frutos P, Torrado S, Perez-Lorenzo ME, Frutos G. A validated quantitative colorimetric assay for gentamicin. J. Pharmaceut. Biomed. 2000;21(6):1149-1159.

[15] Chang H-I, Wang Y. Cell Responses to Surface and Architecture of Tissue Engineering Scaffolds. Regenerative Medicine and Tissue Engineering - Cells Biomaterials 2011 Ed by Prof. Daniel Eberli.

CHAPTER I

Chapter II

CHAPTER II

THERMOSETTING HYDROGEL AND MOLDABLE COMPOSITE SCAFFOLD AS DRUG DELIVERY SYSTEMS FOR OSTEOMYELITIS TREATMENT

ABSTRACT

The present work aimed to design biodegradable drug delivery systems made of chitosan and bovine bone substitutes, able to locally deliver gentamicin, meanwhile acting as scaffold for bone regeneration. A thermosetting composite gel (IsFcG) and a composite moldable scaffold (mCSG) obtained through hydrogel freeze-dryng, were studied. Amount and technique to incorporate gentamicin sulphate into mCS was evaluated optimizing scaffold stability and gentamicin release rate. Gelification resulted to be affected by gentamicin sulphate according to cosolute effect on sol/gel transition. Gentamicin loading into mCS (mCSG) was investigated by 5 different techniques. Positive results in terms of porosity around 80-86% were obtained for mCSG1, mCSG2, mCSG3 and mCSG5, while mCSG4 lost its original 3D structure after freeze-drying process. Gentamicin addition to mCS didn't interfere with scaffold water uptake and retention capability. Gentamicin *in vitro* release was completed in 4 hours, useful in limiting risks of infection during open surgeries. Good results in term of cell seeding were observed for all moldable scaffolds (mCSG1-5). MCSG3 and mCSG5 resulted the best in terms of cell proliferation results. Antimicrobial effect was tested on *E.Coli ATCC 10356* showing bactericidal effect of mCSG3 for 24 hours. Bacteriostatic effect of chitosan was superimposed in the first 4 hours.

Keywords: thermosetting hydrogel, moldable scaffold (mCS), osteomyelitis, gentamicin sulphate.

This chapter to be submit for pubblication.

R.Dorati, A.De Trizio, I.Genta, A. Merelli, T.Modena, B.Conti.

1. INTRODUCTION

Osteomyelitis is an inflammatory bone disease which leads to bone destruction (osteolysis). It can arise by direct contamination (e.g. open fractures and ulcers) or by spreading from blood stream (hematogenous source) or from contiguous site or implant. Surgical interventions for treating bone defects or bone fusion, and involving open surgery, have long air exposure times and potential for surgical injury that can easily lead to infection. Bacteria causing infection often originate from patient's skin as well from operating personals. Moreover, orthopedic implants can be a nidus for infection and infection rate could be higher after an orthopedic general surgery, because the damaged tissue has not blood supply, and bacteria can live and spread, serious infections can be induced around the graft site.

Clinically, physicians are able to classify bone infections in two different categories: acute and chronic infections. The most common form of acute cases is due to blood weakness or damage, known as hematogenous infection. Chronic cases of osteomyelitis infection are less common but they are increasing nowadays, due to more frequent use of prosthetic for joint replacement or fracture repair. Clinical signs of infections persisting for longer than 10 days are associated with development of necrotic bone and chronic osteomyelitis [1]. Infected tissue is usually surrounded by sclerotic and poorly vascularized bone covered by a thickened periosteum, scarred muscle and subcutaneous tissue (involucrum). In order to overcome bone infection, it is important to firstly understand biological infection cascade to prevent and treat such manifestations. Body's first immunological response focuses on collection at infected site of macrophages, neutrophils, and other phagocytic cells, and infection recognition by body signals associated to T-cells and B-cells of specific immune system producing antibodies [2]. High concentration of cells and immunologic agents like histamine trigger an immune response like pain, swelling, redness, heat and function loss. This is generally a beneficial response, but if infection is persistent, this response can lead to necrotic tissue formation [3].

Traditional way of pathogenic bacteria elimination involves surgical removal of necrotic tissue in combination with systemic antibiotic therapy applied for 3-6 weeks with broad-spectrum antibiotic such as vancomycin, ciprofloxacin and gentamicin. Conventional antimicrobial therapy usually promotes bacterial resistance when pathogens change from the familiar plank-tonic (free floating) form into phenotypically different sessile forms forming an organized community of bacteria called biofilm [6]. The surface of devascularized bone and implants are predisposed to bacteria attachment and biofilm formation. First 6 hours post implantation are critical to prevent bacterial adhesion and decisive implant success. Over this period, certain species of adhered bacteria are able to form a biofilm at implant-tissue interface [7].

Therefore, systemic treatment requires high antibiotic dose regimens increasing antibiotic potential hazardous and side effects. On this purpose infusion pumps have been used to locally deliver antibiotic for some acute infections. For these reasons a lot of research is on going concerning design and development of drug delivery systems for osteomyelitis local treatment being more effective and less toxic than conventional systemic antibiotic therapy [4, 5, 10] and few medicinal products are already on the market.

Drug delivery system design for local administration of antibiotic should address to: i) an easily administered formulation by minimally invasive procedure; ii) a drug delivery system with suitable mechanical and structural properties for bone tissue regeneration; iii) drug delivery system ability to deliver high local amounts of antibiotic directly to infection site without requiring an intact vasculature; *iii)* drug release profile including initial fast release followed by prolonged antibiotic release in therapeutic amounts in order to inhibit latent infections [4, 5, 6, 7]. Biofilm-embedded bacteria require much higher concentrations of antibiotics for their elimination compared with their planktonic forms, because antimicrobial molecules must diffuse through biofilm matrix.

Some antibiotic loaded bone grafts are available on the market, namely, Simplex® P, Osteoset-T®, Collatamp®, Septocoll®, Septopal®, Herafill® beads and Stimulan® [8]. These local antibiotic delivery devices elute into joint space or in an infected area with several advantages since they: can achieve a much higher concentration than through systematically administered antibiotic, maximize antibiotic efficacy minimizing its toxicity and potentially reducing bacterial resistance risk. Use of antibiotic loaded polymethylmethacrylate (PMMA) cement is well established in osteomyelitis treatment as long as in arthroplasty. One the most relevant disadvantages of the system is the amount of eluted antibiotic into joint or bone defect area is not always kept at the minimum inhibitory concentration (MIC). Moreover, cement isn't resorbable involving a second surgical intervention to remove it, and PMMA can also act as foreign body on top of which bacteria produce a biofilm, protecting them from antibiotic action. Cancellous bone autograft, calcium sulphate (Osteoset-T®) or phosphate impregnated or soaked in antibiotic solution can also be utilized showing rapid antibiotic release and new bone formation support. Biodegradable scaffold loaded with antibiotic can represent an innovative alternative to PMMA cements. They can act as matrix for bone growth meanwhile releasing antibiotic and gradually being resorbed, they do not need a second surgery to be removed when exhausted. Antibiotic release from a biodegradable scaffold/drug delivery system happens combining diffusion mechanism through the polymer matrix with matrix biodegradation, and it can be modulated according to polymer matrix biodegradation properties. In this way antibiotic activity can be prolonged at the infected site, also preventing biofilm formation. Collagen fleece (Collatamp®) are an example of biodegradable drug delivery system already on the market. The product is biocompatible, however its

fast degradation with quick loss of integrity and poor mechanical properties does not support new bone growth. Moreover, collagen can exert some immunogenical potential [9]. Starting form this background, the present work was aimed to design biodegradable drug delivery systems able to locally deliver gentamicin meanwhile acting as scaffold for bone regeneration. Chitosan was investigated as biomaterial since it is a biocompatible, biomimetic and degradable polymer, with slight antibacterial acitivity; and it promotes osteogenesis and osteoinduction and healing. Exploiting chitosan thermosensitive gelification, thermosetting composite gel (IsFcG) was here investigated as gentamicin delivery system. IsFcG combines chitosan with bovine bone substitutes (BBS Orthoss® granules) in order to improve hydrogel osteoconductive properties. Moreover, starting from the gentamicin loaded thermosetting hydrogel, a composite moldable scaffold loaded with gentamicin was designed and *in vitro* characterized.

The most innovative characteristic is the systems versatility since it can be formulated and used as injectable in situ forming composite gel (IsFcG) or solid moldable scaffold based on the specific application. In form of thermosetting hydrogel, it can be used either as implant coating or it can be injected to fill bone cavity. In form of moldable scaffold, it can be used in a spongy-like structure to be implanted.

2. MATERIAL

Orthoss® spongious granules (Spongious granules 1-2 mm) were supplied by Geistlich Surgery (Geistlich Pharma AG, Wolhusen Switzerland). Chitosan chloride (CL213, Protosan CL213, Mw 300-350 kDa, deacetylation degree 82%, hydrochloric acid content 10-20%) was purchased from Pronova Biomedical, Norway. Glycerol 2-phosphate disodium salt hydrate was purchased from Sigma Aldrich, Milan (Italy). Foetal Bovine Serum (FBS, Eu approved) was purchased from Euro Clone, Milan (Italy). Human adult dermal fibroblasts as primary cells were purchased from International PBI, Milan (Italy). Gentamicin sulphate (Gentamicin C1 $C_{21}H_{43}N_5O_7$, Mw 477.6 g/mol, Gentamicin C2 $C_{20}H_{41}N_5O_7$, Mw 463.6 g/mol, Gentamicin C1a $C_{19}H_{39}N_5O_7$), Mw 449.5 g/mol., Ninhydrin Mw 178.14 g/mol were from Sigma Aldrich. The water used in the preparation of thermogelling polymeric solutions was ultrapure water (Millipore Corporation, Massachusset, USA). Unless specified, all other solvents and reagents were of analytical grade.

3. METHODS

3.1 Preparation of a moldable polymeric/composite scaffold as carrier for gentamicin

Materials and protocol to obtain an *In situ* Forming composite Gel (IsFcG) were set up in a previous work. Briefly, a polymer solution of chitosan chloride (CL213 and sodium salt glycerophosphate (β-GP)) were prepared as vehicle for *in situ* injection of bovine bone sobstitutes (BBS). The thermosensitive solution is in a liquid state at room temperature and it gelifies at 37°C (body temperature) [11]. Chitosan chloride was solubilized in distilled filtered water (Millipore Corporation Massachusetts, USA) at 2.4 % w/v under magnetic stirring for 12 hours, at room temperature. Chitosan CL213 solution was sterilized with saturate steam high pressure (autoclave Vapor Matic,770, Milan, Italy) following the conditions specified in European Pharmacopoeia (15 minutes, 121°C, at 2 atm). β-GP was dissolved in sterile water under magnetic stirring and flitered with 0.22 μm before use, in order to obtain a final concentration of 58 % w/v. Both solutions were cooled at 4°C in an ice bath. The hydrogel was obtained by dropping β-GP solution in chitosan solution at 1:4.8 v/v ratio; the final solution was maintained in ice bath for 1 hour to prevent gelification and subsequently split in a 24 well plate (1ml of thermogelling solution per well) and kept at 37°C. Whenever the gel was formed, the multiwell was stored at -25°C for 3 hours, and then freeze-dried at -48°C 0.1 mbar for 24 hours in order to obtain solid moldable scaffolds (mS). In case of BBS addition, 200 mg of granules were placed in each well before thermogelling solution addition. 1ml of thermogelling solution was added per well and gently mixed in order to achieve an homogeneous suspension and gelified at 37°C. The multiwell was stored at -25°C for 3 hours then the samples were freeze-dried at -48°C 0.1 mbar for 24 hours in order to obtain solid moldable composite scaffolds (mCS). The procedure was performed in aseptic conditions.

Literature reports gentamicin loaded drug delivery systems based on borate bioactive glass, bone cement and polymeric film made of Poly ($_{L}$-lactic-acid) or poly ($_{D,L}$-lactide –co-glycolide) [3, 4, 12-15] but chitosan has not been yet investigated , at our knowledge, and it was here evaluated . As suggested from the literature 4 mg of gentamicin sulphate was incorporated in the thermosetting solution then the influence of gentamicin sulphate addition on thermosensitive gel formation was studied. 5 mg of gentamicin powder were dissolved 827.6 μL of 2.4% w/v chitosan (CL213) sterile solution, following addition of 172.4 μL of 58% w/v β-GP. Thermosensitive gel formation was evaluated upon incubation of 1 mL of thermosetting hydrogel at 37°C to induce gelification; visual hydrogel appearance was controlled at 10 min intervals: 10, 20, 30, 40, 50 and 60 minutes.

Keeping constant the amount of thermosetting solution (1ml) making the moldable scaffold, gentamicin loading to moldable scaffold has been investigated setting up five different protocols in order to select which one could optimize moldable scaffold performances such as stability and

gentamicin release rate (**Figure 1**). Gentamicin loaded moldable scaffold preparation protocols are reported here below:

1) 5 mg of gentamicin powder is added to 827.6 µl of sterile solution of chitosan Cl213, following by 172.4 µl β-GP addition, supplemented with BBS or not and freeze-dried (mSG1 and mCSG1).

2) 4 mg of gentamicin powder is added to the already formed thermosensitive sol-gel (1 ml of Cl213 and β GP) supplemented with BBS or not, and freeze-dried (mSG2 and mCSG2).

3) 1 ml of 4 mg/ml gentamicin solution is added to the pre-formed scaffold and then the scaffold is freeze-dried (mSG3 and mCSG3);

4) 0.1ml of 40 mg/ml gentamicin solution is added to the pre-formed scaffold and then the scaffold is freeze-dried (mSG4 and mCSG4);

5) 1 ml of 4 mg/ml gentamicin solution is added to 200 mg of BBS and adsorbed to granules, the suspension was freeze-dried. Then 1 ml of the thermosensitive sol-gel (Cl213 and β-GP) is added to the BBS granules impregnated with gentamicin, and freeze-dried (mSG5 and mCSG5).

In all cases the final product was a lyophilized solid moldable scaffold (mSG and mCSG).

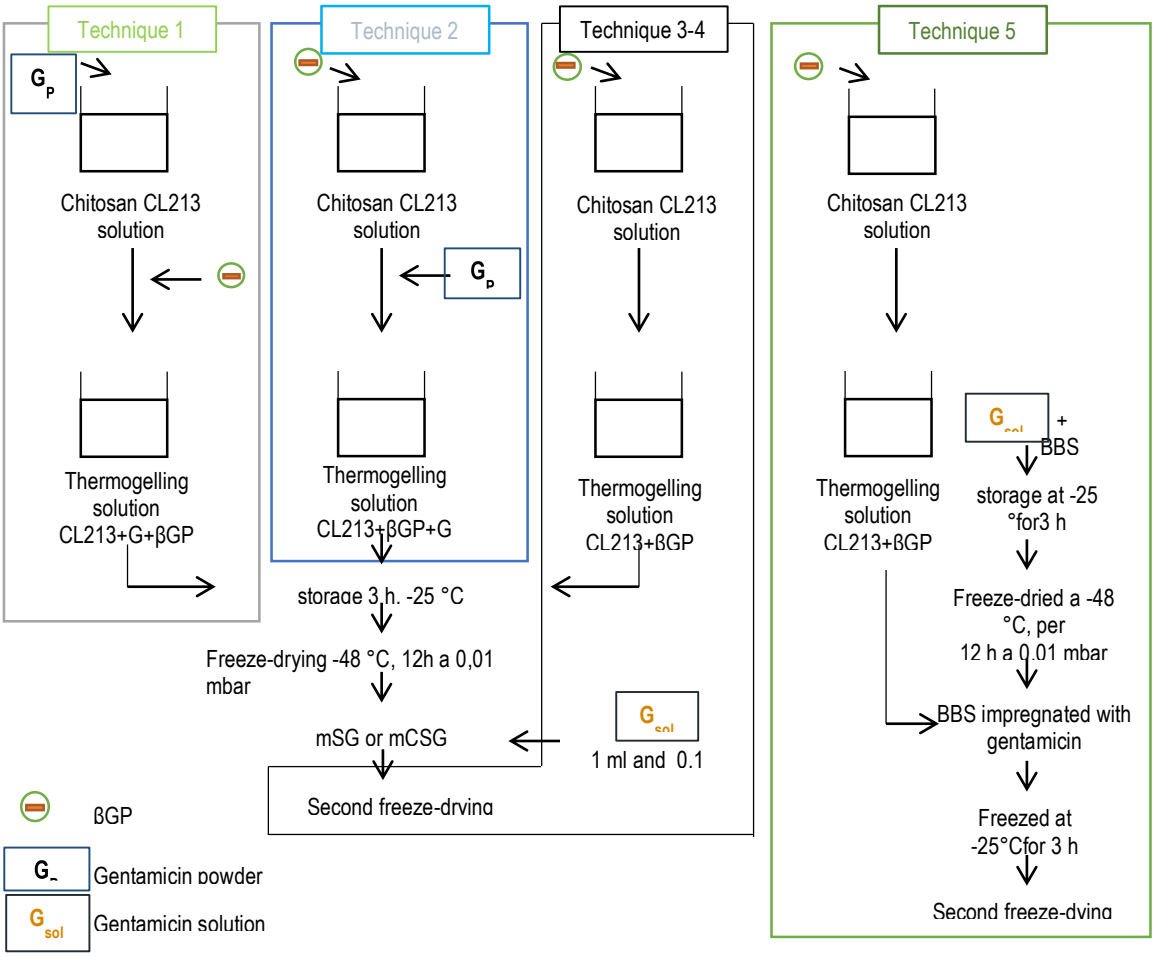

Figure 1: Scheme of five protocols in order to obtain moldable scaffolds loaded with gentamicin (mS1, mS2, mS3, mS4 and mS5) and moldable composite scaffolds loaded with gentamicin (mCS1, mCS2, mCS3, mCS4 and mCS5).

3.2 Rheological behavior of thermosetting gentamicin loaded hydrogel

Rheologic behavior of gentamicin sulphate loaded thermogelling polymeric solution was studied by rotational rheometer (Rheometer Kinexeus Plus, Alfatest, Mi, Italy). CP4/40 cone-plate geometry was employed (1° cone angle, 40 mm diameter) with a gap of about 0.15 mm with a solvent trap used to avoid water evaporation during the test. Apparent viscosity was measured at 25°C and at 37°C (body temperature) increasing shear rate from 0.1-10 s^{-1}. The polymer solution viscoelastic properties were determined by measuring storage modulus (G') and loss modulus (G'') representing elastic and viscous behavior, respectively. Temperature sweep test was performed at constant frequency (1Hz) and shear stress (1 Pa) increasing temperature from 25°C to 70°C in order to evaluate the sol/gel transition. Sol/gel transition temperature is the temperature in which the storage modulus (G') is equal to the

loss modulus (G''). If sol/gel transition was verified, the gel was cooled to reach room temperature to verify its reversibility.

3.3 *In vitro* physical -chemical characterization of moldable composite scaffolds

When a polymeric or a composite polymeric structure (mSG and mCSG) is developed, architecture, surface morphology, *in vitro* release of the loaded drug and biological performance of these structures must be studied.

In vitro physical characterization involved: porosity evaluation, scaffold water uptake, water retention and wettability.

Chemical characterization involved: drug encapsulation efficacy (EE%) determination and *in vitro* release.

Yield Process (%) is always evaluated as proof of production process consistency.

3.3.1 Porosity

mSG and mCSG porosity was measured by a modified liquid displacement method: ethanol was chosen as the displacement liquid because it penetrates easily into the pores, it is a chitosan non-solvent and it does not induce polymer shrinkage or swelling [16] .

Briefly, a weighted polymer scaffold [17] was immersed in a graduated cylinder containing a known volume (V_1) of ethanol. The sample was kept in the non-solvent for 10 min, and then a set of evacuation-repressurization cycles were carried out to force the ethanol into the pore structure. Cycling was continued until no air bubbles were observed from the surface scaffold. The total volume of the ethanol and ethanol-soaked scaffold was then recorded as V_2. The volume difference, (V_2-V_1), was the volume of the scaffold skeleton. The ethanol-soaked scaffold was then removed from the cylinder and the residual ethanol volume was recorded as V_3. The volume (V_1-V_3), that is the ethanol volume retained in the porous scaffold, was defined as the pore volume of the scaffold. The total volume of the scaffold was calculated as follows:

$$V = (V2 - V1) + (V1 - V3) = (V2 - V3) \qquad \text{Eq.1}$$

The porosity of the scaffold (ε) expressed as percentage (%) was calculated by:

$$\varepsilon\ (\%) = \frac{(V1-V3)}{(V2-V3)}\ X\ 100 \qquad \text{Eq.2}$$

The porosity values were determined on five samples and expressed as mean±standard deviation.

3.3.2 Water uptake and water retention (%)

Water uptake and water retention was measured by soaking each sample of mS, mSG, mSC and mCSG in 6 ml of PBS pH 7.4 kept at 37°C in static condition. Swelling behavior was quantified by measuring the change in the sample diameter as a function of incubation time (20 minutes, 10 hours and 7 days) in the medium. The experiment was performed in triplicate.

To assess the ability of water uptaking, the mS and mCS placebo and loaded with the gentamicin of known weight (Wd) were immersed in PBS solution (pH7.4) and incubated at 37°C under static condition for 24 hours. The water uptake percentage was calculated by Equation 3. To measure the Ww, swollen samples were re-weighted after removal of excessive water on the surface using a filter paper.

The ability to retain water is extimated weighting again the samples after centrifugation (CompacStar Cs4,VWR) at 500 rpm for 3 minutes (W'w). The water retention percentage was calculated by the following equation 4:

$$Wu\ (\%) = \frac{Ww - Wd}{Wd}\ X\ 100 \qquad \text{Eq.3}$$

$$Wr\ (\%) = \frac{W'w - Wd}{Wd}\ X\ 100 \qquad \text{Eq.4}$$

Each experiment was repeated three times, and the average value was recorded as the water uptake and water retention value.

3.3.3 Wettability

Wettability can be assessed by the contact angle that a droplet of water has with the materials surface. The static water contact angle (WCA) of the mS, mCS samples placebo and loaded with Gentamicin was measured at room temperature using Lorentzen-Wettre. The liquid used was PBS pH 7.4 and the drop volume was 45 µl.

3.3.4 Morphologic Characterization (SEM)

Scanning electron microscopy (SEM) provides images of the surface of a given samples by scanning it a high energy beam of electrons. SEM was used for analysis of morphology/porosity of the different moldable composite scaffold loaded with Gentamicin (mCSG). For this purpose, all samples were coated with Au via ion-sputtering prior to observation in Electron Microscope (Jeol Cx, Tecman, Tokyo, Japan).

3.3.5 Gentamicin encapsulation efficacy (EE%) determination and *in vitro* release

The encapsulation efficiency (EE%) and the *in vitro* release study were determined by Uv-Vis spectrophotometry at 400 nm by ninhidryn test (UV-1601, UV-Vis spetrophotometer, Shimadzu). The test, is a quantitative way to determine concentrations of an absorbing species in solution affecting the purple colour of the chemical involved. For encapsulation efficiency determination, each scaffolds was dissolved in 2 ml of 0.1 M acetic acid where chitosan is soluble but gentamicin isn't soluble. The resulting suspension was centrifuged at 25°, 16400 r.p.m. for 20 mins, and the pellet was solubilized in 800 µl of distilled filtered water.

The 800µl of gentamicin solution were mixed with 240 µl of ninhidryn solution in PBS (0.2 %w/v) pH 7.4 [18, 19]. The solutions were stirred by vortex and heated at 95°C for 15 minutes in order to induce the reaction between the ninhidryin carboxyl group and the amino groups of gentamicin. At the end of the reaction the solutions were cooled in an ice bath to stop the reaction. mCS and mS placebos were considered as blanks in the performed quantification. Encapsulation efficiency was expressed as percentage of incorporated drug compared to theoretical content after solubilization of the matrix in 0.1 M acetic acid . The Drug content (DC) was calculated as the amount of gentamicin incorporated into the scaffold (mg) per total area of the cylindric scaffold (cm^2). The standard curve was obtained from gentamicin solutions in ultrapure water (concentrations ranging from 50 µg/ml to 500µg/ml, relating the quantity of Gentamicin with the absorbance intensity. The results presented are an average of three measurements.

The *in vitro* release study on the mCSG and mSG was performed in PBS pH 7.4 at 37°C in static condition until Gentamicin release was completed. Gentamicin-loaded scaffolds were weighted and immersed in 7 ml of phosphate buffer solution. Aliquots of 800 µl were withdrawn in predetermined time intervals (and the same volume of fresh medium was added to the suspension) and analysed by UV spectrophotometer using nynhidrin method as explained above. The concentration of Gentamicin released from each samples was calculated from gentamicin calibration curve in PBS pH 7.4 (concentrations ranging from 50 µg/ml to 250 µg/ml). Calculations of the amount of drug released took into account the replacement of aliquots with fresh medium.

3.3.6 Yield process determination

The yield process (%) was calculated following the equation 5, where Wi was considered the weight of the freeze-dried scaffold and W was the initial weight of the materials (Chitosan CL213, β-GP, BBS and gentamicin based on the composition of the mS and mCS).

$$Yield\ Process\ (\%) = \frac{Wi}{W} \times 100 \qquad \text{Eq.5}$$

3.4 Antimicrobial activity of the moldable scaffold loaded with gentamicin

Microbiological assay was performed against *E. coli* (ATCC 10536) in order to determine the antibacterial activity of scaffolds loaded with gentamicin obtained with technique 3. Antibacterial activity was evaluated on: scaffolds containing gentamicin powder (4mg/per scaffold) and placebo scaffold.

The samples were incubated in falcons with 24 ml of ISB (ISO SENSITIVE BROTH) plus 1 ml of *E.Coli* (ATCC 10536) inoculus $10^7 – 10^8$ CFU. A blank sample (24 ml ISB plus 1 ml of *E.Coli* (ATCC 10536) inoculus $10^7 – 10^8$ CFU) was used as control. Samples and control were incubated at 37°C for the set times: 0, 1h, 2h, 4h, 24h. Afterwards 50 µl of incubation broth were withdrawn diluted in EUG (EUGONIC BROTH W/LECITHIN, TX-100 & POLYSORBATE 80) according to standard dilution protocol and placed in 5 ml of sterile water (II dilution, 1:100), 50 µl of the II dilution are withdrawn and placed in 50 ml of sterile water (IV dilution, 1:10000) and so on up to dilution VIII (1:100000000).

1 ml of the diluted samples are seeded on Petri dishes with TSA (Triptone Soya Agar) as culture medium and incubated at 37°C for 24 hours before counting colonies to determine the number CFU/ml and microbicidal effect.

Microbicidal effect (M.E.) is computed as reported in the following equation (Eq.6):

$$M.E = log10\,(CFUsample) - log10(CFUcontrol) \qquad \text{Eq.6}$$

3.5 Biological characterization

3.5.1 Cytotoxicity test

100 µl cell suspension was seeded in 96-well plates at the density 1x 10^5 cells per well and incubated 24 hours to allow cell adherence. The cells were incubated with aqueous solution of gentamicin sulphate ranging from 0.0039 mg/ml to 2.5 mg/ml in order to simulate the amount of gentamicin *in vitro* released from the scaffolds in 24 hours. MTT test was used to extimate the number of living cells because of the ability of 3-(4,5-dimetiltriazole-2-y)-2,5 difeniltetrazole bromide (MTT) to interact with mitocondrial dehydrogenase enzyme only in the living cells forming purple crystals of formazan that accumulate in the cytoplasm of living cells. Briefly, a stock solution of MTT was prepared by dissolving MTT powder in DMEM without FBS (5 mg/ml). 25 µl of MTT solution and 200 µl of DMEM without FBS were added to each well. After 2.5 hours of incubation, the MTT was aspirated off and 200 µl DMSO was added to dissolve the cellular membrane and solubilize the formazan crystal released from the living cells. After 40 minutes, the plate was read in a microplate reader using an wavelenghth of 570 nm and 690 as reference. Untreated cells were taken as control with 100% viability, and cells without addition of MTT were used as blank to calibrate the spectrophotometer to zero absorbance.

3.5.2 Cell culture seeding and proliferation study

The cytocompatibility of the developed mS and mCS placebo and gentamicin sulphate loaded was evaluated using fibroblast cell line as model cells. Cells were grown in Dulbecco's Medium Eagles's medium supplemented with 1% v/v of antibiotic-antimycotic solution and 20% v/v FBS in a humidified atmosphere with 5% CO_2 at 37°C. For expansion, confluent cells cultures were split 1:3 to 1:6 using 0.25% trypsin/EDTA. For cell seeding, samples were sterilized with UV lamp. Samples were immersed in DMEM containing FBS for 2 hours in order to allow the structure swelling and the medium was removed after this time.

To ensure adherence of cells on mS and mCS and mSG and mCSG, cells were centrifuged at 1500 rpm for 5min, and then resuspended in a volume of medium to yield a solution with a density of 2 x 10^4 cell/100 µl. 100 µl of cell suspension were dropped on the top of all scaffold samples. After 2h incubation in a humidified atmosphere at 37°C and 5%CO_2, the scaffold samples were transferred to new wells containing complete medium and further incubated for 2h. The same protocol was applied to the scaffold samples in order to obtain the profiles of fibroblast proliferation in 4 and 7 days [20]. At each time point, the viability and proliferation of the cells was determined using MTT test. 300 µl of MTT solution and 7 ml of DMEM without FBS were added to each well. After 2.5 hours of incubation, 7 ml PBS was added to remove the excess of unreacted MTT. The samples were stirred at 300 rpm in 2 ml of THF for 1.5 hours in order to solubilize the polymer matrix and break the cell membrane to release the formazane crystals. The obtained solutions were analyzed by spectrophotometer at 595 nm. In case of mCS and mCSG, the obtained suspensions were centrifuged at 25°C, 16400 rpm for 20 minutes (5417R Centrifuge, Eppendorf Germany). The polymer solutions separated from the inorganic component were analyzed by spectrophotometer at 595 nm.

4. RESULTS AND DISCUSSION

Preliminary evaluation involved investigating on how gentamicin could affect sol/gel transition process, and therefore hydrogel stability. The interactions involved in gelification process are: i) electrostatic attractions between chitosan ammonium groups and β-GP phosphate group, ii) hydrogen bonds between chitosan chains, due to decreased electrostatic repulsion after neutralization of ammonium groups by β-GP, iii) chitosan-chitosan hydrophobic interactions to compete with the electrostatic repulsion of chitosan chains after neutralization (**Figure 2**). Sol-gel transition occurs in two stages: i) chitosan is partially neutralized by β-GP negative charges ii) heating chitosan in the presence of β-GP would induce proton transfer from chitosan to β-GP so the repulsive chitosan-chitosan electrostatic forces could be overcome by attractive inter chain forces and thereby

induce chitosan precipitation [21, 22].The presence of gentamicin sulphate could interfere with sol/gel transition process because gentamicin amino groups can interact with negative charges of crosslinking agent (βGP) delaying chitosan neutralization step or inhibiting gelification process. In the literature is reported that sol/gel transition could be influenced by presence of cosolutes, such as salts. Effect of salt addition on sol/gel transition depends on position of corresponding salt in the classic Hoffmeister series, which organizes salts based on their "salting out" power towards proteins from aqueous solutions. A common explanation of cosolute effect is competition for water molecules available for solvation, favoring chitosan precipitation. In this prospective, addition of gentamicin sulphate to thermosetting chitosan solution can decrease sol/gel temperature transition due to SO_4^{2-} salting out effect [23, 24]. Gelifying times greater than 20 mins are not suitable for the final application, because BBS granules and the drug, injected as liquid suspension, spread out in the surrounding tissue if hydrogel does not form in a short time (20 mins maximum). Loadings of gentamicin sulphate such as 4, 8 and 12 mg per mL of thermosetting polymer solutions were preliminarly tested (data not reported) and 8 and 12 mg were no longer evaluated since these thermosetting solutions viscosity was too much high at 25°C, preventing easy injection.

Table 1: Composition of Gentamicin loaded hydrogels and gelyfication times at 37°C.

	Scaffold composition				**Sol-gel transition time (min)**	**EE (%)**	**Gent/scaffold (mg)**	**Drug Content (mg/cm^2)**
	CL213 (% w/v)	βGP (% w/v)	BBS (mg)	Gent (mg)				
$mSG1_A$	2	10	-	4	20	98.5	3.94	0.71
$mCSG1_A$	2	10	200	4	18	98.8	3.95	0.72

The influence of gentamicin on sol-gel transition was evaluated on hydrogel composition containing 4mg/mL of gentamicin in presence or not of bovine bone granules: results in **Table 1** show that gentamicin does not interfere with bovine bone granules in order to change sol-gel transition time. Both in presence or not of BBS granules, 4 mg of gentamicin allows gelification of 1 mL hydrogel in 20 minutes. Based on this preliminary study, this hydrogel composition was submitted to rheological measurements.

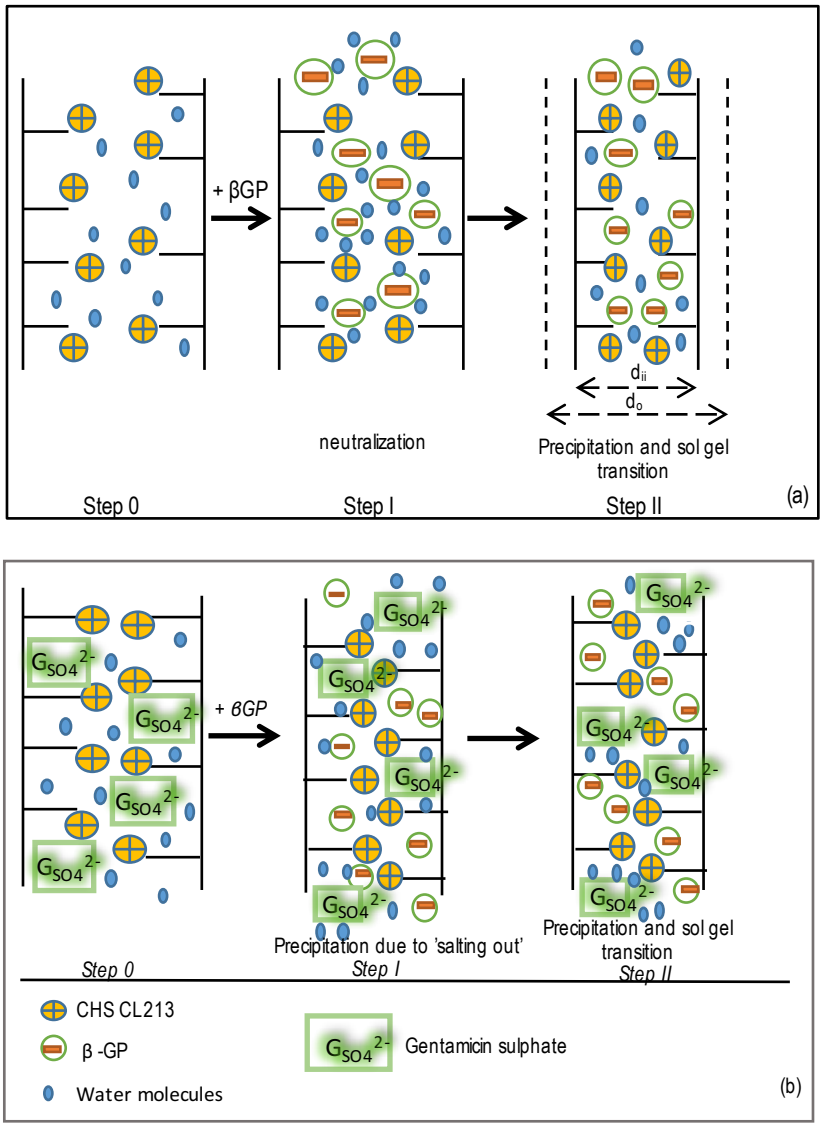

Figure 2: (a) Scheme of chitosan gelification and, (b) Interference of gentamicin sulphate in the gelification process of chitosan and β glycerol phosphate hydrogel (CHS-βGP).

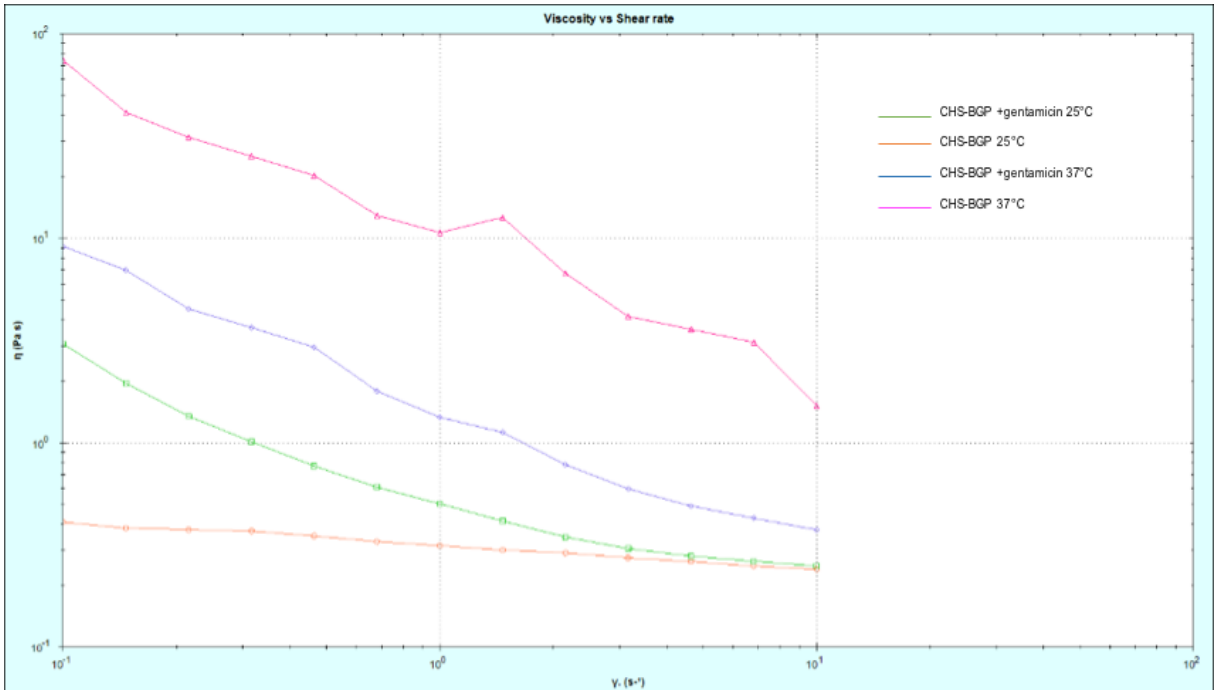

Figure 3: Shear rates/ equilibrium flow curves for chitosan- βGP solution and gentamicin (4 mg) loaded into chitosan- βGP solution at 25°C and 37°C.

The results concerning rheological behavior of gentamicin chitosan-βGP solutions show a pseudoplastic behavior common for polymer solutions. Viscosity was measured increasing shear rate from 0.1-10 sec^{-1} at 25° and 37°C, placebo gel was used as control. The polymer solution containing gentamicin sulphate shows, at low shear rate 10^{-1} γ sec^{-1} and 25°C, 7.5 times viscosity increase with respect to polymer solution without antibiotic (from 0.41 to 3.05 Pa*s). On the contrary, apparent viscosity of the polymer solution with and without gentamicin sulphate at high shear rate 10^{1} and 25°C are very similar, 0.2503 Pa *sec and 0.2408 Pa *sec respectively. Temperature increase from 25°C to 37°C, leads to viscosity increase for CHS-βGP hydrogel both with and without gentamicin sulphate, but apparent viscosity is higher for placebo CHS-βGP hydrogel, both at low and high shear rate (**Figure 3**). Sol/gel transition was evaluated heating from 25° to 70°C. CHS-βGP solutions containing gentamicin results in lower sol/gel transition temperature with respect CHS-βGP solution, 49°and 52° C respectively, demonstrating the influence of SO_4^{2-} anions salting out. In order to evaluate hydrogel thermal reversibility, both CHS-βGP and gentamicin loaded CHS-βGP hydrogels were cooled from 70°C to 25°C and loss modulus (G', red line) and storage modulus (G', blue line) were monitored. The test demonstrated irreversibility for both hydrogels with and without antibiotic, however the G' and G'' decrease during cooling (**Figure 4**).

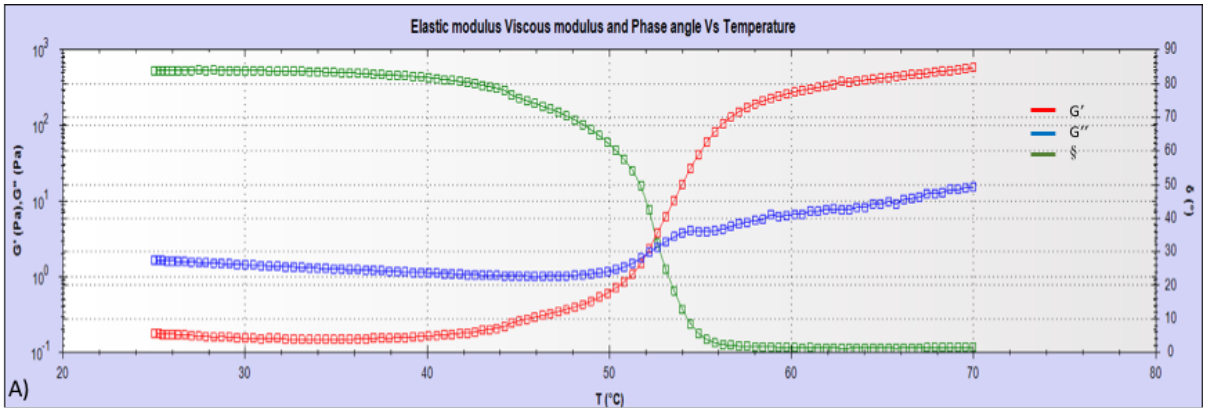

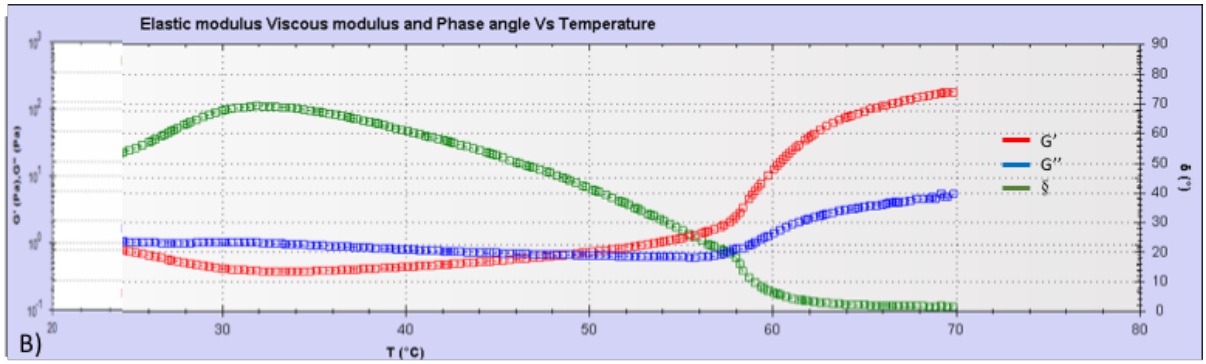

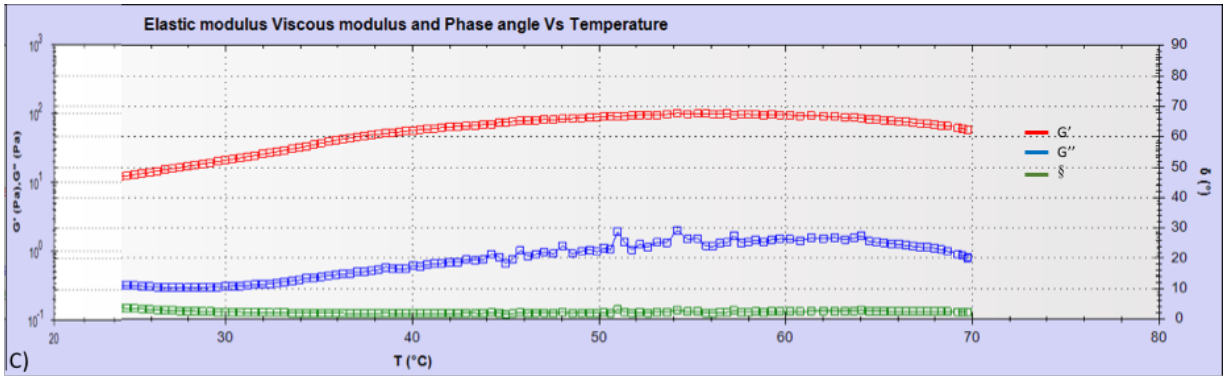

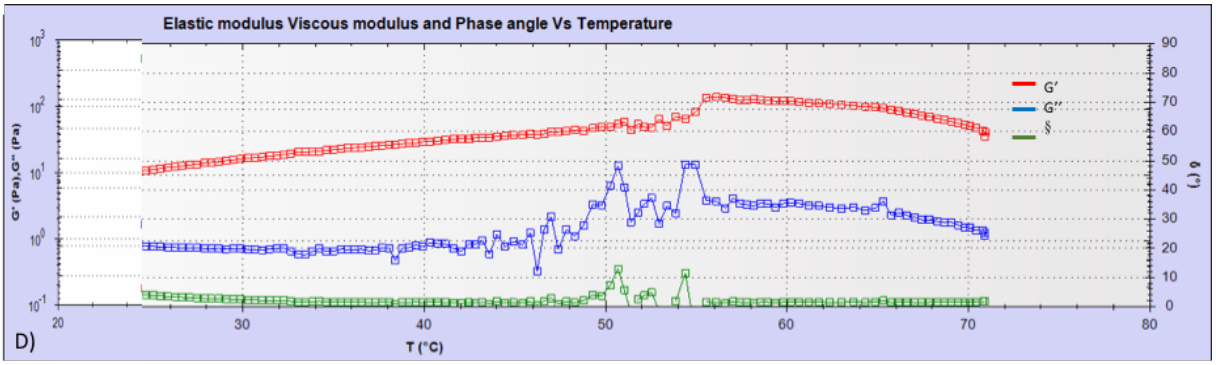

Figure 4: Temperature sweep test curves of CHT-βGP solution from 25°C to 70°C (A) and from 70° to 5°C (C) and 4 mg of gentamicin loaded into CHT-βGP solution from 25°C to 70°C (B) and 70° to 25°C (D).

The composite moldable solid matrix (freeze dried scaffolds) based on chitosan and bovine bone substitute granules were prepared by a simple protocol, reproducible and easily to scale up. 5 different techniques reported in the method section were used, in order to be able to select the most efficient technique to achieve good results in terms of scaffold porosity, yield of process, drug content. Results are reported in **Table 2**.

Positive results in term of porosity around 80-86% are obtained mCS and mS scaffold and the scaffold mCSG1, mSG1, mCSG2, mSG2, mCSG3, mSG3, mCSG5, mSG5 loaded with Gentamicin. Scaffold mCSG4 and mSG4 resulted not to be stable to the freeze-driyng process changing the original tridimensional structure in a bidimensional one. The preparation technique used involved dropping, 0.1 ml of 40mg/ml gentamicin solution, into the already formed and lyophilized scaffold. The final drug amount added to the scaffold was 4 mg, as for all scaffolds, but the higher gentamicin concentration probably causes gentamicin to significantly interact with βGP, destabilizing scaffold structure. Drug content per scaffold expressed as mg/cm^2 didn't show a significant difference depending on the preparation procedure used, and matrices composition. The drug content values are between 0.68±0.06 and 0.72±0.02 mg/cm^2 (**Table 2**) corresponding to 94-99% of encapsulation efficiency. The goal is to formulate a 3D moldable composite scaffold able to locally deliver high gentamicin concentrations, avoiding side effects due to high doses achieved by systemic administration and preventing biofilm formation. Scaffold needs to be biocompatible, with tridimensional structure in order to create an organized structure with a specific size pore distribution to enhance the fluid and nutrient exchange and spatial interaction for the cells. Scaffold degradation should be *in sink* with tissue regeneration rate avoiding infiltration of surrounding tissues, maintaining cavity integrity, preventing distorsion in tissue rearrangement process.

Table 2: Composition and characterization of moldable scaffold and moldable composite scaffold placebo and loaded with Gentamicin.

Scaffold code	CL213 (% w/v)	βGP (% w/v)	BBS (mg)	Gent (mg)	Drug Content (mg/cm^2)	Porosiy (%)	Yield process (%)
mCS	2	10	200	-	-	83,12±2.11	86,66±5,73
mS	2	10	-	-	-	80.23±3.21	63.37±2.52
mCSG1	2	10	200	4	0.69±0.06	81.17±1.44	80.31±6.94
mSG1	2	10	-	4	0.70±0.05	79.82±2.71	64.27±1.63
mCSG2	2	10	200	4	0.71±0.04	81.26±2.55	79.61±0.56
mSG2	2	10	-	4	0.70±0.03	78.45±3.27	68.32±0.32
mCSG3	2	10	200	4	0.72±0.02	85.53±2.18	82.43±1.21
mSG3	2	10	-	4	0.71±0.04	82,42±1.81	85.53±2.76
mCSG4	2	10	200	4	0.71±0.02	75.63±2.64	80.8±0.25
mSG4	2	10	-	4	0.68±0.06	72.46±2.45	62.95±5.53
mCSG5	2	10	200	4	0.70±0.02	86.21±2.32	82.94±3.35
mSG5	2	10	-	4	0.72±0.03	81.24±2.38	63.21±2.55

mCSG3 and mCSG5 showing the best properties in terms of porosity, yield process and drug content, were selected for a deeper characterization in terms of functional properties such as rehydratation capacity, water uptake, water retention, wettability (contact angle). Rehydratation ability, expressed as time (min) needed to complete scaffold rehydratation, was 5 minutes, that is optimal for an immediate use. Moreover, the rehydratated composite scaffolds are easy to handle (after rehydratation) without phenomena of breaking or loss of bovine bone granules following application of a stress simulating surgeon action when implanting the scaffold into body cavity. Gentamicin addition doesn't significantly influence rehydratation time. In terms of water uptake and retention, mCS, mS mCSG3 and mCSG5 are able to absorb high amounts of water (253.96±10.3 to 306.4±7.5 %) and more than 50 % of the absorbed water is retained in the polymer matrix after centrifugation (163.14±5.5 to 180.7±5.8 %). Water uptake is suitable for nutrients and oxygen exchange between external environment and polymer matrix in addition to promoting metabolites release from matrix in the fluids surrounding polymer matrix. Scaffold ability to hold water should promote cell adhesion since cells find an environment suitable for their attachment and proliferation as reported in the

literature [24]. The PL scaffold without BBS granules (mS) is able to absorb and retain higher percentage of water compared to the matrices prepared by combining the polymer with inorganic component (PLc, mCSG3 an mCSG5). Gentamicin addition to scaffold doesn't have an important effect on scaffold ability to absorb and retain water. To complete scaffolds characterization, rehydrated scaffold diameter was measured after soaking in PBS for 20 minutes, 10 hours and 7 days, range from ≈23 % to ≈ 53.84 % of swelling (**Table 3**). No significant diameter changes were detected after 7 days. Scaffold stability was demonstrated also by their ability in retaining BBS granules during all the incubation time.

Table 3: Scaffold functional characterization

Properties	**Scaffold code**			
	mCS	**mS**	**mCSG3**	**mCSG5**
Rehydration time (sec)	5	4	5	5
Wettability (%)	100±0.06	100±0.04	100±0.06	100±0.03
***Water Uptake* (%)**	253.96±10.3	306.43±7.5	260.78±8.6	270.06±7.6
Water retention (%)	163.14±5.5	176.61±6.4	160.14±6.6	180.74±5.8
Swelling (%) 20 min	23.00±4.3	23.07±5.2	30.76±6.4	23.07±4.6
Swelling (%) 10 h	46.15±4.1	53.84±4.7	53.84±4.5	46.15±5.4
Swelling (%) 7 d	46.15±3.5	53.84±2.7	53.84±3.5	53.84±3.4

SEM micographs of mCSG3 and mCSG5 show scaffolds have a tridimensional structure with a high degree of porosity and well interconnected pores. The presence of BBS granules and gentamicin doesn't interfere with the 3D structure of composite scaffold. SEM analysis show macropores with size > 100 µm and including micropores of 20-50 µm (**Figure 5**).

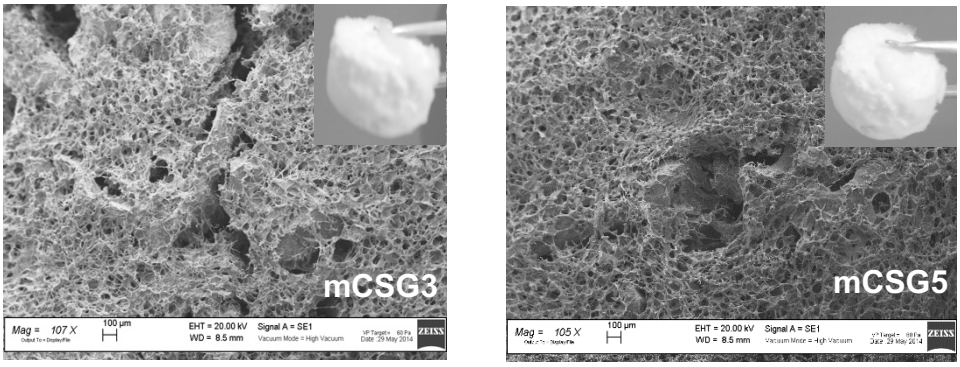

Figure 5: SEM micrographs of gentamicin loaded moldable composite scaffold (mCSG3 and mCSG5). Magnification 100X.

In vitro release study showed gentamicin release was completed in 4 hours of incubation for all scaffolds (**Figure 2a**) with the exception of scaffold mSG4 and mCSG4 showing prolonged drug release up to 120-168 hours, respectively (data not reported). However, the structure of these scaffolds was collapsed upon lyophilization, resulting in low porosity and scarce biological properties. Therefore, scaffolds mSG4 and mCSG4 cannot be considered as suitable systems combining prolonged drug release and tissue regeneration properties. There was no significant difference in gentamicin release rate between scaffold with or without BBS (mCSG and mSG respectively). The amount of Gentamicin released (mg/ml) was always above its MIC value (0.002 mg/ml), **Figure 6**. The rapid and complete release of the gentamicin can be attributed to antibiotic diffusion through the polymer matrix. Moreover, incorporation of a drug, positively charged at pH 7.4, and its rapid release seem not affect substantially scaffold stability [26].

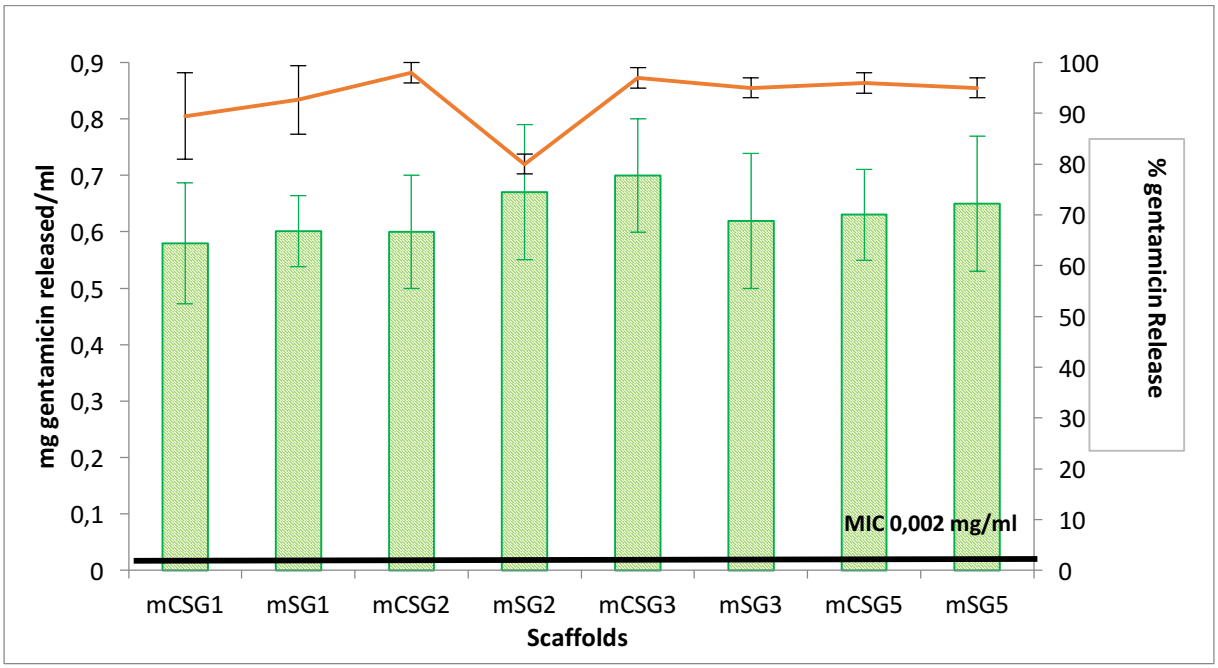

Figure 6: 4 hours *in vitro* release of gentamicin loaded scaffolds mCSG1-5 and mSG1-5 incubated at 37°C in PBS, expressed asreleased % (y right axis) and mg of gentamicin released (y left axis).

Gentamicin loaded scaffolds were tested on *Escherichia coli* ATCC 10356, for their antimicrobic activity (**Figure 7**) showing the antibacterial activity of gentamicin released from the scaffolds is maintained for 24 hours. Placebo composite scaffold (mCS) show antibacterial activity in the first 4 hours incubation with *Escherichia coli:* the behavior is consistent with chitosan antibacterial activity reported in the literature. Antibacterial activity shown by gentamicin loaded scaffolds should take into account this synergistic effect.

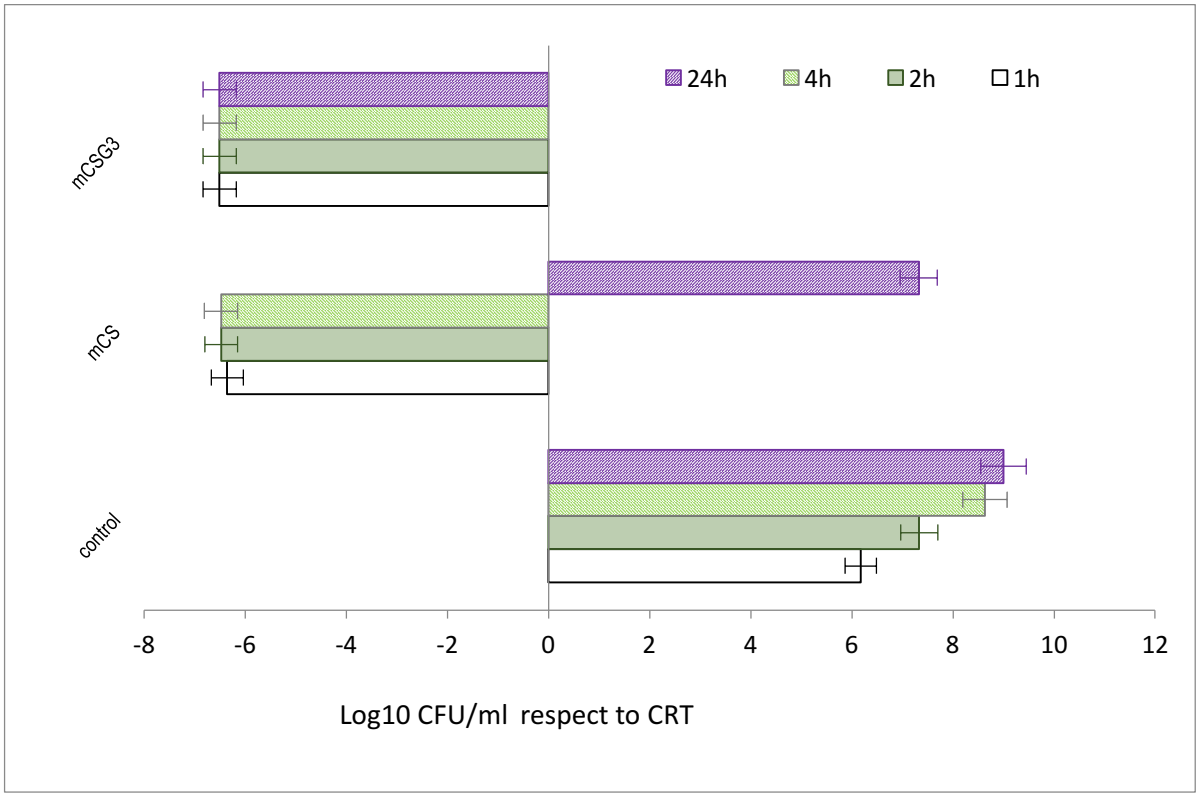

Figure 7: Gent-loaded moldable composite scaffolds (mCSG3) antibacterial activity against *Escherichia coli* ATCC 10356, expressed as change in number of Colony-forming unit (cfu) from initial inoculum. Placebo moldable scaffold (mCS) was used as reference, *Escherichia coli* ATCC 10356 10^8, inoculum was used as control. Data are means and standard deviation of least three independent determinations. MIC 2 µg/ml.

In vitro cytotoxicity study was carried out before *in vitro* proliferation test in order to evaluate possible toxic effect of gentamicin on fibroblast cell line model. Gentamicin concentration range between 1-0.54 mg/ml simulated gentamicin amount released *in vitro* (**Figure 8**).

Cell viability percentages shown in **Figure 8,** demonstrate gentamicin isn't toxic at the concentration tested and doesn't interfere with cell metabolism.

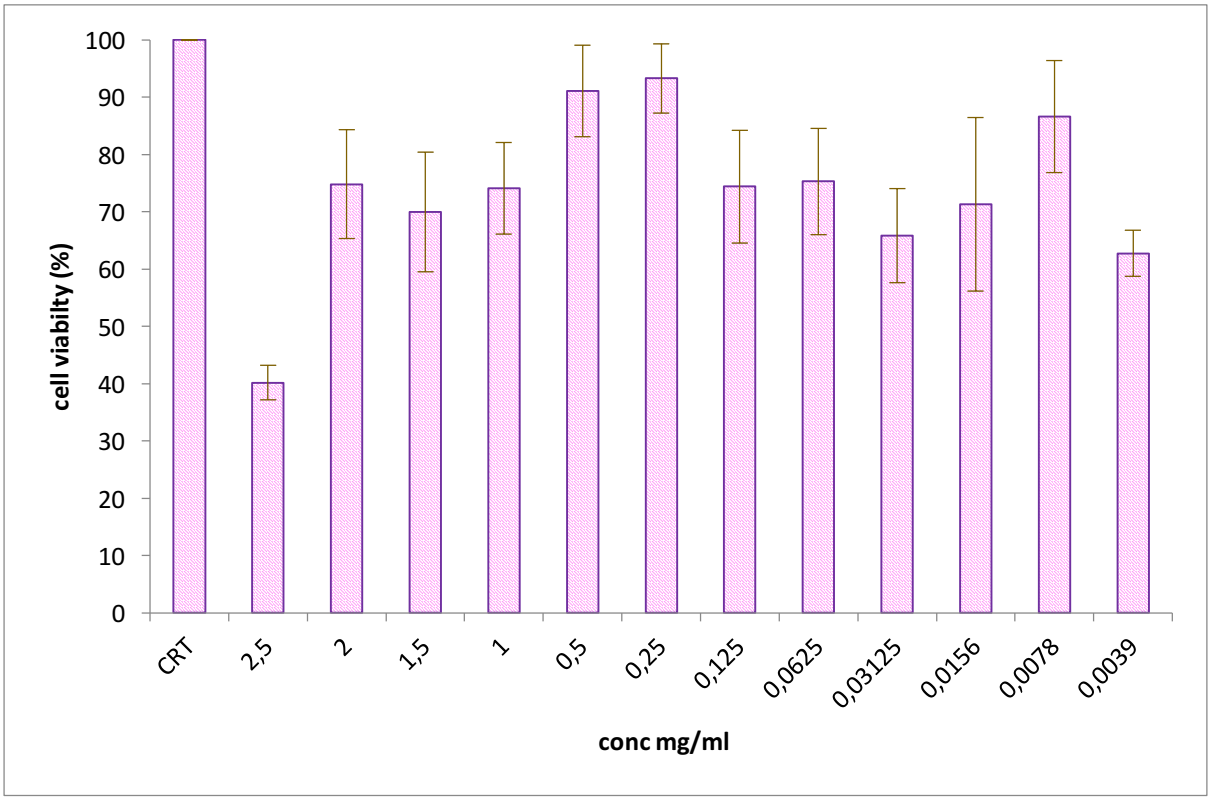

Figure 8: *In vitro* cytotoxicity of gentamicin solutions from 2.5 to 0.0039 mg/ml in DMEM 10% (v/v) FBS, at 37°C and 5% CO_2. Concentration range between 1 and 0.54 mg/ml correspond to the mg of gentamicin/ml released from scaffold.

The results obtained from cell seeding study in **Figure 9** show greater efficiencies for the composite scaffold (mCSG1-5 and mCS) with respect to polymeric scaffold (mSG1-5 and mS). This can be attributed to stiffness of containing BBS composite scaffold promoting cells adhesion. The presence of BBS makes scaffold more stable with a rigid structure after incubation in DMEM at 37°C, 5% CO_2. Gentamicin addition doesn't interfere with cell adhesion on both scaffold surface, containing or not BBS. The best results in term of cell adhesion were observed for composite gentamicin loaded scaffold prepared with technique 3 and 5. These scaffolds (mCSG3 and mCSG5) confirmed to give the best results in terms of structural properties (porosity and pore size) as previously reported (**Table 2**).

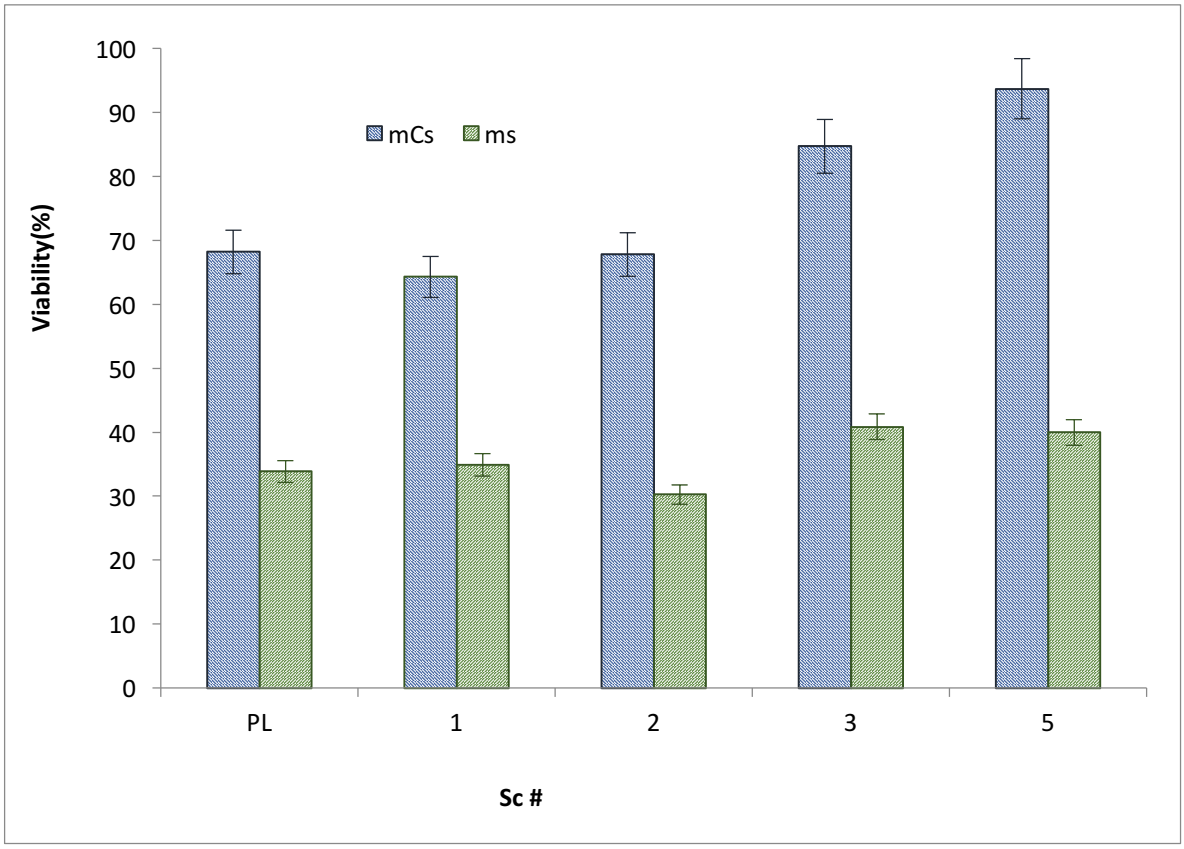

Figure 9: Cell seeding capacity of modable composite scaffold (mCS and mCSG1-5) moldable polymeric scaffolds (mS and mSG1-5). Time of culturing 3h in DMEM 10% (v/v) FBS, at 37°C and 5% CO_2.

Proliferation study was monitored for a short time, 4 and 7 days as reported in **Figure 10**. 2D cultured fibrolasts are the positive control. Composite placebo scaffolds (mCS) shown increased proliferation with respect to polymeric scaffolds (mS) after 4 and 7 days. Gentamicin addition doesn't inhibit the cell proliferation. Most promising results were obtained for scaffolds prepared with protocols 3 and 5. **Figure 10**, shows an important increase of Abs values at 7^{th} day of incubation for both composite (mCSG3 and mCSG5) and polymeric scaffolds (mSG3 and mSG5). In particular scaffold mCSG5, after 7 days of incubation increased of 50% cell growth with respect to 4^{th} day. The low Abs values for scaffolds prepared by techniques 1 and 2 are attributed to their low porosity (78.4±3.2-81.2±2.5%). Scaffolds prepared by techniques 4 were not tested because they collapsed during lyophilization.

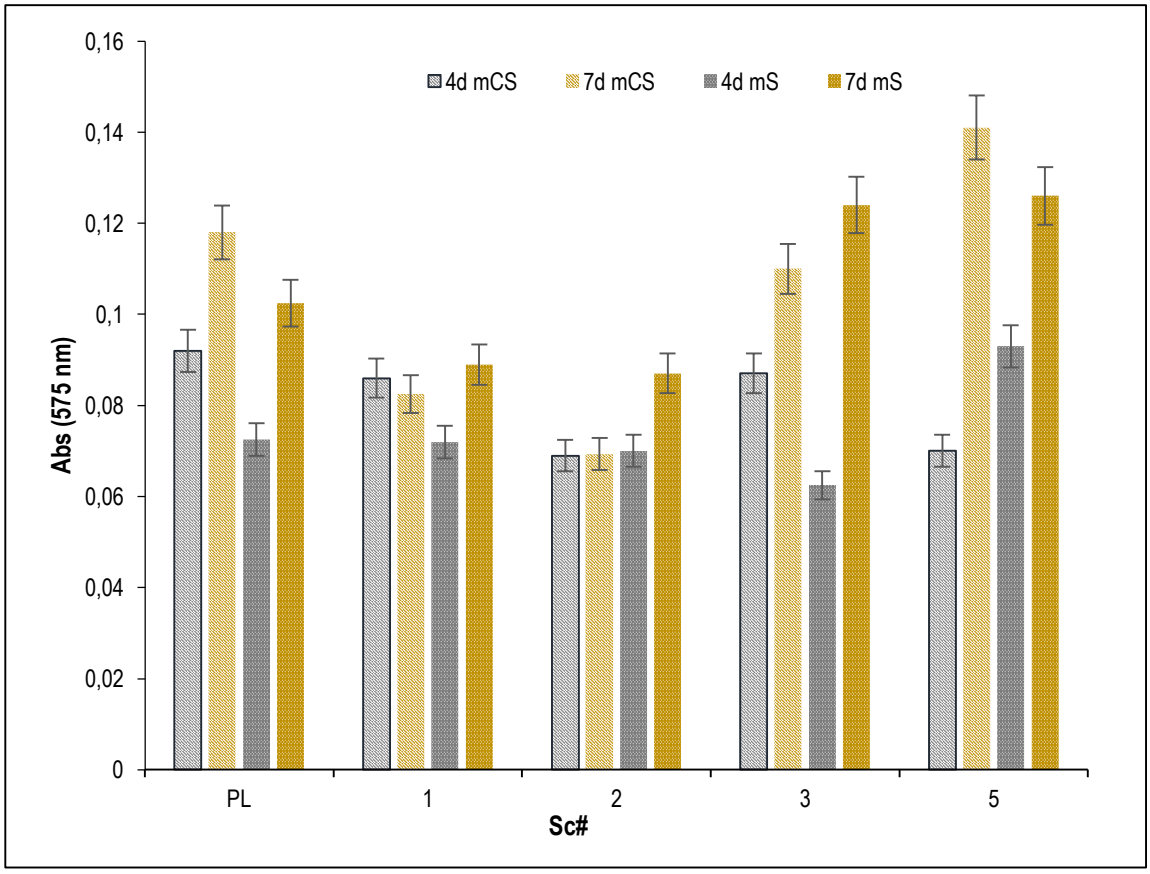

Figure 10: Results of cell proliferation study in DMEM 10% (v/v) FBS, at 37°C and 5% CO_2. Seeding density: 200000 cells/Scaffold.

5. CONCLUSIONS

Chitosan thermosetting hydrogel loaded with gentamicin have been successfully prepared and the amounts of gentamicin giving low viscosity solutions, easily to be injected, and a thermosetting gel have been suitably set up. Attention was addressed to rapid gelification, obtained with the amount of gentamicin loaded and presenting several advantages: i) to facilitate BBS administration as filler of a bone cavity, ii) to prevent loss and consequent distribution of BBS in the surrounding tissue when the liquid suspension is injected in bone cavity, iii) to promote an intimate contact between composite hydrogel and surrounding tissue improving stem cells migration inside scaffold. Moreover, the proposed hydrogel can be spread on prothesis surfaces before implant, in order to reduce infection risk. Freeze-dried moldable composite scaffolds loaded with gentamicin were successfully prepared with suitable properties to be used as filler in bone surgery with anti-osteomyelitis property in order to obtain a stable scaffold for an immediate application by the surgeon. They show 3D structure , cylindrical shape with size of 1.3 cm (diameter) and 0.7 cm (height), they are easily to remodel manually, to cut according to the site of application, so they can be designed to fit with bone

defect and they have a complete and spontaneous rehydration in buffer solution (5 minutes rehydratation time). Meanwhile the loaded gentamicin can provide antibacterial effect in the first stage of therapy, due to the high gentamicin concentration that can be achieved locally in short time (4 hours). Moreover, the technique used to load gentamicin sulphate influences chemical-physical properties and biological performances of the moldable composite scaffold.

6. REFERENCES

[1] Chemotherapy Ksf., Clinical guidelines for the antimicrobial treatment of bone andd joint infection in Korea. Infection and Chemotherapy 46 (2) (2014)

[2] B.Snoddy, J. Ambalangodage, The use of nanomaterials to treat bone infections. Materials Science and Engineering C67 (2016); 822-833.

[3] M. Aviv, I. Berdicevsky, M. Zilberman, Gentamicin-loaded bioresorbable films for prevention of bacterial infections associated with orthopedic implants. journal of Biomedical Materials Research Part A (2006) DOI: 10.1002/jbm.a.31184.

[4] Y.Chang, Tai C-L, Hsieh P-H, Ueng S.W.N, Gentamicin bone cement. Bone Joint Res 2 (No.10) (2013), 220-222.

[5] G-JAt Boo., A. Daniel Arens, W-J Metsemakers, S. Zeiter, R. Richards, D.W. Grijpma, D.Eglin, T.F. Moriarty, Injectable gentamicin-loaded thermo-responsive hyaluronic acid derivative prevents infection in a rabbit model. Acta Biomaterialia 43, (2016) 185-194.

[6] GD Ehrlich, P.Stoodley, Ph.D1, S.Kathju, Y.Zhao, B. R. McLeod, N. Balaban, F.Z. Hu, N.G. Sotereanos, J.W. Costerton, P.S. Stewart, J. Christopher, and Qiao Lin, Engineering Approaches for the Detection and Control of Orthopaedic Biofilm Infections. 437 (2005) 59-66.

[7] M.Zilberman, J.J. Elsner, Antibiotic-eluting medical devices for various applications. Journal of controlled release 130 (2008) 202-215.

[8] T.A.G. van Vugt, J. Geurts, and J. J. Arts Clinical application of antimicrobial bone graft substiutes in ostemyelitis treatment: a systemic review of different bone graft substitutes available in clinical treatment of osteomyelitis. BioMed Research International Volume 2016 (2016) 9 pages.

[9] P.Mihok, J. Murray, R. Williams. Novel antibiotic delivery and novel antimicrobials in prosthetic joint infection. JTO Peer-Reviewed Articles 4 (2016) 52-54.

[10] O.S. Kluin, H.J. Busscher, D. Neut, H.C. van der Mei, Poly(Trimethylene Carbonate) as a carrier for Rifampicin and Vancomycin to target therapy-recalcitrant Staphylococcal Biofilms. Journal of orthopaedic research (2016) 1828-1837.

[11] R.Dorati, C. Colonna, I. Genta, A. De Trizio, T. Modena, H. Kloss, B. Conti, In vitro characterization of an injectable in situ formining composite system for bine regenration. Polymer Degradation and Stability 119 (2015) 151-158.

[12] Z.Xie, X. Cui, C. Zhao, W. Huang, J. Wang, C. Zhanga, Gentamicin-loaded Borate Bioactive Glass eradi ates osteomyelitis due to Escherichia coli in a rabbit model. Antimicrobial Agents and Chemotherapy 57 (2013) 3293-3298.

[13] N.Dunne, F. Buchanan, J. Hill, C. Newe, M.Tunney, A. Brady, and G. Walker , *In vitro* testing of chitosan in gentamicin-loaded bone cement No antimicrobial effect and reduced mechanical performance. Acta orthopaedica79 (6) (2006) 851-860.

[14] Knaepler H. Local appliaction of gentamicin-containing collagen implant in the prophylaxis and treatment of surgical site infection in orthopaedic surgery. International Journal of Surgery 10 (supplement 1) (2012) S15-S20.

[15] DC.Coraca-Huber, A. Wurm, M. Fille, J. Hausdorfer, M. Nogler, K-D Ku, Effect of freezing on the release rate of gentamicin palmitate and gentamicin sulfate from bone tissue. Journal of orthopaedic research (2014) 842-847.

[16] R.Dorati, C. Colonna, I. Genta, T. Modena, B. Conti, Effect of porogen on the physico-chemical properties and degradation performence pf PLGA scaffold. Polymer Degradation and Stability 95 (2010) 694-701.

[17] H.Winkler, P. Haiden, Treatment of chronic bone infection. Operative technique in orthopaedic 26 (Issue 1) (2016) 2-11.

[18] AF. Ismail, M. Awang, F. Mohamed**,** High initial burst release of gentamicin formulated as PLGA microspheres implant for treating orthopeadic infection. Int J Pharm Pharm Sci 4 (Supll 4) (2012) 686-691.

[19] R.Dorati, A. DeTrizio, I. Genta, P. Grisoli, A. Merelli, C.Tomasi, B. Conti, An experimental design approach to the preparation of pegylated polylactide-co-glicolide gentamicin loaded microparticles for local antibiotic delivery. Materials science and engineering C C58 (2016) 909-917.

[20] Thevenot P., A. Nair, J. Dey, J. Yang, and L. Tang, Method to analyze three-dimensional cell distribution and infiltration in degradable scaffold. Tissue Engineering Part C 14(Number 4) (2008) 319-331.

[21] M.Lavertu, D. Filion, and M-D. Buschmann, Heat-induced transfer of protons from chitosan to glycerol phosphate produces chitosan precipitation and gelation. Biomacromolecules 9 (2008) 640-650.

[22] V S.Van.lierberghe, P. Drubruel, and E. Schacht, Bioplolymer-based hydrogels as scaffold for tissue engineering apllications: a Review. Biomacromolecules 12 (2011) 1387-1408.

[23] G. A. ter Boo, D. Arens, W-J. Metsemakers, S. Zeiter, R. G. Richards, D. W. Grijpma, D. Eglin, T. F. Moriarty,

Injectable gentamicin-loaded thermo-responsive hyaluronic acid derivative prevents infection in a rabbit model. Acta Biomaterialia 43 (2016) 185-194.

[24] R.Freitag, and F. Garret-Flaudy, Salt effect on the thermoprecipitation of Poly-(N-isopropylacrylamide) Oligomers from acqueous solution. Langmuir 18 (2002) 3434-3440.

[25] H-I.Chang, and Y. Wang, Cell responce to surface and architecture of tissue engineering scaffolds. Regenerative medicine and tissue engineering-Cells and Biomaterials 27 (2011).

[26] S.Supper, N. Anton, J. Boisclair, N. Seidel, M. Riemenschnitter, C. Curdy, T. Vandamme, Chitosan/glucose 1-phosphate as new stable in situ forming depot system for controlled drug delivery. European Journal of Pharmaceutics and Biopharmaceutics 88 (2014) 361-373.

Chapter III

CHAPTER III

AN EXPERIMENTAL DESIGN APPROACH TO THE PREPARATION OF PEGYLATED POLYLACTIDE-CO-GLICOLIDE GENTAMICIN LOADED MICROPARTICLES FOR LOCAL ANTIBIOTIC DELIVERY

ABSTRACT

The present paper takes into account the DOE application to the preparation process of biodegradable microspheres for osteomyelitis local therapy. With this goal gentamicin loaded Polylactide-co-glycolide-co-polyethylenglycol (PLGA-PEG) microsphere were prepared and investigated. Two preparation protocols (o/w and w/o/w) with different process conditions, and three PLGA-PEG block copolymers with different composition of lactic and glycolic acid and PEG, were tested. A Design Of Experiment (DOE) screening design was applied as an approach to scale up manufacturing step. The results of DOE screening design confirmed that w/o/w technique, the presence of salt and the 15% w/v polymer concentration positively affected the EE% (72.1-97.5%), and span values of particle size distribution (1.03-1.23), while salt addition alone negatively affected the yield process. Process scale up resulted in a decrease of gentamicin EE% that can be attributed to the high volume of water used to remove PVA and NaCl residues. The results of *in vitro* gentamicin release study show prolonged gentamicin release up to three months from the microspheres prepared with salt addition in the dispersing phase; the behavior being consistent with their highly compact structure highlighted by Scanning Electron Microscopy analysis. The prolonged release of gentamicin is maintained even after embedding the biodegradable microspheres into a thermosetting composite gel made of Chitosan and acellular bovine bone matrix (orthoss® granules), and the microbiologic evaluation demonstrated the efficacy of the gentamicin loaded microspheres on *E. coli*. The collected results confirm the feasibility of the scale up of microsphere manufacturing process and the high potential of the microparticulate drug delivery system to be used for the local antibiotic delivery to bone.

Keywords: DoE, Gentamicin, Osteomyelitis, Microspheres, Polylactide-co-glycolide, Polyethylenglycol, bone delivery.

This chapter is based on the following publication:

Materials Science and Engineering C 58 (2016) 909 e 917 Elsevier.

R.Dorati, A. De Trizio, I. Genta, P. Grisoli, A. Merelli, C. Tommasi, B. Conti

1.INTRODUCTION

Quality by Design (QbD) is a rational and orderly paradigm for developing drug products with enhanced quality and robustness, while emphasizing science and risk-based product and process understanding. Therefore, the QbD approach is important also in the early stages of design and development of a drug delivery system. In these terms Design of Experiments (DoE) can help in the selection and set up of a robust preparation process.

The present paper takes into account the DoE application to the preparation process of biodegradable microspheres for osteomyelitis local therapy. Among the postoperative orthopaedic infections, osteomyelitis, mainly caused by *Staphiloccus Aureus*, still remains a severe issue. It frequently develops as a nosocomial infection and can arise from different causes such as implantation of a prosthesis, or a temporary bacteraemia leading to biofilm adhesion and growth on the biomaterial surface. Progressive bone destruction and the formation of sequestra are common osteomyelitis consequences, which are mainly caused by contiguous spread of infection, hematogenous seeding or direct inoculation of microorganisms into intact bone. These infections are particularly complicated and debilitating in immune-compromised patients. The therapy generally involves, a systemic antibiotic treatment from four to six weeks and can develop several undesired side effects as systemic toxicity, patient discomfort and bacterial resistance. Due to these drawbacks, local antibiotic administration has been recognized the key point to improve the treatment of osteomyelitis minimizing the side effects that can rise upon prolonged systemic antibiotic treatment [1, 2]. Gentamicin is an aminoglycoside antibiotic, extensively used for treating many types of infections because it presents a wide bacterial spectrum. However, it has low bioavailability after oral administration and poor cellular penetration, in addition the internalized gentamicin molecules are accumulated into the lysosomial compartment with reduction of its activity. Following parenteral administration gentamicin is rapidly excreted by glomerular filtration resulting in a plasma half-life of 2 h in patients with normal renal function, while its half-life in the renal cortex is 100 h. Therefore, repetitive doses of gentamicin result in renal accumulation and nephrotoxicity. Moreover, also ototoxicity can rise in the prolonged administration of gentamicin due to free radical formation.

For these reasons local delivery of gentamicin was studied, and innovative preparations based on cement and polymeric beads are on the market. Presently inert polymethylmethacrylate (PMMA) beads represent the gold standard for the prevention and the local treatment of chronic osteomyelitis [2]. However, these systems have few disadvantages: manufacturing through methyl acrylate polymerization partially inactivates the antibiotic; the drug delivery systems have low biocompatibility, the active agent release is incomplete and the residual slow release of low amounts of antibiotic

enhances the risk of resistance phenomena. Moreover, the system should be removed when exhausted, with possible problems arising from a second surgery.

The usefulness of biodegradable microspheres loaded with gentamicin is demonstrated by several studies found in the literature involving synthetic biodegradable polymers such as polylactide-co-glycolide, polylactide, polylactide-PEG, and natural polymers such as polyhydroxybutirate and chitosan [3-10]. The biodegradable polymers have the advantage that they do not need to be removed when the drug is exhausted because they degrade and completely disappear from the body. Moreover, the drug release rate and behavior can be modulated at great extent by choosing polymers with different compositions, molecular weights, and also by blending together polymers, or microspheres made of different polymers. It is well known that osteomyelitis treatment needs a burst high dose of antibiotic, to attack the infection, followed by a maintenance one, to completely eradicate it.

Starting from this background, the present study is addressed to the preparation of biodegradable microparticles loaded with gentamicin, and it is focused on the preparation method optimization and scale up through DOE screening. Polylactide-co-glycolide-Polyethylenglycol polymers are here investigated, due to their good biocompatibility and hydrophilic lipophilic molecular balance. DOE has been applied on: *i)* the selection of the type of pegylated polymer for gentamicin (Gent) encapsulation and the suitable technique for the microparticles preparation, *ii)* the process parameters optimization, *iii)* the Gent-loaded microparticles characterization in terms of drug entrapment.

Moreover, a preliminary "in vitro" drug release test simulating the final local drug delivery system is here proposed by an *in situ* forming composite gel made of crosslinked Chitosan/Orthoss ®. The composite *in situ* forming gel should be able to preserve the antibiotic activity, and provide a prolonged release of the antibacterial agent, promoting the cellular penetration and modulating the cellular distribution in order to achieve a more effective therapy for the prevention and treatment of osteomyelitis infection [11].

2.MATERIALS

Gentamicin sulphate (GentamicinC1 $C_{21}H_{43}N_5O_7$, Mw 477.6 g/mol, GentamicinC2 $C_{20}H_{41}N_5O_7$, Mw 463.6 g/mol, GentamicinC1a $C_{19}H_{39}N_5O_7$, Mw449.5 g/mol, was from Sigma Aldrich. PLGA (7525 DLG 3E Mw 35 kDa), Polylactide-co-glycolide-co-polyethylenglycol (PLGA-PEG): 7525 DLG 3C PEG 6000, Mw 45kDa, PEG 60%, 5050 DLG 4C PEG 1500, Mw 47 kDa PEG % 51, 5050 DLG 5C PEG 1500 Mw 70 kDa, PEG 51%), were from Lakeshore Biomaterials, Birmingham, AL, USA. PVA (Mw 85-124 kDa 87-89% hydrolysed), PVA (Mw 85-124 KDa 87-89% hydrolized), methylene chloride, dimethyl sulfoxide, sodium chloride, ninhydrin, Mw 178,14 g/mol, glycerol phosphate disodium salt (β-GP), 216.16 Mw, were from Sigma Aldrich, Milan, Italy.

Orthoss® granules 1-2 mm diameter were granted by Geistlich-Pharma-CH-6110 Wohlusen, Switzerland, as commercially available.

Chitosan chloride CL 213,350-300 kDa was from Pronova (Pronova Biopolymers FMC, 1337 Sandvika, Norway).

3.METHODS

3.1. Microsphere preparation

Two different microparticles preparation methods were evaluated: method 1) single emulsion solvent evaporation, and method 2) double emulsion solvent evaporation.

Each method was performed with four different polymers: one type of PLGA- capped homopolymer and three types of PLGA-PEG uncapped block copolymer n-m-n, where n is PLGA chain and m is the PEG chain.

The 7525 DLG 3E polymer was chosen because of its molecular structure with ends capped esterified carboxyls that inhibits any charge-interaction between the gentamicin positively charged aminogroups. Since the goal was to produce microspheres made of pegylated PLGAs, the capped 7525 DLG 3E polymer was used as control for the development of microspheres.

The 7525 DLG 3C PEG 6000, 5050 DLG 4C PEG 1500, 5050 DLG 5C PEG 1500 block copolymers are biodegradable, biocompatible and FDA authorized for human use. The pegylated polymers have been chosen because they give to microspheres stealth behavior preventing macrophages phagocytosis thus prolonging the duration of the therapeutic effect.

Moreover, the block copolymers have been selected for their hydrophilicity which should facilitate the encapsulation of water-soluble molecules, such as gentamicin. Since the microspheres will be incorporated into an hydrophilic gel polymer matrix made of chitosan, their hydrophilic character can facilitate their homogeneous distribution in the gel.

Method 1) was performed as follows: 10 mg of Gentamicin sulphate was dispersed in 1.2 ml of methylene chloride (DCM) containing the polymer (10-15 % w/v concentration). The dispersion was emulsified with 32 ml of 2% w/v PVA aqueous solution under mechanical stirring (350 rpm for 150 minutes).

Method 2) was performed as follows: 10 mg of gentamicin was dissolved in 133 µl of filtered water, the aqueous solution was dropped into an organic solution containing the polymer dissolved in methylene chloride (10-15 % w/v). The w/o emulsion was kept under mechanical stirring (700 rpm) for 2 minutes. The system was ice-cooled during the process. The first emulsion was dispersed under mechanical stirring in a second aqueous phase made of 32ml 2% w/v PVA solution, to form a double

emulsion. The system was kept under continuous stirring, (350 rpm) for 150 minutes. NaCl (5 % w/v) was dissolved in the external phase of the double emulsion. This salt concentration was used to create an hyperosmotic environment in the external aqueous phase that prevents drug leaking from the microspheres during the preparation process [12].

Both preparation methods were accomplished by two hours solvent evaporation at room temperature. Afterwards the solid microspheres were recovered through centrifugation (3000 rpm for 15 minutes), washed with distilled and filtered (10ml) water, filtered through 0.45 µm AA Millipore membrane (Millipore Corporation, Milano, Italy) and lyophilized (Lio 5P, Cinquepascal s.r.m., Milano, Italy).

Microsphere batch composition and preparation methods are listed in **Table 1**. Each batch was prepared in triplicate.

Table 1: Microsphere batches composition, preparation methods, particle size and Span values.

Batch	Prep Method	Polymer		NaCl (w/v %)	Particle size d_{90} µm	Span
		Type	Conc. (w/v)			
Ms-1	o/w	7525 DLG 3E (capped)	10	-	440.52	3.5
Ms-2	o/w	7525 DLG 3C PEG 6000	10	-	600.03	3.9
Ms-3	o/w	5050 DLG 4C PEG 1500	10	-	567.03	2.8
Ms-4	o/w	5050 DLG 5C PEG 1500	10	-	176.20	3.2
Ms-5	w/o/w	7525 DLG 3E (capped)	10	-	224.66	2.9
Ms-6	w/o/w	7525 DLG 3C PEG 6000	10	-	153.81	3.0
Ms-7	w/o/w	5050 DLG 4C PEG 1500	10	-	290.91	2.0
Ms-8	w/o/w	5050 DLG 5C PEG 1500	10	-	306.74	2.5
Ms-9	w/o/w	7525 DLG 3E (capped)	15	5	280.00	1.2
Ms-10	w/o/w	7525 DLG 3C PEG 6000	15	5	350.10	1.1
Ms-11	w/o/w	5050 DLG 4C PEG 1500	15	5	250.00	1.0
Ms-12	w/o/w	5050 DLG 5C PEG 1500	15	5	375.21	1.2

3.2. Particle size, zeta potential and morphology analysis

Microsphere particle size distribution was measured by laser light diffraction method with Mastersizer 2000 (Malvern Instrument). Microspheres were suspended in filtered water. Results are expressed as d_{90} (µm). Five replicates were performed for each analyzed sample. Zetapotential was measured on

scaled up batches of gentamicin loaded microspheres. Analysis were performed with Zetasizer 2000 (Malvern Instrument) by suspending the microspheres in flitered deionized water. Results are expressed as millivolts surface charge. Five replicates were performed for each analyzed sample.
Microsphere shape and size were analyzed by an optical microscope Opitka B-500 equipped with a digital camera Optika 4083. The images were processed with the software Micrometrics SE Premium.

3.3. Determination of encapsulation efficiency and yield process

The amount of gentamicin encapsulated into microspheres was determined by dispersing accurate weighted amounts (36mg) of microspheres in 400 µl of DMSO under mechanical stirring overnight in order to solubilize the polymer. This was followed by addition of 800 µl of filtered water to precipitate the polymer and extract gentamicin. DMSO is miscible with water; the polymer is soluble in DMSO, but insoluble in water, and it precipitates as soon as water is added to DMSO. The suspensions were centrifuged at 6000 rpm for 15 minutes to separate the polymer. The solution containing the extracted drug was analyzed by ninhydrin colorimetric assay [13, 4].
A calibration curve was obtained starting from gentamicin standards in bidistilled filtered water, at concentrations ranging between 50 and 400 µg/ml. Assay samples were mixed with freshly prepared ninhydrin reagent previously dissolved in PBS pH 7.4 (240 µl, 0,2% w/v), the mixture was vortexed and heated in a water-bath at 95°C (15 minutes) and then cooled in an ice-bath for 10 minutes. Absorbance was measured by UV-spectrophotometer at 400 nm. The blank was made of 240 µl of ninhydrin solution (0,2% w/v) and water /DMSO mixture 2:1 (800 µl).
Encapsulation efficiency was calculated with Eq (a) based on the ratio between actual gentamicin amount to theoretical loading, expressed as percentage.

$$Encapsulation\ Efficiency\ (\%) = \frac{microsphere\ actual\ drug\ content}{microsphere\ theoretical\ starting\ \ drug\ content} \times 100 \qquad (a)$$

The process yields represent the amounts of microspheres recovered starting from the stated amounts of polymer and drug. The parameter is useful to evaluate the efficiency of a manufacturing process, when combined to other parameters such as E.E. and particle size. It is expressed as a w/w percentage and calculated using the following equation:

$$Yield\ of\ process\ \left(\frac{w}{w}\%\right) = \frac{mass\ of\ microspheres\ recovered}{mass\ of\ polymer+drug} \times 100 \qquad (b)$$

3.4. Design of experiment (DOE)

On the basis of the results of the preliminary microspheres preparation experiments a DOE procedure was applied in order to set up the formulation variables.

A full factorial design was performed on each microsphere polymer composition; this is an efficient method indicating the relative significance of a number of variables. Traditional designing of pharmaceutical formulations is based on time consuming approach of changing one variable on time which doesn't take into consideration the joint effect of independent variables. Factorial design can serve as an essential tool to understand the complexity of pharmaceutical formulations.

Screening design identifies significant main effects, rather than interaction effects which are considered an order of magnitude less important.

Considering the two level full factorial design for three factors the design is 2^3. This implies eight runs (except replication or central point runs).

In tabular form, the design is given by **Table 2.**

Microsphere preparation method (Factor X_1), Polymer concentration (Factor X_2) and NaCl concentration (Factor X_3), each one at high and low setting are imposed on a production tool to determine which has the greatest effect on EE% and process yield %.

Two replications were run at each setting. A (full factorial) 2^3 design with two replications for 8*2=16runs.

Running the full complement of all possible factor combinations means that we can estimate all the main and interaction effects. There are three main effects and three to two-factors interactions as seen in this simple linear equation:

$Y= \beta_0 + \beta_1X_1+ \beta_2X_2 + \beta_3X_3 + \beta_{12}X_1X_2 + \beta_{13}X_1X_3 + \beta_{23} X_2X_3.$

Intercept= β_0

Linear terms= $\beta_1X1+ \beta_2X_2 + \beta_3X_3$

Interaction terms= $\beta_{12}X_1X_2 + \beta_{13}X_1X_3 + \beta_{23} X_2X_3$

The coefficients corresponding to linear effects (β_1, β_2 and β_3), to interactions (β_{12}, β_{13}, and β_{23}) were determined from the results of the experiments in order to identify the statically significant term.

Table 2: Three factors and 2 levels full factorial design

Run	Factor (X_1) Preparation method	Factor (X_2) Polymer concentration (% w/v)	Factor (X_3) NaCl concentration (%w/v)
1	o/w (-1)[a]	10 (-1)[a]	5 (+1)[a]
2	w/o/w (+1)	10 (-1)	5 (+1)
3	o/w (-1)	15 (+1)	5 (+1)
4	w/o/w(+1)	15 (+1)	5 (+1)
5	o/w (-1)	10 (-1)	0 (-1)
6	w/o/w (+1)	10 (-1)	0 (-1)
7	o/w (-1)	15 (+1)	0 (-1)
8	w/o/w (+1)	15 (+1)	0 (-1)

[a] Values in parentheses indicate levels of variables.

3.5. Process scale up

The block copolymer 5050DLG4CPEG1500 was exposed to scale up study upon screening design.

The scale factor was 1:7.5 with respect to pilot formulations. The compositions of the polymer, gentamicin and PVA solutions were kept constant, while volumes were increased 7.5 times.

Scaling up the process required an optimization of the protocol in terms of stirring type and speed during the first and second emulsification.

Briefly, the first emulsion was prepared dissolving 1.35 g of polymer in 9 ml of DCM (oily phase) and the obtained solution was homogenized (17500 rpm/2 minutes), by an homogenizer (Ultraturrax Model T25 S25NI8G), with 1 ml gentamicin solution consisting of 75 mg of the drug dissolved in filtered water. The primary emulsion was dispersed into the secondary aqueous continuous phase containing PVA (2% w/v) to produce the double emulsion. This emulsification step was performed by overhead Stirrers (Eurostar digital, IKA Labortechnik) at 350 rpm-min. To facilitate solvent evaporation, and the consequent microparticle formation, the system was maintained under continuous stirring for 2.5 hours at room temperature. The formulations obtained were centrifuged at 3000 rpm for 10 minutes and then washed with 60 ml of double distilled water to remove excess of salt and PVA. Then, the batches were filtered through 0.45 µm mixed cellulose ester membrane filters (Millipore membranes filters), resuspended in 1 ml of water, immediately frozen at -25°C for 12 hours and lyophilized at -48°C for 12h at a pressure of 0.01 mbar (lyophilizer, LIO 5P, Milan, Italy) in order to remove water and residual solvent, which may compromise the stability and safety of the product.

3.6. Thermal Analysis

Thermal stability of gentamicin, placebo and gentamicin-loaded microspheres scaled up batches, was evaluated by both thermogravimetric analysis (TGA) and differential scanning calorimetry (DSC).

TGA measurements were performed on 5 ÷ 10 mg specimens by means of a 2950 thermogravimetric analyzer (TA Instruments, USA), equipped with Pt sample holders. Data were collected from room temperature up to 500°C at a rate of 5°C/min, under nitrogen purge.

DSC measurements were carried out using a 2910 modulated differential scanning calorimeter (TA Instruments, USA), fitted with a standard DSC cell. Samples of 5 ÷ 10 mg were hermetically sealed in aluminium pans and subjected to thermal scans from 20°C up to their decomposition temperature at a heating rate of 5°C/min. The DSC cell was purged with dry nitrogen at 35 ml/min. The system was calibrated both in temperature and enthalpy with standard indium, and a baseline correction was performed by recording a run with empty pans.

3.7. Gentamicin *in vitro* release study from the microspheres

In vitro release study was performed on the scaled up batches by the dialysis method. 270 mg microspheres were suspended in 5ml PBS (pH 7,4) containing 0.1% w/v NaN_3 into a dialysis bag (FLOT-A-LYZER; spectra/Pore ester of cellulose with cut off DA50 KDa). The bag was introduced into a vial containing 12 ml of buffer solution. The test was carried out at 37°C and moderate stirring speed. At scheduled time intervals, 800 µl, out of the 12 ml buffer solution, was removed and replaced with fresh PBS buffer.

The amount of drug released was determined spectrophotometrically at 400 nm wavelength by ninidrin assay. The drug concentration was calculated on the basis of a calibration curve in PBS ($y=0.0029X-0.0513$, $R^2=0.9961$). Analyses were carried out on three samples for each microsphere batch.

3.8. Gentamicin *in vitro* release study from thermosetting gel embedded microspheres

In order to perform a preliminary evaluation of the final delivery system, for local administration to bone, an *in vitro* test was set up embedding the gentamicin loaded microspheres in a thermosetting composite gel, whose preparation has been explained in a previous work [14]. Briefly chitosan chloride aqueous solution (CL 213, 350-300 kDa, 2% w/v) was mixed with glycerol phosphate disodium salt (β-GP 10% w/v) at 4°C under stirring. 1 ml of thermosetting gel was added to a mixture made of 200 mg of Orthoss® granules with 200 mg of gentamicin loaded microspheres in a 24 multiwell (1.2 cm diameter). Thermosetting gel added with free gentamicin was used as control. Gelification was attained by keeping the suspensions at 37°C for 20 mins. The microspheres composite gels were placed

in 6 multiwells and incubated with 3 ml of PBS at 37°C. At scheduled times, 800µl was removed and replaced with fresh PBS buffer. *In vitro* release was followed till to completion of the antibiotic agent release.

3.9. MIC determination from gentamicin loaded microspheres

A microbiological assay was performed against *Escherichia coli* (ATCC 10536) in order to evaluate the antimicrobial properties of gentamicin loaded microparticles. Before testing, bacteria were incubated overnight in a Tryptone Soya Broth (OXOID Ltd., Basingstoke, Hampshire, UK) pH 7.3 at 37 C. Cultures were centrifuged at 224 g for 20 min to separate cells from culture broth and then resuspended in Phosphate Buffered Saline (PBS) at pH 7.3, to obtain $1x10^7$–$1x10^8$ CFU/ml. The antimicrobial activity of gentamicin loaded microparticles was evaluated by the macrodilution broth method, according to Clinical and Laboratory Standards Institute procedures. The minimum inhibitory concentration (MIC) was evaluated after 24 h incubation at 37 °C, as the lowest gentamicin concentration that completely inhibited the formation of visible microbial growth, and it was determined for gentamicin and microparticles loaded with gentamicin; placebo microparticles were used as control.

4. RESULTS AND DISCUSSION

Four different polymers were employed in the preliminary phase of the research study: one PLGA-capped homopolymer and three block copolymers with various compositions of lactic and glycolic acid and PEG percentages. The Mw of the selected polymers ranged between 35 and 70 kDa in order to obtain a prolonged release of gentamicin up to two-three months. The polymers Tg values were between 35 and 40 °C.

The process yields of the batches prepared by o/w emulsification solvent evaporation technique (Ms 1-4) ranged between 28.6 and 66.6 %, higher values (53.8-92.01%) were obtained by w/o/w (Ms 5-8) technique as shown in **Figure 1**. The w/o/w technique (Ms 5-8) also led to E.E. percentages higher (72.5-81.9%) those achieved by o/w method (Ms 1-4, 27.1-72%). The sizes resulted to be averagely smaller for the microparticles obtained by w/o/w with respect to those obtained by the o/w methods, as reported in **Table 1**. Nevertheless, the SPAN value was always very high, greater than 2, independently of the preparation method. (**Table 1**)

The high E.E. percentages observed for the microparticles obtained by the w/o/w method could be ascribed to a more stable structure of the first w/o emulsion during its dropping into the secondary continuous phase, that reduces gentamicin migration into secondary aqueous continuous phase (PVA solution). Gentamicin is an hydrophilic molecule, therefore it partially precipitates when in contact

with the organic phase in the first emulsification step l. The w/o emulsion is then dropped into the PVA solution, the organic phase diffuses into the aqueous phase and evaporates, while, the already precipitated gentamicin, is highly efficiently entrapped (≥ 50%) into the polymeric microparticles. The E.E. percentage values of microspheres based on block copolymers prepared with the w/o/w method were affected by the polymer composition and Mw. The E.E.% of microspheres made of 5050 DLG block copolymer with 51% PEG (with respect to DLG copolymer) is significantly higher (81.05-81.9% vs 73.1%) than that of microspheres made of 7525 DLG and containing 60% PEG (with respect to DLG copolymer). Comparing the polymers with the same composition and different Mws, highest E.E.% is obtained for the microspheres made of higher Mw polymers (5050 DLG 5C PEG1500; E.E.% = 81.9). This can be explained by the viscosity of the w/o emulsion that increases with polymer Mw and lead to a thicker polymer layer at the interface between oil and the external aqueous phase. In terms of microparticle size, the batch based on polymer with higher Mw shows larger d_{90} value (306.74 µm). with respect to those made of lower Mw polymer whose d_{90} value was 290.01 µm.

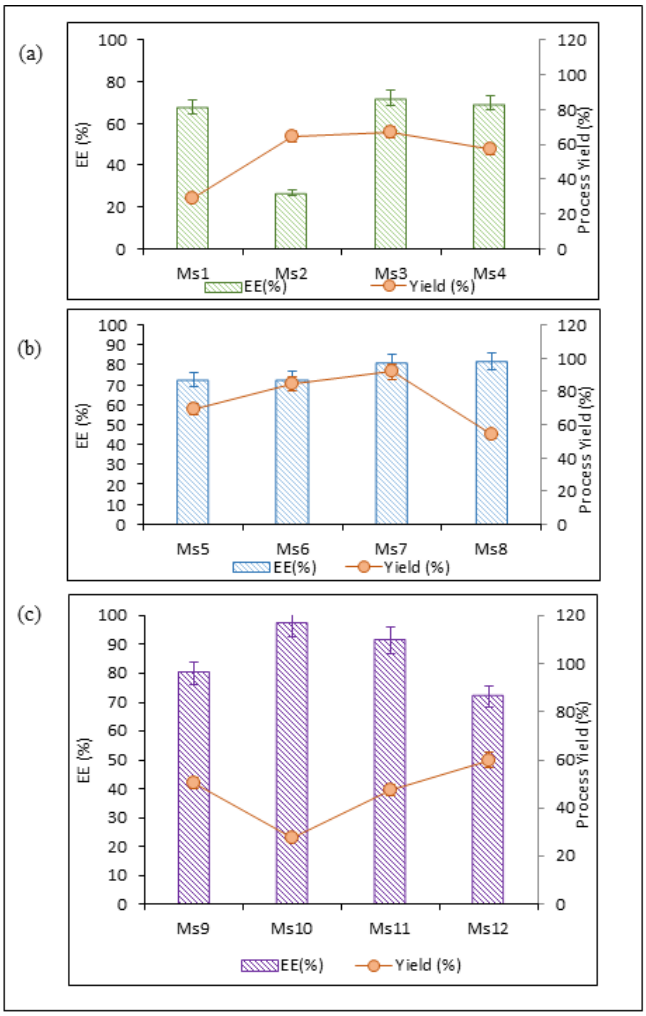

Figure 1: Entrapment Efficiency (EE%) and Process Yields (%) of microparticles (Ms) prepared by: (a) o/w (Ms1-4), (b) w/o/w methods (Ms5-8) (c) w/o/w with salt addition (Ms 9-12).

The light microscope images in **figure 2** show spherical shaped microparticles with wide particle size distribution, for the batches prepared by the single emulsion method (Ms1-4). Aggregation phenomena were detected in batches Ms 2-3 prepared by o/w single emulsion, and were absent in Ms 5-8 prepared by w/o/w emulsion. The highly regular structure shown by the microparticles of batch Ms-6 could be attributed to the high PEG content.

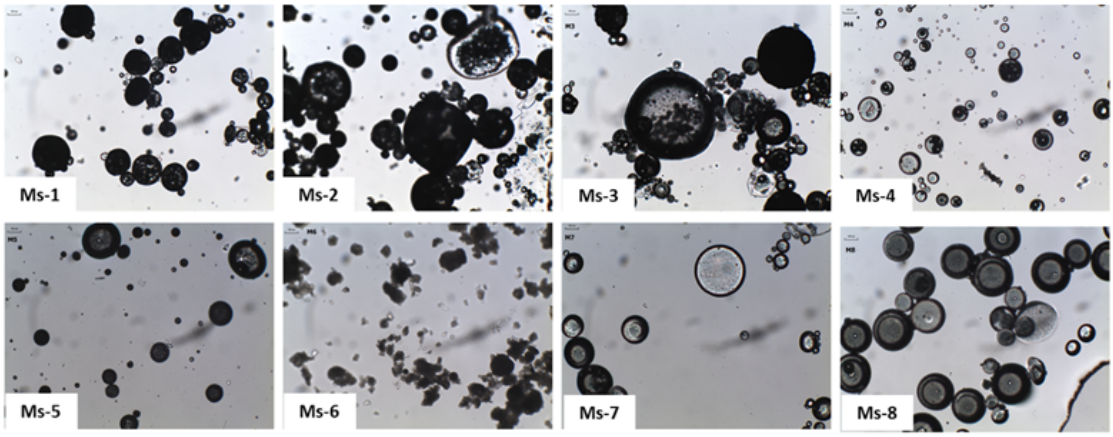

Figure 2: Optical microscope images of microparticles prepared by single emulsion o/w method (Ms-1 – Ms-4) and double emulsion w/o/w solvent evaporation method (Ms-5 – Ms-8).

Microparticles Ms 9-12, prepared by 5% NaCl addition, presented d_{90} values lower than 400 µm and narrow particle size distributions (**Table 1**); the EE% enhanced up to 97.5 % for 15 % w/v polymer concentration (**Figure 1c**). Comparing the process yield values plotted in **Figure 1c** and **1b,** salt addition seems to affect the process yields**.** The increase of E.E. could be ascribed to combined effects of the increased polymer concentration, viscosity and the osmotic pressure gradient, limiting gentamicin diffusion of into the aqueous phase. Moreover, the presence of salt in the PVA solution reduced gentamicin solubility.

As reported in the methods section a DOE study was applied to the formulation of solutions involved in the preparation process and to the preparation process as such. Microsphere preparation process (o/w; w/o/w), polymer concentration (10; 15% w/v) and NaCl concentration in the continuous phase (0; 5 % w/v) were selected as critical experimental factors of the experimental design and their effect on the encapsulation efficiencies and yields process were evaluated with a complete and reduced experimental model.

The E.E.% and process yield % showed R-squared value of 99.96% and 94.05% respectively, indicating a good fit of the linear equation. The experimental design demonstrates that only two variables

(preparation technique and polymer concentration) significantly contribute in the regression of the linear equation for measured E.E.% responses. The positive coefficient related to preparation technique indicates that double emulsion technique is the most appropriate for obtaining good E.E.%, these evidences confirm the preliminary results. The positive effect related to polymer concentration refers to the high improvement in the response (E.E.%) at increasing polymer concentrations. On the contrary the presence of NaCl in the external aqueous phase does not significantly affect E.E.% (**Figure 3a**).

The reduced model obtained subtracting the not significant interactions, between polymer and NaCl concentrations (**Figure 3b**) shows R-squared values about 99.8 % and the main factor, NaCl concentration, results are statistically significant with a positive value. The data indicate the significant role of the main factors in controlling microparticles E.E.% and the relatively little interaction role between the selected variables and the response (Y1; E.E.%).

The Pareto chart in **Figure 3c** shows that all the considered main factors and their interactions are not statistically significant towards process yield %. However, in the reduced model R-squared= 91.15% (**Figure 3d)** demonstrates that NaCl 5 % w/v concentration negatively affects the process yield. This result is consistent with the increased viscosity of PVA outer phase observed after salt addition, that affects microparticles recovering by precipitation and consequently the process yield. Moreover, the high viscosity of the external aqueous phase seems to be responsible of the particle size reduction highlighted in the batches Ms9 – Ms11.

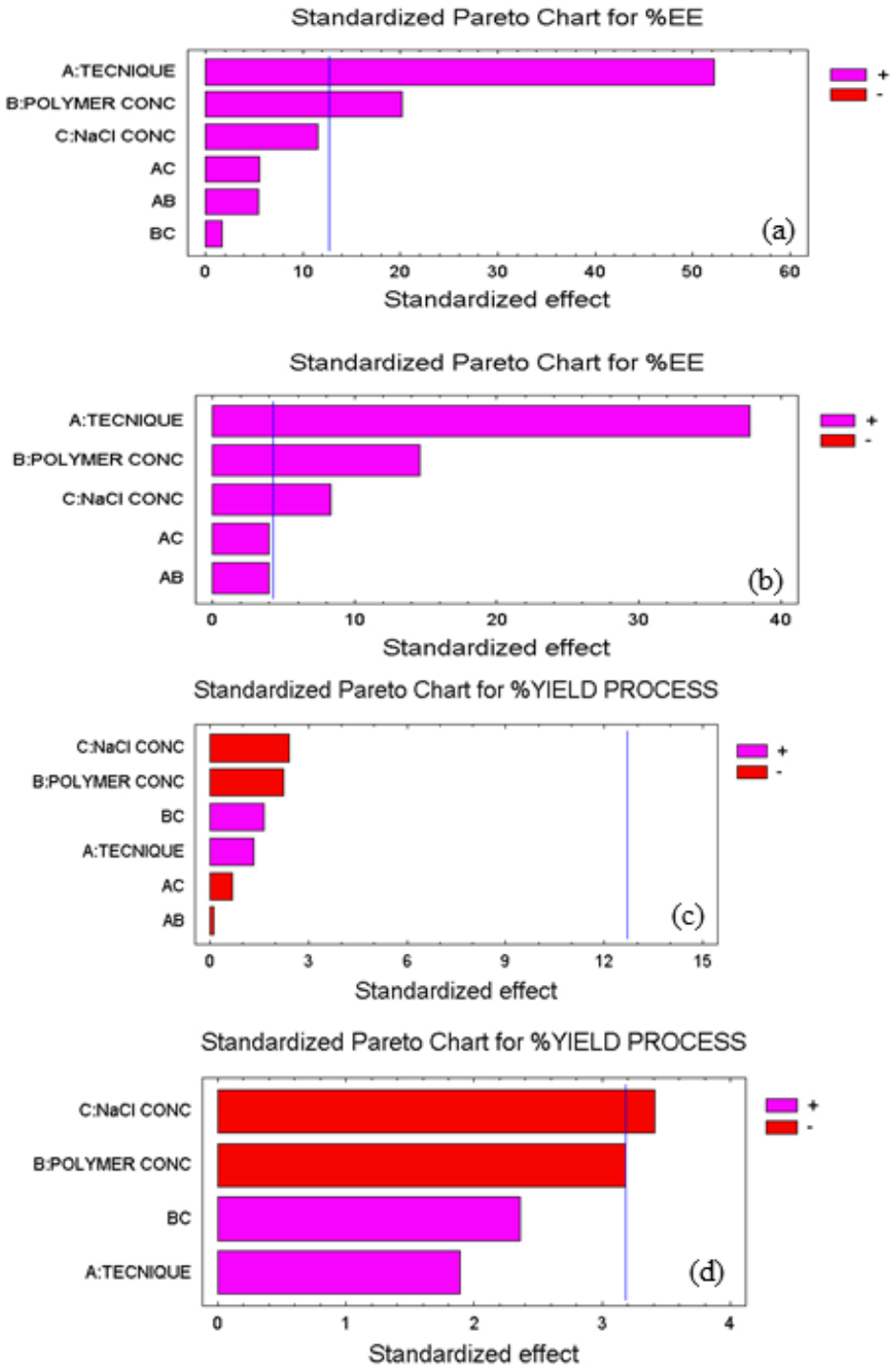

Figure 3: Pareto charts reporting: (a) the effect of the selected variables on the microspheres encapsulation efficiency (EE%); (b) the effect of the selected variables on the microspheres encapsulation efficiency (EE%) with the reduced model; (c) the effect of the selected variables on the microspheres process yield %, (d) the effect of the selected variables on the microspheres process yields, in the reduced model.

The results computed as estimated response surface and shown in **Figure 4** permitted to conclude that the model is linear, therefore further optimization tests were'nt needed.

The results in the Pareto chart confirmed those reported in **Table 1** and **Figure 2** for particle size distribution and yield process respectively: when 5% w/v NaCl was added to the external aqueous phase the microspheres (Ms 9-12 batches) always showed d_{90} value significantly lower, narrower particle size distribution, and higher E.E.%. Considering the E.E.% value (91.4), the size of microparticles (d90 < 300 µm) and the process yield (47.7 %) the batch Ms11 preparation protocol was selected for the scale up and *in vitro* release studies.

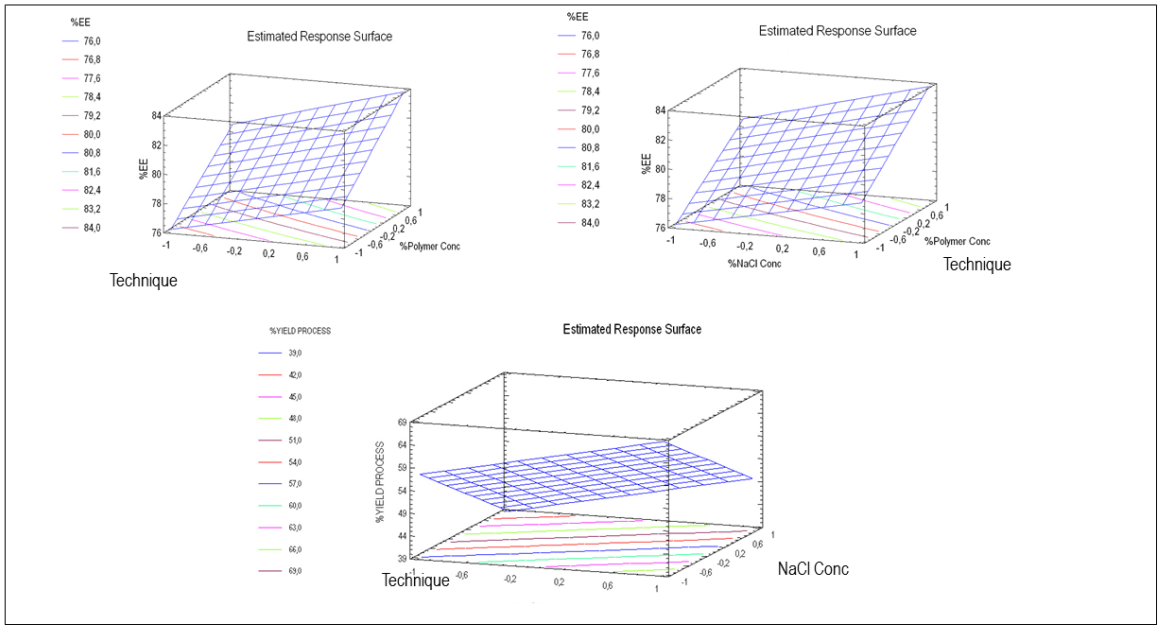

Figure 4: Estimated response surface towards encapsulation efficiency and process yield.

Scanning electron microscopy (SEM) showed that microspheres prepared without NaCl addition have highly porous structure (**Figure 5** b1 and b2), while those prepared with NaCl addition in PVA have a spherical shape and a smooth surface. To justify these results, it was speculated that the salt influenced the arrangement of the chains and their orientation during the organic solvent evaporation.

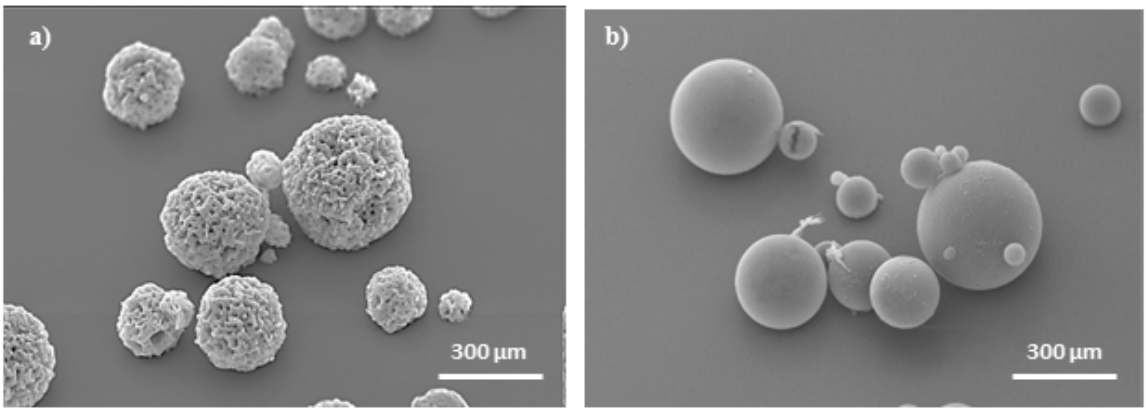

Figure 5: SEM images of the freeze-dried microparticles Ms 7(a) and Ms 11 (b).

On the basis of the screening design the double emulsion technique, the polymer concentration of 15% w/v and NaCl 5% w/v in the PVA solution were selected as the most significant factors and applied to scale up the process with the 5050 DLG 4C PEG1500 polymer. The volume ratios of aqueous internal phase, organic phase and outer aqueous phase were increased 7.5 times by keeping constant polymer, gentamicin and PVA concentrations. The scaled up batch was prepared with the same composition of Ms11; a scaled up batch without salt addition was prepared as control (see **Table 3**). Due to the increased phase volumes, the stirring speed of the first emulsification step was increased up to 17400 rpm, and the second emulsification step was obtained using a paddle stirrer. Process yield values of the scaled up batches ranged between 51.22 ±5.8 -69.66% ±8.8.

Analysis of the scaled up batches (Ms11 – 13) confirmed that salt addition led to a significant reduction of particle size (see **Table 3**). The EE% values of scaled up batches were always significantly lower than those of the corresponding small size batches. These results have been attributed to the higher volumes of water used to remove PVA and salt residuals. In any case, the presence of salt in the external aqueous phase always led to significant E.E.% increase and better gentamicin internalization into the microsphere matrix, as suggested by the zetapotential results (**Table 3**).

Table 3: Characteristics of Scaled up batches (scale up size ratio 1:7.5).

Scaled up Batch n.	Polymer Conc. (%w/v)	NaCl to PVA aqueous (%w/v)	Particles size (µm)	Span	EE%	Process Yield (%)
Ms 13-	15	5	250	1.03	54.89	69.66±8.8
Ms 14-	15	-	290.91	1.33	24.32	51.22±5.8

Figure 6 a) reports a comparison of the TGA traces recorded up to 500°C on gentamicin sulphate, placebo microspheres and microspheres loaded with gentamicin. For what gentamicin is concerned, after an initial mass loss of about 8 wt% related to the presence of moisture, a two-step decomposition falling between 200 and 400 ºC, of the order of 40 wt%, occurred, and a continuous degradation process took place at higher temperatures. Such a thermal behaviour is in fairly good agreement with that reported by A. Thakur [15] in the same temperature range. Both placebo and gentamicin-loaded microspheres TGA thermograms exhibited a tiny loss of moisture below 100 °C followed by the molecule breakdown at about 250 °C and 300 °C, respectively. It is worth noting that according to these experimental results gentamicin-loaded microspheres look more thermally stable than the placebo ones.

The DSC traces of gentamicin, placebo microspheres and gentamicin-loaded microspheres are illustrated in **Figure 6 b**. The measurements were recorded from 20 °C up to the incipient degradation temperature of each sample. The gentamicin thermograph presents an endothermic feature below 200°C due to the moisture release, followed by a series of spikes starting at about 230 °C. Since commercial gentamicin is a complex mixture of gentamicin sulphates with melting points ranging from 94 to 100 °C to 218-237 °C, the latter thermal features can be interpreted as an incipient melting of the gentamicin complex mixture accompanied by the molecule degradation. In both placebo and gentamicin-loaded microspheres DSC thermographs the glass transition temperature of PEG-PLGA, in agreement with previous investigations [16, 17], can hardly be detected and, in agreement with the corresponding TGA traces, do not exhibit significant thermal phenomena up to their decomposition temperatures.

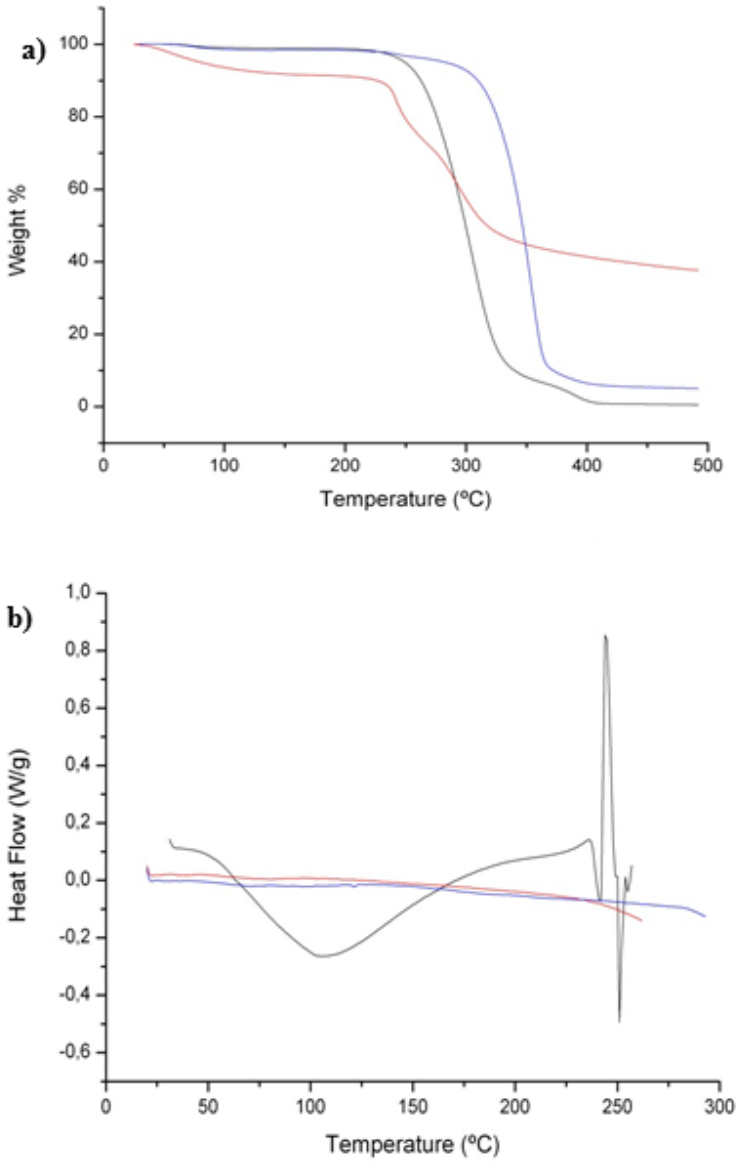

Figure 6: a) TGA behaviour of Gentamicin (red line), placebo microspheres (violet line), Gentamicin loaded microspheres, Ms13 batch (blue line); b) DSC traces of Gentamicin (red line), placebo microspheres (violet line) and Gentamicin loaded microspheres, Ms 13 batch (blue line).

The release profiles of Gentamicin are reported in **Figure 7**; a three phasic release profile was observed for batch Ms13, with about 8.5% (43.61 µg/ml) of drug released in the first 6 hours of incubation followed by a continuous slow release till it reaches 27% (128.59 µg/ml) after forty days and reaching 94% (475.29 µg/ml) in 81 days.

Ms 14 presented a burst release at about 33.2% in the first 6 hours of incubation and the release was completed in three days.

The rapid release of Ms14 could be attributed to the spongy structure of the matrix that results in a higher surface area, with respect to Ms 13, promoting the release of gentamicin. The results are consistent with the use of NaCl and its concentration, being significant variables in the performed DOE. The MIC values of 2 µg/ml for gentamicin powder and 1.7 µg/ml for gentamicin released from the microspheres can be considered not significantly different [18]. Thus the results permit to establish that the microspheres did not interact with the microorganism and they act as prolonged release drug delivery system. Comparing the data in **figure7** with the MIC value of gentamicin determined against *E. coli* it can be stated that the amount of gentamicin released from the microspheres samples (200 mg) is always over the MIC value. Moreover, the data permit to calculated that, in these conditions, an amount of 5.6 mg of microspheres is sufficient to achieve the MIC value.

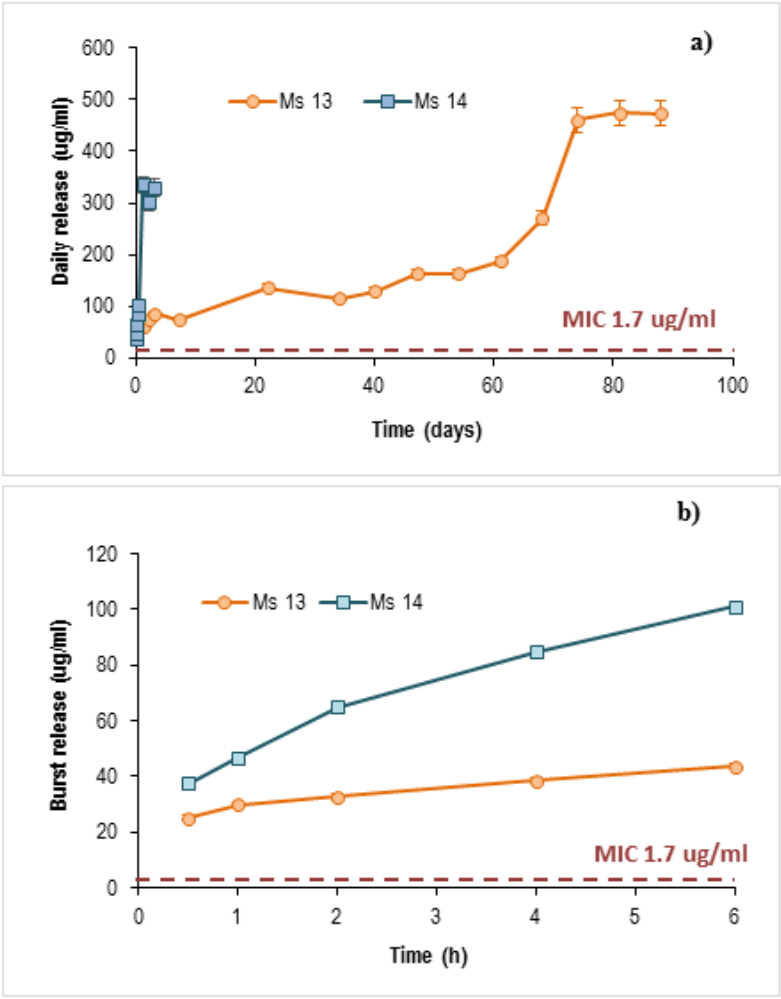

Figure 7: Cumulative amounts (µg/ml) of gentamicin *in vitro* released from Ms14: a) till completion, b) in the first 6 hours incubation, and compared to gentamicin MIC values.

The results of the preliminary *in vitro* release test performed on microspheres (200 mg of Ms13 batch), loaded into the chitosan/Orthoss based composite gel are reported in **figure 8** and compared with the release of gentamicin powder directly loaded into the composite gel, and to gentamicin release from the microspheres directly soaked in the incubation medium. **Figure 8**, shows that the release of gentamicin powder from the composite gel is completed in the first 4 hours, while, in the same time, 8.5% of gentamicin is released from the microspheres and 5.1 % from the composite gel loaded with gentamicin loaded microspheres (Ms13 batch). Chitosan composite gel significantly slow down gentamicin release from the microspheres for the first 40 days. After this time the two release behaviors are superimposable and the chitosan gel completely disrupts after 45 days of incubation releasing the microspheres in the incubation medium. The amount of gentamicin released is always 35 times over the MIC value determined.

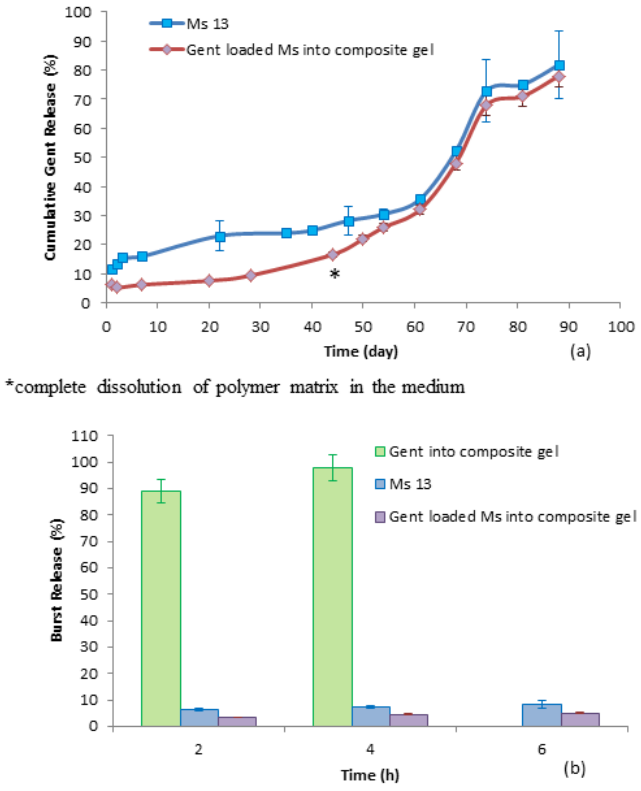

Figure 8: (a) Gentamicin *in vitro* release from Ms 13- batch embedded into the chitosan composite gel compared to the in vitro release of gentamicin from the microspheres directly incubated in PBS. (b). Data collected in the first six hours of incubation of gentamicin incorporated into composite gel, gentamicin loaded in microparticles and gentamicin loaded in microparticles loaded into composite gel. The release is expressed as percentage of cumulative release with respect to the amount encapsulated

5. CONCLUSIONS

In conclusion the work reports an experimental evaluation through DOE screening design of the variables involved in the preparation processes through o/w and w/o/w emulsification solvent evaporation methods of PLGA-PEG- PLGA microspheres loaded with gentamicin. The results obtained permitted the selection of the suitable preparation method and conditions and the scaling up of the microspheres manufacturing process.

The preliminary *in vitro* release study and microbiologic evaluation give the perspective of a product of potential interest in the local delivery of gentamicin for osteomyelitis treatment.

6. REFERENCES

[1] D.Neut, H.Van de Belt, L. Stokroos, J.R. Van Horn, H.C. Van der Mei, H.J. Busscher, Biomaterial-associated infection of gentamicin-loaded PMMA beads in orthopaedic revision surgery,Journal of Antimicrobial Chemotherapy. 48 (2001) 885–891.

[2] T. Wu, Q. Zhang,W. Ren, X.Yi, Z. Zhou, X. Peng, X. Yu, M. Lang, Controlled release of gentamicin from gelatin/genipin reinforced beta-tricalcium phosphate scaffold for the treatment of osteomyelitis, Journal of Materials Chemistry B, 201 (2013) 3304-3313.

[3] P. Shi, Y. Zuo, X. Li, Q. Zou, H. Liu, L. Zhang, Y. Li, Y. S Morsi, Gentamicin-impregnated chitosan/nanohydroxyapatite/ethyl cellulose microspheres granules for chronicosteomyelitis therapy. Journal of Biomedical Materials Research Part A (2009) 1020-1031.

[4]F. I. Ahmad, M. A. Abdalmonemdoolaanea, M. Farahidah, High initial burst release of gentamicin formulated as PLGA microspheres implant for treating orthopaedic infection, International Journal of Pharmacy and Pharmaceutical Sciences, 4, Suppl 4 (2012) 685-691.

[5]C. Lecaroz, M. J. Blanco-Prieto, M. A. Burrell, C. Gamazo, Intracellular killing of Brucella melitensis in human macrophages with microsphere-encapsulated gentamicin, Journal of Antimicrobial Chemotherapy 58 (2006) 549–556.

[6] G.H.Wang, S.J. Liu, S. Wen-Neng Ueng, E.C. Chan, The release of cefazolin and gentamicin from biodegradable PLA/PGA beads, International Journal of Pharmaceutics 273 (2004) 203–212.

[7] J. Ji ,S. Haoa, D. Wua, R. Huangb, Y. Xua, Preparation, characterization and in vitro release of chitosan nanoparticlesloaded with gentamicin and salicylic acid, Carbohydrate Polymers 85 (2011) 803–808.

[8] L. Francis, D. Meng, J. Knowles, T. Keshavarz , A. R. Boccaccini, I. Roy, Controlled Delivery of Gentamicin Using Poly(3-hydroxybutyrate), Microspheres. Int. J. Mol. Sci. 12 (2011) 4294-4314; doi:10.3390/ijms12074294.

[9] M. C. Lecaroz, M. J. Blanco-Prieto, M. A. Campanero, H. Salman, C. Gamazo1, Poly(D,L-Lactide-Coglycolide) Particles Containing Gentamicin: Pharmacokinetics and Pharmacodynamics in *Brucella melitensis*-Infected Mice, Antimicrobial agents and chemotherapy (2007) 1185–1190.

[10] M. R. Virto,_B. Elorzab, S. Torrado, M. Elorza, G. Frutos, Improvement of gentamicin poly(D,L-lactic-co-glycolic acid) microspheres for treatment of osteomyelitis induced by orthopedic procedures, Biomaterials 28 (2007) 877–885.

[11] Q. Xu, S. E. Chin, C. Wang, D. W. Pack, Mechanism of drug release from double-walled PDLLA(PLGA) microspheres, Biomaterials 34 (2013) 3902-3911.

[12]D.Singh, S.Saraf, V.K.Dixit, S.Saraf, Formulation optimization of Gentamicin loaded Eudragit RS100 microspheres using factorial design study, Biol. Pharm. Bull. 31 (2008) 662-667.

[13] P. Frutos, S.Torrado, M.E. Perez-Lorenzo, G. Frutos, A validate quantitative colorimetricassay for gentamicin, Journal of Pharmaceutical and Biomedical Analysis 21 (2000) 1149-1159.

[14] R. Dorati, I. Genta, B. Conti, H. Klöss, K. Martin, An injectable *in situ* forming composite gel to guide bone regeneration: design and development of technology platform, European Cells and Materials 24. Suppl. 1 (2012) 14.

[15]A. Thakur,R. K. Wanchoo, and P. Singh, Hydrogels of Poly(acrylamide-*co*-acrylic acid):*In-vitro* Study on Release of Gentamicin Sulfate, Chem. Biochem. Eng. Q. 25 (4) (2011) 471–482.

[16] R. Dorati, I. Genta, C.Tomasi, T. Modena, C. Colonna, F. Pavanetto, P. Perugini, B.Conti, Polyethylenglycol-co-poly-D,L-lactide copolymer based microspheres: preparation, characterization and delivery of a model protein, Journal of Microencapsulation 25 (2008) 330-338.

[17] R. Dorati, C. Colonna, C. Tomasi, I. Genta, T. Modena, A. Faucitano, A. Buttafava, B. Conti, γ-irradiation of PEGd,lPLA and PEG-PLGA multiblock copolymers: effect of oxygen and EPR investigation, AAPS Pharm. Sci. Tech. 9 (2008)718-25.

[18] S.M Abdelghany, D. J Quinn, R. J Ingram, B. F Gilmore, R. F Donnelly, C.C Taggart, C.J Scott, Gentamicin-loaded nanoparticle show improved antimicrobial effects towards Pseudomonas Aeruginosa infections, International Journal of Nanomedicine (2012) 4053-4063.

CHAPTER III

Chapter IV

CHAPTER IV

FORMULATION AND *IN VITRO* CHARACTERIZATION OF A COMPOSITE BIODEGRADABLE SCAFFOLD AS ANTIBIOTIC DELIVERY SYSTEM AND REGENERATIVE DEVICE FOR BONE.

Abstract

A biodegradable composite scaffold, useful as tridimensional bone regenerative scaffold (3D) and antibiotic delivery system (DDs), is here formulated and characterized. The device, called as 3D-DDS, is an injectable or moldable scaffold based on chitosan chloride crosslinked with glycerol 2-phosphate disodium salt and laden with bovine bone substitute (BBs) granules and gentamicin loaded polylactide-co-glycolide-co-poly ethilenglycol (PLGA-PEG) microparticles. 3D-DDS characterization results show that microparticles are homogeneously distributed in the composite matrix, and do not interfere with scaffold stability. The lyophilized 3D-DDS has high rehydration ability and is able to restrain physically bovine bone granules and microparticles up to 45 days in *in vitro* simulated conditions. Bactericidal action is high in the first 4h and it accounts for superimposable effect of gentamicin release and bacteriostatic chitosan properties; sustained gentamicin bactericidal effect is evident up to 14 days.

Keywords: antibiotic local delivery; bone regeneration; biodegradable polymers; chitosan; poly lactide-co-glycolide; poly ethyleneglycol; microparticles.

This chapter is based on the following publication:

Journal of Drug Delivery Science and Tecnology 35 (2016) 124-133 Elsevier.

R. Dorati, A. De Trizio, I. Genta, A. Merelli, T. Modena, B. Conti

1. INTRODUCTION

Surgical site infections in orthopedic surgery and bone trauma account for about 15% of all nosocomial infections [1]. In particular, osteomyelitis is a chronic recurrent infection that can rise after open fractures and implant-related infections or following treatment of fractures and prosthetic joint replacements. Osteomyelitis can be treated by medical or surgical therapy, and in the worst-case amputation of the infected part is needed with consequent reconstruction of the resected tissue. The problem is significant in the case of periprosthetic implant infections, known as septic failures, because of prolonged hospitalization, high risk of relapses with poor healing outcomes, and high costs involved in the treatments, which amount to $70,000/per episode in USA [2].

The treatment usually undergoes several stages: drainage of the site, debridement of the necrotic tissue, bone dead space management, soft tissue coverage, and restoration of blood supply. The most important and critical step is the management of dead space, namely the void space between soft tissue and bone defect generated from surgical resection. An appropriate management of the dead space reduces the risks of persistent infection at the originally infected site and of distortion of surrounding tissues maintaining the physical integrity of site. Generally, the dead space management is performed by insertion of autologous vascularized tissue, soft tissue transplant, antibiotic impregnated bandage and bone grafting. Currently, antibiotic loaded beads represent the gold standards for the dead space management; they are based on inert material, polymetilmethacrylate (PMMA), and loaded with a broad spectrum antibacterial agent such as gentamicin. They are easily inserted in the required body cavity; nevertheless, they need to be removed when exhausted by a second surgery with associated risk of further infection, painful and high cost [3].

In spite of the innovative treatments, the literature highlights that chronic osteomyelitis is still a challenging condition to treat [4]. Recurrence of infection is well known, and successful treatment needs a multidisciplinary team approach.

Since one therapeutic approach is the bone grafting with implantation of natural bone substitute, the goal of the present work is to design a bone grafting combined with a drug delivery system (3D-DDs). The 3D-DDs could be injectable or moldable and it is composed by natural biocompatible biodegradable polymer combined with decellularized bone matrix (Bovine Bone susbstitute- BBs) and with gentamicin loaded biodegradable microparticles.

The advantages of 3D-DDS are multiple, it is ready to be used, injectable through a cannula or inserted through minimally invasive surgical procedure, easy to be placed into irregular body cavities and to fit perfectly irregular site maintaining its physical integrity.

The moldable 3D scaffold is designed for invasive surgical procedures; it can be cut, hidrated and extemporaneously remodeled by surgeon in order to fit the bone defect. It is obtained by lyophilization of injectable composite scaffold and the high porosity and the spongy like structure typical of lyophilized scaffolds allow the rapid hydration of scaffold in blood or physiological fluids unchanging its physical structure.

The 3D-DDs represents a new generation of surgical scaffolds obtained by combination of bone grafting and drug delivery system, they can be useful in orthopedic medical practice because they can provide the prevention or the complete treatment of infection improving, simultaneously, the tissue regeneration reducing the healing process. The injectable and mouldable 3D-DDSs present several advantages: they are biodegradable, biomimetic and they promote local and extended gentamicin delivery to the bone. Moreover, they could be loaded with antibiotic combinations reducing the risk of bacterial resistance, and due to their *in situ* gelification, they can create intimate contact with the surrounding tissue promoting the diffusion of stem cells and avoid the failure of surgical procedure due to the cavity distortion. Furthermore, the amount of antibiotic loaded into the system can be adjusted in order to achieve its desired time specific release profile. Eventually, the local delivery of the antibiotic at the site of action can dramatically reduce the antibiotic side effects arising from a systemic administration.

The potential limitation and/or drawback of the proposed 3D-DDs could be associated with potential accumulation phenomena of antibiotic due to a slow residual release of antibiotic, which can evoke bacterial resistance. This critical aspect has been considered and evaluated in the present work.

Gentamicin (Gent) has been chosen since it is a wide bacterial spectrum aminoglycoside antibiotic extensively used for treating many types of infections including osteomyelitis. It has plasma half-life of 2 hours in patients with normal renal function, while its half-life in the renal cortex is 100 hours. Systemic administration of gentamicin can rise diverse problems and side effects. The antibiotic has low bioavailability after oral administration and poor cellular penetration; in addition, the internalized gentamicin molecules are accumulated into the lysosomal compartment with reduction of its activity. Since it is excreted by glomerular filtration, repetitive doses of gentamicin can result in renal accumulation and nephrotoxicity. Due to these characteristics and criticalities, gentamicin is a good candidate for local administration, in order to reduce side effects caused by systemic administration whilst improving the therapeutic ones.

Biodegradable biocompatible polymers have been widely investigated as carriers for gentamicin because of their advantageous properties [5-8]. Polylactide-co-glycolide-co-polyethylenglycol (PLGA-PEG) has been selected as biodegradable, biocompatible constituent of the microparticle matrix, the presence of polyethylene-glycol (PEG) gives the hydrophilic-lipophilic molecular balance, suitable to

improve gentamicin loading, and fosters microparticles loading into the chitosan hydrogel. The preformulative and formulative phase, involving the optimization of gentamicin loaded microparticles preparation method, has been carried out in a previous work throughout design of experiments (DOE) together with the characterization of gentamicin loaded microparticles [9].

Chitosan was selected as the polymeric component to prepare composite scaffold. It is a natural hydrophilic polymer, it allows the formation of a thermogelling polymer solution in the presence of glycerol phosphate disodium salt (βGP). The lyophilized formulation, obtained combining the thermogelling polymer solution with the bovine bone substitute (BBs) granules (Orthoss®), has been designed, prepared and characterized in previous works by the same authors [10, 11]. The composite scaffold has been proposed for bone regeneration, as filler system with osteogenic and osteoconductive properties.

Starting from this background, the present work deals with the formulation study of a 3D composite scaffold loaded with gentamicin loaded microparticles (3D-DDS) capable to prevent or treat the osteomielyties achiving gentamicin prolonged release and support the regeneration of new tissue. In these terms, the scaffold loaded with gentamicin loaded microspheres is here proposed as a biodegradable drug delivery system for the local delivery of antibiotic to bone, and promoting bone regeneration ad composite scaffold as scaffold for tissue regeneration. The study involves the preparation of gentamicin loaded 3D-DDS and its complete characterization in terms of physico-chemical and bactericidal properties as well as stability.

2. MATERIALS

Gentamicin sulphate (Gentamicin C1 $C_{21}H_{43}N_5O_7$, Mw 477.6 g/mol, Gentamicin C2 $C_{20}H_{41}N_5O_7$, Mw 463.6 g/mol, Gentamicin C1a $C_{19}H_{39}N_5O_7$, Mw 449.5 g/mol), was from Sigma Aldrich. 5050 DLG 4C PEG 1500 (Mw 47 kDa PEG % 51) was from Lakeshore Biomaterials (Birmingham, AL, USA), PVA (Mw 85-124 KDa 87-89% hydrolized), methylene chloride, dimethyl sulfoxide, sodium chloride, ninhydrin, Mw 178,14 g/mol, glycerol 2-phosphate disodium salt hydrate (β-GP) 216.16 Mw, were from Sigma Aldrich, (Sigma Aldrich Milan, Italy).

Orthoss® granules were supplied by Geistlich Surgery (Geistlich Pharma AG, Wolhusen Switzerland), with size and size distribution of d_{10} 141.437 mm, d_{50} 721.029 mm and d_{90} 1340.246 mm, Span value 1.663. Chitosan chloride CL213, Protosan CL213, deacetylation degree 82%, hydrochloric acid content 10-20%, Mw 350 KDa was purchased from Pronova Biomedical (Pronova Biomedical, Norway). Human adult dermal fibroblasts as primary cells were purchased from International PBI, (PBI, Milan,Italy). Distilled water was filtered through 0.22 µm membrane filters (Millipore

Corporation, Massachusset, USA) before use. Unless specified, all other solvents and reagents were of analytical grade.

3. METHODS

3.1. Preparation of gentamicin microparticles

Microparticles preparation was performed as reported in a previous work by the authors [9]. Microparticle formulations were prepared by double emulsion with evaporation of solvent. Briefly, primary emulsion was prepared by homogenizing of 7.5% w/v gentamicin aqueous solution (1 ml) into 9 ml of 5050 DLG 5C PEG1500 polymer solution (15% w/v) in methylene chloride, at 17,500 rpm for 2 minutes. The obtained emulsion was dispersed into a secondary aqueous continuous phase containing PVA (2% w/v) and NaCl (5% w/v); the system was maintained under stirring at 350 rpm, and solvent evaporation was carried out in 2.5 hours at room temperature. The solid microparticles were recovered through centrifugation (3000 rpm for 15 minutes), washed with water (10 ml), filtered through 0.45 µm AA Millipore membrane (Millipore Corporation, Milano, Italy), and lyophilized (Lio 5P, Cinquepascal s.r.m., Milano, Italy) for 24 hours, −50°C, 0.01 bar (Lio 5P, Cinquepascal s.r.l., MI, Italy).

The amount of gentamicin encapsulated into microspheres was determined by ninhydrin colorimetric assay as reported in a previous work of the authors [9]. Briefly, weighed amounts of microspheres (36 mg) were dissolved in 400 µl of DMSO keeping under magnetical stirring for 12 hours. Gentamicin was extracted by addition of filtered water (800 µl) and separate from organic phase, containing polymer, by centrifugation at 6000 rpm for 15 minutes. The aqueous phase was analyzed by ninhydrin colorimetric assay with UV-spectrophotometer at 400 nm. Ninhydrin solution (0.2% w/v) and water /DMSO mixture 2:1 were used as controls. Drug content is expressed as the weight % of drug with respect to the microsphere batch weight.

3.2. Gentamicin loaded 3D-DDS preparation

The placebo scaffolds were prepared according to the method previously set up by the authors to obtain a thermosetting gel scaffold [11]. Briefly, chitosan chloride CL 213 aqueous solution (2% w/v) was mixed with β-GP aqueous solution (10 % w/v), the system was kept at 4°C under stirring for 1 h to obtained an homogeneous solution. Thermosetting polymer solution (1 ml) was combined with 200 mg of bovine bone granules (Orthoss® granules,1-2 mm) at room temperature, gelification of thermosetting polymer solution was completed in 10-15 minutes at 37°C.

The moldable scaffold was obtained by lyophilization of composite system for 24 hours, at −50°C, 0.01 bar. Scaffolds loaded with gentamicin powder were prepared following the same explained

procedure adding gentamicin powder into chitosan chloride aqueous solution before mixing with β-GP solution. The scaffolds embedded with gentamicin loaded microparticles (3D-DDS) were prepared by mixing gentamicin loaded microparticles at different increasing amounts (6, 12, 24, 36 and 48 mg) with 200 mg of bovine bone granules. Mild stirring was used to facilitate the homogeneous incorporation of granules and microparticles in the polymer solution and to avoid precipitation phenomena with consequent phase separation [9, 10].

The amount of gentamicin loaded PLGA-PEG lyophilized microparticles (24 and 12 mg) were selected on the base of: *i)* preliminary results related to the physical stability of composite scaffold after loading different increasing amounts of gentamicin loaded microparticles (6, 12, 24, 36 and 48 mg) and *ii)* gentamicin *in vitro* release profile from 3D-DDS (see section 2.2.4.). iii) Moreover, preliminary bacterial challenge studies (see section 2.2.5) were performed in order to evaluate the suitability of selected gentamicin microparticles amounts.

3.3. Scaffold characterization

3.3.1. Scanning Electron Microscopy

SEM analyses were performed by a Scanning Electron Microscope (SEM) (Jeol, Cx, Temcan, Jed, Tokyo; J). Samples were sputtered with an Au/Pd coating in argon atmosphere. Placebo scaffolds, composite scaffolds and gentamicin microparticles loaded into composite scaffolds were observed in their cross section.

3.3.2. Porosity and compressive strength

Scaffolds porosity was measured by a liquid displacement method as previously reported [10, 12]. Briefly, a weighed polymer scaffold (W), after being soaked for 10 min in a graduated cylinder containing a known volume (V_1) of not solvent (ethanol), underwent to evacuation and depressurization cycles until no air bubbles were observed from the scaffold surface. The total volume of ethanol plus ethanol-soaked scaffold was recorded as V_2 and the calculated volume difference (V_2-V_1) corresponded to the scaffold skeleton volume. The ethanol volume residual in the graduated cylinder after ethanol-soaked scaffold withdrawn was recorded as V_3. The volume difference (V_1- V_3), corresponding to the volume of ethanol absorbed in the porous scaffold, and was defined as the scaffold pore volume.

The scaffold porosity expressed as percentage (%) was calculated by the following equation:

$$\varepsilon(\%) = \frac{(V1-V3)}{(V2-V3)} X\ 100 \qquad \text{(a)}$$

The porosity values were determined on five samples and expressed as mean ± standard deviation. The compressive strength was measured with an electromagnetic testing machine (Enduratec Elf 3200, Bose Corporation, Eden Prairie, MN, USA) applying a force of 220 N. Compression tests were performed under displacement control, at a velocity of 0.1 mm/s until the sample was 40% of initial height. The compressive modulus was calculated as the average of five measurements per scaffold and expressed as mean ±standard deviation (sd).

3.3.3. Water uptake and retention

Dried polymeric scaffolds (composite placebo scaffold and gentamicin loaded scaffolds and 3D-DDS) were rehydrated by soaking in 6 ml of PBS pH 7.4 containing 0.1 %w/v of NaN_3 at 37°C.

$$Water\ uptake\ (\%) = \frac{(Ww - Wd)}{(Wd)}\ X\ 100 \qquad \text{(b)}$$

where, W_w is the weight of the scaffold after incubation in PBS (wet state) and W_d is the weight of scaffold in the dried state, before incubation.

Water retention capability was estimated after centrifugation of the scaffold at 500 rpm for 3 min. Water retention was determined according to the equation (c):

$$Water\ retention\ (\%) = \frac{(W'w - Wd)}{(Wd)}\ x\ 100 \qquad \text{(c)}$$

W'_w is the weight of wet scaffold after centrifugation and W_d is the weight of scaffold before incubation (dried state).

3.3.4. Gentamicin *in vitro* release from the 3D-DDS

The 3D-DDS loaded with 12 mg and 24mg of gentamicin loaded microparticles were incubated in 3 ml of PBS at 37°C. At scheduled times; 800µl of buffer was removed and replaced with fresh PBS. *In vitro* release was followed till to reach the complete release of antibiotic agent. The amount of gentamicin released was determined spectrophotometrically at 400 nm wavelength by ninidrin assay. The drug concentration was calculated based on a calibration curve in PBS (y=0.0029X-0.0513, R^2=0.9961). Analyses were carried out on three samples for each 3D-DDS microparticle loading and the results are expressed as the mean ± standard deviation (n=3).

3.3.5. Bacterial challenge studies

The microbiological assay was performed against *E. coli* (ATCC 10536) in order to determine the antibacterial activity of scaffolds loaded with gentamicin microparticles. Firstly, the minimum inhibitory concentration (MIC) of gentamicin loaded scaffolds, gentamicin loaded microparticles and

3D-DDS was evaluated by the macrodilution broth method, according to Clinical and Laboratory Standards Institute procedures [13]. MIC was evaluated after 24h incubation
at 37 °C, as the lowest gentamicin concentration that completely inhibited the formation of visible microbial growth.

Bacterial challenging was performed on scaffolds containing gentamicin powder (200, 250, 500, 1000, 4000 µg/per scaffold), scaffolds loaded with gentamicin microparticles (12 and 24 mg of microparticles corresponding to 250 and 500 µg of gentamicin), scaffold loaded with placebo microparticles, placebo microparticles and gentamicin powder. The amounts of gentamicin and gentamicin microspheres were selected according to the MIC test and the *in vitro* release data discussed in a previous work [9].

For the bacterial challenging, the samples were incubated in 24 ml of Iso Sensitest Broth (ISB) containing 1 ml of *E.Coli* (ATCC 10536) culture at $10^7 – 10^8$ colony-forming units (CFU). A blank sample, namely 24 ml of ISB plus containing1 ml of *E.Coli* ATCC 10536 at $10^7 – 10^8$ CFU, was used as control. Samples and controls were incubated at 37°C, at scheduled times 50 µl of broth were withdrawn and diluted with eugonic broth supplemented with lecithin, triton 100 (Tx-100) and polysorbate 90 according to the standard dilution protocol. Diluted samples (1:100, 1:10000 and 1:100000000) were seeded on Petri dishes with Triptone Soya Agar (TSA) and incubated at 37°C for 24 hours. After 24 h, the colonies were counted to determine the number of colony-forming units per ml (CFU/ml) and to define the microbicidal effect.

The microbicidal effect (M.E.) was calculated as reported in the following equation:

$$M.E. = \log_{10}(CFU\ control) - \log_{10}(CFU\ sample) \qquad \text{(d)}$$

3.3.6. Cell seeding capacity and long-term culture study

The study was mainly focused on the cell adhesion and long-term proliferation comparing placebo chitosan composite scaffold, gentamicin loaded composite scaffold and 3D-DDS.

Adult dermal fibroblasts, purchased as primary cells from International PBI (Milan, Italy), were cultured in DMEM supplemented with 10% FBS and 1% antibiotic solution (100 U/ml penicillin, 100 ug/ml streptomycin); cell seeding capacity and long-term culture were performed on fibroblast at cell division cycle # 6.

The samples (composite placebo scaffolds, gentamicin loaded scaffolds and 3D-DDS) were fixed in 6 well culture plates and conditioned with DMEM supplemented with 10% FBS, for 4 h. After conditioning, the media was removed and cells suspension (2 x 10^5 cells/50 µl DMEM) was seeded onto each scaffold surface. Fresh DMEM was added to each well to completely submerge scaffolds

into the media (8 ml), samples were incubated at 37°C, 5% CO_2 for 3 h to assess cell-seeding capacity and for 28 days to evaluate long-term cell growth. At scheduled times, samples were collected and the cell mitochondrial activity was determined by a slightly modified MTT assay, based on a spectrophotometric technique [5, 10].

3.3.7. Scaffold stability evaluation *in vitro*

Scaffold stability was evaluated in *in vitro* simulated physiologic conditions (PBS 3.75 mM, pH 7.4 at 37°C) following several parameters: i) ability of scaffold to holding back microparticles and bovine bone granules into swollen composite matrix (by gravimetric analysis); ii) loss of chitosan scaffold mass (by gravimetric analysis) and iii) variation of chitosan and PLGA-PEG molecular weight (Mw) by gel permeation chromatography.

3.3.7.1. Scaffold ability in holding back microparticles and bovine bone granules

Composite chitosan scaffolds containing microparticles were immersed in PBS (6ml) and kept at 37°C, in static conditions. Composite scaffold with no addition of microparticles was used as control. At fixed time points, PBS volume was removed and filtered on a filter paper in order to recover microparticles and BBS granules released from scaffold during incubation. After liophilization, microparticles were collected and percentage of released microparticles, Mps (%), was determined as followed:

$$Mps\ (\%) = \frac{M1-M2}{w}\ X\ 100 \qquad \text{(e)}$$

where, M_1 is the weight of microparticles released by composite scaffold containing microparticles, while M_2 is the weight of BBs granules release by the control (composite scaffold with no addition of microparticles). Each value was normalized to the amount of microparticles incorporated into the scaffolds (12 mg).

The percentage of released BBS granules, BBs (%), was calculated as follow, equation (f):

$$BBs\ (\%) = \frac{M2-M3}{200}\ X\ 100 \qquad \text{(f)}$$

where, M_2 is the weight of BBs granules release by composite scaffold and M_3 is the weight of composite scaffold with no addition of BBs granules. Each value was normalized to the amount of BBs granules incorporated into the scaffolds (200 mg).

The assay was designed and performed in simulated physiological conditions (PBS 3.75 mM, pH 7.4 at 37°C) in order to determine the ability of composite scaffold to holding back both polymeric microparticles and BBs granules into swollen hydrogel matrix.

3.3.7.2. Scaffold mass remaining

The scaffolds were immersed in PBS, pH 7.4 at 37°C, until physical integrity was completely lost. The test was performed to determine the mass remaining profile and it is useful to define the scaffold stability in simulated physiologic conditions. At scheduled time points (3, 7, 14, 21 and 28 days) scaffolds were recovered, lyophilized (-50 °C, 0.01 bar for 24 h) and weighed (W_f), and their weight was compared to the initial one (Wi). The mass remaining percentage was calculate using equation (g):

$$Mass\ remaining\ (\%) = 100 - [\left(\frac{Wi - Wf}{Wi}\right) X\ 100] \quad \text{(g)}$$

where, Wi is the initial weight of the scaffold before incubation and Wf is the final weight, after incubation and freeze-drying. The test was carried out on 3D-DDS loaded with 12 and 24 mg of Gentamicin microparticles (Batches 2 and 3, **Table 1**), composite scaffolds placebo (PL) were used as control. Results are expressed as the mean ± standard deviation (n=5).

3.3.7.3. Degradation study

The *in vitro* degradation behaviour of chitosan and PLGA-PEG microparticles incorporated into 3D-DDS was evaluated as markers of 3D-DDS stability. The study was performed on the same samples (composite scaffolds containing 12 and 24 mg of Gentamicin loaded microparticles) used for the two previous tests to allow the correlation of all results and to explain scaffold stability. Indeed, the ability of scaffold to restrain physically the microparticles and bovine bone granules, as well as the mass remaining can be affected by the degradation of chitosan matrix and PLGA-PEG microparticles. Moreover, the hydrolysis of PLGA-PEG can affect the degradation behavior of chitosan matrix due to pH shift of microenvironment. Briefly, 3D-DDS samples loaded with microparticles were incubated in physiologic simulated conditions, in PBS with 0.1 w/v % NaN_3 at pH 7.4, at 37 °C for 28 days. The incubation buffer was withdrawn, collected and replaced with fresh PBS buffer at regular time intervals (twice a week). At scheduled times (3, 7, 10, 14, 21 and 28 days) the scaffolds were recovered, washed with distilled water and lyophilized at -50 °C, 0.01 bar for 24 h. The chitosan weight-average molecular weight (Mw) and number average molecular weight (Mn) were determined by Gel Permeation Chromatography (GPC). The samples for GPC analysis was prepared as follows: scaffolds were soaked in tetrahydrofuran (THF) at a concentration of 1-2 mg/ml to dissolve PLGA-PEG microparticles. The suspensions were centrifugated at 16,400 rpm for 20 min and supernatant and pellet were recovered. The pellet was treated with acetic acid (0.1 M) to solubilized chitosan polymer, while the supernatant was analysed as such. All solutions were diluted in the proper solvent and filtered through 0.45 µm filter taking in consideration membrane compatibility.

GPC apparatus consists of a guard column, two or three columns connected in series, a pump (Varian 9010, Milan, Italy), a RI detector (Prostar 355, Varian Milan, Italy), and software for Mw distribution computing (Galaxie Ws, ver. 1.8 Single-Instrument, Varian Milan, Italy). The analysis was performed at constant temperature, using 1 ml/min as flow. The results are expressed as means ± sd (n=5). Here below a summary of the columns, eluents and standards used for the analysis:

Chitosan analysis – 2 M $NaNO_3$ and 0.01 M NaH_2PO_4 as eluents, PL aquagel-OH Guard 8 mm, 50 - 7.5 mm, (Agilent, Milan, Italy) guard column and two PL aquagel-OH MIXED-H 8 mm columns (300 – 7.5 mm) connected in series. The Mw was calculated on the base of calibration curve using pullans (polysaccharides) in the range between 5.9-708 KDa as standards. PLGA-PEG analysis – eluent tetrahydrofuran with BHT, Phenogel 10E 4 Å µm, 300 x 7.8 mm (Phenomenex, Milan, Italy) guard column and two Phenogel 10E 3 Å µm and 500 Å columns connected in series. In this case the Mw was calculated on the base of calibration curve using polystyrene in the range between 1.4-950 KDa as standards.

4. RESULTS AND DISCUSSION

PLGA-PEG microparticles loaded with gentamicin resulted to have reproducible drug loading, 2.21± 0.11 w/w %. Increasing amount of gentamicin loaded PLGA-PEG microparticles (6, 12, 24, 36, 48 mg) were embedded into thermosensitive composite system based on chitosan/β-glycerophosphate and bovine bone granules. The gelification of composite system was completed in 15 minutes only with an amount of microparticles below 24 mg (**Table 1**) while higher amount of solid microparticles seemed to hamper chitosan gelification in the stated conditions. The gelified 3D-DDS was freeze-dried to obtain a moldable scaffold (**Figure 1**).

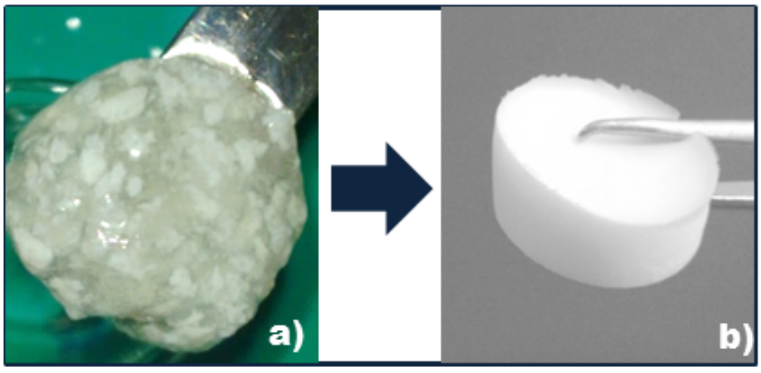

Figure 1: Images of 3D/DDs after gelification (a) and lyophilization (b).

The release of gentamicin from the 3D-DDS was completed in about 80 days, no burst effect was highlighted. As expected, the release of gentamicin from the composite scaffolds loaded with

gentamicin powder was completed in 4 hours. Therefore, the incapsulation of gentamicin in PLGA-PEG microparticles is crucial to slow down gentamicin release from the composite scaffolds and reach an extended release profile.

Table 1: Characterization of 3D-DDSs containing different amount of gentamicin loaded microparticles per scaffold: gelification time and gentamicin release (4 hours and 90 days).

Batch #	mg of gentamicin loaded microparticles/ per scaffold	Gelification time (min)	% of Gentamicin released	
			in 4 hours	in 90 days
1	6	15	3.9	80
2	12	15	5.1	80
3	24	15	8.4	90
4	36	nd*	-	-
5	48	nd*	-	-

*nd: not detectable because microparticles hampered the gelification process.

Preliminary microbiologic evaluation was performed on chitosan composite scaffolds containing gentamicin powder and on gentamicin loaded microparticles. The test was assessed in order to assess MIC values of gentamicin loaded as such into the scaffolds and into PLGA-PEG microparticles; as well as to set up the dose of gentamicin to load into the composite scaffolds. No statistical difference was highlighted between MIC values, indeed MIC of gentamicin powder resulted to be 2 μg/ml, while MIC of gentamicin microparticles was 1.7 μg/ml. These results could be attributed to the rapid release profile of antibiotic agent from composite scaffolds, 100% of drug was released in 4 hours. Different amounts of gentamicin (200 - 4000 μg/per scaffold) was loaded into composite scaffolds in order to screen the bactericidal effect in a wide dose range. As reported in the literature, the chitosan matrix itself has bacteriostatic properties hindering the bacterial growth but it does not have bactericidal properties [14]. The data reported in **Figure 2** prove the antimicrobial effect of chitosan composite placebo (PL) scaffold, this effect was detected in the first 4 h of incubation, and it disappears after 24 hours. Therefore, in testing scaffolds loaded with gentamicin powder the bactericidal effect revealed in the first 4 hours includes both the antimicrobial effect of chitosan matrix and the bactericidal effect of antibiotic agent; while the antimicrobial effect revealed after 24 hours was attributed uniquely to gentamicin. Comparing the bactericidal data collected in the first hour of incubation, it is evident that chitosan composite scaffold containing 250 μg of gentamicin (Sc 250 μg) has higher bactericidal effect than chitosan composite scaffold loaded with 200 μg (Sc 250 μg). Nevertheless, no further increase

in bactericidal effect was observed for scaffolds loaded with gentamicin amount > 250 µg (Sc 500 µg, Sc 1000 µg and Sc 4000 µg). On the base of this evidence, gentamicin amounts opted for the present research study were 250 and 500 µg of gentamicin/per scaffold. 12 and 24 mg of microparticles were selected as the highest doses providing bactericidal effect, since the PLGA-PEG microparticles drug loading was 2.21 % w/w and taking into account the gentamicin release profile (**Table 1**).

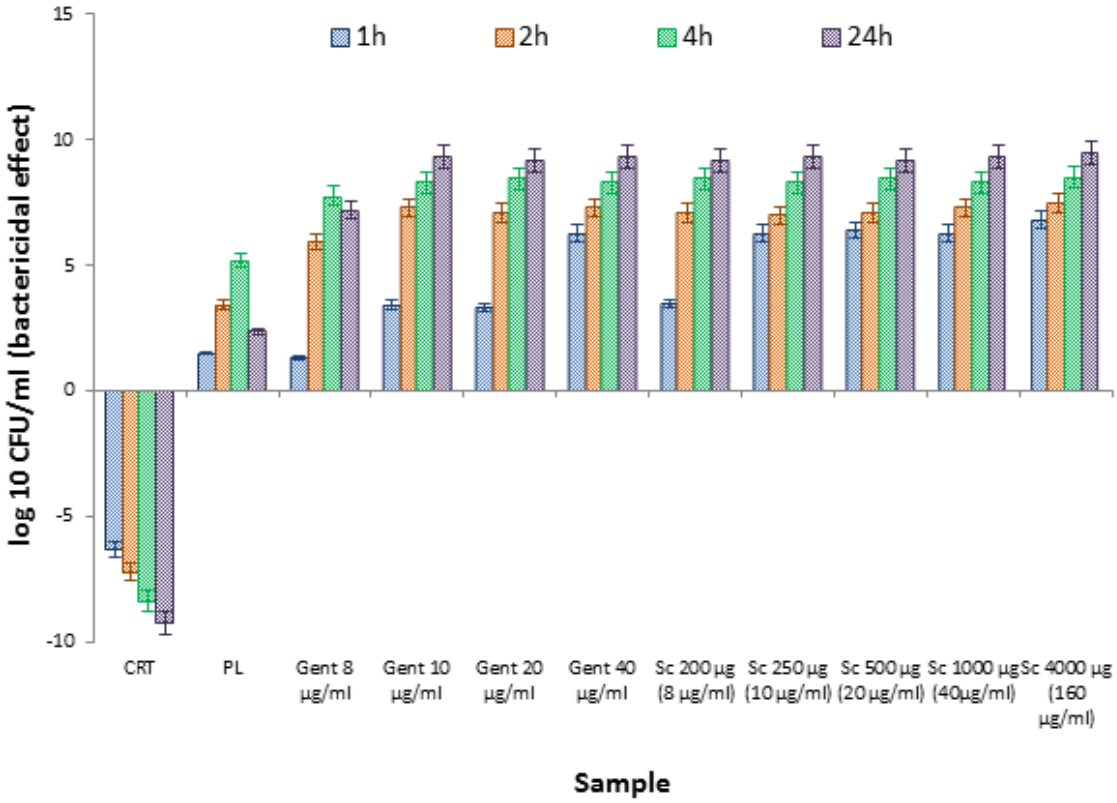

Figure 2: Antibacterial activity of Gent-loaded chitosan composite scaffolds (Sc 200 µg/ml, Sc 250 µg/ml, Sc 500 µg/ml, Sc 1000 µg/ml and Sc 4000 µg/ml) against *Escherichia coli* ATCC 10356. The data are expressed as difference in the number of Colony-forming unit (CFU) from the initial inoculum, means ± sd (n=3). Composite placebo scaffold (PL) and solution of gentamicin at different concentrations (Gent 8 µg/ml, Gent 10 µg/ml, Gent 10 µg/ml and Gent 10 µg/ml) were used as controls. The concentration reported after scaffold name indicates the concentration of gentamicin into scaffold.

The antimicrobial activity results against *Escherichia coli* ATCC 10356 are plotted in **Figure 3.** Placebo microparticles (Mps PL) did not have any bactericidal effect and the behavior of placebo microparticles embedded into chitosan composite scaffold (Sc Mps PL) was superimposable to that of chitosan composite scaffold (PL). Gentamicin microparticles (Gent Mps) had the highest

bactericidal effect in the first 4 hours of incubation, however the antimicrobial activity was maintained for 336 hours (fourteen days). The antimicrobial activity of 3D-DDS (Sc Mps Gent) resulted to be comparable to the one of gentamicin loaded microparticles (Mps Gent). Indeed, the highest value was measured after 4 hours of incubation (log_{10} CFU/ml 7.26) and it was maintained up to 14 days of incubation (log_{10} CFU/ml 1.65). The impact of chitosan antimicrobial activity on the formulation is limited to the first 4 hours and is a positive synergic to the formulation.

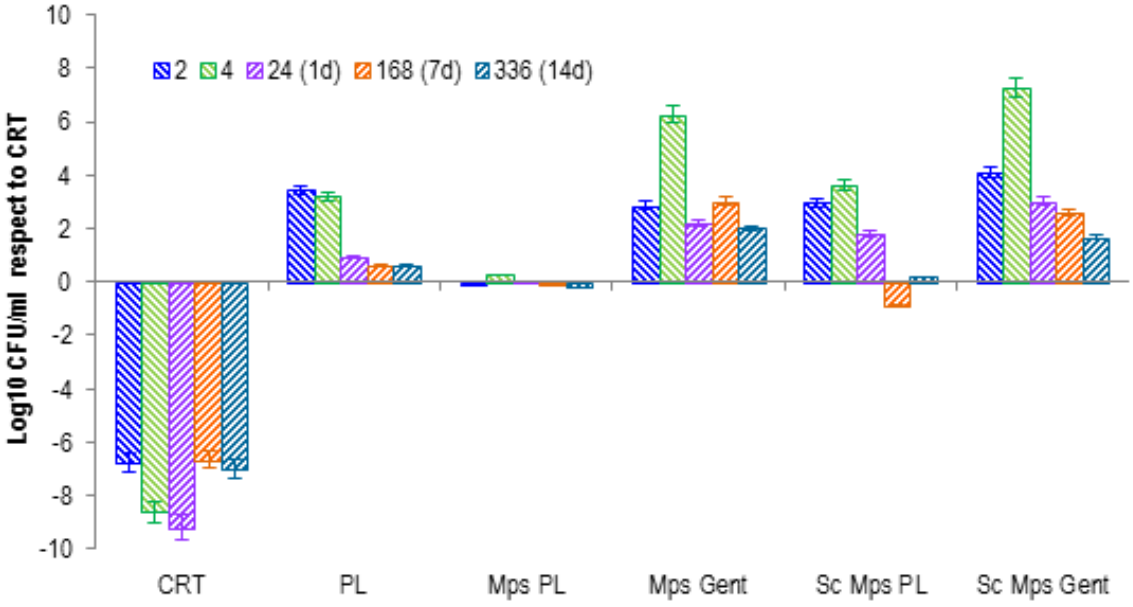

Figure 3: Antibacterial activity against *Escherichia coli* ATCC 10356 of Gent-loaded microparticles (Mps Gent) and 3D-DDS (Sc Mps Gent), the activity is expressed as change in the number of Colony-forming unit (CFU) from the initial inoculum. Composite placebo scaffold (PL), microparticles placebo (Mps PL) and microparticles placebo incorporated into composite scaffold (Sc Mps PL) were used as controls. Data are expressed as means ± sd (n=3).

Results of morphologic characterization show that PLGA-PEG microparticles are uniformly distributed throughout the chitosan matrix (**Figure 4 a**) with no separation phase phenomena. The presence of bovine bone granules (BBs) and microparticles do not interfere with microarchitecture of the composite scaffold (**Figure 4 b and c**) and the tridimensional spongy structure was maintained intact, no evidence of pore size reduction, interconnectivity occlusion was detected by SEM analysis (**Figure 4 d, e and f**).

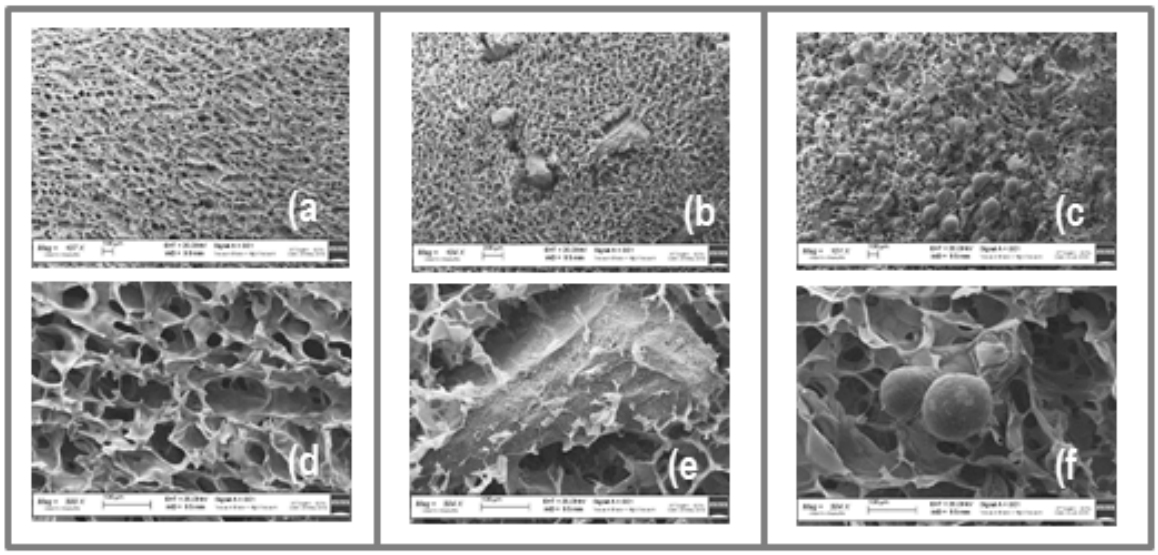

Figure 4: SEM micrographs of composite scaffolds: a) and d) composite placebo scaffold, b) and e) gentamicin loaded composite scaffold, c) and f) composite scaffold loaded with gentamicin PLGA-PEG microparticles (3D-DDS). Magnification 100x and 500x.

The water uptake of the 3D-DDS scaffold was in the range of 250.5-260.5 %, **Table 2**. This proves that the hydrophilic character of pegylated PLGA microparticles did not extensively affect on water uptake with respect to the placebo chitosan composite scaffold. The results showed that the 3D-DDSs loaded with 12 mg of Mps have the highest swelling properties (260.5%) and the 3D-DDSs with 24 mg of Mps have swelling behavior similar to placebo chitosan composite scaffold (253.96%). The water retention values of 3D-DDSs were not statistical different to the values measured for controls, chitosan and chitosan composite scaffolds (176.6 and163.14%, respectively) and the behaviour was independent to the amount of microparticles loaded into the scaffold.

All the scaffolds had porosity in the range of 80-95%; the steric effect of microparticles embedded into chitosan composite scaffolds did not alter the porosity of scaffolds. The compressive strength of 3D-DDSs in dry condition was also evaluated: DDs exhibits compressive strength of about 90-92 MPa, similar to the one detected for placebo chitosan composite scaffolds (96±0.6 MPa). Trabecular bone has been reported to display a compressive strength of 2-10 MPa, and cortical bone possesses much higher compressive strength, ranging from 100-230 MPa [15].

These experimental results are in agreement with the results of morphologic characterization; indeed, the presence of Mps into composite scaffolds does not vary their microarchitecture and the physico- and mechanical-properties (water uptake, water retention and compressive strength).

Table 2: Physico-chemical characterization of scaffolds: water uptake (%), water retention (%), porosity (%) and compressive strength (MPa).

Properties*Scaffolds*	**Chitosan scaffold**	**Chitosan composite scaffold**	**3D-DDSs – Mps loading**	
			12 mg	**24 mg**
Water Uptake (%)	306.4±7.5	253.96±10.3	260.5±5.5	250.5±10.5
Water retention (%)	176.6±6.4	163.14±5.5	170.7±6.5	175.7±7.3
Porosity (%)	91±3	89±6	88±5	85±5
Compressive strength (MPa)	36±0.08	96±0.6	92±0.5	90±0.7

The stability of the 3D-DDS was evaluated in terms of Mps and BBs granules release from chitosan composite scaffold, scaffold mass remaining and chitosan Mw variation. 9 % of BBs were released in the first 7 days, followed by a gradual release of BBs granules for six weeks. After 45 days, BBS granules release was faster and it was completed in almost 12 weeks, which corresponds to the time required for the complete dissolution of the chitosan matrix in the medium.

For the PLGA-PEG microparticles, the release rate was faster that the rate observed for BBs granules: indeed, 75 % of particles were released from composite scaffold in the first two weeks of incubation. These evidences could be attributed to the high porosity of composite scaffold and to the fast hydration of chitosan polymer matrix (**Figure 5**).

Further evaluation *in vivo* will be performed, taking into account that the scaffold environment in a narrow cavity could show less chance to release the BBS and the microparticles, consequently reducing the spreading of them in the surrounding tissue improving the osteoconductive property of the BBS and prolonged release of the gentamicin from the microparticles in infected tissue.

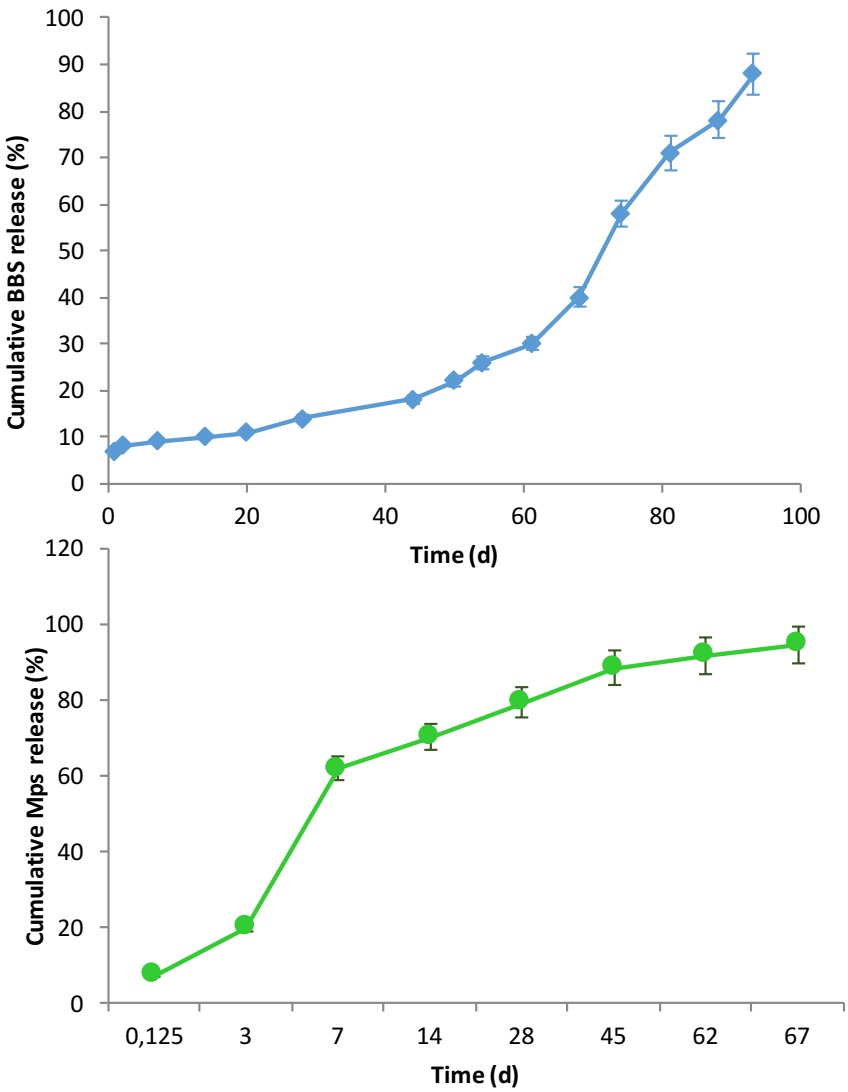

Figure 5: a) Cumulative release of bovine bone substitute (BBS) and b) Micropartcles (Mps) from Gent-loaded Mp chitosan composite scaffold as function of incubation time in PBS pH 7.4 for 74 and 67 days respectively. The values are means ± SD (n=5).

The mass remaining and Mw variation results are plotted in **Figure 6 and 7**, respectively. Placebo composite scaffold and 3D-DDS scaffolds loaded with two different microparticles doses (12 and 24 mg) present similar degradation trends. The mass remaining curves showed that the incorporation of Mp has not significant effect on the early phase 14 days, but after this time the mass loss rate was statistically increased. In particular, the incorporation of 24 mg of Mps led to fast reduction of mass remaining value reaching 75% in 14 days, while for 3D-DDSs loaded with 12 mg of Mps 75% of mass remaining was observed only after 21 days of incubation. All scaffolds lose their physical integrity when a mass remaining value of 5-6 % was reached.

The rapid mass loss of scaffolds containing PLGA-PEG microparticles could be linked to hydrolitic degradation of PLGA-PEG microparticles, the time dependent degradation of PLGA-PEG microparticles could cause shifts of pH into the scaffold microenvironment, at these conditions the hydrolytic reactions are catalyzed. This speculation is well correlated to mass remaining data and it is further supported by GPC analysis.

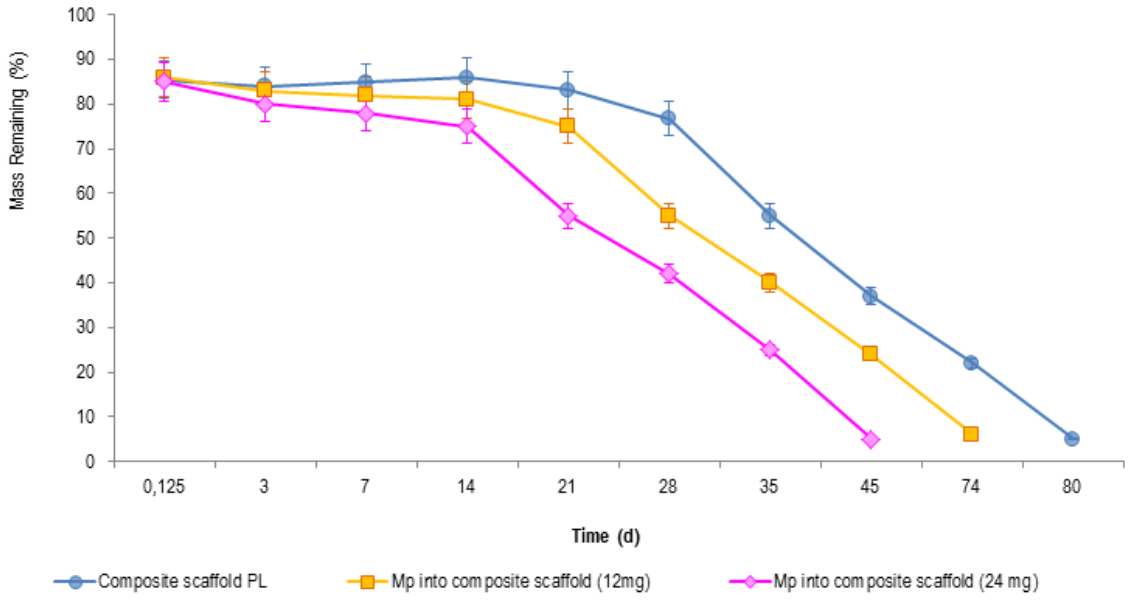

Figure 6: Mass remaining (%)of composite placebo scaffold (composite scaffold PL) and of 3D-DDS containing 12 mg of Mps (Mp into composite scaffold - 12 mg) and 24 mg of Mps (Mp into composite scaffold - 24 mg) as a function of incubation time. Samples were incubated in DMEM supplemented with 10% v/v FBS, at 37°C for 28 days. The values are expressed as means ± sd (n=5).

Results of GPC analysis in **Figure 7 a** report the values of chitosan Mw along incubation in DMEM supplemented with 10% v/v FBS, at 37°C, for 28 days. Chitosan Mw reduction is significantly higher for 3D-DDSs with respect to placebo composite scaffold, moreover the extect of reduction was dependent to amount of microparticles incorporated into composite scaffolds. GPC results revealed that the rate and the extent of polymer degradation were greater for scaffolds with the highest Mps content, 24 mg. These evidences confirm that the presence of PLGA-PEG microparticles into chitosan matrix have a destabilizing effect towards the polymer.

Looking to curves in **Figure 6 a**, an apparent increase of chitosan Mw is shown between day 5th and 15th, followed by the dramatic decrease of polymer Mw. The increase of Mw, detected in the first phase of degradation process, was due to the dissolution of small oligomers into the media which

inplicates the increase of the weight average molecaluar weight. After day 15th, the Mw reduction became significant and the behaviour is consistent with mass loss profiles (**Figure 6**).

The results of GPC analysis on the PLGA-PEG microparticles embedded into chitosan scaffolds (3D-DDS) and exposed to *in vitro* degradation test (**Figure 7b**) show that Mw reduction is significant slower for the microparticles embedded into scaffold with respect to free PLGA-PEG microparticles. The chitosan matrix seems to exert a protective effect towards PLGA-PEG polymer, slowing down its degradation rate.

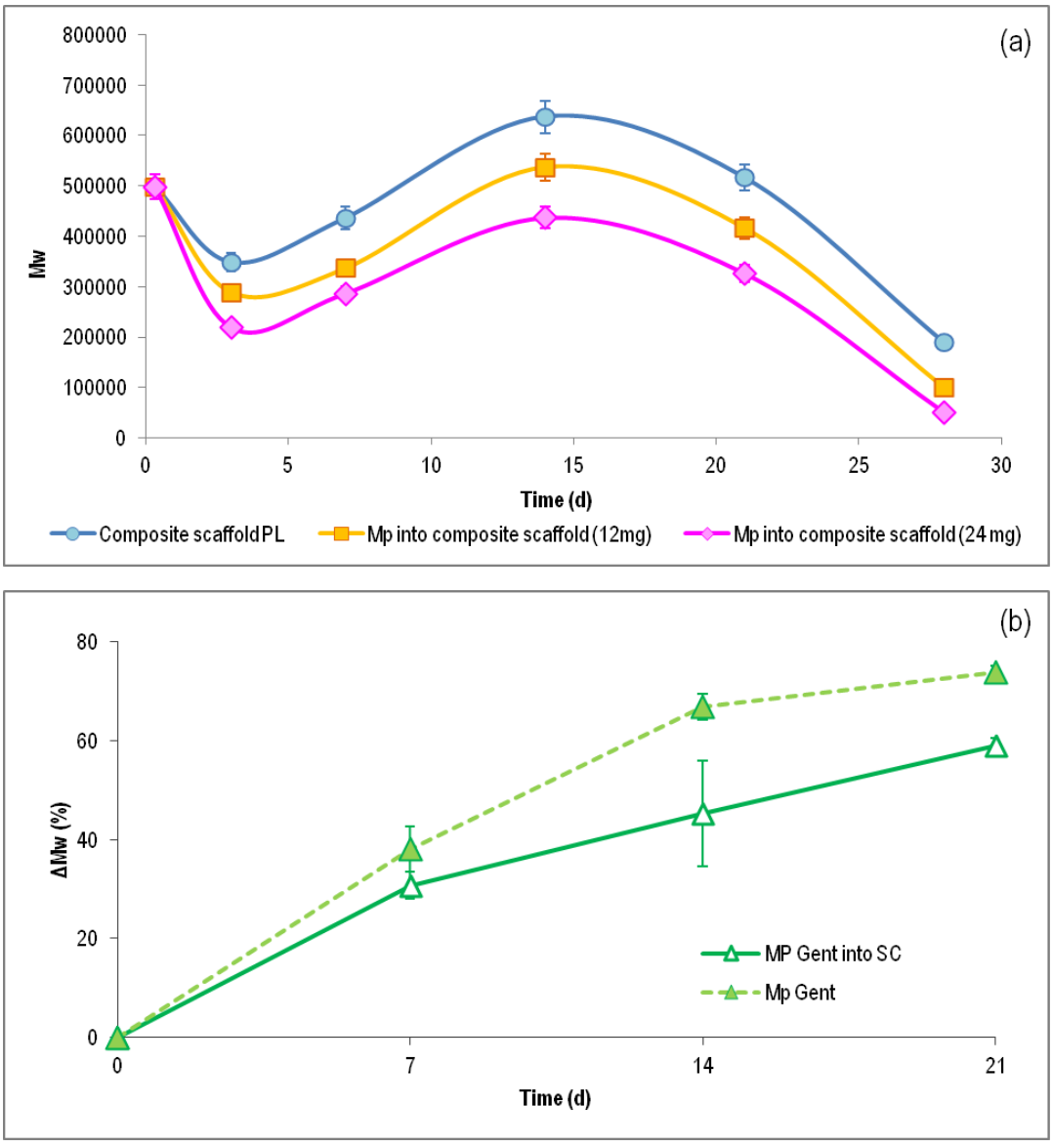

Figure 7: GPC results of *in vitro* degradation test: (a) Mw of composite scaffold (PL), 3D-DDS (12 mg Mps loading) and 3D-DDS (24 mg Mps loading) as function of incubation time; (b) molecular weight variation (ΔMw %) of PLGA/PEG microparticles as a function of incubation time. Samples were incubated in DMEM supplemented with 10% v/v FBS, for 18 days. The values are expressed as means ± sd (n=5).

The results of cell adhesion study showed that the incorporation of Mps did significantly affect cell adhesion to the scaffolds. All samples showed comparable cell adhesion properties: absorbance (Abs) values ranged from 0.09-0.13 in the first 3 hours. Long-term cell proliferation study (**Figure 8**) demonstrated similar cells growth trend and no important differences were highlighted between 3D-DDSs (Mp into composite scaffold 12 mg and Mp composite scaffold 24 mg) and control (Composite scaffold PL).

The composite scaffold containing microparticles seems to be a good microenvironment for cells attachment and proliferation; the good interconnectivity and hight porosity of composite scaffolds allow the diffusion of oxygen and nutrients inside the scaffolds and removal of cell waste toxic products. The degradation of chitosan matrix and PLGA-PEG microparticles look like not interfere with the cell growth.

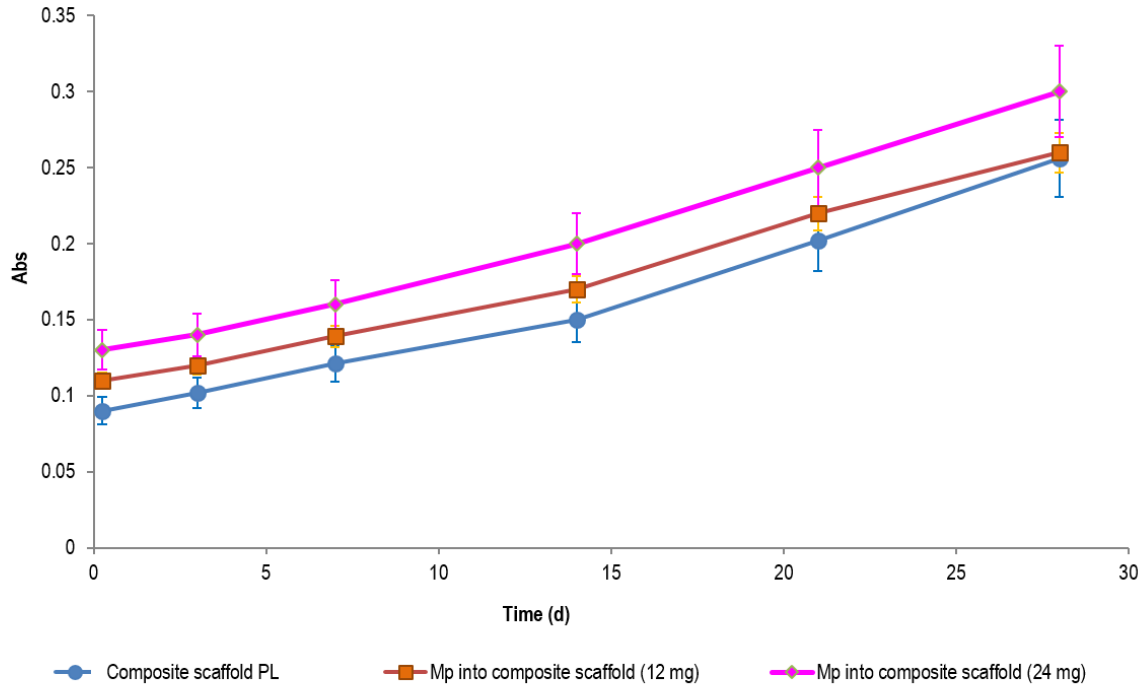

Figure 8: Long-term cell growth study of composite scaffold placebo (Composite scaffold PL) and microparticles incorporated into composite scaffolds (Mp into composite scaffold 12 mg and Mp into composite scaffold 24 mg). Samples were incubated in DMEM supplemented with 10% FBS, for 28 days at 37°C 5% CO_2. The values are expressed as means ± sd (n=5).

5. CONCLUSIONS

The literature on this topic reports that bacterial infection remains a major problem in orthopedic procedures. Moreover, it is well known that local delivery of antibiotics offers a better alternative to systemic administration, since it allows to reach high antibiotic concentration at the site of action and to limit the drug side effects.

This is particularly important in the initial post-surgery time, in order to prevent the formation of biofilm onto prosthesis surface.

The study introduces a biodegradable moldable and/or injectable system that can be useful as filler at prosthesis implantation site and as antibiotic delivery system. The final proof of concept has two actions: it is a 3D biodegradable scaffold promoting bone regeneration and a drug delivery system for local delivery of gentamicin to bone. The present work introduces the formulation study and *in vitro* characterization of the 3D-DDS. The results obtained permit to prove the feasibility of the 3D-DDS in its preliminary proof of concept. The study throw the basis for a further *in vivo* study and a product formulation, either as injectable *in situ* gelifying devices, or as moldable 3D-DDS scaffolds. Sterilization is one of the issue that has to be investigated for the final formulation set up. The proposed 3D-DDS is a composite polymer based system and unlikely it could undergo terminal sterilization by saturated steam. Therefore, a suitable sterilization process should be investigated combining different sterilization methods such as ionizing irradiation for the PLGA-PEG microparticles and BBs granules, saturated steam sterilization for other components, and assembling the product in aseptic area.

ACKNOWLEDGEMENTS

The authors thank Geistlich-Pharma AG for granting Orthoss® spongious granules for the research purposes.

6. REFERENCES

[1]L.Uçkay, P. Hoffmeyer, D. Lew, D. Pittet, Prevention of surgical site infections in orthopedic surgery and bone trauma: state-of-the-art update. J. Hosp. Infect. 84(663) (2013) 5–12.

[2]T. Stanton, J. Haas, M. Phillips, I. Immerman, Study points to savings with infection-screening program before TJR. *AAOS Now* 2010. Available from: http://www.aaos.org/news/aaosnow/mar10/clinical10.asp.Accessed 1 June 2011.

[3]D.Neut, H.Van de Belt, L. Stokroos, J.R. Van Horn, H.C. Van der Mei, H.J. Busscher, Biomaterial-associated infection of gentamicin-loaded PMMA beads in orthopaedic revision surgery,Journal of Antimicrobial Chemotherapy. 48 (2001) 885–891.

[4] K. C Pandey, Optimal management of chronic osteomyelitis: current perspectives. Orthopedic Research and Reviews. 7 (2015) 71–81.

[5]Harun Ismail, Ahmad Fahmi and Doolaanea, Abd Monem and Awang, Mohamed, Mohamed, Farahidah High initial burst release of gentamicin formulated as PLGA microspheres implant for treating orthopaedic infection. International Journal of Pharmacy and Pharmaceutical Sciences, 4(4) (2012) 685-691.

[6] G.H. Wang, S.J. Liu, S. Wen-Neng Ueng, E.C. Chan, The release of cefazolin and gentamicin from biodegradable PLA/PGA beads. International Journal of Pharmaceutics 273 (2004) 203–212.

[7] L. Francis, D. Meng, J. Knowles, T. Keshavarz, A. R. Boccaccini, I. Roy, Controlled delivery of gentamicin using poly(3-hydroxybutyrate) microspheres. Int. J. Mol. Sci. 12 (2011) 4294-4314.

[8] M. C. Lecaroz, M. J. Blanco-Prieto, M. A. Campanero, H. Salman, C. Gamazo, Poly(D,L-Lactide-co-Glycolide) particles containing gentamicin: pharmacokinetics and pharmacodynamics in *Brucella melitensis*-infected mice. Antimicrobial agents and chemotherapy (2007) 1185–1190.

[9] R. Dorati, A. DeTrizio, I. Genta , P. Grisoli , A. Merelli,C. Tomasi, B. Conti, An experimental design approach to the preparation of pegylatedpolylactide-co-glicolide gentamicin loaded microparticles for localantibiotic delivery. Materials Science and Engineering C 58 (2016) 909–917.

[10] R Dorati, I Genta, B Conti, H. Klöss, K. Martin, An injectable *in situ* forming composite gel to guide bone regeneration: design and development of technology platform. European Cells and Materials 24 (1) (2012) 14.

[11] R. Dorati, C. Colonna, I. Genta, A. De Trizio, T. Modena, H. Kloss, B. Conti, In vitro characterization of an injectable in situ forming composite system for bone reconstruction. Polymer Degradation and Stability 119 (2015) 151-158.

[12] R. Dorati, C. Colonna, I. Genta, T. Modena, B. Conti, Effect of porogen on the physico-chemical properties and degradation performance of PLGA scaffolds. Polymer Degradation and Stability 95 (2010) 694-701.

[13] M.A. Wikler, National Committee for Clinical Laboratory Standards, Methods for Dilution Antimicrobial Susceptibility Test for Bacteria that Grow Aerobically, eighth ed., Approved Standard M7-A8, National Committee for Clinical Laboratory Standards, Wayne, PA, US, 29(2) (2009).

[14] M. Kong, X. G. Chen, K.Xing, H.J. Park, Antimicrobial properties of chitosan and mode of action: a state of the art review. International Journal of Food Microbiology 144(1) (2010) 51-63.

[15] R.Huiskes, B.Van Rietbergen, in: V.C. Mow, R.Huiskes (Eds.), Biomechanics of Bone in basic Orthopaedic Biomechanics and Mechano-Biology, Chpt 4 third ed., Lippincot Williams and Wilkins Philadelphia, 2005, pp 123-179.

CHAPTER IV

Chapter V

CHAPTER V

PLGA-PEG/PLGA-H GENTAMICIN LOADED NANOPARTICLES: PREPARATION, FORMULATION STUDY AND *IN VITRO* CHARACTERIZATION

ABSTRACT

The s/o/w technique was selected for gentamicin incapsulation using PLGA-PEG, as biodegradable and biocompatible polymer. The critical points are: achievement of high payload into nanoparticles (Nps), stability after freeze-drying and resuspendability of nanoparticles. For this purpose, several process parameters were set up in order to optimize particles size, size distribution and focusing on gentamicin EE% improvement. On the base of a screening design, PLGA-PEG concentration was selected as the most significant factor influencing particles size (nm), most appropriate polymer concentration resulted to be 12.5 mg/ml in order to obtain small size Nps. Stirring rate is the most influencing factors for size distribution (PI), and 700 rpm permits to obtain an homogeneous Nps dispersion (PI=1, a narrow distribution). Moreover, increasing solvent/non solvent ratio (S/nS) from 0.2 to 0.5 is possible to improve drug contet (DC, 4.38 μg of gentamicin/mg of nanoparticles). Further experimental parameters were investigated to optimize drug content: polymer composition (PLGA-PEG and PLGA-H), PVA concentration into external aqueous solution, amount of methanol (MetOH) added to PVA external aqueous solution. A second 2^3 screening design permits to obtain a DC ≈12 μg of gentamicin/mg of nanoparticles. Since Nps resuspendability after centrifugation is a critical step, curing conditions (temperature and time used for solvent evaporation) were studied and suitabily set up at 4°C and 5 hours, Nps resuspension after centrifugation was optimized. It can be concluded that gentamicin is effectively entrapped in PLGA-PEG/PLGA-H Nps by modified s/o/w technique and the enhanced drug loading can be obtained by varying experimental conditions.

Keywords: s/o/w technique, gentamicin, Polylctide-co-glycolide-co-polyethylenglycole (PLGA-PEG), Polylactide-co-glycolide (PLGA), DoE, lyophilization.

This chapter to be submit for pubblication.

A. De Trizio, R. Dorati, T. Modena, I. Genta, B. Conti

1. INTRODUCTION

Gentamicin is an aminoglycoside antibiotic used to treat several types of bacterial infections. These may include bone infections, endocarditis, pelvic inflammatory disease, meningitis, pneumonia, urinary tract infections and sepsis among others. Moreover, it is the preferred antibiotic to treat nosocomial infections.

Gentamicin is a small drug molecule (Mw 477.596 g/mol); classified as BCS (biopharmaceutical classification system) class III because of its high water solubility and poor cellular penetration. Gentamicin binds irreversibly to 30S ribosomal subunit, inhibits an initiation complex formation with mRNA, preventing protein synthesis and resulting in cell bacteria death. Additionally, as all aminoglycoside antibiotics, gentamicin can cause membrane damage altering ionic concentration [1].

As already mentioned, aminoglycoside-gentamicin can be used for treating infections caused by bacteria as *Escherichia Coli, Pseudomonas Aureus and Staphylococcus Aureous.* These bacteria are the dominating cause of osteomyelitis. Osteomyelitis is one of the devastating bone diseases, especially in the chronic stage, in which vascularized tissues renders systemic antibiotic administration inefficacious.

Conventional treatment of osteomyelitis involves firstly debridement of infected bone tissue, followed by intravenous administration of antibiotics at high concentration for following 4-6 weeks. The conventional multiple dosing regimens result in adverse reactions due to fast gentamicin clearance or its unfavorable biodistribution, causing nephrontoxicity and ototoxicity. Generally, strict antiseptic operative procedure is suggested to prevent infection during surgery, including a local antibiotic therapy using antibiotic-impregnates or antibiotic-loaded cements [2]. Even if using antibiotic-impregnated cements represents the gold standard treatment, the use of these products remains controversial because of poor drug release rate, unreasonable drug-loaded quantity and antibiotic resistance onset [3].

A biodegradable antibiotic local nanoparticulate drug delivery system (Nps DDS) could be a promising strategy to overcome drawbacks of antibiotic-impregnated or -loaded cements: NpS DDS could provide an appropriate drug release kinetic supplying an effective and efficacious local therapeutic concentration of antibiotic at infection locus [3, 4]. Moreover, Nps DDs could present antimicrobial activity by themselves improving the effectiveness and safety antibiotic administration.

Nanotechnology has emerged as a promising approach both for restoring or enhancing activity of old and conventional antimicrobial agents and for treating intracellular infections by providing intracellular targeting and sustained release of drug inside infected cells. Nps DDS may lead to an improvement in drug cellular accumulation and a reduction of the required dosing frequency improving patient

compliance and efficacy of antimicrobial therapy. It could be promising to overcome the microbial resistance [5].

According to their sub-micro size, nanoparticles efficiently cross biological barrier improving drug bioavailability and permanence time in infected site, protecting drug from degradation and achieving gradual release pattern [1]. In this context, loading gentamicin in polymeric nanoparticles could be interesting in treating osteomyelitis infections [6, 9].

According to literature review, it was found that several authors studied preparation of gentamicin loaded nanoparticles based on PLGA using different method as w/o/w and s/o/w evaporation techniques [6-8].

The aim of the present work was to design and characterize gentamicin-loaded PLGA-PEG nanoparticles in order to obtain a controlled release system. Nanoparticles have prepared by s/o/w method and formulations have been characterized with regard to size, size distribution, drug content and drug release. In the first part of present research project, two different full factorial screening experimental designs have been used to optimize process-parameters. The effect of several process parameters have investigated to reduce particles size and to enhance drug encapsulation. *In vitro* release tests were performed on optimized formulation in PBS pH 7.4, 37°C in static conditions. In order to understand kinetic and mechanism of drug release, release data were fitted with four kinetic equations, as zero order, first order, Higuchi model and Korsmeyer–Peppas model. A design of experiment (DoE) approach has adopted to investigate the influence of all process parameters. DoE allows to evaluate interactions between process variables and to control methodically them during nanoparticle synthesis. In the second part, formulation phase, a freeze-dried powder has developed optimizing freeze-drying protocol using a mixture design.

2. MATERIALS

Gentamicin sulphate (Gentamicin C1 $C_{21}H_{43}N_5O_7$, Mw 477.6 g/mol, Gentamicin C2 $C_{20}H_{41}N_5O_7$, Mw 463.6 g/mol, Gentamicin C1a $C_{19}H_{39}N_5O_7$, Mw 449.5 g/mol was from Sigma Aldrich. Polylactide-co-glycolide (PLGA-H, 7525 DLG 3A Mw 25 kDa) and Polylactide-co-glycolide-co-polyethylenglycol (PLGA-PEG, 5050 DLG 5C PEG 1500 Mw 70 kDa, PEG 51%) were from Lakeshore Biomaterials, Birmingham, AL, USA. PVA (Mw 85-124 kDa 87-89% hydrolyzed), Polyvinylpirrolidone (PVP K17, Mw 17KDa and PVP K32, Mw 32KDa), sodium carboxymethylcellulosa (SCM, Mw 90KDa) methanol, ethanol, acetone, dichloromethane, dimethyl sulfoxide, ninhydrin, Mw 178.14 g/mol were from Sigma Aldrich, Milan, Italy.

3 METHODS

3.1 Preparation of nanoparticles

Nanoparticles were prepared using a modified solid/oil/water extraction method (s/o/w). Briefly, 3.5 mg of gentamicin was dissolved in 0.1 ml of distilled water. The gentamicin solution was then added to 2 ml of acetone containing different amounts of polymer (50 or 25 mg). The diffusion of water into acetone contribute to solid gentamicin precipitation. The suspension was stirred by vortex at 30,000 rpm/min for 1 minute and then added to different volumes of PVA solutions at 1 % w/v (10 or 5 ml). Following acetone phase diffusion into the aqueous PVA phase contributed to the formation of gentamicin-loaded nanoparticles.

3.2 Optimization protocol by Experimental of Design (DoE)

s/o/w technique was submitted to a screening design (2^3) to investigate: a) effect of polymer concentration (mg/ml), b) volumetric ratio between solvent (acetone, S) and non-solvent (PVA aqueous solution, nS) and c) stirring rate (rpm), keeping polymer (2ml) volume constant. These factors (input) have selected because they strongly influenced particle size (nm), size distribution (PDI) and drug content (μg of gentamicin entrapped/mg of nanoparticles). Eight batches were prepared for 2^3 full factorial design to study the effect of three independent variables (input) on each response (output). Each factors were tested at two level designed as -1 and +1 (**Table 1**).

Equation 1 is:

$Y= \beta_0 + \beta_1X_1+ \beta_2X_2 + \beta_3X_3 + \beta_{12}X1X2 + \beta_{13}X1X3 + \beta_{23}$ X2X3.

Intercept= β_0

Linear terms= $\beta_1X_1+ \beta_2X_2 + \beta_3X_3$

Interaction terms= $\beta_{12}X1X2 + \beta_{13}X1X3 + \beta_{23}$ X2X3

The coefficients corresponding to linear effects (β_1, β_2 and β_3), to interactions (β_{12}, β_{13}, and β_{23}) were determined from the results of all experiments in order to identify a statistically significant term. Diagrammatic representations of values per each response (pareto chart and response surface) resulted to be very helpful to explain the relationship between independent and dependent variables.

Table 1: Factors and factor level studied in the screening experimental design (2^3=8 batches).

Batches #	Polymer concentration(mg/ml)	S/nS ratio (v/v)	Stirring rate (rpm)
1	12.5 (-1)	0.2 (-1)	350 (-1)
2	12.5 (-1)	0.5 (+1)	350 (-1)
3	12.5 (-1)	0.2 (-1)	700 (+1)
4	12.5 (-1)	0.5 (+1)	700 (+1)
5	25 (+1)	0.2 (-1)	350 (-1)
6	25 (+1)	0.5 (+1)	350 (-1)
7	25 (+1)	0.2 (-1)	700 (+1)
8	25 (+1)	0.5 (+1)	700 (+1)

After this screening design, other factors such as: a) type of polymer solvent, b) polymer composition, c) PVA concentration in the outer phase, d) addition of methanol and ethanol in PVA outer phase, were investigated in order to improve gentamicin drug content. A second 2^3 full factorial design has performed using Statgraphics Centurion software (**Table 2)** and it has designed based on preliminary experimental results (**Table 5**). Eight batches were prepared for the 2^3 full factorial design, keeping constant the polymer concentration (12.5 mg/ml), solvent/non solvent ratio (0.5 v/v) and stirring rate (700 rpm) as already set up from the first screening design.

This second study was assessed in order to optimize the effect of: a) polymer composition (PLGA-PEG and PLGA-H), b) PVA concentration (%w/v) and c) addition of a different percentage of a non-solvent (MetOH) into PVA outer solution, on three responses as gentamicin DC, particles size and size distribution. Each factor was tested at two levels designated as -1, and +1 (**Table 2**). This second experimental screening design has planned to improve gentamicin drug content maintaining constant values of particle size and particle size distribution obtained from the first screening design. The regression equation for the response was calculated using equation 2:

$Y= \beta_0 + \beta_4X_4+ \beta_5X_5+ \beta_6X_6 + \beta_{45}X4X5 + \beta_{46}X4X6 + \beta_{56}$ X5X6

Response in the above equation Y is the measured response associated with each factor level combination: βo is the intercept, β is the coefficient of terms X, X4, X5 and X6, which are the studied factors; X4X5, X4X6 and X5X6 are the interaction between variables.

Response surface and pareto charts methodology set a mathematical trend in the experimental design for determining the influence of each experimental factor and their interactions for a given response. Two replications were run for each screening design.

Table 2: Runs parameter for the second full factorial, screening experimental design (2^3=8 batches).

Batches #	Polymer composition (PLGA-PEG/PLGA-H)	PVA (% w/v)	MetOH (% v/v)
9	70/30 (-1)	0.25 (-1)	30 (-1)
10	70/30 (-1)	0.5 (+1)	30 (-1)
11	70/30 (-1)	0.25 (-1)	60 (+1)
12	70/30 (-1)	0.5 (+1)	60 (+1)
13	30/70 (+1)	0.25 (-1)	30 (-1)
14	30/70 (+1)	0.5 (+1)	30 (-1)
15	30/70 (+1)	0.25 (-1)	60 (+1)
16	30/70 (+1)	0.5 (+1)	60 (+1)

3.3 Redispersability and lyophilization study of nanoparticles

The nanoparticle formulation selected from the two screening designs (Np 13, in **Table 2**) was purified by centrifugation at 16400 rpm, 4°C for 20 minutes. The suspension was freeze at -25°c for 1hour and then -40°c for 12 hours and then liophylized at -48°c at 0.01 mbar for 24 h (lyophilizer, LIO 5P, Milan, Italy). Lyophilization can generate many stresses induce aggregation and in some cases irreversible nanoparticles fusion. For this reason, cryoprotectant solution must be added to the suspension of nanoparticles before lyophilization to protect these fragile systems. Polyvinylpirrolidone (PVP K17 and/or PVP K32 and sodiomethylcarboxycellulosa (SMC) are chosen as cryoprotectants in order to obtain a 1:2 w/w weight ratio between nanoparticles and cryoprotectant. The lyophilized nanoparticles formulation in the presence of cryoprotectant was rehydrated in 500 µl of sterile water (the same volume of cryoprotectant solution). In order to investigate the influence of cryoprotectant as such or their mixture a new experimental approach, Mixture Design has applied. The mixtures design selected for the study is the simplex centroid (centroid), this includes in 2q-1 different blends design (q number of components) generated from the processing of: i) pure components (1,0 ,0), binary mixtures (1/2, 1/2, 0), ternary mixtures (1/3, 1/3, 1/3) until reaching the selected centroid (1/q, 1/q, 1 /q), in our case the centroid corresponds to the ternary mixture. The three components of the mixture are: i) polyvinylpyrrolidone PVP K17 ii) polyvinylpyrrolidone PVP K32 and iii) sodium carboxymethyl cellulose (SCM). In the case of binary, each component of the mixture must correspond to 100 and for the ternary mixtures, each component is 66.6 %. The particle size was determined before and after freeze-drying to calculate the ratio between final and initial size (S_f/S_i) [10].

Table 3: Runs parameter for the stability study after freeze-drying of the nanoparticles using a mixture design.

Batches #	PVP K17*	PVP K32*	SCM*
1	2	0	0
2	0	2	0
3	0	0	2
4	1	1	0
5	0	1	1
6	0.66	0.66	0.66
7	0.66	0.66	0.66
8	0.66	0.66	0.66

*(w/w is the weight ratio between cryoprotectans and nanoparticles)

3.4 Characterization of nanoparticles

3.4.1 Particle size and Surface charge

Particle size and polidispersability index (PDI) were determined by dynamic light scattering (DLS) by using ZetaSizer (NICOMP 380 ZLS, Particles Sizing System, Santa Barbara, California, USA). Each fresh formulation was dispersed in distilled water and appropriately diluted reaching a concentration of 13 µg/ml. Zeta potential was evaluated using ZetaSizer (NICOMP 380 ZLS, Particles Sizing System, Santa Barbara, California, USA). Each fresh formulation was dispersed in PBS (10 mM) at concentration of 13 µg/ml. All measurements were carried out in triplicate.

3.4.2 Morphology

Shape and surface morphology of nanoparticle formulation were examined with a transmission electron microscopy (TEM) (TEM 208 S, Philips NL). 15 µl of Nps suspension was placed on a 300 mesh copper grid covered with Formvar film (AGAR Scientifc, Stansed, UK). The excess liquid was removed with filter paper, and then 10 µL of 1% uranyl acetate was added on to grids and left standing for 10 s, after that liquid in excess was removed by filter paper and sample analyzed.

3.4.3 Drug content

13 mg of Nps formulation was dispersed into 1 ml of DMSO, the dispersion was stirred at 300 rpm for 5 h to ensure complete dissolution of nanoparticles. The resulting solution was centrifuged at 16400 rpm, 25°C for 20 minutes and pellet was reconstituted in 2 ml of distilled water and stirred for 12 h to

solubilize the extracted gentamicin. Both supernatants, in DMSO and in distillated water containing gentamicin were analyzed by UV-spectroscopy at λ 400 nm after reaction with nynidrin [14, 15]. In regards to the nynidrin assay: 800 µl of supernatant was mixed with a ninhydrin solution in PBS pH 7.4 (240 µl, 0.2 % w/), the mixture was vortexed and heated in a water-bath at 95°c (15 minutes) and then cooled in an ice-bath for 10 minutes.

A calibration curve in DMSO (50-500 µg/m, R^2=0.9879) and in water (50-500 µg/ml, R^2=0.9909) was used for gentamicin quantification. Drug Content (DC) has calculated using equation 3, considering the contribution from DMSO and distillated water:

$$DC=\frac{\text{weight of gentamicin extracted (µg)}}{\text{weight of dried nanoparticles (mg)}} \qquad \text{Equation 3}$$

3.4.4 *In vitro* release study

In vitro release profile of gentamicin from gentamycin-loaded nanoparticles was performed as follows: 90 mg of lyophilized nanoparticles composed by 30 mg of gentamicin nanoparticles optimized formulation and 60 mg of cryoprotectant selected from DoE mixture, were suspended in 1 ml of PBS pH 7.4, at 37°C. At each time point (0.25, 0.5, 1, 2, 4, 6, 8, 10 hours), nanoparticles were centrifuges (20 minutes, 25°c at 16400 rpm) and 800 µl have collected and replaced by an equal amount of fresh PBS. The amount of gentamicin released in PBS at each time point was detected by reaction with ninhidryn and then quantified by UV-Vis spectrophotometer (UV-1601, Shimadzu, Japan) at 400 nm and calculated using a calibration curve in PBS (33.3-275 µg/ml, R^2=0.9979). The release study has been conducted until to reach 100% of release. Gentamicin as such (1 mg) underwent a dissolution test in the same experimental conditions. All experiments have performed in triplicate. To analyze the *in vitro* drug release data four kinetic models were used to describe release kinetics.

The zero order Eq (4) explains the release from systems where rate of drug release is concentration independent [11].

$$C = K_{0t}t \qquad \text{Eq (4)}$$

Where C is the concentration of drug at time t, t is the time and K_0 is zero-order rate constant express in concentration/time unit.

The first order Eq (5) explains the release from systems where rate of drug release is concentration dependent.

$$\log C_0 - \log C = K_1 t/2.303 \qquad \text{Eq (5)}$$

Where C_0 is the initial concentration of drug and K_1 is the first order rate constant.

Higuchi model describes the release from insoluble matrix as square root of time dependent process based on fickian diffusion Eq (6) [12].

$C = K_h\sqrt{t}$ Eq (6)

Where, K_h is the constant which reflect system design variables.

Korsmeyer-Peppas model describes the release of drug from a polymeric system (Eq 7).

$M_t/M_\infty = KK_{hp}t^n$ Eq (7)

Where M_t/M_∞ is the fraction of drug released at time t, K_{hp} is the rate constant and n is the release exponent.

3.5 Statistical analysis

All experiments were based on three independent samples and the experiments were repeated for three times. Results were reported as mean±standard deviation. Moreover, analysis of variance (ANOVA) and p-value< 0.05 were used to assess statistical significance.

4.RESULTS AND DISCUSSION

Physical properties, as particles size, size distribution and drug content (DC) are summarized in **Table 4**. All PLGA-PEG nanoparticles were prepared using a s/o/w procedure, several process parameters have been evaluated to optimize size, size distribution and DC.

Keeping constant PLGA-PEG concentration at 12.5 mg/ml, and stirring rate at 350 rpm, increase of S/nS ratio causes an important increment of size and size distribution (Batch # 1 and 2). As reported in literature, S/nS ratio is a critical parameter having an important role in nanoparticle formation [16]; no statistical differences have been highlighted in term of drug content.

The increment of stirring rate up to 700 rpm (Batch #4) allows reduction of size (240.0±0.54 nm) and size distribution values (0.130 ± 0.57). A slightly increase of drug content value was observed, reaching 4.38±2.45 µg gentamicin sulphate/mg nanoparticles. Low drug content values can be due both to the high solubility of the drug in aqueous solution (50 mg/ml) and the large surface area of nanoparticles, which facilitate gentamicin diffusion into external aqueous phase during nanoparticles preparation. Nanoparticles prepared with polymer concentration of 25 mg/ml show size > 500 nm. Only for batch #7 no statistical variations of size were detected; nevertheless, polydispersity index (PDI) was larger (1.230±0.24). In terms of drug content, high polymer concentration doesn't affect the entrapment of gentamicin.

Table 4: Effect of PLGA-PEG concentration, S/nS ratio and stirring rate on size, size distribution (PDI) zeta potential (mV) and drug content (DC).

Batch #	PLGA-PEG (mg/ml)	S/nS ratio (v/v)	Stirring rate (rpm)	Size (nm)	PDI	Zeta potential (mV)	DC
1	12.5	0.2	350	199.4±54.4	0.27±0.47	-1.06±0.56	1.54±0.70
2	12.5	0.5	350	384.6±58.7	0.30±0.43	-0.37±0.98	1.73±0.32
3	12.5	0.2	700	410.7±42.4	0.10±0.99	-1.28±0.67	1.68±0.86
4	12.5	0.5	700	240.0±54.6	0.13±0.57	0.36±0.84	4.38±2.45
5	25	0.2	350	855.5±46.7	0.27±1.28	-0.96±0.88	1.36±0.67
6	25	0.5	350	507.8±47.9	0.18±2.71	-5.23±0.43	1.55±0.67
7	25	0.2	700	381.5±57.9	1.23±0.24	-2.36±0.75	2.45±1.78
8	25	0.5	700	919.3±53.2	0.14±2.45	-5.54±0.59	2.34±1.68

*Drug content was reported as **µg/mg of nanopartcles**

From data reported in **Table 4** polymer concentration, S/nS ratio and stirring rate have been selected as the most critical process parameters for the formulation of gentamicin-loaded nanoparticles. These parameters have further studied in order to increase gentamicin content in PLGA-PEG nanoparticles. The data reported in **Table 4** were applied for a 2^3 randomized screening design (DoE), the three factors were evaluated at two different levels, summarizing all possible combinations.

PLGA-PEG polymer concentration (25-12.5 mg/ml), S/nS ratio (0.5-0.2 v/v) and stirring rate (700-350 rpm) have chosen as independent variables whereas particle size, size distribution and drug content were selected as dependent variables (outputs). Terms with $p<0.05$ were considered statistically significance and retained in the reduced model.

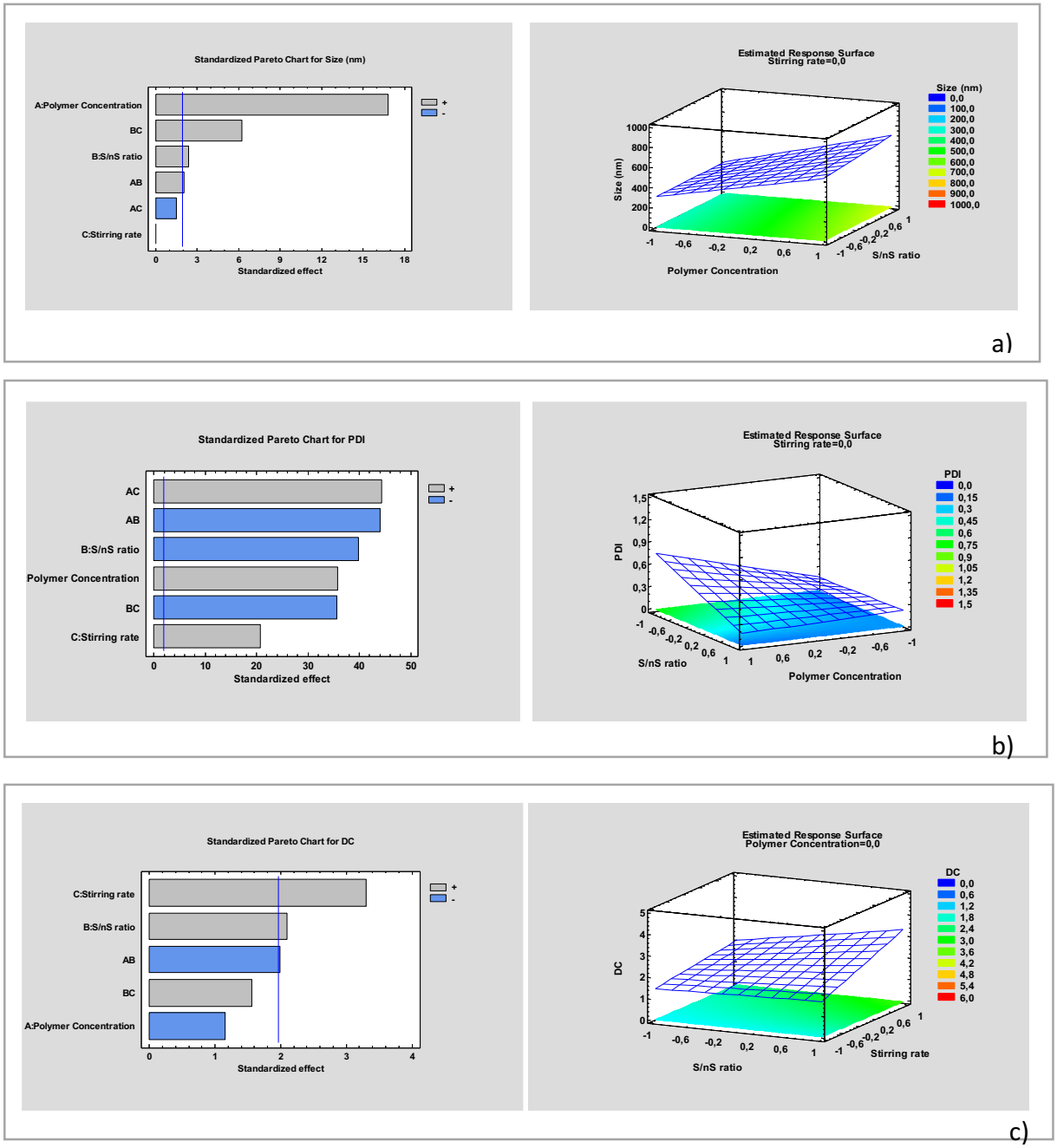

Figure 1: Estimated Response Surface and pareto chart for particle size (a), size distribution (b) and DC (c) of the screening design.

In **Figure 1a** the Pareto Chart and Estimated Response Surface of mean diameter versus polymer concentration and S/nS ratio (significant factors) show a linear model, namely Nps particles size is linearly dependent to polymer concentration and S/nS ratio. Higher particles size values were observed at high polymer concentration and at high S/nS ratio.

The coefficients, that are over the blue line (significant limit) having p value <0.05 are highly significant (Pareto Chart **Figure 1a**). The interaction BC, between ratio S/nS (B) and stirring rate (C) presents a p

value < 0.05, thus it contributes on an increase of mean particle size. Nevertheless, factor C, stirring rate, doesn't have any significant effect on mean diameter. Equation of the full model is here reported:

Size (nm) = 487.313 + 178.637 X polymer concentration + 25.5375 X S/nS ratio + 0.4875 X stirring rate + 21.9125 X polymer concentration X S/nS ratio -16.1875 X Polymer concentration stirring rate + 66.1625 X S/nS ratio X stirring rate

R^2 squared is a measure of total variability explained by the model. R^2 squared value of the model was 61.10 indicating that the model can explain 61.10 of variability around the mean.

The pareto chart of the model shows that polymer concentration and S/nS ratio significantly ($p<0.05$) influenced output, mean particle size. Particle size values were bigger (507.8±47.9 - 919.3±53.2 nm) for formulations with high polymer concentration (25 mg/ml) and high S/nS ratio (0.5)

A value of PDI close to 0 indicates homogeneous dispersion, while PDI values higher than 0.3 represent heterogeneous distribution. Low PDI has measured at low value of both polymer concentration and stirring rate and at high value of S/nS ratio (**Figure 1b**).

The pareto chart of the full model for PDI shows that all factors were significant (p-value<0.05) contributing in output prediction (PDI), (**Figure 1b**). Full model analysis of variance (ANOVA) showed a R^2 square value of 87.42, the equation is reported here below:

PDI = 0.327+ 0.12675 X Polymer concentration-0.14075 X S/nS ratio + 0.0735X Stirring rate- 0.156 X Polymer concentration S/nS ratio+ 0.15675 X Polymer concentration stirring rate- 0.12575 X S/nS ratio X stirring rate

At high of S/ns ratio (0.5 v/v) PDI is lower indicating a narrow particle size distribution of nanoparticles, instead for high polymer concentration (25 mg/ml) and high stirring rate (700 rpm) nanoparticles suspension is non uniform with some aggregation phenomena.

As observed for mean particles size and PDI outputs, DC response surface shows a linear model, thus no further experiments were designed. From response surface, high value of S/nS ratio and stirring rate, that are output significant factors, improve DC (**Figure 1c**).

The DC pareto chart of full model doesn't has any significant factors; the interactions AC, between stirring rate (B) and polymer concentration (A) was discarded (**Figure 1c**). High DC value was observed at high stirring rate (700 rpm) and high S/nS ratio value (0.5). ANOVA of reduced model show a R^2 squared value of 84.07. The reduced model has the following equation:

DC (μg/mg Nps) = 2.12875-0.20375X Polymer concentration + 0.37125 X S/nS ratio + 0.5875 X stirring rate- 0.35125X Polymer concentration X S/nS ratio

DC pareto chart indicates that Stirring rate and S/nS ratio have significantly important influence.
This preliminary screening design demonstrates that a polymer concentration at low level (12.5 mg/ml) contributes to reduce both particles size and PDI; S/nS ratio at high level (0.5) positively influences DC and PDI value, and it negatively affects the mean particle size. Stirring rate is the most important factor affecting DC: the highest DC value was measured at high stirring rate value. On the base of preliminary results summarized in **Table 4**, and of the statistical values of DoE experimental, process parameters used to formulation batch #4 were selected. Nevertheless, further attempts have made to improve gentamicin DC. Effect of several processes variables has been evaluated, as the solvent used to dissolve polymer, polymer composition and composition of external aqueous phase with regard to PVA concentration and addition of an alcohol. The effect of all process parameters was investigated on DC, particle size and size particle distribution (**Table 5**).

- *Effect of solvent*

Solvents, used to dissolve polymer, have an important role in the preparation of Nps, affecting both size and DC. Solvent diffusion into the outer phase should be fast enough to permit polymer precipitation and drug entrapment inside formed nanoparticles. It is important to evaluate solvent affinity and external aqueous phase (no solvent) in order to control solvent diffusion towards aqueous phase [13] . Acetone and DMSO have selected because of their capability to dissolve polymers and their dielectric constant. Solvent dielectric constant provides a measure of solvents polarity and it can be an acceptable predictor of solvent ability to dissolve ionic compound.
Acetone and DMSO have been selected for preparing of PLGA-PEG Nps containing gentamicin. Acetone is the most common solvent used in s/o/w technique because is able to dissolve PLGA polymer and it has a low dielectric constant (ε=20.5 at 25°C), while DMSO is a polar solvent with high dielectric constant (ε=46.4 at 25°C). DMSO solvent shows low affinity for PVA aqueous phase hampering solvent diffusion from polymer matrix to the outer phase, while the high affinity of acetone with PVA aqueous solution should facilitate diffusion of polymer solvent into external aqueous phase reducing time needed for polymer precipitation and potentially increasing drug entrapment. Batches # 4 and 9 were prepared with acetone and DMSO, respectively. On the base of data reported in **Table 5**, acetone remains the optimal solvent for preparing PLGA-PEG Nps using s/o/w technique. Indeed, the formulation obtained solubilizing PLGA-PEG polymer in DMSO (Batch # 9) show particles size > 1 μm due to aggregates formation during polymer precipitation.

- *Effect of polymers*

The effect of polymer composition has also investigated using PLGA copolymer and PLGA-PEG block copolymer. DC data depend on polymer composition; the data obtained for Batch #10 were not comparable to Batch #4.

DC (27.31 μg/mg of nanoparticles) is 8 times higher with respect to PLGA-PEG formulation (Batch #4) probably due to ionic interaction between carboxyl groups of PLGA-H and amino groups of gentamicin sulphate.

PLGA-PEG and PLGA-H polymer were mixed at different ratio (70:30, 50:50, 30:70). As expected, the reduction of PLGA % in organic phase causes an important decrease of DC reaching 0.2 μg of Gentamicin per mg of nanoparticles. Batches obtained mixing PLGA-H with PLGA-PEG show higher particles size and size distribution compared with Batches #4 and 10. Only Batch #12 (PLGA-PEG/PLGA-H ratio, 50:50) shows similar results in terms of size and size distribution, nevertheless low DC value has been measured (0.94 μg/mg of nanoparticles). The ratio PLGA-PEG/PLGA-H 30:70 (Batch #11) was selected and further parameters were optimized changing PVA concentration and addition of an alcohol into external phase.

- *Effect of PVA concentration and addition of alcohol into external aqueous phase*

PVA concentration affects external aqueous phase viscosity and consequently acetone diffusion rate from polymer matrix to external aqueous phase: external aqueous phase viscosity is reduced decreasing PVA concentration promoting solvent diffusion. The rapid diffusion of polymer solvent could promote drug entrapment into polymer matrix and facilitates small nanoparticles formation. On the opposite, lower external aqueous phase viscosity could facilitate gentamicin diffusion from the embryonic nanoparticles. Considering the two competitive effects, results of Batches #14 and #15 demonstrates gentamicin diffusion into the external aqueous phase prevales. In fact, at low PVA percentages (0.5 and 0.25% w/v), DC values were lower with respect to Batch #11 at and particles size value was very high. The concomitant reduction of PVA concentration and addition of alcohols into external aqueous phase was investigated. Alcohols are characterized by low dielectric constant which affects gentamicin solubility and its capability to escape into external aqueous phase. Two different alcohols have evaluated: ethanol (EtOH, ε=24.6 at 25°C) and methanol (MetOH, ε=32.7 at 25°C). Addition of alcohol to external aqueous phase should reduce PVA aqueous phase dielectric constant increasing DC values. Batch #16 and 17 were prepared using decreasing PVA percentages (0.5 % and 0.25%) and adding 30% v/v of ethanol. The results show an important significant of DC which is dependent on ethanol addition despite PVA concentration. Nevertheless, nanoparticles size increases reaching 1μm.

Table 5: Optimization of organic phase and aqueous phase.

Batches #	Organic phase			Aqueous phase			Results				
	PLGA-PEG (%)	PLGA (%)	Solvent	PVA (%, w/v)	Alcholos		DC (µg/mg Np)	Size (nm)	PI	Z Potenzial (mV)	Process Yield (%)
					EtOH (%v/v)	MetOH (%v/v)					
4	100	0	Acetone	1	-	-	4.38±2.45	240.0±54.6	0.13±0.57	0.36±0.84	45±2.34
9	100	0	DMSO	1	-	-	-	>1000±14.5	1.21±3.56	-7.13±3.1	-
10	0	100	Acetone	1	-	-	27.31±4.3	286±43.9	0.02±0.65	-3.18±2.4	43±5.8
11	30	70	Acetone	1	-	-	5.6±2.3	326±10.1	0.6±0.78	-2.7±1.1	45±6.9
12	50	50	Acetone	1	-	-	0.94±0.5	236±25.4	0,01±0.64	0.28±0.4	43±5.3
13	70	30	Acetone	1	-	-	0.2±0.4	410.9±2.6	0.26±0.53	0.3±0.3	42±6.9
14	30	70	Acetone	0.5	-	-	1.54±0.7	787±59.5	0.57±0.45	-1.86±0.7	36±8.3
15	30	70	Acetone	0.25	-	-	2.3±0.2	801.5±49.3	0.61±0.32	-9.7±0.4	42±3.7
16	30	70	Acetone	0.5	30	-	19±1.4	973±23.4	0.71±0.21	-0.1±0.9	57±5.4
17	30	70	Acetone	0.25	30	-	7.10±2.3	672±33.2	0.24±0.26	-1.2±0.5	40±6.4
18	30	70	Acetone	0.25	20	-	5.47±2.2	647±39.1	0.27±0.34	-1.02±0.4	39±4.8
19	30	70	Acetone	0.25	40	-	6.54±2.6	763±14.7	0.09±0.54	-1.23±0,9	42±4.3
20	30	70	Acetone	0.25	60	-	54±1.4	1000±6.8	0.63±0.39	-0.73±0.7	62±5.7
21	30	70	Acetone	0.25	-	30	11.59±1.5	310±11.7	0.13±0.43	1.3±0.6	60±8.5

Different percentage of ethanol (20, 30 40 and 60% v/v) were tested maintaining constant PVA percentage at 0.25% w/v, Batch #17-20. The best results regarding particles size and DC were obtained for Batch #17.

Batch #21 was prepared using same process parameters of Batch# 17 but methanol (MetOH) has used instead of ethanol (EtOH). Addition of 30% v/v of MetOH to external aqueous phase allows to increase DC to 12 µg/mg nanoparticles keeping size at 310±111nm. The effect cannot be explained by MetOH dielectric constant, being higher than EtOH dielectric constant. However, PLGA-PEG/PLGA-H polymer has slight higher affinity for EtOH compared to MetOH, and this can slow down Nps precipitation with consequent higher gentamicin diffusion.

In conclusion, polymer composition, PVA concentration (% w/v) and addition of MetOH into aqueous phase were the most significant variables influencing DC and size of Nps.

This preliminary study (**Table 5**) using an empirical approach has enhanced through a full factorial experimental design in order to statistically evaluate selected variables and to investigate their interaction. The interactions among polymer composition, PVA concentration and methanol addition were examined using a 2^3 full factorial design by Statgraphic centurion Software. Polymer composition (PLGA-PEG/PLGA-H ratios 70:30 and 30:70), PVA concentration (0.25, 0.5% w/v) and methanol percentages (30, 60 %v/v) were defined as inputs, while size (nm) and size distribution and DC (μg/mgNp) were the outputs. In **Table 6** run parameters and responses for 2^3 (three factors at two levels) random screening design are summarized. Data analysis (**Figure 2a**) from pareto chart show that PVA concentration and the addition of MetOH to PVA aqueous solution has a significant (p-value<0.05) impact on the DC (μg/mgNp). In particular formulations with high PVA concentration (0.5 %w/v) and high percentage of MetOH added to PVA solution (60% v/v) present lower DC but their interaction, although is not so significant has a positive influence on DC. The response surface show a linear model in which the DC highest value should be obtained for 0.25% w/v PVA composition with 30 %v/v of MetOH.

The predictive reduced model for DC is given in the equation, showing a R^2 squared of 87.12%:

DC (μg/mgNp) = 9.73137 + 1.00125 X Polymer composition – 5.5165 X PVA %w/v – 5.2335 X MetOH %v/v+ 6.0755 X PVA %w/vX MetOH %w/v

Data for PDI (**Figure 2b**) from pareto chart indicates that only PVA% w/v concentration positively influences on the response. Low PDI value was detected at lowest PVA polymer concentration (0.25 % w/v). The response surface of PVA % w/v versus polymer composition shows low PDI value indicating homogeneous suspension at polymer ratio PLGA-PEG/PLGA-H 30/70 and PVA concentration 0.25 % w/v. The equation based on the statistical reduced model (R^2-squared= 96.05%) is:

PDI = 0.266-0.1185 X Polymer composition+ 0.259 X PVA %w/v + 0.03 X MetOH %w/v – 0.164 X Polymer composition X PVA %w/v + 0.195 X Polymer composition X MetOH %w/v

Pareto chart analysis (**Figure 2c**) shows that both methanol addition and the interaction between methanol and PVA % w/v concentration have a significant effect on particle size. Particles with size > 500 nm were obtained at high value of factors C, which is MetOH at high level (60% v/v). Moreover,

PVA concentration (% w/v) doesn't have a significant influence on the response (size) but the interaction between PVA concentration (% w/v) and MetOH addition in PVA external solution has a significant impact on particle size. Smallest particles size (nm) is obtained with the addition of low percentage of MetOH (30% w/v) at lower PVA concentration of 0.25 % w/v, as it shown by response surface for the particle size (nm). The equation based on this statistical design (R^2 squared= 87.29%) of the reduced model were reported:

Size (nm) = 356.95- 38.4 x Polymer composition+ 259.7 X PVA %w/V + 456.25 X MetOH %v/v – 488.7 X PVA%w/v X MetOH %v/v

In conclusions, particles size and DC of nanoparticles depend on methanol addition into external aqueous phase and PVA polymer concentration, while PDI is a result of polymer composition and PVA concentration. On the base of this second screening full factorial design, Batch Np# 25 was selected for a further deeper investigation on stability after freeze-drying, morphology, *in vitro* release.

Table 6: Runs parameters and responses for 2^3(three factors at two level) full factorial screening design.

Batch #	PLGA-PEG/PLGA-H Ratio	PVA (%, w/v)	MEtOH (%, v/v)	Size (nm)	PI	Zeta potential (mV)	DC (µg/mg Nps)
21	70:30	0.25	30	365.5±7.9	0.23±0.66	0.67±0.5	8.87±2.3
22	70:30	0.5	30	643.9±5.3	0.56±0.75	0.34±0.2	3.87±2.4
23	70:30	0.25	60	711.6±6.6	0.33±0.67	-0,46±0.3	4.22±1.6
24	70:30	0.5	60	650.1±8.5	0.52±0.45	0.54±0.1	6.54±1.4
25	30:70	0.25	30	310±11.7	0.13±0.43	1.3±0.6	11.59±1.5
26	30:70	0.5	30	551.1±9.5	0.26±0.54	-0.61±0.3	5.56±2.0
27	30:70	0.25	60	876.4±10.4	0.39±0.32	0.44±0.7	5.78±1.3
28	30:70	0.5	60	480.2±6.8	0.45±0.21	-0.72±1.0	4.57±0.7

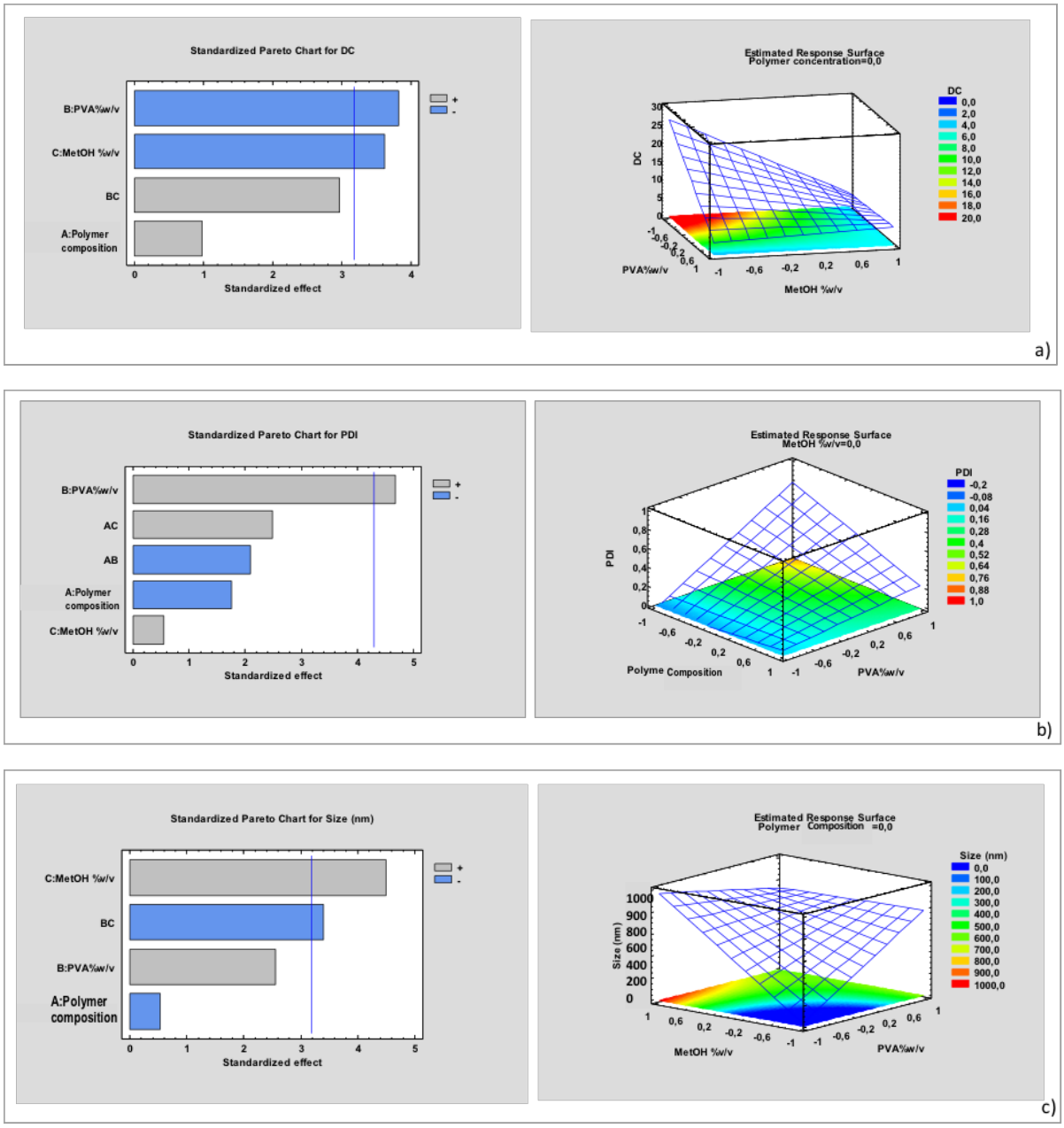

Figure 2: DoE analysis of a full factorial design: Pareto chart and Estimated Response Surface for DC (a), size distribution (b) and particle size (c).

After the optimization study by DoE, Batch #25 has been purified by centrifuge and suspended in distilled water. Several experimental conditions, during Nps preparation and Nps recovery, were optimized (**Table 7**), it was demonstrated that prolonging curing time from 4 to 5 hours, it is possible to limit aggregation phenomena after recovering by centrifugation (condition B, **Table 7**). Moreover, pellet recovery requires a gradual addition of water and cycles of vigorous stirring by vortex and sonication. The different resuspension and curing conditions did not affect DC.

As reported in **Table 7** Batch #25 selected after the optimization study was suspended in 12 minutes following conditions C.

Table 7: Resuspendability after centrifuge at 16400 rpm, 4°C for 20 minutes for optimized gentamicin loaded nanoparticles (NpG 25).

Resuspension Conditions	Curing conditions		Results				
	Temperature (°C)	Time (h)	Size (nm)	PI	DC (µg/mg Nps)	Resuspendability ***	Time (min)
A*	4	4	353.2±15.4	0.1±0.64	12.31±1.5	±	30±2.3
B*	4	5	330±13.7	0.1±0.72	10.85±1.5	+	20±1.1
C**	4	5	284.5±10.7	0.15±0.68	12.20±1.5	+	12±0.5

* Batch was resuspended in 200 µl of sterile water and maintained under agitation (30,000 rpm).

**Batch was progressively suspended in sterile water (100 µl + 100 µl), after each addition, the formulation was maintained under agitation for 60 sec (30,000 rpm). Then suspension was sonicated for 5 min and further agitated for 5 min.

*** Keys: (+) suspended nanoparticles, (–) complete polymer precipitation (no nanoparticle formation) and (±) mixture of suspended nanoparticles and polymer precipitation

The results in **Table 8** show that PVP K17 and K32 seem to stabilize the nanoparticles during freeze-drying; S_f/S_i ratio values are 1 and 1.19, respectively, confirming that there aren't aggregation phenomena. All formulations containing cryoprotectants show good aspect after lyophilization with no evidence of collapse phenomena except for Batch with freeze-drying condition 3, as reported in **Table 8**. This is probably due to high viscosity of SCM solution that limits re-hydratation of lyophilized nanoparticles. Samples containing SCM show S_f/S_i values >1.17 highlighting aggregation phenomena. The single cryoprotectants, their mixture and resuspending conditions have submitted to a Mixture design study using Statgraph software.

Table 8: Runs parameters and results of Mixture Design study.

Freeze-drying conditions	Cryoprotectants (w/w)*			Results		
	PVP K17	PVP K32	SCM	S_f/S_i**	PI	Zeta potential (mV)
1	2	-	-	1.0	0.179	-1.25
2	-	2	-	1.19	0.116	-1.50
3	-	-	2	1.8	0.564	-3.28
4	1	1	-	1.08	0.501	-0.34
5	-	1	1	1.17	0.934	-0.3
6	1	-	1	5.55	0.684	-0.274
7	0.66	0.66	0.66	2.42	0.355	-1.24
8	0.66	0.66	0.66	2.56	0.342	-1.56
9	0.66	0.66	0.66	2.31	0.450	-1.10

*mg cryoprotectants/mg nanoparticelle

** S_f/S_i particles size of nanoparticles before (D_i) and after (D_f) freeze-dried

$S_f/S_i = 1$ without aggregation phenomena

$S_f/S_i > 1$ aggregation phenomena

Results are plotted in a simplex centroid, mixture design by statgraphics software (**Figure 3**). PVP K17, PVP K32 and SCM corresponds to vertex, binary mixture and ternary mixture combining the three cryprotectans must give a total amount that correspond two times the weight of the nanoparticles. The most appropriate model for this mixture design is a special cubic design because the R-squared is 99.88%, while linear and quadratic designs show a R-squared of 20.97 % and 97.66%, respectively. Response surface plot shows that SCM exhibits a S_f/S_i higher respect to PVP K17 and PVP K32.

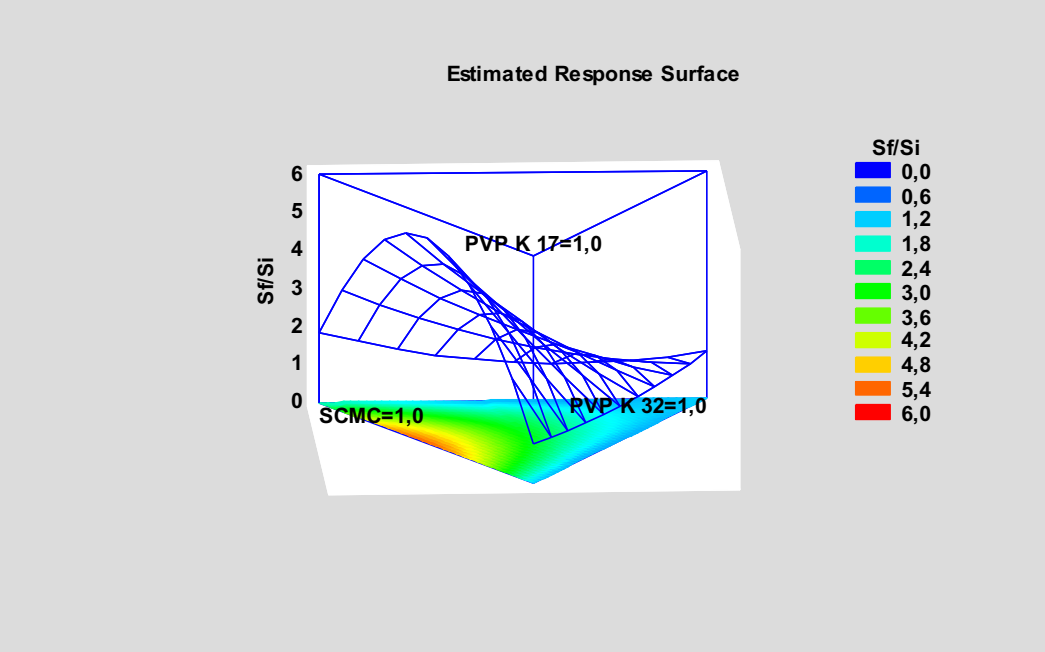

Figure 3: Response Surface of the Mixture design using the special cubic model.

Nanoparticles suspension (Batch #25) were analyzed by TEM after freeze-drying with cryoprotectant (**Figure 4**). Gentamicin loaded nanoparticles before freeze-drying were spherical in shape with average size of about 300 nm, confirming the data from dynamic light scattering. Nanoparticles freeze-dried without the addition of cryoprotectans show important aggregation phenomena. No variations of particle shape and size were highlighted for nanoparticles freeze-dried in presence of PVP K17 and mixture of PVP K 17 and PVP K 32 (**Figure 4c and d**). Nevertheless, sample freeze-dried with the binary mixture displays more inter-particle bridges linking nanoparticles.

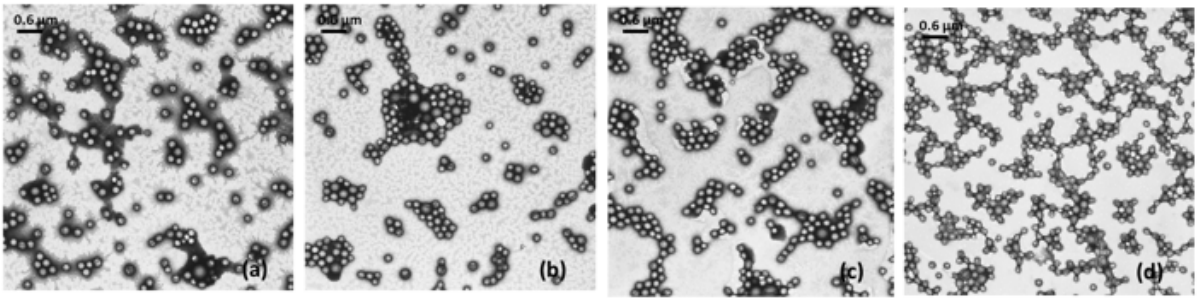

Figure 4: TEM micrograph showing the morphology of the optimized gentamicin loaded nanoparticles (batch #25): after centrifuge (a), after freeze-drying without cryoprotectants (b) and with PVP K17 (c) a binary mixture of PVP K17 and PVP K 32 (d).

The release of gentamicin from loaded nanoparticles (batch #25) was evaluated in PBS pH 7.4 in order to mimic physiological conditions. Gentamicin loaded Nps show a biphasic release profile with nearly 40% of gentamicin released after 1 hours and 70 % after 2 hours. The complete release was reached in 10 hours (**Figure 5**).

Following plots were made for kinetic study: cumulative % drug release vs time (zero order kintetic model); log cumulative % drug remaining vs time (first order kinetic model); cumulative % square root drug release vs of time (Higuchi model) and log cumulative % drug release vs log time (Korsmeyer-Peppas model).

In the **Table 9,** R^2 is correlation value, n is release exponent. On the base of the best fit with the highest correlation (R^2) value, gentamicin loaded nanoparticles follow Higuchi model with release exponent value slope 0.5352. The n value indicates that the release mechanism is Ficknan diffusion [17].

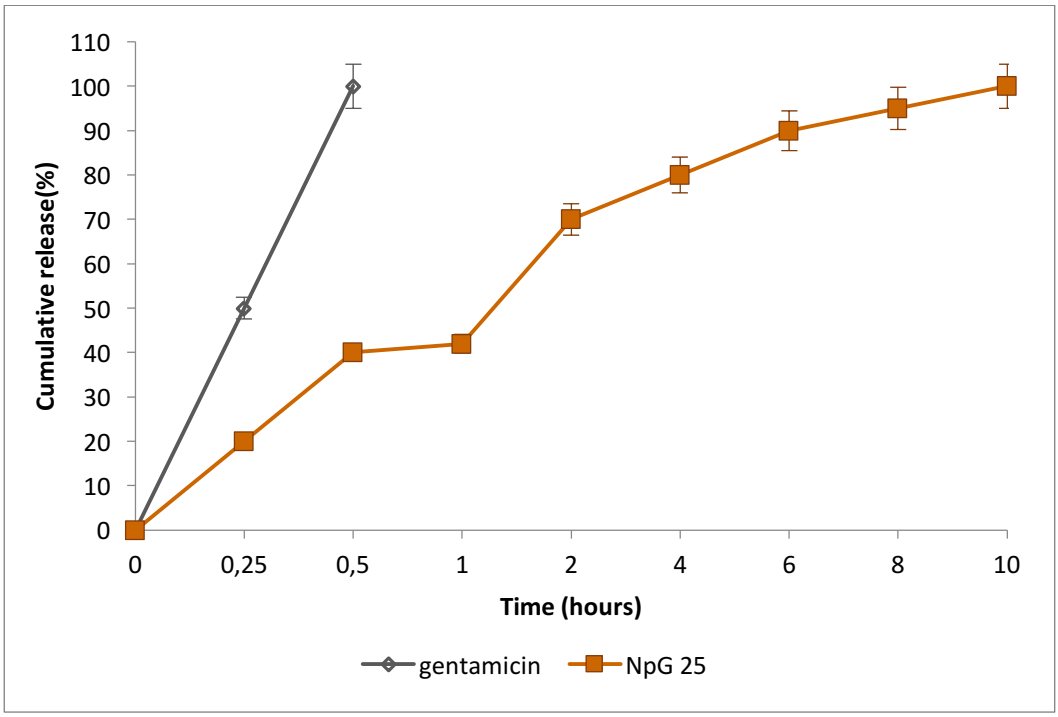

Figure 5: *In vitro* release profile of Batch #25 freeze-dried formulation in PBS pH 7.4 at 37°C, *in sink* condition, free gentamicin *in vitro* dissolution has been used as control.

Table 9: Results of model fitting for optimized gentamicin loaded nanoparticles (Batch #25).

Models	n	Slope	R^2
Zero order	0.1039	0.85671	45.81
First order	0.015	0.77978	3.8281
Higuchi	3.2864	0.93953	24.539
Korsmeyer-Peppas	0.5352	0.79909	1.6538

5. CONCLUSIONS

On the base of the present investigation it is possible to conclude that the preparation of gentamicin loaded nanoparticles by s/o/w technique is governed by several process variables, such as polymer concentration and composition, stirring rate, S/nS ratio, PVA concentration and addition of alcohols into PVA solution. A systemic study of all these variables has been performed and valuable results have been obtained. Using s/o/w technique the most important factors for reducing the size of nanoparticles is polymer composition, polymer concentration, stirring rate, S/nS ratio and PVA w/v%. While more factors are involved for improving drug content, as polymer composition and the addition of methanol into external aqueous phase. DC of 12 µg/mg nanoparticles has achieved mixing PLGA-PEG polymer with PLGA-H, using a sufficient amount of surfactant (PVA) and reducing the dielectric constant of external aqueous phase. On the base of the optimization of all process variables, gentamicin loaded nanoparticles have been successfully formulated with a good reproducibility and yield process.

6. REFERENCES:

[1] P. Sabaeifard, A. Abdi-Ali,R. M.Soudi, C.Gamazo, M.J.Irache, Amikacin loaded PLGA nanoparticles against Pseudomonas aeruginosa. European Journal of Pharmaceutical Sciences 93 (2016) 392-398.

[2] Y. Cai, J. You S.Kundu, J.Yao, Multifuncional nano-hydroxuapatite and alginate/gelatin based sticky gel composite for potential bone regeneration. Materials and Chemistry and Physics 181(2016) 227-233.

[3] L.Saidykhan, A.B.Z.M. Bakar, Y.Rukayadi, U. A.Kura, Y. S.Latifah, Development of nanoantibiotic delivery syste, using cockle shell-derived aragonite nanoparticles for treatment of osteomyelitis. International Journal of Nanomedicine. 11 (2016) 661-673.

[4] X.Qi X.Qin, R. Yang, J. Qin, W. Li, K.Luan, Z.Wu, L. Song, Intra-articular administration of chitosan Thermossensitive in situ hydrogel combined with diclofenac sodium-loaded alginate microspheres. journal of Pharmaceutical Sciences 105 (2016) 122-130 .

[5] T.Isa, A.Z. Zakarial, Rykayadi Y.,Hezmee M., Jaji Z., Iman U., Hammadi I., Mahmood K. Antibacterial activity of ciprofloxacina-encapsulated cockle shells calcium carbonate (aragonite) nanoparticles and its biocompatability in macrophages J774A.1. international journal of Molecular Sciences 17 (2016).

[6] S.M. Abdelghany, D.J. Quinn, R.J. Ingram, B.F. Gilmore, R.F. Donnelly, C.C. Taggart, C.J. Scott, Gentamicin-loaded nanoparticles show improved antimicrobial effects towards Pseudomonas aeruginosa infection. International Journal of Nanomedicine 7 (2012) 4053-4063.

[7] U.Posadowoska, Gentamicin loaded PLGA nanoparticles as local drug delivery system for the osteomyelitis treatment. Acta of Bioengineering and Biomechanics 17 (2015)41-48.

[8] C. Lecaroz, C.Gamazo, M.J.Blanco-Prieto, Nanocarriers with gentamicin to treat intracellular pathogens. Journal of nanoscience and nanotechnology 6 (2006) 3296-3302;.

[9] T. Sadat. Improved drug loading and antibacterial activity of minocycline-loaded PLGA nanoparticles prepared by solid/oil/water ion pairing method. International Journal of Nanomedicine 7 (2012) 221-234;.

[10] W.Abedelwahed, G. Degobert, H.Fessi A pilot study of freeze-drying of poly(epsilon-caprolactone) nanocapsules stabilized by poly(vinyl alcohol): Formulation and process optimization. International Journal of Pharmaceutica 309 (2006)178-188 .

[11] S.Dash, P. N. Murthy, L. Nath P. Chowdhury, Kinetic modeling on drug release from controlled drug delivery systems. Acta Poloniae Pharmaceutica-Drug Research 67 (2010) 217-223.

[12] E.Cova, M. Colombo,S.Inghilleri, M.Morosini, S.Miserere, J. Peñaranda-Avila, B. Santini, D.Piloni, S.Magni, F.Gramatica, D.Prosperi, F.Meloni, Antibody-engineered nanoparticles selectively inhibit mesenchymal cells isolated from patients with chronic lung allograft dysfunction. Nanomedicine 10 (2015) 9-23.

[13] K.S.Yadav, S Jacob, G Sachdeva, K Chuttani, AK Mishra, KK Sawant, Modified nanoprecipitation method for preparation of cytarabine-loaded PLGA nanoparticles. AAPS PharmSciTech 11 (2010) 1456-1465.

[14] R.Dorati, A. DeTrizio, I. Genta, P. Grisoli, A. Merelli, C Tomasi, B. Conti, An experimental design approach to the preparation of pegylated polylactide-co-glicolide gentamicin loaded microparticles for local antibiotic delivery. Materials science and engineering C 58 (2016) 909-917.

[15] R. Dorati, A. De Trizio, I. Genta, A. Merelli, T. Modena, B. Conti, Formulation and in vitro characterization of a composite biodegradable scaffold as antibiotic delivery system and regenerative device of bone. Journal of drug delivery science and technology 35 (2016) 124-133.

[16] Bilati U. Development of a nanoprecipitation method intended for the entrapment of hydrophilic drugs into nanoparticles. European Journal of Pharmaceutical Sciences 2005;24.

[17] P.G.V. Christoper C. Vijaya Raghavan, K. Siddharth, M. Siva Selva Kumar, R. Hari Prasad, Formulation and optimization of coated PLGA –Zidovudine nanoparticles using factorial design and in vitro in vivo evaluations to determine brain targeting efficiency. Saudi Pharmaceutical Journal 22 (2014) 133-140.

Chapter VI

CHAPTER VI

FUNCTIONALIZED NATURAL BASED EUMELANIN NANOPARTICLES AS CARRIERS FOR LOCAL GENTAMICIN DELIVERY

ABSTRACT

Eumelanin is a heteropolymer that spontaneously self-assembles in round shaped micelles of nanometric size. Herein, by utilizing the intriguing properties of polydopamine (PD), we modified natural based eumelanin nanoparticles surface by dopamine self-polymerization (FEUNp), aiming to facilitate conjugation through its bioactive functional groups and improving its hydrophilicity. Morphological studies by SEM, TEM, and AFM confirmed that eumelanin nanoparticles were successfully coated with PD layer and that the FEUNp possess spherical shape (230.04±8.25 nm). From FTIR and XPS analysis, the chemical functional group and elemental analysis showed an individual indole or indoline structures spectrum at 1600 cm^{-1} and a mass ratio of C:N was 9.08, respectively. Quartz-crystal microbalance with dissipation monitoring (QCM-D) and thermal gravimetric analysis (TGA) showed the successful adsorption of dopamine to the surface of eumelanin nanoparticles and a weight ratio of eumelanin nanoparticles/dopamine of 1/2.46 in the wet state and 1/0.20 in the dry state. Moreover, the negatively surface charges of -36.60±0.45 mV also reinforced the presence of PD covering. In further step, FEUNp loaded with gentamicin sulphate were studied as carriers to enable localized delivery for osteomyelitis therapy. The drug efficiency was 32.42±3.21 with a ζ-potential close to the neutrality (-1.84±0.58 mV). The microbial effect of FEUNp-GS on *Staphylococcus aureus* and *Escherichia coli* were tested by serial dilution. The antibacterial effect demonstrated gentamicin sustained released from the FEUNp after 24 h that IC_{50} was 110.60 µg/mL, IC_{90}: 216.39 µg/mL for *S.aureus* and IC_{50} of 54.13 µg/mL, IC_{90} of 101.25 µg/mL for *E.coli*. Therefore FEUNp nanoparticles can be further evaluated as localized drug delivery systems in different infection diseases and wound healing treatments.

Keywords: Eumelanin nanoparticles; Polydopamine; Surface modification; Gentamicin; Osteomyelitis

This chapter to be submit for pubblication.

A. De Trizio, P.Srisuk, R.Costa,A.Fraga,T.Modena,I.Genta,R.Dorati,B.Conti, R.Reis,V.M.Correlo

1. INTRODUCTION

Eumelanin is a subtype of melanin pigments, it is a dark brownish heteropolymer that spontaneously self-assembles in round shaped micelles of nanometric size [1]. It is a well-known biological pigment useful for photo-protection, radical scavenging, antioxidant, and amorphous semiconductor [2]. Sepia ink from cuttlefish (*Sepia officinalis*) is the main source of pure eumelanin, which commonly is used as standard for natural eumelanin [3]. Despite significant eumelanin's research efforts, natural based eumelanin insolubility strongly restricts its pharmaceutical use. Common strategies of nanoparticle functionalization involve noncovalent physisorption or covalent conjugation with the desired ligand. The lack of reactive functional groups necessitates the activation of nanoparticle surface with a reactive linker, followed by exhaustive purification processes to remove catalyst and excess of reactants. Alternatively, nanoparticles can be produced using pre-functionalized polymers, where functional ligands are covalently conjugated to polymers. The synthesis of the polymer-ligand conjugate can be inefficient and needs to be tailored for each ligand [4]. Surface modification of eumelanin nanoparticles plays an important role in facilitating conjugation through its bioactive functional groups, improving nanoparticle hydrophilicity, hematocompatability and colloidal stability [5]. Another innovative method to functionalize nanoparticle surface exploits dopamine self-polymerization, a simple and versatile surface modification method, applicable to a variety of nanocarriers irrespective of their chemical reactivity, overcoming complexity and inefficiency involved in traditional nanoparticles functionalization processes [4]. Polydopamine (PD), adhesive macromolecule inspired by catechol-rich marine mussel adhesive proteins offers remarkable multipurpose properties of naturally occurring eumelanin in terms of electrical, optical and magnetic properties [6]. Another important property of PD lies in its chemical structure possessing many functional groups such as amines, catechols, and imines [7]. These functional groups could be starting point for covalent immobilization with ligands aiming to achieve drug delivery systems with tailored properties. In fact, many methods currently used to modify nanoparticle surface are inefficient and laborious. Nanoparticles surface functionalization with PD, including gold nanorods [8], gold nanoparticles [9], silver nanoparticles [10, 11], magnetic nanoparticles [12, 13], silicon dioxide particles [14], graphene oxide nanosheets [15], gentamicin liposome-impregnated calcium sulfate [16], has been investigated with the aim of achieving targeted drug delivery systems. Gentamicin sulphate (GS) is classified as an aminoglycoside antibiotic to treat or prevent acute or chronic Gram-positive and Gram-negative infections. Its action mechanism involves irreversible inhibition of bacteria 30S ribosomal subunit leading to bacterial t-RNA molecule misreading [17]. However, GS use should be strictly monitored in order to reduce development of drugs multi-resistance among microorganisms.

An example of gentamicin use by systemic administration is treatment of osteomyelitis, a severe bone infection proven or strongly suspected to be due to Gram-positive and Gram-negative microorganisms. Osteomyelitis is a heterogeneous infectious and inflammatory disease of bone and joints, mostly caused by *Staphylococcus aureus* [18]. In general, it occurs in children and adults predominantly caused by hematogenous seeding and injury to bone, joints, and adjacent soft tissue, respectively [19]. High risk to get an infection is directly associated with a weaken immune system including diabetes, rheumatoid arthritis, AIDS, etc [20]. One of osteomyelitis recommended treatment involves aminoglycoside administration. Even if GS is one of the choices for osteomyelitis treatment, low success rates are achieved in bone and joints infections due to anatomical and physiological bone characteristics [21]. Moreover, nephrotoxicity and ototoxicity are well-known gentamicin side effects associated with its systemic administration, and the latter being related to free radicals [22]. On the purpose, free-radical scavengers as aspirin, glutathione, aminoguanidine and edaravone are supplemented to inhibit gentamicin ototoxicity. All these drawbacks addressed studies on GS delivery systems allowing drug localized and sustained release and improving GS therapeutic outcomes [23]. For examples, GS loaded poly (lactide-co-glycolide) nanoparticles or doped with gelatin/genipin reinforced beta-tricalcium phosphate hydrogel performed significant growth inhibition of *Staphylococcus aureus* both *in vitro* and *in vivo*. Other studies such as those on local administration of GS-containing polymethylmethacrylate (PMMA) beads or GS loaded into collagen sponges, and combination therapy with systemic administration of cefazolin, showed that GS-collagen sponges were able to reduce bacterial colony count more than GS-PMMA beads after 4 weeks [24-26].

In this work eumelanin nanoparticles loaded with GS and coated with PD are proposed as potential candidate for GS local delivery in osteomyelitis treatment by formulation into a locally injectable thermosensitive hydrogel or moldable biodegradable scaffold [27]. Eumelanin can usefully act as scavengers able to react with the free radicals, thus reducing GS toxicity. Exploiting PD bioadhesive properties, FEUNp loaded with GS could be formulated also into dermal or transdermal dosage forms such as gels, ointments or lotions, prolonging formulation residence time at the application site and achieving GS prolonged release. Therefore, FEUNp nanoparticles can be further evaluated as localized drug delivery systems in skin infections and wound healing treatments.

2. MATERIALS

Sepia officinalis (100%) ink was purchased from Nortindal Sea Products S.L. (Tolosa, Spain). Dopamine hydrochloride, TRIZMA™-hydrochloride, phosphate buffered saline (PBS), gentamicin sulfate and ninhydrin were provided from Sigma-Aldrich (Saint Louis, MO, USA). All other reagents were of analytical grade.

3. METHODS

3.1 Preparation and purification of natural based eumelanin nanoparticles

Cuttlefish ink was purified following a method previously described [1]. Briefly, a stock suspension of ink was obtained by dissolving 100 g of commercial ink in 200 mL of ultrapure water. The purification of ink suspension was performed by centrifugation at a speed of 12100 rpm for 15 min at 5°C (5810R, Eppendorf, Germany), then discarded supernatants, the precipitated black slurry was resuspended in ultrapure water. This process was repeated for at least 20 cycles. Afterwards samples were frozen at -80°C and lyophilized for 48 h. The final black pellets were collected and used throughout this study.

3.2 Synthesis of functionalized eumelanin nanoparticles and gentamicin loading

Synthesis of functionalized eumelanin nanoparticles was carried out in an open flask under constant mechanical stirring. About 12.5 mg of eumelanin nanoparticles (EUNp) was suspended in 25 mL of TRIS buffer (10 mM, pH~8.5). The suspension was stirred at 300 rpm and sonicated for 1 h at 40°C. At this state, pH of the system was increased to 10, and then decreased to 8.5 after addition of dopamine hydrochloride in order to obtain the following dopamine final concentrations 0.125, 0.25, 0.5 and 1.0 mg/mL, respectively. The obtained suspensions were stirred overnight at room temperature. Self-polymerized polydopamine-coated eumelanin nanoparticles were collected by centrifugation at a speed of 12100 rpm for 15 min at 5°C (5810R, Eppendorf, Germany) and then washed with ultrapure water for 3 times to ensure for removing of all unpolymerized residues. The functionalized eumelanin nanoparticles (FEUNp) were frozen at -80°C and lyophilized for 12 h, to be stored for further analysis. The different formulation of FEUNp are summarized in **Table 1**.

Table 1: Functionalized eumelanin nanoparticles composition

Formulations	Eumelanin Nanoparticles (mg)	Dopamine HCl (mg)	Mass Ratio
FEUNp1	12.5	3.125	1:0.25
FEUNp2	12.5	6.25	1:0.5
FEUNp3	12.5	12.5	1:1
FEUNp4	12.5	25	1:2

FEUNp3 resulted to be the best formulation in terms of homogeneous dopamine film coating. From the preliminary results (SEM images), dopamine deposition on the surface of natural based eumelanin nanoparticles FEUNp1 and FEUNp2 was not homogeneous all over the Nps surface, while FEUNp4

resulted in an excess of dopamine with enucleation. Therefore, FEUNp3 composition was chosen and gentamicin loading performed as follows: after FEUNp3 centrifugation, 12.5 mg of FEUNp3 were resuspended in a solution of gentamicin sulphate in TRIS buffer (10mM, pH~8.5) and gently stirred at 600 rpm at room temperature. The amount of gentamicin and stirring time were varied as showed in **Table 2.**

Table 2: Gentamicin loading into functionalized eumelanin nanoparticles

Formulations	FEUNp3 (mg)	Gentamicin(GS) (mg)	Time (min)	Mass Ratio (FEUNp:GS)
FEUNp-GS1	12.5	25	30	1:2
FEUNp-GS2	12.5	25	60	1:2
FEUNp-GS3	12.5	50	30	1:4
FEUNp-GS4	12.5	50	60	1:4

3.3 Morphological study

Surface morphological studies of eumelanin nanoparticles and functionalized eumelanin nanoparticles were carried out by scanning electron microscope; SEM (Leica Cambridge S-360, UK). All samples after freeze-drying were suspended in ultrapure water at a final concentration of 0.025 mg/mL and sonicated for 1 h. After sonication, the samples were dried on glass slides at room temperature and sputted with platinum before observation. Coated samples were examined at an acceleration voltage of 25 kV, micrograph was captured at a magnification of 30.00 KX and 80.00 KX. The same batches of functionalized nanoparticles were analyzed by TEM, magnification at 200000 X. Briefly, 10 µL of samples were mounted on formvar/carbon film coated mesh nickel grids and left standing for 2 min. The excess liquid was removed with filter paper, and then 10 µL of 1% uranyl acetate was added onto the grids and left standing for 10 s, after which liquid in excess was removed by filter paper, and sample was analyzed. The surface roughness and tri-dimensional images of FEUNp1, 2, 3, and 4 were assessed using AFM Dimension Icon (Bruker, USA) operating in PeakForce Tapping (ScanAsyst) in air. AFM cantilevers (ScanAsyst-Air, Bruker) made of silicon nitride with a spring constant of 0.4 N/m and frequency of 70 kHz were used.

3.4 Particle size and zeta potential

The dark black color of the FEUNp is a crucial interference factor for the analyzing of particle size by dynamic light scattering technique. All images of FEUNP with a high resolution of 512x533 pixel, performing as representative of bulk samples were taken by SEM at the magnification of 30.00 KX and

subsequently processed using ImageJ software. The particle sizes were quantified by binary images in segmentation (black and white in pixel). In ImageJ software, scale as distance in pixel and threshold were set up in order to calibrate the whole all images. The 'Analyze Particles' feature was provided and generated a table of particle areas and average diameters. Size distribution is plotted as the mean diameter ± standard deviation. Dynamic light scattering technique with Zetasizer (Nano ZS, Malvern Instruments, UK) was used to analyze polydispersity index (PDI) and zeta potential of EUNp and FEUNp. Before measurements, all samples were diluted with purified water pH 7.4 to a final concentration of 0.025 mg/mL in a clean Malvern quartz cuvette. All experiments were carried out at 25^{o}C.

3.5 Elemental and functional group analysis

The functional group of eumelanin nanoparticles (EUNp), dopamine hydrochloride, polydopamine (PD), functionalized eumelanin nanoparticles (FEUNp) and gentamicin loaded functionalized eumelanin nanoparticles (FEUNp-GS) were examined by Fourier-transform infrared spectrometer; FTIR (IRPrestige21, Shimadzu, Japan). All samples were pressed into potassium bromide (KBr) pellet prior measurements. All spectra were taken ranging from 2000 to 500 cm^{-1}. Elemental analysis was carried out by an X-ray Photoelectron Spectroscope; XPS (Axis Supra, Kratos, UK) on the EUNp, dopamine hydrochloride, PD, and FEUNp. X-ray beam was a common tool to evaluate samples and photoelectron detector was set at 45°off-normal. High-energy resolution spectra were collected using a pass energy of 69.0 eV with a step size of 0.125 eV.

3.6 Quantitative total mass analysis of polydopamine (PD) coating eumelanin nanoparticles

The quantitative total dry mass analysis of FEUNp and EUNps were evaluated by thermogravimetric analysis. All samples including EUNp, PD, and the selected formulation; FEUNp3 were analyzed by the simultaneous thermal analyzer (STA7200, Hitachi, Japan) under nitrogen environment at a flow rate of 40 mL/min and a heating rate of 10°C/min from 40 to 800°C. In other words, the quantitative total wet mass analysis of PD coated was evaluated by QCM-D (Q-Sense E4 model from Biolin Scientific, Sweden) which used to monitor the adsorption of dopamine to EUNp in the same condition as TGA analysis. Gold-coated AT-cut quartz sensors (Q-sense, ref. QSX 301) pre-coated with polydopamine from the spin coater (WS-650Hzb-23NPPB-UD-3, LAURELL, USA) were used as substrates. Sensors were excited simultaneously at a constant temperature of 25 ºC at multiple overtones: 1st, 3rd, 5th, 7th, 9th, 11th and 13th, corresponding to 5, 15, 25, 35, 45, 55, and 65 MHz, respectively. EUNps in suspension (0.5 mg/mL in Tris buffer, pH~8.5) were flushed using a peristaltic pump set to 50 µL·min^{-1} for 24 h. Then, a solution of dopamine (0.5 mg/mL) was flushed at the same speed until the frequency (ΔF_n) and dissipation (ΔD_n)

variations reached a stable value (i.e., ΔF_n<5% per hour, considering that 100% was the maximum ΔF_n value at a given time). The adsorption of the materials was intercalated by a rinsing step with Tris buffer for 15 min to remove loosely bonded Np. To estimate the weight ratio of EUNp and dopamine HCL coupled to the sensors surface, the Voigt-based viscoelastic model was used [28], following interface provided by the QTools software (version 3.1.25.604, by Q-Sense). The model follows Equation (1) and Equation (2):

$$\Delta F \approx -\frac{1}{2\pi\rho_0 h_0}\left\{\frac{\eta_3}{\delta_3}+\sum_{j=k}\left[h_j\rho_j\omega-2h_j\left(\frac{\eta_3}{\delta_3}\right)^2\frac{\eta_j\omega^2}{\mu_j{}^2+\omega^2\eta_j{}^2}\right]\right\} \quad (1)$$

$$\Delta D \approx \frac{1}{2\pi f\rho_0 h_0}\left\{\frac{\eta_3}{\delta_3}+\sum_{j=k}\left[2h_j\left(\frac{\eta_3}{\delta_3}\right)^2\frac{\mu_j\omega}{\mu_j{}^2+\omega^2\eta_j{}^2}\right]\right\} \quad (2)$$

where, considering a total of k thin viscoelastic layers, ρ_0 and h_0 are the density and thickness of quartz crystal, η_3 is the viscosity of the bulk liquid, δ_3 is the viscous penetration depth of the shear wave in the bulk liquid, ρ_3 is liquid density, μ is the elastic shear modulus of an overlayer, and ω is oscillation angular frequency. The model was used considering a constant solvent viscosity of 0.001 Pa, film density between 1100-1300 kg·m^{-3}, and solvent density between 1000-1015 kg.m^{-3}. Calculation was made using at least three overtones until the total error, χ^2, was minimized.

3.7 Encapsulation efficiency of gentamicin in functionalized eumelanin nanoparticles

Encapsulation efficiency of gentamicin sulphate was determined by an indirect spectrophotometric method using ninhydrin reagent [27]. Briefly, ninhydrin reagent was dissolved in PBS buffer (pH ~7.4) at a final concentration of 2 mg/mL. Two hundred and forty microliters of ninhydrin solution were mixed with 800 µL of the supernatant of functionalized nanoparticles containing un-encapsulated gentamicin. Subsequently, the solution was incubated in a water bath at 95°C for about 15 min and then cooled in an ice bath (~10 min). Absorbance was measured at a wavelength of 400 nm and gentamicin sulfate solution was used as the control. Gentamicin concentration was calculated by a calibration curve (100-1000 µg/ml in TRIS-HCl buffer 10mM, pH ~8.5). Encapsulation efficiency (EE %) was calculated from the following Equation (3):

$$EE\ (\%) = \frac{Wi-Wt}{Wi}\ X100 \quad (3)$$

Where W_i stands for amount of gentamicin added to FEUNp suspension and W_t for free gentamicin in the supernatant after gentamicin absorption onto FEUNp.

The production yield (%) represents the amounts of FEUNp-GS recovered after gentamicin absorption process on FEUNp. It is expressed as a percentage of weight (w/w) and calculated using this Equation (4):

$$Yield\ (\%) = \frac{Wr}{Wi}\ X100 \qquad (4)$$

Where W_r stands for total recovering mass FEUNp-GS and W_i for total initial mass of FEUNp.

3.8 The release profile of gentamicin loaded functionalized eumelanin nanoparticles

The release profile of gentamicin from FEUNp-GS1 was evaluated using dialysis tubes (Micro Float-A-Lyzer Dialysis Device (3.5-5 KDa), Spectrum Labs, USA). Initially, dialysis tubes were rinsed with 10%v/v ethanol and purified water. Five hundred microliters of the nanoparticles suspension in PBS (pH~7.4) was filled into the tubes and then they were fully immersed in 90 mL of PBS under constant stirring at 60 rpm, 37°C for 24 h. At specific time points, an aliquot of 800 µL sample was withdrawn and replaced by an equal amount of fresh PBS. After reaction with ninhydrin, the amount of released gentamycin at each time points was quantified by UV-Vis spectrophotometer analysis (UV-1601, Shimadzu, Japan) at 400 nm and calculated by using a calibration curve (30-300 µg/mL). All experiments were performed in triplicate.

To find out the mechanism of drug release, firstly 60% of drug release data were fitted to Korsmeyer-Peppas equation by using equation 5, plotting log cumulative percentage drug release *versus* log time [29]:

$$M_t / M_\infty = kt^n \qquad (5)$$

M_t / M_∞ where a fraction of drug is released at time t, k is the release rate constant and n is the release exponent. The n value is the diffusional exponent which characterizes the transport mechanism.

3.9 Antimicrobial effect

The antimicrobial effect of the nanoparticles was determined by performing a 16 two-fold serial dilutions of the test material (gentamicin and gentamicin loaded FEUNp) in a 96-well-U-bottom microtiter plate. To each well $1x10^5$ CFU of the bacterial suspension was added. The plates were prepared in duplicate and placed in an incubator set at 37°C for 24 h. Serial 10-fold dilutions of the suspension were plated on nutrient LB. Bacterial colony formation was counted after 24 h of incubation at 37°C. Following ASTM guidelines, the reported value for the limit of detection for microbiological purposes should be "< the dilution value" if no colonies are recovered; therefore, the limit of detection for our experiments is $1\log_{10}$ CFU/mL. All countable colonies, even those below the countable range, were counted and reported as an estimated count. The IC_{50} and IC_{90} of each drug

were determined as the lowest concentrations of antibiotic that inhibit the growth of a microorganism by either half or 90%, respectively.

3.10 Statistic analysis

All results are expressed as mean ±SD of three independent experiments. For statistical analysis from SEM and TEM images was measured by ImageJ software.

4. RESULTS AND DISCUSSION

Natural based eumelanin nanoparticles obtained, after removing small fractions and other impurities from cuttlefish (*Sepia Officinalis*) ink are depicted in **Figure 1**. The mean diameter, measure by ImageJ software and polydispersity index (PDI) determined dynamic light scattering, of natural based eumelanin nanoparticles, were 141.17±10.16 nm and 0.22 ± 0.02 nm, respectively. Due to black color of FEUNp, results of particle size analysis by Zetasizer were not reliable, and only PDI values can be considered. SEM images have shown spherical shape with smooth surface, as well as the previous study from Srisuk et al. [1]: this morphology usefully favors for nanoparticle coating. In this study, natural based eumelanin nanoparticles were also used as a control before functionalization. For the purpose of synergetic effect of the layer of polydopamine (PD) coating on eumelanin nanoparticles (EUNp), the functionalization was conducted by PD self-polymerization. SEM images of dopamine hydrochloride at different concentrations (0.125, 0.25, 0.5 and 1.0 mg/mL) have shown a spontaneous nucleation of dopamine into nanoparticles (Data not shown). From SEM images, it was observed that the particles provided a spherical shape, nevertheless they were also prompt to fuse and agglomeration. At the concentration of 0.25 mg/mL, the average size was lower than 50 nm. While, at the concentration of 0.5 mg/mL, functionalized nanoparticles were completely fused and its average size was 70 nm. Morover, at a concentration of 1.0 mg/mL, the average size was not uniform in the range between 70 and 200 nm. (Data not shown)

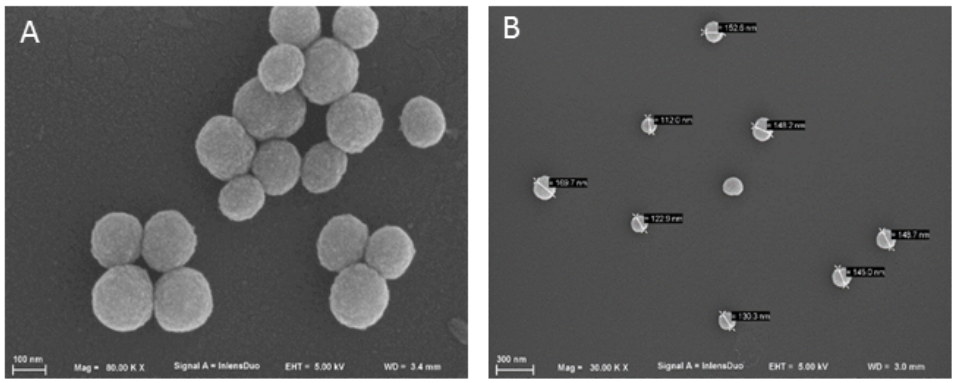

Figure 1: SEM images of eumelanin nanoparticles (EUNp), magnification at (A) 80.00 KX and (B) 30.00 KX.

The emphasis of this work is to demonstrate the occurred interaction between polydopamine and eumelanin nanoparticles, through data acquisition from several different equipment and techniques. When EUNp and PD weight ratios were 1:0.25 and 1:0.5 (FEUNp1 and FEUNp2), surface roughness was lower than with the higher weight ratios of 1:1 and 1:2 (FEUNp3 and FEUNp4) (**Figure 2**), as shown by SEM analysis. Due to deposition of PD layer, on FEUNp4 (1:2) it is possible to observe the presence of particulate PD aggregation, not only on EUNp surface, but also extra PD aggregation (**Figure 2** (D)). For eumelanin nanoparticles functionalization with PD, when dopamine solution was incubated with eumelanin nanoparticle suspension, the self-polymerized PD had a capability of highly potential wrapping tendency on the surrounding system due to the preference of auto-nucleation nanoparticles surface. After reaction, functionalized eumelanin nanoparticles (FEUNp) were able to maintain their original spherical shape, but roughness was increased. However, aggregation was still found probably due to PD excellent adhesion property. Moreover, its catechol groups (phenolic C-OH groups) can also be controlled by altering dopamine hydrochloride solution concentration.

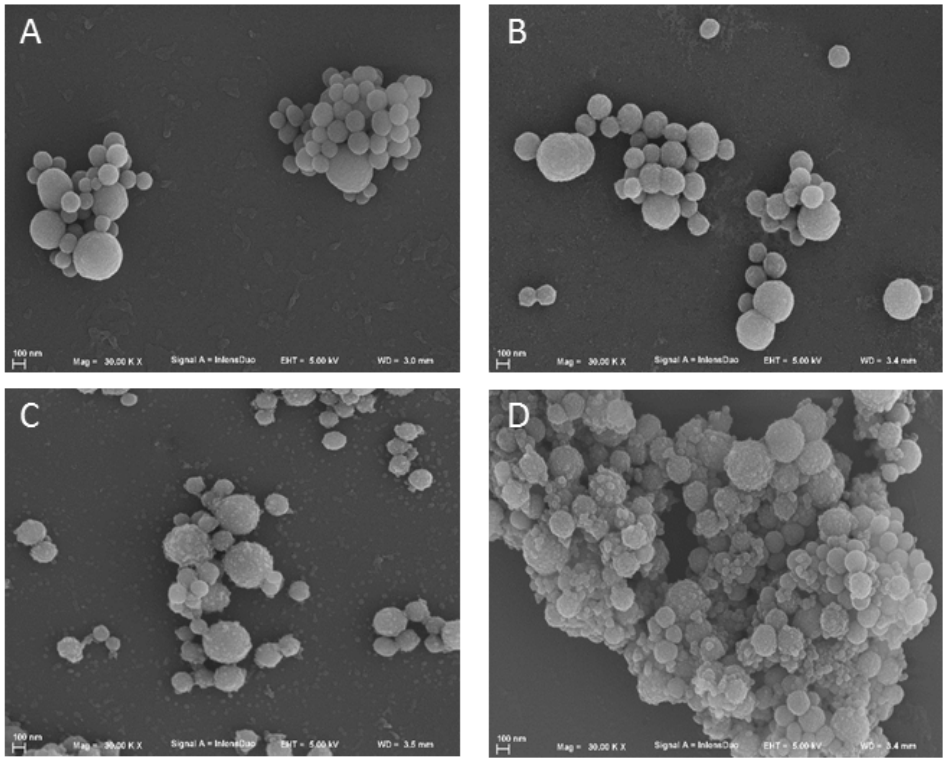

Figure 2: SEM images of (A) FEUNp1, (B) FEUNp2, (C) FEUNp3 and (D) FEUNp4 at 30.00 KX.

The morphology of functionalized eumelanin nanoparticles is examined by TEM as depicted in **Figure 3**. By this method it was possible to observe that all functionalized eumelanin nanoparticles have spherical shape similar to the original eumelanin nanoparticles. However, PD layer structure was visualized and confirmed by TEM, as shown in **Figure 3**, in which a clear contrast emerged between the core and the layer of PD segments. For FEUNp1 (**Figure 3** (A)) and FEUNp2 (**Figure 3** (B)), the PD layer was not homogeneous when compared with FEUNp3 and FEUNp4 (**Figure 3** (D)). However, the best outcomes were obtained for the condition FEUNp3 (weight ratio of 1:1) where deposition of homogeneous PD layer on nanoparticles surface without any self-nucleation of PD was highlighted. Even thought, the mechanism of the deposition of a PD layer on EUNp surface has not yet been clearly explained, from the obtained results two different mechanism can be suggested: i) by random nanoaggregation on the nanoparticles or ii) by interaction of dopamine oligomers and a monomers forming interconnected layers on nanoparticles surface. In theory, the surface morphologies of FEUNp is dependent on initial dopamine concentration which influenced the relative rate of nucleation and PD growth process. In this context, we believed that PD-assisted surface modification process is due to catechol groups (C-OH groups) which exposed to the surrounding basic environment and provokes dopamine nucleation into PD layer exclusively on eumelanin nanoparticles surface. Successively, this nuclei of polymerized dopamine is grown in terms of size and then finally fused together forming a PD

layer on the surface of EUNp. Therefore, the formation of PD layer may be attributed to the dual effect of PD nucleation and growth process on EUNp surface, which is based on the initial dopamine concentration [30, 31].

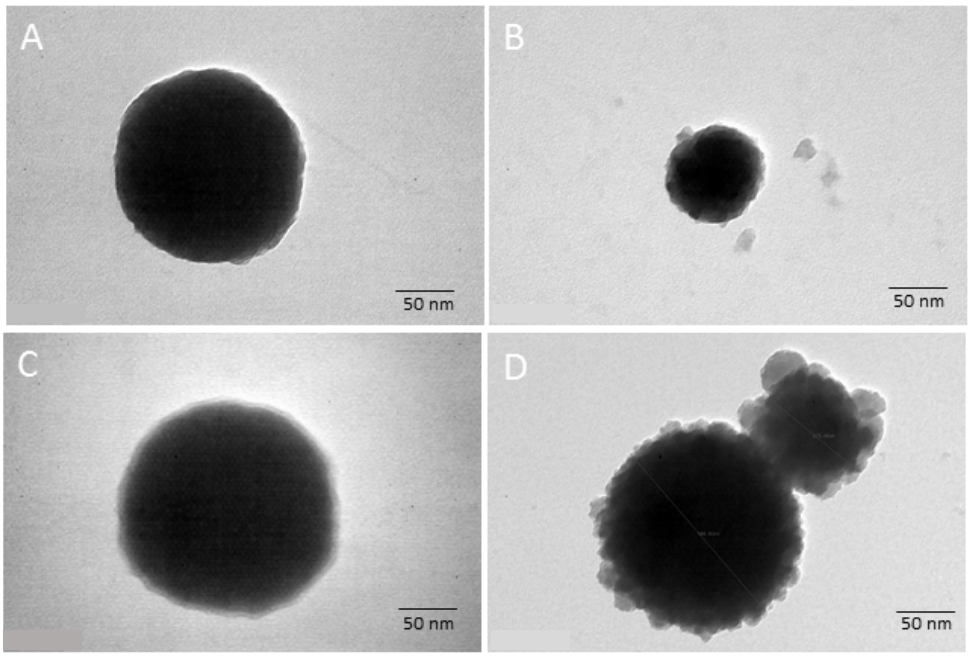

Figure 3: TEM images of FEUNp1 (A), FEUNp2 (B), FEUNp3 (C), and FEUNp4 (D) at 200000 X.

AFM images show that FEUNp have spherical uniform shape, confirming the results obtained by SEM and TEM techniques (**Figure 4**). As expected, FEUNp roughness is increased with the highest weight ratio of EUNp and dopamine (1:2) (**Figure 4**). Particles size values obtained by TEM and AFM was similar. Surface functionalization of natural based eumelanin nanoparticles with several types of biomolecules coul be suitable to deliver therapeutic agents to cells, demonstrating the great promise of the PD coating for biomedical applications. In the literature is reported that PD coating could make the funcionalized nanoparticles that escape from the lysosomes to cytosol and appear close to the nucleus (nuclear delivery of nanoparticles) [32].

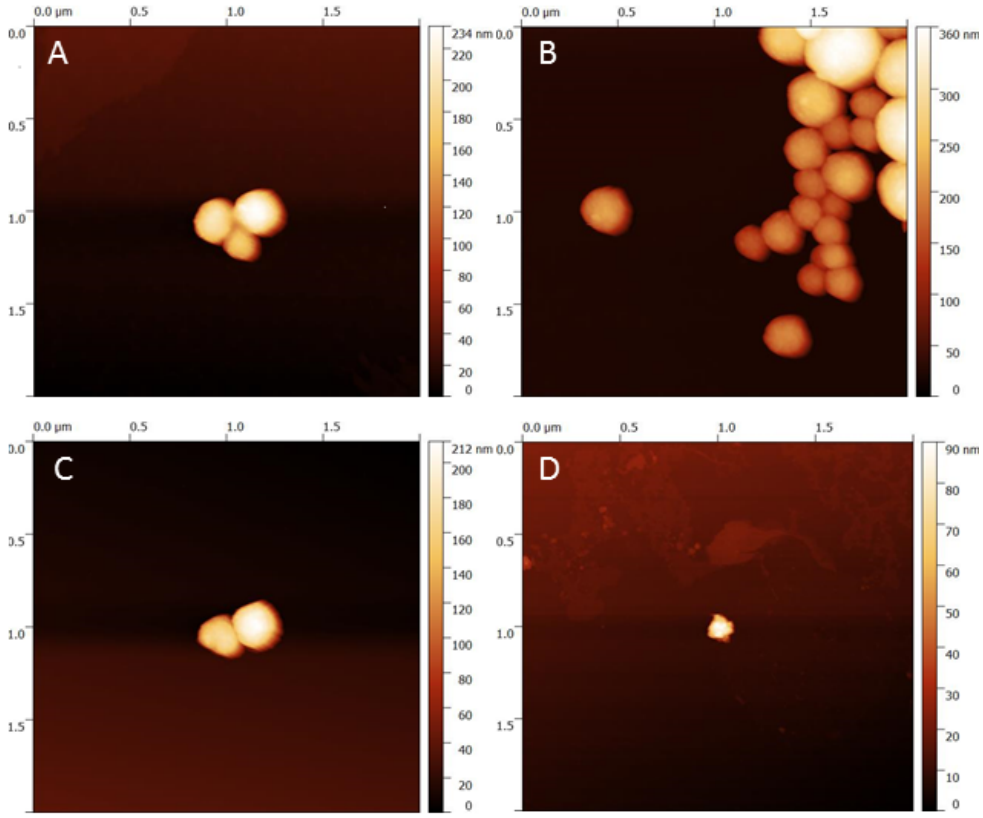

Figure 4: AFM images of the FEUNp1 (A), 2 (B), 3 (C) and 4 (D), corresponding to the EUNp coated with PD, EUNp were incubated in different amount of solubilized dopamine hydrochloride in TRIS-HCl buffer (10 nM, pH ~8.5) under oxidizing conditions.

The average size, polydispersity index (PDI) zeta potential and yield process (%) of the FEUNp1 to FEUNp4, EUNp, and PD are shown in **Table 3.** The average size of EUNp and PD at the same concentration (0.5 mg/mL) are 141.17±10.16 and 67.35±2.05 nm, respectively. The confirmation of dopamine self-polymerization in a nanoparticulate system is proven by nanoaggregation in the absence of substrate in basic condition. The average size of all FEUNp is larger than EUNp (> 200 nm) and this could be ascribed to the PD surface coating layer on EUNp. PDI of EUNp, PD and FEUNp ranged between 0.22±0.02 to 0.28±0.003 nm, corresponding to homogeneous size distribution. FEUNp4 with EUNp and PD at the highest weight ratio (1:2) show PDI value about 0.37±0.02 indicating presence of nanometric PD aggregation. Zeta potential (ζ) evaluation describes nanoparticles stability by electrostatic repulsion. In **Table 3,** the zeta potential (ζ) of all samples is negatively valued, but when increasing dopamine hydrochloride concentration, zeta potential (ζ) of FEUNp reaches a value closed to PD (-33.46±0.58 mV). It could be another confirmation of the external PD layer on eumelanin nanoparticles surface. In terms of yield (%), FEUNps show values between 45.34±0.56 and 50.46±0.38, particularly, the best yield (%) results of this study is obtained for FEUNp3.

Table 3: Size, zeta potential, polydispersity index of EUNp, PD and FEUNp1 to 4 with different mass ratios of EUNp and PD.

Sample	Size (nm)*	PDI**	ζ (mV)**	Yield (%)
EUNp (0.5 mg/mL)	141.17±10.16	0.22±0.02	-43.13±0.86	54.70±0.45
PD (0.5 mg/mL)	67.35±2.05	0.28±0.003	-33.46±0.58	33.54±0.88
FEUNp1	225.56±11.25	0.23±0.012	-40.13±0.87	45.34±0.56
FEUNp2	228.77±3.15	0.25±0.03	-34.90±0.78	46,89±0.44
FEUNp3	230.04±8.25	0.23±0.02	-36.60±0.45	50.46±0.38
FEUNp4	236.03±5.76	0.37±0.02	-37.20±0.76	48,59±0.48

*Size (nm) was calculated from SEM images using the ImageJ software for the analysis particle.

**PDI and zeta potential (mV) were calculated from the light scattering measurements in purified water. All values are expressed as average±SD of three independent measurements. The selected concentration is 0.025 mg/mL

For better understanding the mechanism underlying FEUNp formation, EUNp, PD and FEUNp, elemental analysis was performed by X-ray photoelectron spectroscopy (XPS). From **Table 4,** elemental analysis of the percentage of PD atomic composition is compared to theoretical dopamine composition. Nitrogen elemental atomic, which is attributed to eumelanin nanoparticles imino groups is higher than PD [33]. These results show the percentage of carbon from EUNp and PD are 68.39 and 74.98%, respectively. While, the percentages of oxygen are 21.27 and 19.34%, in EUNp and PD, respectively. This results confirm a fully delocalized structure of PD layer on EUNp surface because the quantitative analysis by XPS is the contribution of both EUNp and PD. PD layer is very thin (< 10nm, from TEM images) and inhomogeneous. As mentioned, the C/N ratio can explain about the composition of FEUNp, because C/N ratio (6.61) in EUNp is less than C/N ratio in the PD (13.20). Moreover, C/N ratios in FEUNp1 to 4 are in the range corresponding to PD. In particular, FEUNp4, composed of the highest EU/PD weight ratio (1:2) has PD amounts two times higher than EUNp and C/N (10.54) ratio is the highest close to PD C/N ratio (13.20).

Table 4: Atomic composition of dopamine, PD, EUNp and FEUNp1 to 4 for the different mass ratios between EUNp and PD determined by XPS.

Samples	%C	%O	%N	C/N ratio
Dopamine HCl	77.29	15.84	6.87	11.25
PD	74.98	19.34	5.68	13.20
EUNp	68.39	21.27	10.34	6.61
FEUNp1	70.32	21.12	9.45	7.44
FEUNp2	69.30	21.74	8.96	7.73
FEUNp3	72.57	19.44	7.99	9.08
FEUNp4	72.68	20.43	6.89	10.54

In the experiments, we report IR analysis of self-polymerized polydopamine (PD) on the surface of eumelanin nanoparticles (**Figure 5A**). However, IR spectra of PD have not been clearly observed, because of low signal and low amount of reacted PD. Although PD cannot clearly be detected as opposite of dopamine (data not shown), PD formation on eumelanin nanoparticles is observed, indicating the presence of PD and supporting the mechanism of self-polymerization [34]. As shown in **figure 5A**, PD shows peaks at 1344 and 1600 cm^{-1}, associated with indole ring or indoline structures supporting the proposed structure as reported in the literature [35]. Moreover, the characteristic peaks of PD in the functionalized nanoparticles are in the same region but not of same intensities [36]. In **Figure 5B** spectra of eumelanin nanoparticles display the characteristic bonds that also appear in PD spectra, demonstrating the same chemical skeleton between EUNp and PD. However, they are slightly different with the peaks at 1600 and 1344 cm^{-1}, broadened and shifted to higher wavenumber of 1618 and 1377 cm^{-1}. Moreover, gentamicin loaded functionalized eumelanin nanoparticles (FEUNp-GS1) show a peak at 1120 cm^{-1} which is attributed to the sulphur content in the form of S-O stretch.

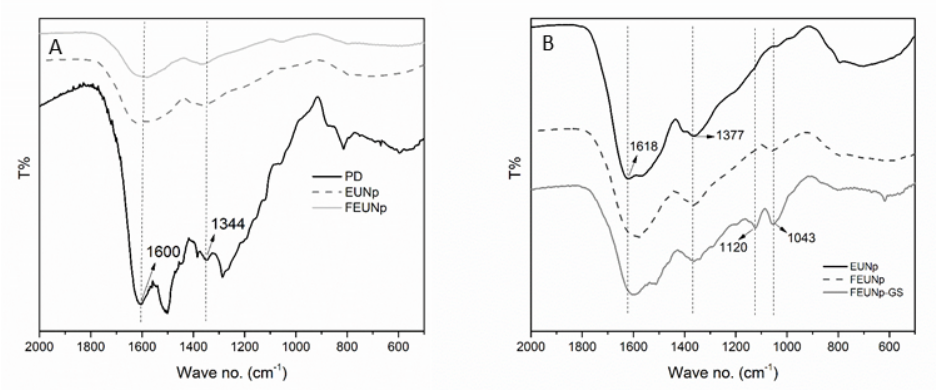

Figure 5: (A) Infrared spectra of polydopamine (PD), eumelanin nanoparticles (EUNp) and functionalized eumelanin nanoparticles (FEUNp). (B) Infrared spectra of eumelanin nanoparticles (EUNp) and functionalized eumelanin nanoparticles, and functionalized eumelanin nanoparticles loaded gentamicin (FEUNp-GS).

Thermogravimetric analysis (TGA) were conducted for PD, EUNp and FEUNp3. The experiment was carried out in a temperature range of 25° to 800°C with nitrogen atmosphere. **Figure 6** reports PD, EUNp, and FEUNp thermograms weight remaining being 98.85, 43.87 and 60.30 %, for PD, EUNp and FEUNp, respectively. After analysis, it is observed that PD tolerated high temperatures for at least up to 800°C (98.85% mass remaining) without significant thermograph changes. Instead, EUNp did not show thermal stability because the % weight residual was about 43.87% at 800°C (**Figure 6**). FEUNp3 demonstrated performances with good thermal stability, good stability which can be attributed to the additional PD layer. Moreover, weight of PD layer, as calculated in dry state from thermogravimetric analysis, is approximatively 95 µg with a weight ratio (1:0.2) of EUNp and PD by using the carbon yield at 800°C.

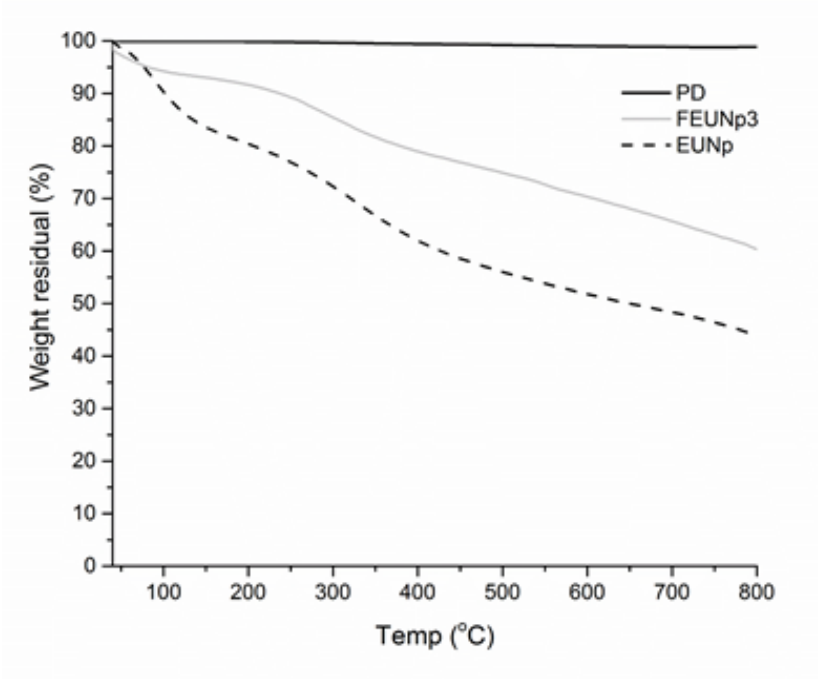

Figure 6: Weight residual % of polydopamine (PD), eumelanin nanoparticles (EUNp), and functionalized eumelanin nanoparticles with 1:1 of mass ratio (FEUNp3).

Adsorption of dopamine to EUNp surface was monitored using a quartz-crystal microbalance with dissipation monitoring (QCM-D). The QCM-D is an analytical equipment capable of detecting surface density changes in the order of ng/cm^2 at the surface of gold-coated quartz crystals [37]. Prior to QCM-D, crystals were spin-coated with PD in order to allow the attachment of EUNp to the surface. This approach was adapted from Thörn et al, who previously used the QCM-D to quantify lipase and feruloyl esterase immobilization into mesoporous silica particles, the latter attached to APTMS-functionalized sensor surfaces [38]. **Figure 7** shows the frequency and dissipation variations caused by sequential attachment of EUNp and PD, normalized to the 5th overtone (25 MHz).

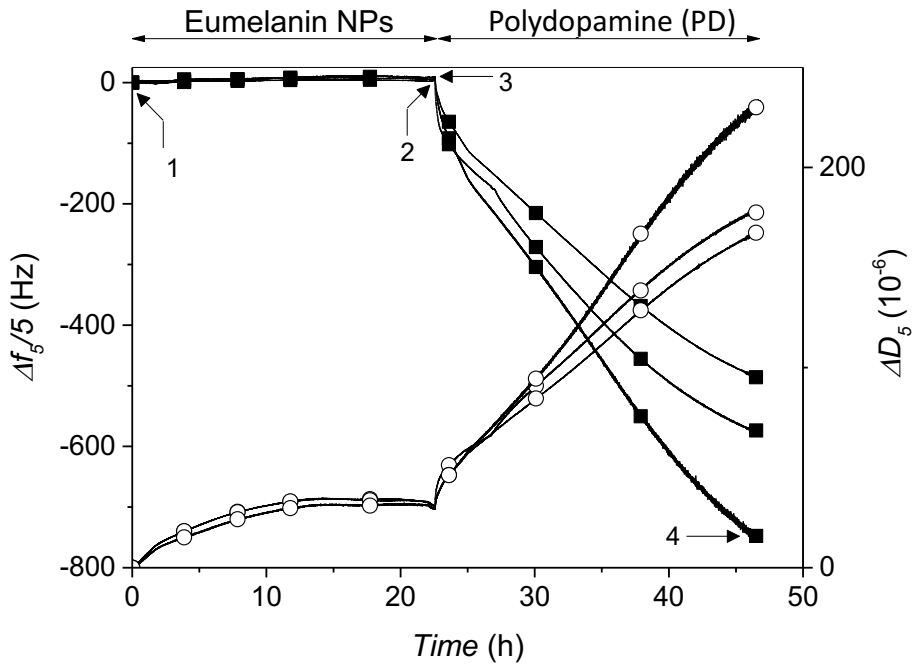

Figure 7: QCM-D monitoring of normalized frequency (Δf_n/n, ■) and dissipation (ΔD_n, ○) obtained at the 5th overtone. Numbers refer to adsorption of eumelanin nanoparticles (1), adsorption of polydopamine (3) and rinsing (2 and 4). Rinsing steps are too short to be seen.

During QCM-D acquisition, the adsorption of mass to the sensor's surface is usually identified by a decrease in Δf. As observed, flushing EUNp for 24 h resulted in a $\Delta F_5/5$ variation close to 0 Hz. However, one can observe that ΔD_5 increased (30.8±1.61 × 10^{-6}). ΔD provides evidence about the film's viscoelastic properties: a soft component often leads to an increase of the dissipation values due to energy loss from the crystal's oscillation, whereas smaller dissipation values are obtained for rigid components [39-40]. The soft character evidenced by ΔD, it is also associated with high water content. The hydration of spin-coated PD layer is discarded since the experiments were carried out in a stable buffer immersed environment from t=0. Therefore, the variations observed for this time period show that nanoparticles coupled with high amounts of water adsorbed to the surface. After immobilizing EUNp, dopamine solution was injected for 22 hours (i.e., time necessary to reach the stop condition of Δf_n<5% per hour). By the end of this time period, PD adsorption contributed to $\Delta f_5/5$ and ΔD variations of about -610 Hz and 160×10^{-6}, respectively.

The QCM-D monitoring data was used as input for the Voigt-based viscoelastic model (Eq. 1 and 2) to calculate the mass of material attached to the crystal's surface in each adsorption stage. By doing this it was possible to estimate a correlation between EUNp and PD necessary to develop a full coating. In average, the coating of 1 g of EUNp requires 2.46±0.3 g of PD. The QCM-D results, alongside the

application of the Voigt-based model, demonstrate the successful EUNp-PD interaction occurring during coating formation. For the comparison of dry state from TGA and wet state from QCM-D at optimized condition of dopamine (0.5 mg/mL), system water uptake was about 92 % demonstrating a hydrophilic nature of PD coating layer.

After prime-coating of EUNp with PD in the 1:1 ratio (FEUNp3), from the literature, amine terminated functional ligands such as folate, cRGD, peptide, polymer ligands can be incorporated to the EUNp via the PD surface [4]. In our work, since gentamicin molecule has primary amines group, the amine groups can react with PD via Schiff base reaction in oxidizing condition. As reported [4], PD functionalization provides many advantages in order to easily and conveniently binding many biomolecules. Moreover, PD is able to improve adhesion and proliferation of many kinds of cells with good biocompatibility. Due to zwitterion property of PD in different acid-base condition, in acid condition, PD layer is positively charged and allows good permeability of negatively charged small molecules, but it is negatively charged and allows good permeability of positively charged molecules in basic condition. FEUNp3 was incubated with different amounts of gentamicin, as reported in **Table 2** in order to achieve FEUNp3: gentamicin of the ratios of 1:2 and 1:4 with the different incubation time in TRIS-HCl buffer (pH ~8.5) for 30 or 60 min. When system pH is 8.5, gentamicin is close to its pKa (8.2), 50% is protonated and can be adsorbed to FEUNp surface. **Table 5** presents ζ-potential, PDI and particle size of the produced nanoparticles (FEUNp- GS1 to FEUNp-GS4). ζ-potential of all formulations is closed to neutrality that is an influence of gentamicin positive charge on FEUNp surface. Based on SEM images, the particle size distribution of FEUNp-GS varied from 232.121±6.15 to 238.051±8.50 nm. Moreover, SEM image (**Figure 8**) did not reveal any visible difference in morphology between the FEUNp and PD. Aggregation is observed by DLS and is confirmed by SEM, showing high PDI values for all formulations: 0.431±1.34 (FEUNp-GS1) and 0.60±1.64 (FEUNp-GS4). Higher amount of gentamicin (FEUNp-GS3 and FEUNp-GS4), correspond to lower encapsulation efficiency (EE %) between 16.32±2.45% and 17.97±3.09% that is attributed to gentamicin hydrophilicity (water solubility~50mg/mL). Moreover, incubation time does not affect EE%. Therefore, the layer of PD coating probably offers catechol groups to functionalize EUNp with gentamicin.

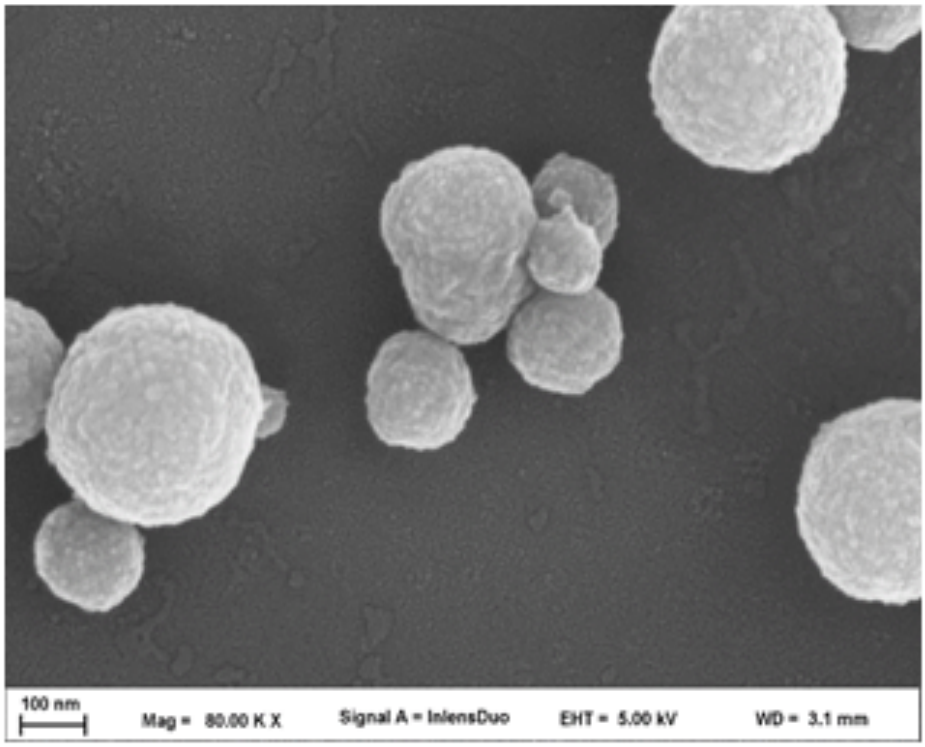

Figure 8: SEM image of FEUNp-GS3, magnification at 80.00 KX.

Table 5: Size, zeta potential, polydispersity indices parameters FEUNp-GS from 1 to 4 with amount of gentamicin (25 or 50 mg) and stirring time (30 or 60 min).

Samples	Size(nm)*	PDI**	ζ(mV)**	EE (%)	Yield (%)
FEUNp-GS1	236.031±7.24	0.431±0.03	-1.84±0.58	32.42±3.21	44.34±0.67
FEUNp-GS2	238.051±8.50	0.44±0.09	-2.78±0.76	29.48±2.13	42.67±0.88
FEUNp-GS3	232.121±6.15	0.56±0.04	-4.32±0.54	17.97±3.09	39.54±0.78
FEUNp-GS4	235.231±7.12	0.60±0.06	-5.73±0.78	16.32±2.45	40.56±0.65

*Size (nm) was calculated from SEM images using the ImageJ software for the analysis particle.

**PDI and zeta potential (mV) were calculated from light scattering measurements in purified water, values are expressed as average±SD of three measurements. The selected concentration is 0.025mg/ml

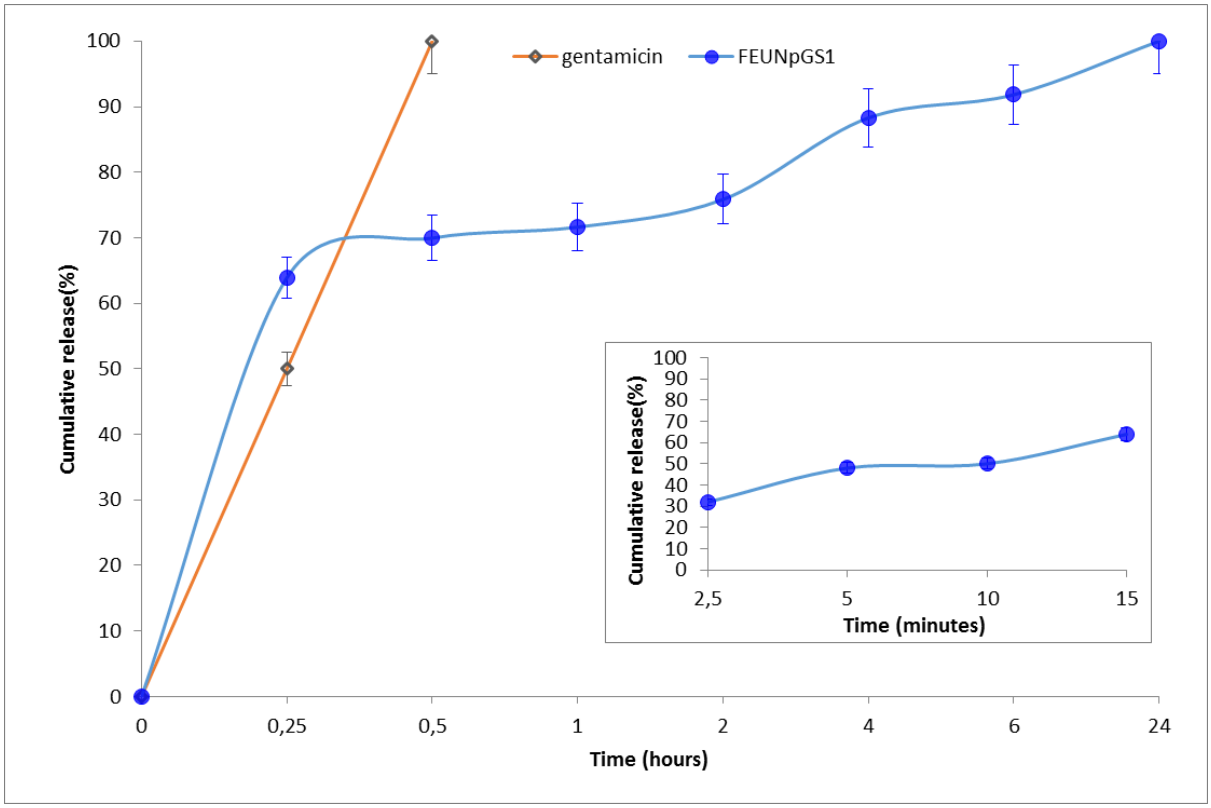

Figure 9: Cumulative release profile of FEUNp-GS1 from 0 min up to 24 h.

FEUNp-GS1 with the best results in terms of EE%, size, size distribution (PDI), zeta potential (ζ) and yield process was submitted to *in vitro* release test in PBS buffer pH 7.4 in dynamic condition at 37°C. The release profile exhibits an initial burst release about 63.90 % in 15 min reaching 71.63% in 1 h, followed by sustained release behavior up to 24 h **(Figure 9)**. The best fitting data of the percentage of released gentamicin and considering data up to 60% (15 min) to Korsmeyer and Peppas equation, exponential diffusion was found to be 0.2116 (R^2= 0.9083), this value indicates Fickian release [41]. FEUNp-GS1 with higher gentamicin loading indicates gentamicin molecules are not covalently bond, but they are absorbed onto the surface of FEUNp which contributed to the greater initial release. During the first hour of the release study, high gentamicin concentration gradient acts as diffusional driving force. Subsequently, after 1 h gentamicin release slows down. It can be hypothesized the behavior is due to high porosity with large porous of PD coating layers in functionalized eumelanin nanoparticles structure, (**Figure 8**) [42, 43].

In this study, we set out to determine whether FEUNp-GS1 presented an antimicrobial effect against *Staphylococcus aureus* and *Escherichia coli*, two opportunistic microorganisms that can cause a wide variety of osteomyelitis in humans. Gentamicin sulphate is an antibiotic used to treat several types of bacterial infections in osteomyelitis, including *S. aureus* and *E. coli*. As an aminoglycoside, gentamicin is able to bind to the 30S subunit of the bacterial ribosome, interrupting protein synthesis and

promoting cell death. Indeed, we observed that free gentamicin solution was able to inhibit *S. aureus* growth by half (IC_{50}), at concentrations of 10.33 µg/mL (**Figure 10A**), while complete inhibition of bacterial growth (IC_{90}) was achieved at concentrations of 18.06 µg/mL (**Figure 10A**). FEUNp-GS1 also observed an antimicrobial effect against *S. aureus*, although this conjugated required higher concentrations of gentamicin released to obtain the same effects as free gentamicin solution (**Figure 10B**; IC_{50}: 110.60 µg/mL and IC_{90}: 216.39 µg/mL). Importantly, the antimicrobial effect of gentamicin released from FEUNp-GS1 was not due to the nanoparticle itself, since FEUNp alone was not able to prevent bacterial proliferation (data not shown).

Similar results were observed with *E. coli*. Approximately 2.62 µg/mL of gentamicin solution were required to prevent *E. coli* growth by half (**Figure 10C**) and 3.15 µg/mL to completely inhibit proliferation (**Figure 10C**); while gentamicin loaded FEUNp presented an IC_{50} of 54.13 µg/mL and IC_{90} of 101.25 µg/mL (**Figure 10D**). The FEUNp also had no influence on *E. coli* growth *in vitro* (data not shown). Together, these *in vitro* results confirm that FEUNp-GS1 is effective in inhibiting the proliferation of two important bacteria as known to be responsible for osteomyelitis treatment. Therefore, FEUNp-GS1 nanoparticles can be viable alternative carriers to antibiotic alone, as a localized drug delivery system for osteomyelitis treatment. The efforts to develop new generation of antimicrobial drugs with expansion of drug-resistant pathogens is contributed to develop new modern formulation strategy for treating bacterial infection. In the field of bone infectious diseases, nanoparticles could eradicate biofilm formation which protect bacteria from the action of antimicrobial agents. In this prospective, functionalized nanoparticles could be an alternative chance to prevent the formation of the biofilm. Further evaluations should be performed in different animal models of infection, in order to establish its *in vivo* antimicrobial effect.

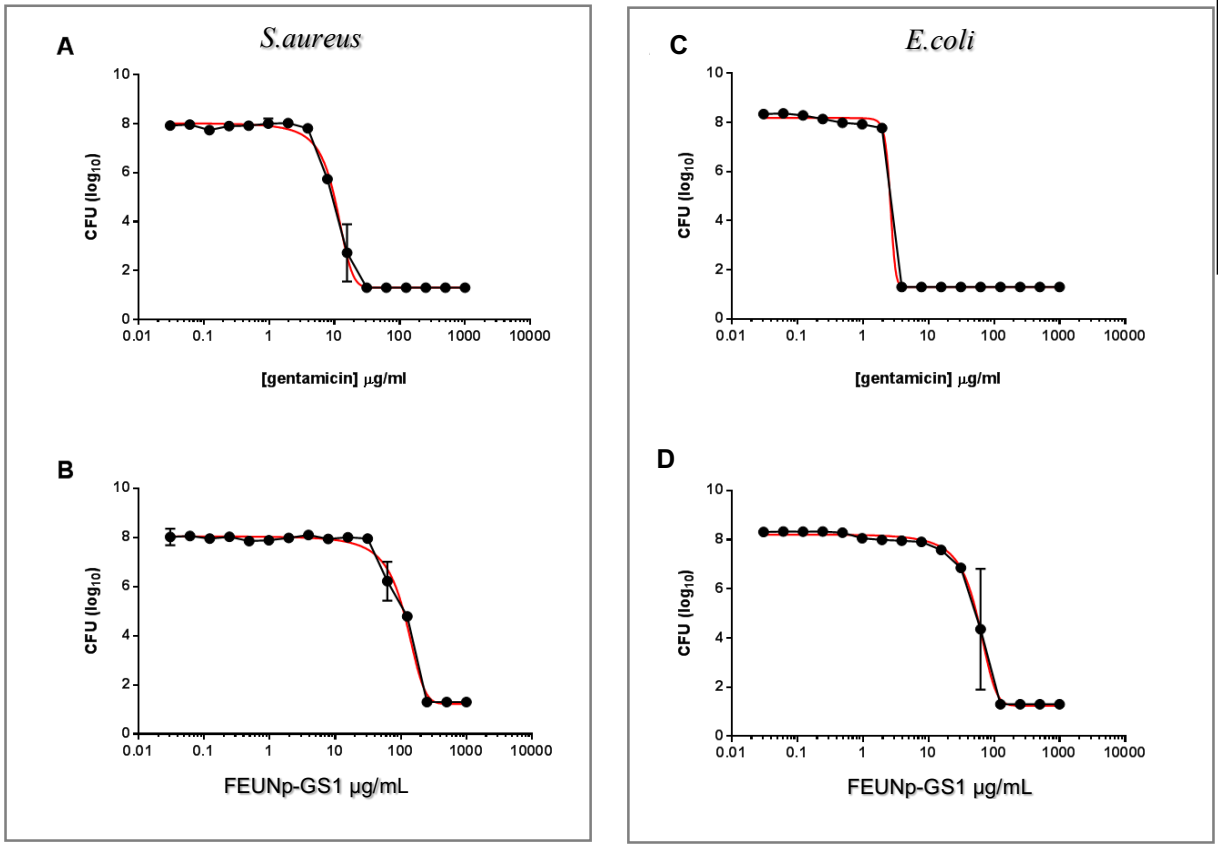

Figure 10: Antimicrobial effect of free gentamicin and gentamicin loaded FEUNp against *S. aureus* and *E. coli*. Cultures of 1x10^5 CFU of *S. aureus* and *E. coli* were incubated with increasing concentrations of gentamicin (A and C) or gentamicin loaded FEUNp (B and D). After 24 h of incubation, CFU were performed to determine bacterial viability. Data points represent the mean ± SEM (n=2). Plots represent one experiment of 4 independent experiments.

5. CONCLUSIONS

Even if the full application of the fate of natural based eumelanin nanoparticles is a really hard task, we believe that the functionalization by self-polymerized bioadhesive polydopamine is a simple method to increase their utility in drug delivery system. Indeed, this study, dealing with the funcionalized eumelanin nanoparticlesand entrapped gentamicin are both successfully fabricated. The physical and chemical characterization are confirmed that the extra layer of polydopamine is generated covering the surface of eumelanin nanoparticles. Moreover, entrapped eumelanin nanoparticles, release profile and antimicrobial effect are also supporting their capabilities as localized carriers. The proposed proof of concept is focused on the drug delivery system application in osteomyelitis infectious disease. On this purpose, Nps could be formulated in an injectable in situ forming hydrogel for local administration. However, Nps could be loaded with diverse bioactive

molecules and could be formulated in ointments and/or lotions for topical administration on skin. Eventually, the proposed natural based eumelanin nanoparticlesare a versatile system for delivery of drugs.

ACKNOWLEDGEMENTS

The authors would like to thank the European Union (Horizon 2020) funded project FoReCaST (n° 668983). Khon Kaen University, Thailand provided financial support to Pathomthat Srisuk. Rui R. Costa acknowledges the financial support from Fundação para a Ciência e Tecnologia (grant SFRH/BPD/95446/2013), "Fundo Social Europeu" (FSE), and "Programa Operacional de Potencial Humano" (POPH). The FCT fellowship distinction attributed to Vitor M. Correlo under the Investigator FCT program (IF/01214/2014) is also greatly acknowledged.

6. REFERENCES

[1] P.Srisuk, V.M Correlo, I.B. Lenor, P. Palladino, R. Reis, Effect of Melanomal Proteins on Sepia Melanin Assembly. Journal of Macromolecular Science, Part B, 54 (2015) 1532-1540.

[2] P.Meredith, and T. Sarna, The physical and chemical properties of eumelanin. Pigment Cell Research, 19(6) (2006) 572-594.

[3] L.Zeise, R.B. Addison, and M.R. Chedekel, Bio-analytical Studies of Eumelanins. I. Characterization of Melanin the Particle. Pigment Cell Research, 3 (1990) 48-53.

[4] J.Park, T.F. Brust, H.J. Lee, S.C. Lee, V.J. Watts, and Y.Yeo, Polydopamine-based simple and versatile surface modification of polymeric nano drug carriers. ACS Nano, 8(4) (2014) 3347-3356.

[5] X.Gu, Y. Zhang, H.Sun, X. Song, C. Fu, and P. Dong **,** Mussel-inspired Polydopamine Coated Iron Oxide Nanoparticles for Biomedical Application. Journal of Nanomaterials, (2015) 12 pages.

[6] M.D'Ischia, A. Napolitano, V. Ball, C-T Chen and M,J; Buehler, Polydopamine and Eumelanin: From Structure–Property Relationships to a Unified Tailoring Strategy. Accounts of Chemical Research, 47(12) (2014) 3541-3550.

[7] S.M Kang, N.S. Hwang, J. Yeom, S.Y:Park, P.B. Messersmith, I.S. Choi, R. Langer, D.G: Anderson and H. Lee, One-step multipurpose surface functionalization by adhesive catecholamine. Advanced functional materials 22(14) (2012) 2949-2955.

[8] K.C.L Black, J. Yi, J.G. Riviera, D.C. Zelasko-Leon and P.B. Messersmith, Polydopamine-enabled surface functionalization of gold nanorods for cancer cell-targeted imaging and photothermal therapy. Nanomedicine, 8(1) (2012) 17-28.

[9] C. Li, Z. Liu, and P. Yao, Gold nanoparticles coated with a polydopamine layer and dextran brush surface for diagnosis and highly efficient photothermal therapy of tumors. RSC Advances, 6(39) (2016) 33083-33091.

[10] S.Hong, K.Y. Kim,H.J. Wook, S.Y.Park, K.D. Lee and H.Lee, Attenuation of the *in vivo* toxicity of biomaterials by polydopamine surface modification. Nanomedicine, 6(5) (2011) 793-801.

[11] Y.Liao, Y. Wang, X. Fengc, W. Wanga, F. Xua, L.Zhanga, Antibacterial surfaces through dopamine functionalization and silver nanoparticle immobilization. Materials Chemistry and Physics, 121 (2010) 534-540.

[12] M.Zhang, X. Zhsng, X. he, L. Chen and Y. Zhang, A self-assembled polydopamine film on the surface of magnetic nanoparticles for specific capture of protein. Nanoscale, 10 (2012) 3141-3147.

[13] R.Mrówczyński , R. Turcu, C. Leostean, H. A. Scheidt and J. Liebscher, New versatile polydopamine coated functionalized magnetic nanoparticles. Materials Chemistry and Physics, 138 (2013) 295-302.

[14] S.P Le-Masurier, H.T.T. Duong, C. Boyer and A.M: Granville, Surface modification of polydopamine coated particles via glycopolymer brush synthesis for protein binding and FLIM testing. Polymer Chemistry, 6(13) (2015) 2504-2511.

[15] W.Hu, G. He, H. Zhang, X. Wu, J. Li, Z. Zhao, Y. Qiao, Z. Lu, Y. Liu and C. M. Li, Polydopamine-Functionalization of Graphene Oxide to Enable Dual Signal Amplification for Sensitive Surface Plasmon Resonance Imaging Detection of Biomarker. Analytical Chemistry, 86(9) (2014) 4488-4493.

[16] T.Hui, Z.T.GangYou, Y.MuyaoLi, J. Jing, Treatment of osteomyelitis by liposomal gentamicin-impregnated calcium sulfate. Archives of Orthopaedic and Trauma Surgery, 129(10) (2009) 1301-1308.

[17] J.S.Gogia, J.P. Meehan, P. E. Di Cesare, and A.A. Jamali, Local Antibiotic Therapy in Osteomyelitis. Seminars in Plastic Surgery, 23(2) (2009) 100-107.

[18] D.P.Lew,and F.A. Waldvogel Osteomyelitis. New England Journal of Medicine, 336(14) (1997) 999-1007.

[19] P.J.Carek, L.M. Dickerson, and J.L. Sack, Diagnosis and management of osteomyelitis. American family physician, 63(12) (2001) 2413-2420.

[20] T.T.Yoshikawa, and B.A. Cunha, Osteomyelitis in Elderly Patients. Clinical Infectious Diseases, 35(3) (2002) 287-293.

[21] D.P.Lew, and F.A. Waldvogel, Osteomyelitis. The Lancet, 364 (2004) 369-379.

[22] J.Ji, S. Haoa, D. Wua, R. Huangb, Y. Xu , Preparation, characterization and in vitro release of chitosan nanoparticles loaded with gentamicin and salicylic acid. Carbohydrate Polymers, 85 (2011) 803-808

[23] U. Posadowska, M. Brzychczy-Włoch, and E. Pamuła, Gentamicin loaded PLGA nanoparticles as local drug delivery system for the osteomyelitis treatment. Acta of Bioengineering and Biomechanics, 17(3) (2015).

[24] V. Mendel, H.-J. Simanowski, H.C. Scholz, H. Heymann, Therapy with gentamicin-PMMA beads, gentamicin-collagen sponge, and cefazolin for experimental osteomyelitis due to Staphylococcus aureus in rats. Archives of Orthopaedic and Trauma Surgery, 125(6) (2005) 363-368.

[25] R.P.Evans, and C.L. Nelson, Gentamicin-impregnated polymethylmethacrylate beads compared with systemic antibiotic therapy in the treatment of chronic osteomyelitis. Clinical orthopaedics and related research, 295 (1993) 37-42.

[26] T. Wu, Q. Zhang, W. Ren, X. Yi, , Controlled release of gentamicin from gelatin/genipin reinforced beta-tricalcium phosphate scaffold for the treatment of osteomyelitis. Journal of Materials Chemistry B, 1(26) (2013) 3304-3313.

[27] R.Dorati, A. De Trizio, P. Grisoli, A. Merelli, I. Genta, T. Modena, B. Conti, An experimental design approach to the preparation of pegylated polylactide-co-glicolide gentamicin loaded microparticles for local antibiotic delivery. Materials Science and Engineering C, 58 (2016).

[28] M.V.Voinova, M. Rodahl, M Jonson and B. Kasemo, Viscoelastic acoustic response of layered polymer films at fluid-solid interfaces: continuum mechanics approach. Physica Scripta, 59(5) (1999) 391-399.

[29] S.Dash, P.N Murthy, L. Nath, P. Chowdhury, Kinetic modeling on drug release from controlled drug delivery system. Acta Poloniae Pharmaceutica-Drug Research, 67 (2010) 217-223.

[30] Z. Li, K.Zhao, C. Wua, K. Zhaoa, B. Pengb, Z. Deng, Polydopamine-assisted synthesis of raspberry-like nanocomposite particles for superhydrophobic and superoleophilic surfaces. Colloids and surface A:Physicochemical and Engineering Aspects, 470 (2015) 80-91.

[31] J.H.Cant, Y-C. Wang, D. G. Castnerand, A. G. Shard, A technique for calculation of shell thicknesses for core-shell-shell nanoaprticles from XPS data. Surface and Interface Ananlysis 48 (2015).

[32] L. Xiangsheng, C. jiesming, L. Huan, J. Qiao, R.Kefeng and J. Jian, Mussel-Inspired Polydopamine: a biocompaticle and ultrastable coating for nanoparticles in vivo, ACs Nano 7 (2013) 9384-9395.

[33]F. Bernsmann, A. Ponche, C. Ringwald, J. Hemmerlè, J. Raya, B. Bechinger, J. C. Voegel, P. Schaaf and V. Ball, Characterization of Dopamine- Melanin Growth on silicon oxide, J. Phys. Chem C 113 (2009) 8234-8242

[34] S.Habibi, A. Nematollahzadeh, S. A. Mousavi, Nano-scale modification of polysulfone membrane matrix and the surface for the separation of chromium ions from water. Chemical Engineering Journal 267 (2015) 306-316.

[35] D.R.Daniel, D.J. Miller,B.D. Freeman,D. R. Paul, and C.W. Bielawski, Elucidating the strucure of Poly(dopamine). Langmuir, 28 (2012) 6428-6435.

[36] H.Luo, Facile synthesis of novel size-controlled antibacterial hybrid spheres using silver nanoparticles loaded with poly-dopamine shperes. RSC Adv., 5 (2015).

[37] K.A.Marx, Quartz Crystal Microbalance: A Useful Tool for Studying Thin Polymer Films and Complex Biomolecular Systems at the Solution−Surface Interface. Biomacromolecules, 4(5) (2003)1099-1120.

[38] C.Thörn, H. Gustafsson, and L. Olsson, QCM-D as a method for monitoring enzyme immobilization in mesoporous silica particles. Microporous and Mesoporous Materials, 176 (2013) 71-77.

[39] N.-J.Cho, et al., Employing Two Different Quartz Crystal Microbalance Models To Study Changes in Viscoelastic Behavior upon Transformation of Lipid Vesicles to a Bilayer on a Gold Surface. Analytical Chemistry, 79(18) (2007) 7027-7035.

[40] F.Höök, et al., Variations in Coupled Water, Viscoelastic Properties, and Film Thickness of a Mefp-1 Protein Film during Adsorption and Cross-Linking: A Quartz Crystal Microbalance with Dissipation Monitoring, Ellipsometry, and Surface Plasmon Resonance Study. Analytical Chemistry, 73(24) (2001) 5796-5804.

[41] k.S. Yadav and K.K.Sawanrìt, Modified nanoprecipitation method for preparation of Cytarabine.loaded PLGA nanoparticles. AAPS PharmSciTech, 11 (3) 1458-1465.

[42] A. Namatollahzadeh, A. Shojaei, JM Abdekhodaia, B. Sellergren, Molecularly imprinted polydopamine nano-layer on the pore surface of porous particles for protein capture in HPLC column. Journal of colloide e Interface Science 404 (2013) 117-126

[43] E. Ghesemian, A. Vatanara, R. Najafabadi, R. M. Rouni, K. Gilani, M. Darabi, Preparation, characterization and optimization of sildenafil loaded PLGA nanoparticles by statistical factorial design. Journal of Pharmaceutical Science 21 (68) (2013) 1-10.

Conclusion and future perspective

GENERAL CONCLUSION AND FUTURE PERSPECTIVE

As explained in the general introduction and all along my thesis, the experimental work done developed a project on bone regeneration combined to antibiotic therapy, by innovative drug delivery systems. All together the collected data confirm the flexibility of the composite polymer matrix in the design of antibiotic delivery system for osteomyelitis local therapy.

The thermo-gelling solution (chitosan-βGP) incorporating bovine bone substitutes (BBS) forms by freeze-drying a 3D porous moldable scaffold with a combination of excellent biofunctionality and mechanical properties (**Chapter I**). In particular the presence of BBS into thermogelling solution positively influences biological response enhancing cell attachment and cell proliferation. 3D structure of moldable composite scaffolds (mCS) has adequate mechanical properties in order to support the physiologic loads developed at tissue site (e.g bone). Moreover, highly microporous structure permits diffusion of cells, nutrients and metabolic products throughout scaffold. The developed systems could be promising candidates for bone regeneration both as injectable for minimal invasive procedure or moldable form, which enables easy rehydration for implantation by surgical procedure (**Chapter I and II**). Additionally, the scaffold demonstrates to be a suitable vehicle for gentamicin sulphate (**Chapter II**). In the presence of gentamicin sulphate rapid irreversible gelification of thermogelling solution is highlighted, and interference of gentamicin with gelifying process is hypotesized (**Chapter II**). Satisfactory biological performances have been obtained for moldable scaffolds due to their high porosity, high water retention ability and antimicrobial efficacy. In order to fulfill prolonged antibiotic release, microparticles based on PLGA-PEG copolymers were developed by Design of Experiment (DoE), and finalized to achieve gentamicin sustained release reaching complete release in 3 months. On the base of the results, the gentamicin loaded microparticles were embedded into thermos-gelling solutions showing a similar prolonged release of gentamicin until 3 months (**Chapter III**). It should be also underlined that the moldable composite scaffold is able to physically retain BBS and microparticles up to 45 days in *in vitro* simulated conditions (**Chapter IV**). Moreover, moldable scaffolds loaded with gentamicin combines bacteriostatic chitosan properties and sustained gentamicin bactericidal effect up to 14 days (**Chapter IV**). Therefore, this novel system could be preferred to conventional osteomyelitis therapy.

Scarce results are reported in the literature regarding nanoparticulate drug delivery approach with gentamicin to overcome biofilm formation. The carried out preliminary experimentals (**Chapter V**) through DoE screening, permitted to set up the optimized conditions achieving gentamicin loaded PLGA-PEG/PLGA-H nanoparticles with good encapsulation efficiency. Moreover, lyophilized

nanoparticles have been obtained with good resuspendability and stability. Lyophilization process was studied by a DoE mixture design and different cryoprotectans. (**Chapter V**).

Finally, during my Erasmus in Portugal at 3B's Research group I studied gentamicin loading into polydopamine surface modified eumelanin nanoparticles. I perfomed a deep physical-chemical characterization of nanoparticles by microscopy technique (SEM, AFM and TEM) and gravimetrical analysis (TGA and QCM-D) obtaining interesting results and confirming the effectively interaction between eumelanin nanoparticles and polydopamine (**Chapetr VI**). The results can be exploited in future work on the polydopamine polymer.

Future prospectives involve:

As long as chitosan composite scaffolds is concerned, to complete the formulation study with evaluation of possible sterilization processes.

As long as gentamicin PLGA-PEG/PLGA-H nanoparticles is concerned, to develop antimicrobial study on standard bacterial (*Escherichia coli* ATCC25922) as quality control and bacteria strains Gram + and Gram – clinical isolate; to study gentamicin loaded nanoparticles efficacy on biofilm formation.

As long as polydopoamine/eumelanin nanoparticles is concerned, to formulate the drug delivery systems into a thermosensitive hydrogel or moldable biodegradable scaffold for osteomyelitis treatment.

Additionally, due to bioadhesive polydopamine properties the functionalized nanoparticles loaded with gentamicin will be further studied to be formulated into a dermal or transdermal forms for would healing treatment.